



Gas-condensate Reservoir Performance
Modelling.

PhD Thesis

Foad Faraji

A thesis submitted in partial fulfilment of the requirements of the
Teesside University for the degree of Doctor of Philosophy

December 2020

ABSTRACT

Accurate prediction of gas-condensate reservoir performance below the saturation pressure is an inherent problem. This is due to the compositional variation and phase change during the depletion process. In doing so, ensuring accurate reservoir performance modelling for various pressure – volume – temperature (PVT) properties such as two phase “gas/condensate” viscosities and compressibility factor (Z factor) in desired reservoir conditions are particularly important. However, the existing viscosities and Z factor models cannot capture fluid flow complexity of gas-condensate reservoirs below the saturation pressure for modelling purposes.

The major contribution of the thesis is development of new gas/condensate viscosity and two-phase Z factor models using comprehensive experimental data sets. The data sets are representing downhole and reservoir condition. In the development process, an investigation on the use of soft computing techniques such as Support Vector Machine (SVM), Artificial Neural Network (ANN) and fuzzy logic (Mamdani & TSK) has been carried out. It is found that developed TSK fuzzy logic approaches offer the most accurate viscosity and two-phase Z factor prediction. The developed models can predict viscosity and two-phase Z factor of gas-condensate reservoirs in high pressure high temperature (HPHT) conditions with variety of non-hydrocarbon contents and they are not limited within geographical location.

The impact of viscosity and two-phase Z factor models towards the production calculation was the ultimate interest of this research. This led to further contribution on proposing the new method for computation of gas-condensate reservoir production rate performance, which involves integrating pseudopressure integral with volumetric material balance. For the computation of production rate, dynamic three-phase effective permeability has also been adopted. Distinctively, the proposed method provides better level of accuracy to compositional commercial simulation software in term of production forecast and economic impact of gas-condensate wells. Furthermore, the proposed method offers simpler computational procedures, where less input parameters are required.

Keywords: Gas-condensate, gas-condensate PVTs, Viscosity, Compressibility factor (Z factor), Soft Computing approach, Artificial Neural Network (ANN), Fuzzy Logic.

ACKNOWLEDGEMENT

I would like to express my sincere appreciation to my supervisory team, Dr. Johnson Ugwu, Professor. Farhad Nabhani and Dr. Perk Lin Chong for their continuous support and guidance throughout this research. I extend my appreciation to Teesside University for providing the fund under graduate tutor scheme. I also would like to thanks all my friends for their support during my study.

LIST OF PUBLICATIONS

Published Articles:

1. Development of inflow performance model in high temperature gas-condensate reservoirs published in Journal of Petroleum Science and Engineering (JPSE)

<https://www.sciencedirect.com/science/article/abs/pii/S0920410519305819>

2. Modelling viscosity of liquid dropout near wellbore region in gas condensate reservoirs using modern numerical approaches published in Journal of Petroleum Science and Engineering (JPSE).

<https://www.sciencedirect.com/science/article/abs/pii/S0920410519310253>

3. Development of new gas-condensate viscosity correlation using TSK fuzzy logic approach (Under review)

4. Modelling of gas condensate viscosity using fuzzy logic based on different membership functions (Under review).

TABLE OF CONTENTS

COVER PAGE	0
ABSTRACT	i
ACKNOWLEDGEMENT	ii
LIST OF PUBLICATIONS	iii
TABLE OF CONTENTS	iv
LIST OF TABLES	ix
LIST OF FIGURES	xi
NOMENCLATURE	xvi
CHAPTER 1 INTRODUCTION.....	1
1.1 Background	1
1.2 Gas-condensate characteristics.....	3
1.3 Gas-condensate flow behaviour	5
1.3.1 Phase behaviour	5
1.3.2 Drawdown behaviour	6
1.4 Problem Statement	8
1.5 Research aim and objectives.....	10
1.6 Proposed approach	11
1.7 Organization of the thesis	11
CHAPTER 2 WELL DELIVERABILITY MODELLING OF GAS-CONDENSATE RESERVOIRS.....	15
2.1 Introduction	15
2.2 Gas Rate Theory	16
2.3 Well Deliverability Theory	19
2.3.1 Modelling Fluid Properties.....	26
2.3.2 Compressibility Factor (Z factor)	31

2.3.3 Density of the mixture	32
2.3.4 Formation Volume Factor of Gas-Condensate Mixture	34
2.3.5 Solution Gas to Oil Ratio (Rs)	40
2.3.6 Viscosity (Gas/Condensate).....	42
2.3.7 Drawdown Behaviour on modelling.....	46
2.4 Summary	48
CHAPTER 3 METHODOLOGY AND CONCEPTUAL FRAMEWORK	50
3.1 Introduction.....	50
3.2 Pressure – Volume –Temperature (PVT) modelling	50
3.3 Approaches of Well Deliverability Modelling	51
3.4 Current Study Approach	53
3.5 Major Work Steps	54
3.6 Data Acquisition and Validation	55
3.7 Summary	56
CHAPTER 4 IMPROVEMENT OF GAS-CONDENSATE FLUID VISCOSITY PREDICTION.....	57
4.1 Introduction.....	57
4.2 Assessment of gas phase viscosity models.....	58
4.2.1 Lohrenz – Bray – Clark (LBC), 1964	58
4.2.2 Lee – Gonzalez – Eakin (LGE).....	60
4.2.3 Londono – Archer – Blasingame (LAB).....	61
4.2.4 Sutton, (2005)	62
4.2.5 Elsharkawy (2006)	63
4.3 Assessment of condensate (oil) phase viscosity models	66
4.3.1 Data acquisition.....	67
4.3.2 Beggs and Robinsons, (1975).....	68
4.3.3 De Ghetto et al., (1994).....	69

4.3.4 Elsharkawy and Alikhan (1999).....	69
4.3.5 Bergman and Sutton, (2007).....	70
4.3.6 Kartoatmodjo and Schmidt, (1991).....	70
4.3.7 Results of existing models.....	71
4.4 Machine Learning (ML) Approach.....	75
4.4.1 Support Vector Machine (SVM).....	77
4.4.2 Artificial Neural Network (ANN).....	84
4.4.3 Results and discussion	90
4.5 Fuzzy Logic Approach	94
4.6 Takagi – Sugeno – Kang (TSK) Fuzzy approach.....	97
4.6.1 Fuzzy Clustering	99
4.6.2 Setting the membership function.....	101
4.6.3 Determination of constants.....	103
4.6.4 Development of new correlation.....	105
4.6.5 Results and discussions.....	106
4.7 Mamdani Fuzzy Approach	114
4.7.1 Fuzzy Engine process.....	114
4.7.2 Membership Functions (MFs) fuzzification.....	116
4.7.3 Mamdani Fuzzy Inference System	119
4.7.4 Defuzzification in Mamdani approach	121
4.7.5 Results and Discussion.....	122
4.8 Computational efficiency of the developed models.....	127
4.9 Summary	128
CHAPTER 5 DEVELOPMENT OF TWO-PHASE Z FACTOR OF GAS-CONDENSATE MIXTURE	130
5.1 Introduction.....	130
5.2 Preliminary theory of Z factor calculation.....	131

5.3 Assessment of Z factor models.....	133
5.3.1 Hall-Yarborough (1973).....	135
5.3.2 Dranchuk – Abu – Kassem (1975)	136
5.3.3 Beggs and Brill (1973).....	137
5.3.4 Rayes et al., (1992).....	137
5.3.5 Azizi et al., (2010)	138
5.3.6 Data bank.....	139
5.3.7 Results of literature models.....	141
5.4 Development of new Z factor models	148
5.4.1 Cascade Forward Neural Network (CFNN)	149
5.4.2 Feed Forward Backpropagation Neural Networks.....	152
5.4.3 Adaptive Neuro Fuzzy Inference System (ANFIS)	157
5.4.4 Proposed ANFIS structure	161
5.4.5 Clustering (Partitioning) of the data.....	166
5.4.6 Results and discussion	172
5.5 Summary	186
CHAPTER 6 PRODUCTION PROFILE FORECAST USING WELL TEST DATA..	188
6.1 Introduction.....	188
6.2 Pressure Transient Test (PTA) and two-phase pseudopressure approach ..	189
6.3 Computation of production profile in relation to gas/condensate viscosity and Z factor in HPHT gas-condensate well.....	196
6.3.1 Construction of pressure – volume – temperature (PVT) relationship....	199
6.3.2 Mathematical manipulation of pseudopressure integral	200
6.3.3 Material balance calculation	207
6.3.4 Validation of new production profile	210
6.3.5 Results and discussion	213
6.4 Summary	219

CHAPTER 7 CONCLUSIONS AND RECOMMENDATIONS	221
7.1 Introduction.....	221
7.2 Improve accuracies of gas-condensate viscosity.....	221
7.2.1 Improvement of two-phase gas-condensate Z factor	222
7.2.2 Effectiveness of viscosities and two-phase Z factor models for producing accurate production profile.....	224
7.3 Recommendation for future work.....	225
REFERENCES.....	226
APPENDIX A: Sample of collected data for development of condensate viscosity models.....	265
APPENDIX B: The developed Matlab codes for prediction of Two-phase Z factor	266
B1. Cascade Forward Neural Network (CFNN) code	266
B2. Feed Forward Neural Network (FFNN) code.....	266
B3. The Developed ANFIS code for prediction of two-phase Z factor.....	267
APPENDIX C: Sample calculation of inflow performance relationship (IPR) for HTHP gas condensate well.....	273
APPENDIX D: The developed Eclipse – 300 code for prediction of well inflow performance of HPHT gas condensate well	274

LIST OF TABLES

Table 1.1. Compositions and properties of several reservoir fluids (Whitson and Brulé, 2000, p. 2).....	4
Table 4.1. Statistical information of the data bank.....	68
Table 4.2. The original and tuned form of the employed literature correlations for predicting condensate liquid viscosity.	74
Table 4.3. The optimum values of the LSSVM parameters.....	82
Table 4.4. Statistical error performance of the LSSVM.	84
Table 4.5. Statistical parameters of developed ML based models and utilized correlations for prediction of condensate viscosity.	92
Table 4.6. The range of constants and input parameters of proposed condensate viscosity model.....	106
Table 4.7. Statistical accuracy of condensate phase viscosity models.	108
Table 4.8. Fuzzy rules defined for estimation of condensate viscosity in gas-condensate reservoirs.....	121
Table 4.9. Statistical error comparison between Mamdani fuzzy approach with three MFs and existing literature models for prediction of condensate viscosity.	123
Table 5.1. Coefficients of Azizi et al., (2010) Z factor correlation.	139
Table 5.2. Statistical description of the data used for development of compressibility factor.....	141
Table 5.3. Performance of employed literature models in predicting two-phase Z factor of gas-condensate systems.....	142
Table 5.4. The relation between the number of neurons and coefficient of determination for 1 hidden layer CFNN, using Levenberg – Marquardt (LM) as training algorithm.	151
Table 5.5. Statistical parameters and convergence time of FFNN with one hidden layer and using LM algorithm.....	155
Table 5.6. Statistical parameters and convergence time of FFNN with one hidden layer and using BR algorithm for training.....	156
Table 5.7. The description and details of the utilized membership functions for prediction of gas-condensate two-phase Z factor using ANFIS.....	163
Table 5.8. Performance of the developed ANFIS model using various membership function.....	166

Table 5.9. Effect of clustering radius on number of fuzzy rules and the performance of the model (1 st iteration).....	169
Table 5.10. Effect of clustering radius on number of fuzzy rules and the performance of the model (2 st iteration).....	170
Table 5.11. Statistical error computation of the developed models in prediction of gas-condensate's two-phase Z factor below the saturation pressure.....	173
Table 5.12. Constant Volume Depletion (CVD) results on North Sea gas-condensate sample at temperature of 394K (Danesh, 1998, pp. 53–56).....	1
Table 5.13. Constant Volume Depletion (CVD) results on sour gas-condensate sample (Elsharkawy, 2002).....	2
Table 5.14. Statistical measurement of the developed models and literature models for prediction two-phase Z factor of two gas-condensate samples as a function of P_{pr}	182
Table 6.1. Reservoir and fluid property of studied gas-condensate well after (Economides et al., (1989).	197
Table 6.2. Pressure build up data for (KAL – 5) obtained from (Economides et al., (1989).....	198
Table 6.3. Statistical error analysis of the developed analytical technique for predicting gas and condensate rates in (KAL – 5).	217

LIST OF FIGURES

Figure 1.1. USA Natural Gas withdrawals (EIA, 2020).....	1
Figure 1.2. Breakdown of Gazprom Group’s explored hydrocarbon reserves in Russian regions (Gazprom, 2019).....	2
Figure 1.3. Typical phase diagram of gas condensate systems (Modified from Fan et al., 2005).	6
Figure 1.4. Gas/condensate flow in three regions.	8
Figure 1.5. The flow chart indicates organization of the thesis for each chapter.	14
Figure 2.1. Typical plot of gas pressure function vs pressure where the area between P_{wf} and P_R representing the integral in 2.2.	19
Figure 2.2. Schematic diagram of traditional black oil formulation of PVT model.	27
Figure 2.3 schematic diagram of modified black oil (MBO) model.	29
Figure 2.4. Typical gas-condensate formation volume factor as a function pf pressure.	36
Figure 2.5. Solution gas to oil ratio (R_s) for North Sea gas-condensate sample at $T=280^\circ\text{F}$ (Modified from Whitson and Torp, 1983).	40
Figure 4.1. The prediction performance of existing literature models in estimating gas phase viscosity of gas-condensate reservoirs below the saturation pressure.	65
Figure 4.2. Plot of calculated viscosity using new developed model against measured viscosity data.....	66
Figure 4.3. Cross plot of the experimental condensate viscosity versus predicted condensate viscosity using employed literature correlations and refined results.	73
Figure 4.4 Machine Learning Block Diagram.	76
Figure 4.5. Performance of LSSVM in predicting condensate (oil) viscosity in training and testing stage.....	83
Figure 4.6. Graphical error analysis of LSSVM performance for predicting condensate (oil) viscosity.....	83
Figure 4.7. Schematic illustration of the ANN structure and computational steps to measure output.	85
Figure 4.8. Developed ANN model architecture for prediction of condensate viscosity.	88
Figure 4.9. Prediction performance of developed ANN network for condensate liquid viscosity in training (A) and testing (B) stage.	89

Figure 4.10. Prediction performance of the developed LSSVM condensate viscosity model as a function of pressure for three independent samples.	90
Figure 4.11. Prediction performance of developed ANN condensate viscosity model as a function of pressure for three independent samples.	90
Figure 4.12. Statistical performance comparison of tuned literature models against developed ANN and LSSVM models (AARD% and RMSE) for prediction of condensate viscosity.	92
Figure 4.13. Statistical performance comparison of tuned literature models against developed ANN and LSSVM models (R^2) for prediction of condensate viscosity.	93
Figure 4.14. Outline of the TSK fuzzy algorithm.	98
Figure 4.15. Optimum number of cluster for the training data sets using validity function (VRC), for condensate viscosity input data.	101
Figure 4.16. Gaussian membership function for detecting fuzzy clusters.	103
Figure 4.17. Gaussian membership function for input 1 “pressure”	104
Figure 4.18. Architecture of constructed TSK fuzzy model for predicting condensate viscosity.	106
Figure 4.19. Cross plot of estimated against condensate viscosity measurements of existing literature correlation, ANN, LSSVM and TSK Fuzzy method.	109
Figure 4.20. Residual plot of relative error percentage for different viscosity models as a function of reservoir pressure.	111
Figure 4.21. Residual plot of relative error percentage for different viscosity models as a function of reservoir temperature.	112
Figure 4.22. Experimental prediction capability of the developed TSK fuzzy model as a function pressure (A), solution gas to oil ratio (B) and temperature (C).	113
Figure 4.23. The relation between pressure and solution gas to oil ratio (R_s) for the utilized databank.	114
Figure 4.24. General architecture of a Fuzzy Logic System (FLS).	115
Figure 4.25. The constructed gaussian membership function representing (A) pressure (B) temperature (C) solution gas to oil ratio and (D) condensate viscosity.	117
Figure 4.26. The constructed triangular membership function representing (a) pressure (b) temperature (c) solution gas to oil ratio and (d) condensate viscosity.	118

Figure 4.27. The constructed trapezoid membership functions (A) pressure (B) temperature (C) solution gas to oil ratio and (D) the condensate viscosity.....	119
Figure 4.28. Architecture of the fuzzy inference (FIS) system for predicting condensate viscosity using Gaussian membership function.....	122
Figure 4.29. Performance prediction of Gaussian based MFs Mamdani fuzzy model in predicting condensate viscosity.....	124
Figure 4.30. Performance prediction of triangular based MFs Mamdani fuzzy model in predicting condensate viscosity.....	124
Figure 4.31. Performance prediction of trapezoidal based MFs Mamdani fuzzy model in predicting condensate viscosity.....	125
Figure 4.32. Performance of utilized literature correlations and Mamdani fuzzy model with gaussian MFs for predicting condensate viscosity as a function of pressure; sample from Coats, (1986).....	126
Figure 4.33. Performance of literature correlations along with gaussian fuzzy approach in predicting condensate viscosity as a function of solution gas to oil ratio R_s ; sample from Coats, (1986).	127
Figure. 4.34. Computational efficiency of the developed AI models (00:00:00 stands for Hour: Minute: Second).	128
Figure 5.1. Scatter plot of five literature models in prediction of two-phase compressibility factor of gas condensate reservoirs below the saturation pressure.	143
Figure 5.2. Graph of relative error utilizing literature models for prediction of two-phase Z factor.	144
Figure 5.3. Residual plot of relative error percentage of utilized literature correlations in predicting gas-condensate two-phase Z factor as a function of pseudo reduced pressure (P_{pr}).	147
Figure 5.4. Residual plot of relative error percentage of literature models in predicting two-phase Z factor of gas-condensate systems as a function of pseudo reduced temperature (T_{pr}).	148
Figure 5.5. Architecture of the cascade forward (CFNN) neural network used in this study.....	149
Figure 5.6. Cascade forward neural network with three hidden layer constructed in Matlab for prediction of two-phase Z factor.	150

Figure 5.7. Feed Forward Artificial Neural Network structure used for prediction of Z factor.	153
Figure 5.8. Comparison of constructed feed-forward neural network (FFNN) performance with different number of neurons in hidden layer.....	157
Figure 5.9. Proposed FFNN for prediction gas condensate two-phase compressibility factor.	157
Figure 5.10. Schematic illustration of type – 3 fuzzy reasoning (a); ANFIS structure type – 3 (b).....	159
Figure 5.11. Proposed ANFIS architecture for prediction of gas condensate two-phase Z factor.	162
Figure 5.12. Structure of proposed ANFIS model for prediction of two-phase Z factor of gas condensate reservoirs.	171
Figure 5.13. Architecture of Takagi – Sugeno fuzzy model for prediction of gas condensate two-phase Z factor.	171
Figure 5.14. Cross plot and relative error of utilized three machine learning models in predicting two-phase Z factor at training, validation and testing stage.	175
Figure 5.15. Residual plot of relative error percentage of intelligent models in predicting two-phase Z factor as a function of pseudo reduced pressure (P_{pr}).	175
Figure 5.16. Residual plot of relative error percentage of intelligent models in predicting two-phase Z factor as a function of pseudo reduced temperature (T_{pr}).	176
Figure 5.17. Error comparison of all utilized literature models and the developed ML based approached in prediction of gas-condensate two-phase Z factor.	176
Figure 5.18. Error comparison of all utilized literature models and the developed ML based approaches in prediction of two-phase Z factor.....	177
Figure 5.19. Testing different methods in predicting experimental Z factor as a function of Ppr for sour gas-condensate sample.....	184
Figure 5.20. Prediction of Z factor as a function of P_{pr} for sweet gas condensate sample.....	185
Figure 5.21. Relevancy factor (r) for each input variables.	185
Figure 6.1. Horner plot for pressure build up test (Earlougher, 1977).	195
Figure 6.2. construction of PVT table for KAL – 5 gas-condensate well.....	200
Figure 6.3. Horner plot for KAL – 5 gas-condensate well.....	203
Figure 6.4. Plot of gas flow rate vs total ΔmP_{gt} for KAL – 5.....	207
Figure 6.5. Schematic illustration of 3D created model in Eclipse 300.....	211

Figure 6.6. Condensate saturation curve a result of the CVD experiment of the reservoir fluid.....	211
Figure 6.7. Phase diagram of the reservoir fluid in standard pressure and temperature.	212
Figure 6.8. Variation of gas and oil (condensate) viscosity with pressure in KAL – 5.	213
Figure 6.9. Gas phase effective permeability.	215
Figure 6.10. Relative permeability ratio (gas to oil) as a function of pressure for high temperature (354°F) gas condensate well.....	215
Figure 6.11. Gas production profile for KAL – 5 using analytical method incorporated with various ML techniques in generating PVT properties.....	216
Figure 6.12. Gas production profile for KAL – 5 using analytical method incorporated with various ML techniques in generating PVT properties.....	216
Figure 6.13. Statistical error results between analytical pseudopressure approach and compositional simulation results for perdition of gas phase production profile in KAL – 5.....	218
Figure 6.14. Statistical error results between analytical pseudopressure approach and compositional simulation results for perdition of oil phase production profile in KAL – 5.....	218

NOMENCLATURE

Symbols	
A	Cross sectional area of fluid flow, m ²
API	American Petroleum Institute, degree
ANN	Artificial Neural Network
ANFIS	Adaptive Neuro Fuzzy Inference System
b	Bias unit of SVM function
B	Turbulent flow parameter
B _{gd}	Dry gas formation volume factor , ft ³ /scf
B _g	Gas formation volume factor, ft ³ /scf
BHFP	Bottom-hole flowing pressure, psia
B _o	Oil formation volume factor, bbl/STB
BO	Black oil
Bob*	Correlating parameter of oil formation volume factor
c	Number of clusters
c _t	Total compressibility of fluid
CVD	Constant Volume Depletion
D	Non-Darcy flow multiplier in gas rate equation
dp/dt	Pressure rate of change in time, psia
dp/dx	Pressure gradient in x direction
dp/dr	Pressure gradient in radial flow
EOS	Equation of state
FL	Fuzzy Logic
f _x	Regression function of SVM
g	Sigmoid function of ANN network
HPHT	high pressure high temperature
J	Cost function in ANN and SVM
K	absolute permeability, millidarcy
K _{rg}	gas phase relative permeability, millidarcy (md)
K _{ro}	oil phase relative permeability, millidarcy (md)
K _g /K _o	Gas to oil permeability ratio
LSSVM	Lease Square Support Vector
M _g	Gas molecular weight, lbm/lbm mol
M _o	Oil molecular weight, lbm/lbm mol
ML	Machine Learning
MBO	Modified black oil
M _i	Molecular weight of each component
m _p	Pseudopressure function, MMpsi ² /cp
M _{C7+}	Molecular weight of hydrocarbon plus fractions
M _o	Surface oil (condensate liquid) molecular weight
n	Deliverability exponent in well deliverability equation; Mole of gas in ideal gas law, lb-mol
N _c	Dimensionless capillary number
P _{dew}	Dew-point pressure, psia
P _{wf}	Bottom-hole flowing pressure, psia
P _r	Average reservoir pressure, psia

P_{sc}	Pressure at standard condition, psia
P_{sep}	Separator pressure, psia
P_{pc}	Pressure pseudocritical properties
PVT	Pressure – Volume – Temperature
P^*	Pressure at interface between region 1 and region 2, psia
q_g	Surface gas flow rate, scf/day
q_o	Surface oil flow rate, STB/day
r_e	External drainage radius, ft
r_s	Solution oil to gas ratio (OGR)
r_w	Wellbore radius, ft
r_p	Total producing gas to oil ratio for calculating well stream gravity, scf/STB
R	Universal gas constant
R_{pi}	Producing gas to oil ratio, scf/STB
R_s	Solution gas to oil ratio, scf/STB
S	Skin factor
S_{or}	Critical oil saturation,
SVM	Support Vector Machine
SS	Overall cluster variable
S_{wi}	Irreducible water saturation
S_g	Gas saturation
S_o	Oil saturation
S_{total}	Total skin factor
T_{sc}	Temperature at standard condition, Kelvin
T_{sep}	Separator temperature, Rankine R
T_{pc}	Temperature pseudocritical properties
T_r	Reduced temperature
V_{pc}	Volume pseudocritical properties, ft ³ /lbm mol
W^T	Transposed matrix of SVM
Z	Z factor, compressibility factor, deviation factor
Greek letters	
μ_g	Gas viscosity, centipoise (cp)
μ_o	Oil (condensate liquid) viscosity, cp
μ_{od}	Dead oil viscosity, cp
μ_{ob}	Live oil viscosity, cp
μ_c	Condensate liquid viscosity, cp
$\mu_A(x)$	Ambiguous membership of component x in universe μ
γ_g	Specific gravity of gas
γ_o	Specific gravity of oil
γ_w	Well stream gravity
$\bar{\gamma}_w$	Average well stream gravity
$\bar{\gamma}_o$	Average surface oil gravity
γ_{API}	API gravity
ρ_g	Density of gas phase, lbm/ft ³
ρ_o	Density of oil (condensate liquid) phase, lbm/ft ³

μ	Viscosity of mixture, cp
ζ	Viscosity reducing parameter, cp ⁻¹
μ^*	Law pressure gas mixture viscosity, cp
ρ_r	Reduced density, lbm/ft ³
γ	Tuning parameter of SVM
$\varphi(x)$	Kernel function in SVM
ξ_k	Slack variable of SVM
Δp_{gt}	Total gas pseudopressure function, psi/cp

CHAPTER 1

INTRODUCTION

1.1 Background

Increasing energy demand worldwide and quest for cheaper and cleaner source of energy place natural gas and gas-condensate reservoirs in a unique position in today's energy market. The global move to use natural gas is an evolution in energy market that is changing economic and the environment for the better (Tillerson, 2015). Figure (1.1) shows the continuous increase of demand for natural gas in United State since 1980. Figure (1.2) highlights the explored hydrocarbon reserves in Russia, which include substantial amount of gas-condensate fields. This also demonstrate the strong share market of gas-condensate reservoirs in the world. Gas-condensate reservoirs are playing an important role in respond to the huge global energy market. It has been reported that gas-condensate reservoirs accounts for 68% of all giant gas reservoirs (reservoirs larger than $10^{12}m^3$) worldwide (Zhang *et al.*, 2019). Examples of some of the giant's gas-condensate fields around the globe are Arun field in Indonesia, Shtokmanovskoye field in Russia, North field in Qatar (South Pars field in Iran) and Cupiagua field in Colombia.

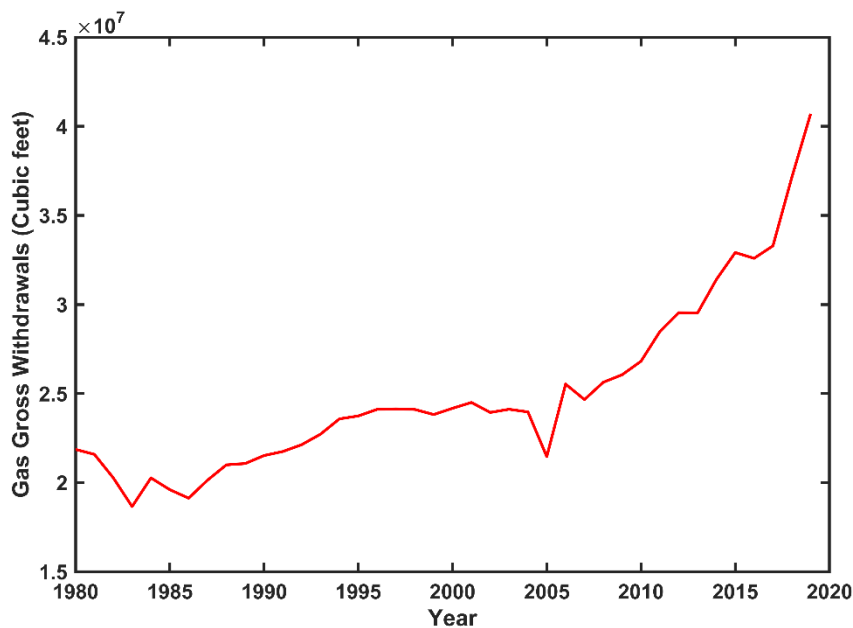


Figure 1.1. USA Natural Gas withdrawals (EIA, 2020).



Figure 1.2. Breakdown of Gazprom Group's explored hydrocarbon reserves in Russian regions (Gazprom, 2019).

Another example of a giant gas-condensate reserve is Khuff gas-condensate reservoir known as north field in Qatar and south pars field in Iran. Khuff is the world biggest gas-condensate reservoir in the world, holds between 1000 – 2000 trillion cubic feet initial gas in place and 30 to 70 billion barrels of condensate in place. However, these important source of energy are suffering from productivity decline and losing its most valuable hydrocarbon source in the depth of the reservoir. This is due to the reduction of bottom-hole flowing pressure (P_{wf}) to below the saturation (dew point) pressure, which trigger condensate (liquid) drop out from the gas phase. This liquid drop out has a significant impact on gas relative permeability and lead to production decline. For example well productivity in the Arun field, in North Sumatra, Indonesia, declined significantly 10 years after the production began and it creates serious problem as the reservoir could not produce the required gas to meet contractual obligation (Fan *et al.*, 2005). In Arun field, which its operator is ExxonMobile, the production loss in some wells were greater than 50% (Afidick, Kaczorowski and Bette, 1994; Ayyalasomayajula, Silpngarmmlers and Kamath, 2005). Another example is Britannia gas-condensate field where the productivity declined between 50 – 60% in the first year of production even before stabilization of the fluid flow occurs (Göktaş, Macmillan and Thrasher, 2010). Shell and Petroleum development Oman reported 60% loss of productivity of the wells in one of the fields (Smits, Van der Post and Al Shaidi, 2001).

This reduction in deliverability and losing production was due to the accumulation of the liquid phase (condensate) near the wellbore region. To understand the well deliverability reduction in gas-condensate reservoirs the phenomenon will be explained in the following section.

1.2 Gas-condensate characteristics

Gas-condensate reservoirs are a class of hydrocarbon reservoirs that characterized by production of surface gas and varying quantities of stock-tank-oil (STO). The STO usually known as “condensate” or “distillate”. In this study the “condensate” phrase is used for stock tank oil. Classification of the hydrocarbon reservoirs are important for modelling and also selecting appropriate engineering practices. As illustrated in Table 1.1 hydrocarbon reservoirs are classified in terms of composition and other fluid properties to dry gas, wet gas, gas-condensate, near-critical oil, volatile oil and black oil. The composition and reservoir condition (temperature and pressure) would determine the category the reservoir fluid. For a given composition, a reservoir fluid can be classified to different category with different pressure and temperature. Gas-condensate fluids typically exhibit condensate (oil) to gas ratio (OGR's) ranging from 5 to 350 barrel of liquid per million standard cubic feet (STB/MMscf). The API gravity of gas-condensate fluid, which is measure of weight or density, is between 40° to 60° API (Whitson and Brulé, 2000). Most well known gas-condensate reservoirs are found in the range of 5000 to 10000 feet deep, at pressure of 3000 to 8000 psia and temperature of 200°F to 400°F (Moses, 1986; Moses and Donohoe, 1987). These wide range of pressure, temperature and compositions of gas-condensate reservoirs lead to wider definitions in literature. However, one of the widely accepted definition is in terms of temperature as if the reservoir temperature located between critical temperature ($T_c = 127^\circ F$) and cricondentherm temperature ($T_{ct} = 250^\circ F$) the reservoir classified as gas-condensate reservoirs (Whitson and Brulé, 2000; Thomas, Bennion and Andersen, 2009; Ahmed, 2010). To further settle wide definition of gas-condensate reservoirs two main characteristics that distinguish all gas-condensate reservoirs from other type of hydrocarbon systems are introduced by Raghavan and Jones, (1996) as follow:

- The condensation of the gas at reservoir conditions during isothermal depletion.
- The retrograde and revaporization of the condensate liquid by further decline in pressure (Raghavan and Jones, 1996).

The above characteristics of gas-condensate reservoirs can be related to fluid behaviour below the saturation pressure. The fluid behaviour is divided into two sections of phase behaviour and drawdown behaviour. The fluid behaviour is major contributor to productivity decline in gas-condensate reservoirs below the dew point pressure. The fluid behaviour is explained in the following section and in wider context it will be related to the productivity decline.

Table 1.1. Compositions and properties of several reservoir fluids (Whitson and Brulé, 2000).

Compositions (mol%)						
Component	Dry Gas	Wet Gas	Gas- Condensate	Critical Oil	Volatile Oil	Black Oil
CO ₂	0.10	1.41	2.37	1.30	0.93	0.02
N ₂	2.07	0.25	0.31	0.56	0.21	0.34
C ₁	86.12	92.46	73.19	69.44	58.77	34.62
C ₂	5.91	3.18	7.80	7.88	7.57	4.11
C ₃	3.58	1.01	3.55	4.26	4.09	1.01
i-C ₄	1.72	0.28	0.71	0.89	0.91	0.76
n-C ₄	-----	0.24	1.45	2.14	2.09	0.49
i-C ₅	0.50	0.13	0.64	0.90	0.77	0.43
n-C ₅	-----	0.08	0.68	1.13	1.15	0.21
C ₆	-----	0.14	1.09	1.46	1.75	1.61
C ₇₊	-----	0.82	8.21	10.04	21.76	56.40
Properties						
MC ₇₊	-----	130	184	219	228	274
γ_{C7+}	-----	0.763	0.816	0.839	0.858	0.920
K_{wC7+}	-----	12	11.95	11.98	11.83	11.47
GOR, scf/STB	∞	105000	5450	3650	1490	300
OGR, STB/MMscf	0	10	180	275	-----	-----
API gravity	-----	57	49	45	38	24
γ_g	-----	0.61	0.70	0.71	0.70	0.63
P_{sat} , psia	-----	3430	5650	7015	5420	5810
B_{sat} , ft ³ /scf	-----	0.0051	0.0039	2.78	1.73	1.16
ρ_{sat} , lbm/ft ³	-----	9.61	26.7	30.7	38.2	51.4

1.3 Gas-condensate flow behaviour

1.3.1 Phase behaviour

Gas-condensate reservoir behaviour is a function of two parameters of phase envelope of the fluid and condition of the reservoir (Roussennac, 2001). A typical phase envelope (P-T diagram) of gas-condensate fluid shown in Figure 1.3. These phase envelop diagram consists of bubble point line (where first bubbles of gas vaporizes from the liquid content) and dew point line (where first droplet of liquid condenses from the gas phase). The bubblepoint line and dew point line meet at the mixture critical point. The critical point is representing a state where all intensive properties of gas and liquid phases are equal (Ahmed, 2010; Craft and Hawkin, 2015). The cricondentherm and cricondenbar are maximum temperature and pressure respectively that above them the mixture is only in the form of gas or liquid (only one phase).

As the reservoir produces, the formation temperature normally doesnot change (isothermal behaviour) but the average reservoir pressure and flowing bottom hole pressure varies. In gas-condensate reservoirs the fluid is initially in single phase (point B on the graph Figure. 1.3), which consists of predominantly methane “C₁” and other short chain hydrocarbons, called heavy ends. Isothermal pressure depletion to below the dew point line cause heavy end hydrocarbons drop out of the solution and form the liquid inside the reservoir (Between point B₁ and B₂). The liquid phase known as condensate liquid has zero mobility ratio to the associated gas between B₁ and B₂. At this point only gas flows where the heavy end hydrocarbons left behind in the reservoir. This phenomenon causes a compositional changes of the reservoir mixture.

Further reservoir pressure decline lead to further accumulation of the liquid to the maximum level at point B₂ (known as critical oil saturation). At this point condensate liquid have enough energy to overcome the gravity segregation in porous media and move towards the wellbore simultaneously with gas phase. The dashed lines on the phase diagram represents the percentage of the vaopur phase (gas phase) in the mixture. Some gas-condensate phase diagrams shown the amount of liquid percentage inside the two phase region. However in Figure 1.3 the amount of gas phase shown in two-phase region.

Additional reduction of reservoir pressure, move down point B₂ towards point B₃. Between point B₂ and point B₃ the accumulated condensate liquid vaporizes and turn

back to gases state. At point B₃ most of the condensate liquid revaporizes and the reservoir fluid is only in the form of gas (100% vapour). This thermodynamically anomalous phenomenon first noticed by Kuenen, (1892) and he called it “retrograde condensation”.

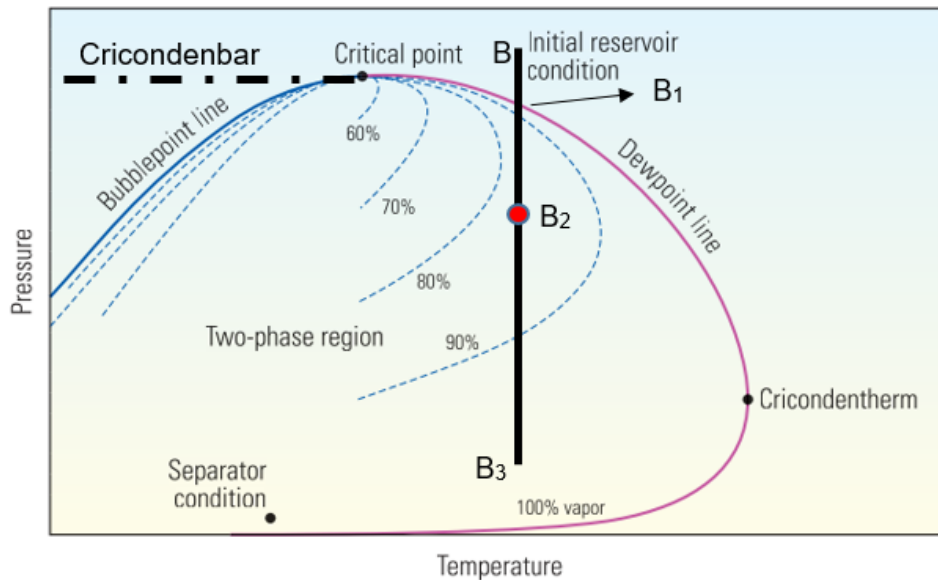


Figure 1.3. Typical phase diagram of gas condensate systems (Modified from Fan *et al.*, 2005).

Condensate drop out significantly alter the permeability of the reservoir formation to the gas flow and fundamentally change the drawdown behaviour of the reservoir near the wellbore region. The amount of liquid phase not only depends on compositions of the mixture shown in Table 1.1, also to the other reservoir behaviour and production strategy (depletion model of recovery). This amount of generated condensate normally determines if the reservoir is lean or rich gas-condensate. If the reservoir generates small amount of liquid normally less than 100 barrels per million square cubic feet the gas-condensate known as lean whereas if the amount of liquid between 150 to 300 barrels per million square cubic feet its known as rich gas-condensate reservoir.

1.3.2 Drawdown behaviour

If depletion drive system is selected as mode of recovery for any hydrocarbon reservoirs, the energy for producing hydrocarbon on the surface comes from the difference between formation pressure gradient (reservoir pressure) and bottomhole flowing pressure (P_{wf}) of the wells. The P_{wf} is the pressure at the formation of the wellbore of the producing well (Ahmed, 2010, p. 354). In gas-condensate reservoirs with depletion mode of recovery when reservoir pressure declined due to the

production, P_{wf} of the wells need to be changed to compensate reservoir pressure decline, and keep the pressure gradient to meet predetermined rate on the surface. The relation between a well constrained P_{wf} and the rate of the production known as well deliverability (Fevang, 1995).

When the P_{wf} keeps decreasing to reach the point known as dew point pressure (the point where first drop of liquid evolve from gas), physics of the flow inside the reservoir is changing and three flow regions are established. These three main flow regions proposed by Fevang, (1995) extending from wellbore outward and illustrated in Figure 1.4. These regions are gradually changing during lifetime of a gas-condensate reservoir. The P_{wf} controls the production of hydrocarbon fluids on the surface. If P_{wf} is above the dew point pressure, the fluid in the reservoir is single phase and region 3 exist. If P_{wf} goes down to below the dew point pressure, region 2 starts to grow and two-phases of gas and condensate (oil) are exist as shown in Figure 1.4. In region 2 only gas flows toward the wellbore and condensate (oil) phase is immobile. The saturation of condensate phase is increasing with time and reaches critical condensate saturation (S_{or}). When the maximum S_{or} is reached the transition is starting from region 2 to region 1, where both phases are flowing toward the wellbore.

Region 1 is the main source of deliverability loss in gas-condensate wells because of higher pressure drop in this region caused by condensate accumulation. Condensate accumulation in region 1, would decrease gas phase permeability to flow sharply.

The amount of condensate saturation in region 1 is a function of fluid properties that entering this region and the production rate (Fevang, 1995; Roussennac, 2001).

These properties consist of viscosity of the original mixture, formation volume factor and solution oil to gas ratio. Condensate drop out further apart the behaviour of the gas-condensate reservoir mixture from ideal gas law. This deviation is determined by compressibility factor (Z factor). Among the fluid properties condensate (oil) viscosity in each depletion stage has the highest uncertainty for the purpose of the modelling in such reservoirs. Accurate Z factor prediction also plays a key role for reliable modelling of gas-condensate well deliverability (Fevang, 1995; Fevang and Whitson, 1996; Mott, 2002; Whitson and Kuntadi, 2005)

The main objective of this research is to develop several models for accurate prediction of the gas/condensate (oil) viscosity as well as Z factor. The developed models will be used for reliable prediction of gas-condensate well production forecast.

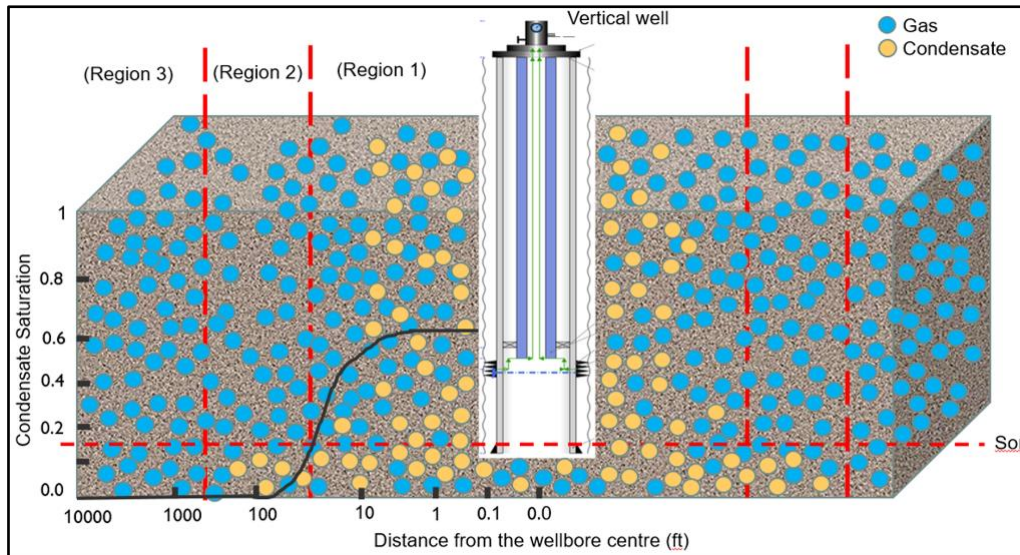


Figure 1.4. Gas/condensate flow in three regions.

1.4 Problem Statement

A reliable model that accurately simulate phase and drawdown behaviour and their effect on gas-condensate well performance is highly desirable for financial projection and field production planning. The focus of this research is in developing well deliverability (productivity) model and condensate blockage effect with an emphasis on accurate prediction of phase behaviour. Although extensive research have been conducted in general well deliverability modelling of gas-condensate reservoirs, there is still outstanding issues and shortfall in this area. We highlights some of these difficulties in following.

Developing accurate and reliable gas-condensate system well deliverability model, governed by accurate fluid phase behaviour, which require well define pressure – volume – temperature (PVT) model. A PVT model describes key phase, viscosity and volumetric behaviour of hydrocarbon mixture that are dictating the recovery of gas and oil at the surface (Whitson et al., 1999). For gas-condensate mixture, a PVT model for all reservoir pressure and temperature conditions cannot accurately define certain properties (e.g., viscosity, compressibility factor, hydrocarbon plus characterization). For example a PVT model such as equation of state (EOS) often have difficulty of matching compositional variation of gas and condensate dropout in near critical gas-condensate systems. Among the PVT properties condensate viscosities are difficult to predict and has the largest prediction uncertainty using any PVT models (Fevang,

1995; Whitson, Fevang and Yang, 1999; Mott, 2002). This is mainly due to inadequacy of the available methods in prediction of condensate viscosity and unavailability of experimental condensate viscosity data to tune the existing models (Fevang, 1995; Whitson, Fevang and Yang, 1999; Mott, 2002; Al-Meshari *et al.*, 2007; Yang *et al.*, 2007).

Unavailability of experimental data is due to the absence of reservoir sample to carry out laboratory experiments for gas-condensate systems. This is because obtaining representative sample of gas-condensate reservoirs are extremely difficult than other type of hydrocarbon systems (e.g., black oil). The difficulty of sampling is due to condensation of liquid during sampling process, which leads to incorrect estimation of gas/condensate percentage and erroneous estimation of reservoir composition (Ahmed, 2010, p. 171).

Compressibility factor (Z factor) is another PVT property that its accurate estimation is always needed to develop an accurate PVT model, and consequently for a reliable gas-condensate well deliverability model (Whitson, Fevang and Yang, 1999). Accurate estimation of Z factor cannot be overemphasized in gas reserve evaluation, material balance calculation, reservoir simulation studies, analytical models, well testing and gas/condensate processing calculations (Rayes *et al.*, 1992; Heidaryan, Moghadasi and Rahimi, 2010; Sun *et al.*, 2012).

Ideally, condensate viscosity and Z factor should be estimated using laboratory experiments, however lack of enough experimental data for the reasons mentioned earlier, motivated to use correlations and EOS extensively in current literature. Using correlations and EOS for estimation of these PVT properties has several problems that will be explained in the following.

There are many EOSs in literature for determination of PVT properties (e.g., Peng and Robinson, 1976; Redlich and Kwong, 1949; Soave- Redlich-Kwong, 1972; Van der Waals, 1873). However, all EOSs are implicit in nature; this means for instance Z factor is estimated as a root of EOSs. This makes using EOSs for estimation of gas-condensate Z factor computationally inconvenient for engineering purposes. Furthermore their performance deteriorate for estimation of gas-condensate mixture because of convergence problem they face for near critical point when the phase change occurs (Sarkar, Danesh and Todd, 1991; Elsharkawy, 2006; Shokir, 2008; Sun *et al.*, 2012).

For estimation of condensate viscosity, the industry heavily rely on correlations, which their prediction accuracy is very limited especially for near critical gas-condensate fluids and all thermodynamic conditions. A few issues of using correlations for prediction of condensate viscosity are as follow.

- Existing condensate viscosity correlations in current literature were developed with simple assumption of single-phase dry gas and their applicability for estimation of gas-condensate viscosity below the dew point pressure, where the two-phase flow exist is arguable.
- Most of available correlations in literature have limited applicability to specific range (e.g., pressure, temperature and viscosity).
- For high pressure high temperature (HPHT) conditions, which majority of gas-condensate reservoirs are located, using correlations for estimation of viscosity is uncertain due to lack of measured data (Al-Meshari *et al.*, 2007; Sun *et al.*, 2012).

Based on the above shortfalls in literature in relation to sufficient models that can well define phase behaviour of gas-condensate fluid below the saturation pressure, the aim and objectives of this study are defined and presented in following section.

1.5 Research aim and objectives

The ultimate aim of this study is to develop an accurate gas-condensate well deliverability (productivity) model with an emphasis on accurate determination of phase behaviour.

Based on the gaps in current literature highlighted in section 1.4 for accurate modelling of PVT properties the following objectives are defined.

- I. Investigate the accuracy and applicability of current existing literature models for estimation of gas/condensate viscosity and Z factor in lean/rich gas-condensate reservoirs.
- II. Development of reliable and accurate gas/condensate viscosity, that can cope with non-linearity of gas-condensate mixture below the saturation pressure.
- III. Developing several models to accurately estimate Z factor of gas-condensate reservoirs below the saturation pressure.

- IV. Investigate the effect of dynamic of condensate build up near well bore region on well inflow performance and production profile through utilizing the developed viscosity and Z factor models.

1.6 Proposed approach

The following methodologies and approaches were adopted to achieve aim and objectives of the study.

- I. An extensive gas-condensate laboratory experimental and field data were collected to investigate the accuracy of existing gas/condensate PVT models for prediction of gas/condensate viscosity and two-phase Z factor.
- II. Non-linear regression has performed to optimize several literature models in order to characterize phase behaviour of gas-condensate mixture through accurate estimation of viscosity and two-phase Z factor.
- III. Sophisticated algorithms of Machine Learning (ML) including Support Vector Machine (SVM), Artificial Neural Network (ANN), Fuzzy Logic (TSK and Mamdani) and Adaptive Neuro Fuzzy Inference System (ANFIS) were employed to develop several gas/condensate viscosity and two-phase Z factor models.
- IV. The optimized and the developed gas/condensate viscosity and two-phase Z factor models in this study employed for better characterization of gas-condensate mixture phase behaviour below the saturation pressure and in establishing an accurate PVT model.
- V. A well-defined PVT model in this study is used for generating reliable production profile of gas-condensate reservoirs experiencing liquid drop out, through utilizing three regions pseudopressure approach for well inflow calculation and volumetric material balance for well production forecast.

1.7 Organization of the thesis

The thesis comprises of seven chapters as follow:

Chapter 1 provides the background information and highlights the challenges of gas-condensate performance modelling. It also covers aims, objectives and proposed approaches in this study.

Chapter 2 covers the literature and relevant theory of fluid flow in porous media in relation to gas-condensate well deliverability modelling. Various factors that are influencing the modelling were also discussed.

Chapter 3 outlines methodologies and current modelling approaches of gas-condensate wells undergoing depletion. The approaches and methodologies undertaken in this study have been discussed in this chapter.

Chapter 4 investigates the applicability of existing literature models (correlations and equation of state based models) for prediction of gas-condensate viscosity below the saturation pressure. Several existing condensate viscosity models in literature have been optimized using experimental data and presented in this chapter. Machine learning techniques including regression, Artificial Neural Network (ANN), Least Square Support Vector Machine (LSSVM) and Fuzzy Logic [Takagi-Sugeno-Kang (TSK) and Mamdani] were extensively used in developing new models. The new models can be used for reliable prediction of gas/condensate viscosity of gas-condensate reservoirs below the saturation pressure as an alternative approach to EOSs.

Chapter 5 assesses the accuracy of the existing literature models for prediction of gas-condensate two-phase Z factor below the saturation pressure using comprehensive data bank. Then several new two-phase Z factor models based on Cascade Forward Neural Network (CFNN), Feed Forward Neural Network (FFNN) and Adaptive Neuro Fuzzy Inference System (ANFIS) were developed. Development of new models including structure of each network are described in details.

Chapter 6 presents well deliverability forecast of gas-condensate reservoirs in tight formation using back pressure equation and three regions pseudopressure integral for computation of well inflow performance. Pressure Transient Analysis (PTA) test of a gas-condensate well is used for computation of effective permeability of gas/condensate phases. Three regions pseudopressure integral was incorporated with the developed gas/condensate viscosity as well as the developed two-phase Z factor model. The detail description of volumetric material balance used for reservoir depletion is provided. A new production forecast for a gas-condensate field case study

is generated utilizing three regions pseudopressure integral incorporated with material balance method. Furthermore, the detail of compositional reservoir simulation using Eclipse 300 is given in this chapter.

Chapter 7 presents the conclusion and recommendations of the research and provides future research avenue.

The flow chart in Figure 1.5 illustrates the organization of the thesis and the tasks that have been carried out throughout each chapters.

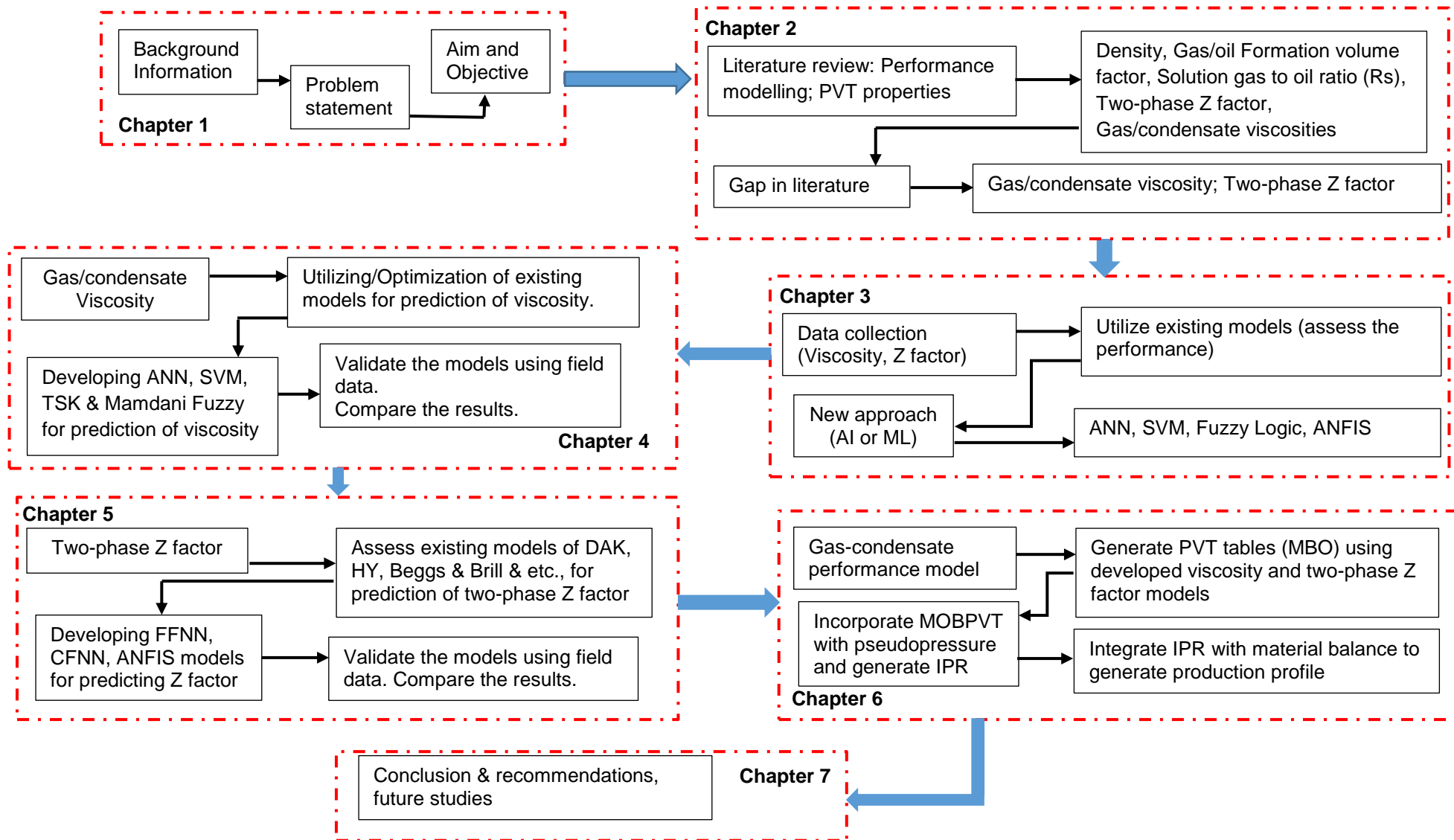


Figure 1.5. The flow chart indicates organization of the thesis for each chapter.

CHAPTER 2

WELL DELIVERABILITY MODELLING OF GAS CONDENSATE RESERVOIRS

2.1 Introduction

This chapter provides a critical review towards the modelling of gas-condensate reservoirs below the dew point pressure. Various modelling approaches have been critically reviewed and evaluated. The influence of condensate drop out when the reservoir pressure depleted to below the dew point pressure on modelling approaches are also discussed.

Modelling and calculation of well deliverability in gas-condensate reservoirs is a historical issue without simple solution (Fevang and Whitson 1996). Reliable calculation of well deliverability requires great understanding of phase and drawdown behaviour in reservoir condition. Gravity segregation of the heavy hydrocarbon components in gas-condensate reservoirs, trigger liquidation of these heavy ends below the saturation pressure. Increasing the saturation of the hydrocarbon liquid in the reservoir will create condensate blockage near the wellbore region. Consequently, the productivity of the wells in gas-condensate field will dramatically reduce due to the condensate blockage (Thornton, 1946; Kniazeff and Naville, 1965; Daltaban, 1985; Vo, Jones and Raghavan, 1989; Raghavan and Jones, 1996). In gas-condensate reservoirs, the initial phase is gas but typically, the fluid of interest is condensate (oil) because of higher profitability that produced condensate can bring to the project. The condensate loss is one of the greatest economical concerns because of its valuable heavier components of the original reservoir fluid, which trapped in the depth of the reservoir (Roussennac, 2001).

This chapter provides fundamental of fluid flow inside porous media in relation to the gas-condensate flow behaviour and well deliverability modelling. First gas flow theory and fundamentals are discussed then the parameters that required for well deliverability modelling and phase behaviour are highlighted. Critical review of each parameter is provided in respective chapter.

2.2 Gas Rate Theory

The fluid flow equations for describing fluid behaviour in hydrocarbon reservoir are in many forms depending on combination of variables such as type of flow, type of fluid and number of mobile phases in the reservoirs (Ahmed, 2010). By combining the fluid transport equation (Darcy's law) with continuity equation for material balance, the appropriate fluid flow equation can be developed for hydrocarbon reservoirs. Fundamental principle of fluid flow in porous media defined by Darcy's law proposed by Henry Darcy (1856). Darcy equation in the form of 2.1 states that the apparent velocity (v) of a homogeneous fluid in a porous media with absolute permeability of k is directly proportional to the pressure difference (d_p) and inversely proportional to fluid viscosity (μ) in a radial flow (d_r). The negative sign represents the inverse direction of pressure gradient with respect to direction of flow.

$$v = \frac{q}{A} = -\frac{k}{\mu} \frac{\partial p}{\partial r} \quad 2.1$$

Integrating Darcy's law yields gas flow rate (q_g) equation in a pseudosteady state for any well geometry (e.g. vertically fractured, radial and horizontal wells) as shown in 2.2. Gas flow rate in equation 2.2 is written in terms of gas formation volume factor (B_g) or equivalent gas compressibility factor (Z).

$$\left\{ \begin{array}{l} q_g = C \times \int_{P_{wf}}^{P_R} \frac{1}{\mu_g B_g} dp \\ \text{or} \\ q_g = C^* \times \int_{P_{wf}}^{P_R} \frac{P}{\mu_g Z} dp \end{array} \right\} \quad 2.2$$

C includes basic reservoir properties and for vertical/horizontal unfractured wells, is defined as follow:

$$\left\{ \begin{array}{l} C = \frac{2\pi a k h}{\ln\left(\frac{r_e}{r_w}\right) - 0.75 + s + Dq_g} \\ C^* = C \frac{T_{sc}}{P_{sc} T_R} \end{array} \right\} \quad 2.3$$

Where a represents conversion factor of $1/(2\pi \cdot 141.2)$ for field units, and $a = 1$ for SI units, s is skin factor, k is absolute permeability of the formation, h is reservoir thickness, r_e is drainage radius, r_w is wellbore radius, T_{sc} and P_{sc} are temperature and

pressure at standard condition (sc) and T_R is temperature at reservoir condition. The unique relationship between pressures and gas properties in pressure integral of equation 2.2 proposed by Al-Hussainy et al., (1966) and commonly known as pseudopressure integral.

Gas rate equation in 2.2 is valid within laminar flow region where Reynolds number is less than 2000. However, in a radial flow system the flow velocity increases significantly near the wellbore region and flow becomes turbulent. Therefore, gas rate equation shown in 2.2 no longer follows a linear relationship between velocity and pressure drop of Darcy's law in higher gas velocity. Subsequently the gas rate changes to Forchheimer, (1901) quadratic form as follow.

$$Aq_g + Bq_g^2 = \int_{P_{wf}}^{P_R} \frac{P}{\mu_g Z} dp \quad 2.4$$

Where A and B are,

$$A = \frac{\ln\left(\frac{r_e}{r_w}\right) - 0.75 + s}{2\pi akh} \quad 2.5$$

$$B = \frac{D}{2\pi akh} \quad 2.6$$

D is non-Darcy or turbulent flow factor and can be calculated by the following equation.

$$D = \frac{3.161 \times 10^{-12} \left[\frac{\beta T \gamma_g}{\mu_g h^2 r_w} \right] kh}{1422T} \quad 2.7$$

Where the turbulent parameter $\beta = 1.88(10^{-10})K^{-1.47}\phi^{-0.53}$, T is temperature in Rankine, γ_g is gas specific gravity and ϕ is the porosity of the reservoir formation. The turbulent flow is contributing to additional pressure drop around the wellbore region. This is particularly important in gas-condensate reservoirs because accumulation of the liquid around the wellbore in region 1 introduces additional skin damage, which in return add extra pressure drop into the system.

Plotting the function inside the integral " $P/(\mu_g Z)$ or $1/(\mu_g Bg)$ " against the reservoir pressure yields a graph shown in Figure. 2.1 with three distinct regions. Substituting

2.5 and 2.6 in Forchheimer gas rate equation 2.4 resulted a pseudo-psteady state equation for estimating gas flow in porous media in three forms representing three areas of the graph in 2.1. The low-pressure region known as region 1, where pressure is usually less than 2000psia and pressure function $P/(\mu_g Z)$ or $1/(\mu_g Bg)$ exhibit a linear relationship with pressure. The following equation can be used for exact calculation of gas flow rate when $P < 2000$ psia.

$$q_g = \frac{kh(P_R^2 - P_{wf}^2)}{1422T(\mu_g Z)_{average} \left[\ln\left(\frac{r_e}{r_w}\right) - 0.75 + s + Dq_g \right]} \quad 2.8$$

The above method known as pressure squared approximation method. The product of $(\mu_g Z)$ in 2.8 is assumed to be constant for pressures below 2000psia.

In second region the relationship between $P/(\mu_g Z)$ or $1/(\mu_g Bg)$ and pressure is a curvature shape. In this region, both bottom-hole flowing pressure (P_{wf}) and average reservoir pressure (P_R) are between 2000 – 3000psia. To estimate gas flow rate when pressure is between aforementioned values, the following equation known as pressure approximation method is used.

$$q_g = \frac{7.08 \times (10^{-6})kh(P_R - P_{wf})}{(\mu_g \beta_g)_{average} T \left[\ln\left(\frac{r_e}{r_w}\right) - 0.75 + s + Dq_g \right]} \quad 2.9$$

The third region is devoted to high pressure region with pressures (P_{wf} and P_R) between 3000 – 5000psia. In this pressure region the relationship between pressure and $P/(\mu_g Z)$ or $1/(\mu_g Bg)$ become almost constant as this can be observed from the graph. The gas flow rate in this region can be estimated by real gas potential or pseudopressure form in pressure region between $3000 < P < 5000$ psia.

$$q_g = \frac{kh(m_{pr} - m_{p_{wf}})}{1422T \left[\ln\left(\frac{r_e}{r_w}\right) - 0.75 + s + Dq_g \right]} \quad 2.10$$

Where m_p is pseudopressure integral shown in Forchheimer gas rate equation of 2.4.

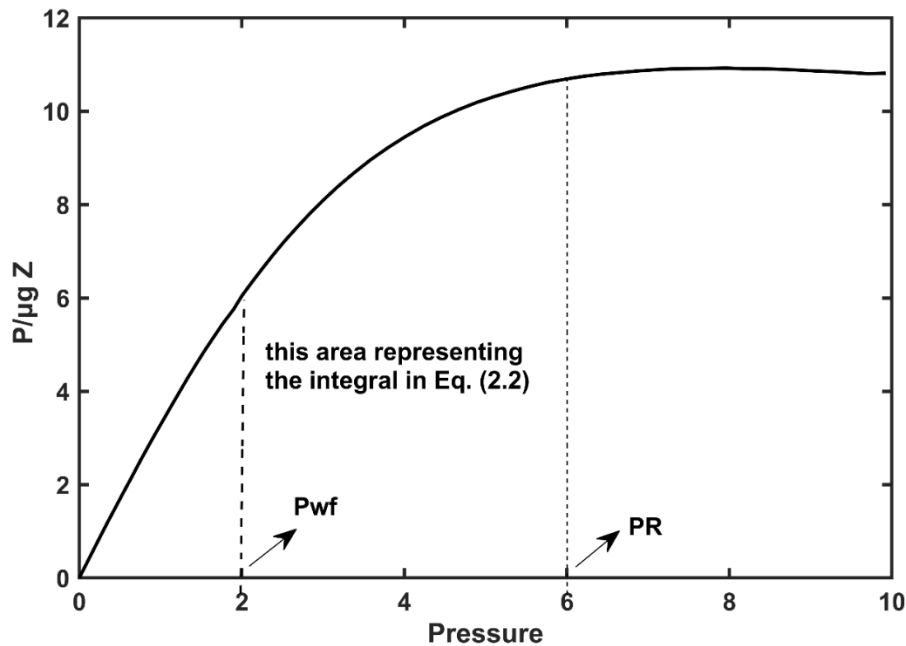


Figure 2.1. Typical plot of gas pressure function vs pressure where the area between P_{wf} and P_R representing the integral in 2.2.

The derived gas flow rate equations in either forms of 2.8 to 2.10 are implicit, where direct determination of q_g is not possible. Furthermore for determination of gas flow rate in high pressure region because the product of $P/(\mu_g Z)$ is almost constant, the pressure integral has simple analytical solution, which is not suitable for rate-time forecasting of a gas well above 3000psia.

Rawlins and Schellhardt, (1936) proposed a simple back pressure equation which relate gas flow rate to bottom-hole flowing pressure (P_{wf}) regardless of value of P_{wf} . The Rawlins and Schellhardt, (1936) is known as well deliverability equation and is discussed in following section.

2.3 Well Deliverability Theory

Rawlins and Schellhardt, (1936) developed an empirical equation known as backpressure equation, that defines relationship between the gas flow rate and some constraint average reservoir pressure (P_R) and bottom hole flowing pressure (P_{wf}). Their empirical equation shown in 2.11 is widely accepted in petroleum industry for estimating gas flow rate (Eilerts, Sumner and Potts, 1965; Gondouin, Iffly and Husson, 1967; Fevang, 1995; Akhimiona and Wiggins, 2005; Al-Attar and Al-Zuhair, 2009; Ogunrewo, 2014). The equation also referred as backpressure equation or well deliverability equation.

$$q_g = C(P_R^2 - P_{wf}^2)^n \quad 2.11$$

Where q_g , P_R , P_{wf} and C are defined in 2.4 to 2.6 and n is deliverability exponent.

Well deliverability equation in 2.12 was developed, as a result of testing several hundred gas rates of gas wells in different fields. The square terms in backpressure equation accounts for pressure dependent of the pseudopressure integral. The exponent n represents degree of flow velocity in non-Darcy flow and is depending on flowing conditions. This exponent is between 0.5 – 1, where 1 representing completely laminar flow and 0.5 for fully turbulent flow. Pressure squared terms ($P_R^2 - P_{wf}^2$) can be replaced by ΔP^2 .

The well deliverability equation is valid for calculating gas flow rate for reservoir pressure of less than 2500 psia. If the average reservoir pressure (P_R) is greater than 2500 psia, then ΔP^2 should be replaced by ΔP . If the coefficients of n and C are known, the gas flow rate at the surface for any bottom-hole flowing pressure (P_{wf}) can be estimated from well deliverability equation. Plotting q_g vs. P_{wf} results in constructing Inflow Performance Relationship (IPR) curves. IPR curve is demonstrating ability of the reservoir to produce gas/condensate to the wellbore (Sousa, Garcia and Waltrich, 2017).

In gas-condensate reservoirs undergoing depletion, accumulation of condensate drop out near wellbore region creates condensate blockage, which introduce extra pressure drop. This would results in well productivity reduction at the surface. Condensate blockage and its effect on well deliverability should be considered for reliable and accurate prediction of gas-condensate well performance. Introducing condensate blockage into well deliverability equation in 2.11 has been an active area of research for many years. Some of the attempts by many scholars will be reviewed here.

Muskat, (1949) was first that addressed condensate blockage in gas-condensate reservoirs operating below the dew point pressure. He introduced a simple method for estimating the radius of the condensate blockage as a function of time, gas rate, reservoir rock and fluid properties. Fetkovich, (1973) used Muskat's results and highlighted condensate blockage problem by introducing a skin factor as a function of gas rate and time for use in standard dry gas equation of 2.4. Eilerts, (1964) was

among the first that numerically solved partial differential equation for transient flow in gas-condensate reservoir. Then Kniazeff and Naville, (1965) continued numerical solution of Eilerts, (1964) for a radial gas-condensate's well deliverability. Both studies confirmed reduction in well deliverability as a results of condensation blockage.

Gondouin et al., (1967) extended the work of Kniazeff and Naville, (1965) by performing black oil simulations, showing the effect of condensate blockage and non-Darcy flow on well deliverability. They used deliverability equation to measure gas flow rate. The work of Gondouin et al., (1967) is a significant contribution in understanding of gas-condensate reservoirs and well deliverability improvement. They showed change of formation permeability in near wellbore region and also reservoir fluid characteristic due to the condensate blockage.

In all above studies, the concept of single-phase pseudopressure approach shown in equation 2.8 was utilized. However, gas-condensate reservoirs experiencing two-phase flow near wellbore region and gas rate equation representing two phases are more adequate. Therefore, the concept of two-phase pseudopressure approach later introduced for gas-condensate well deliverability modelling, which will be explained in following.

Pseudopressure (m_p) is an integral over pressure presented in 2.8, which expresses gas rate through reservoir to the wellbore. O'Dell and Miller, (1967) presented the first gas rate equation using pseudopressure function (m_p) to describe the effect of condensate blockage. Their results were indicated a significant reduction in well deliverability for even small condensate blockage. Their equation is valid when the radius of the blockage around the wellbore is small, which means the P_{wf} is considerably above the dew point pressure. The pseudopressure integral used by O'Dell and Miller, (1967) is based on two regions consisting gas and condensate phase. They were among the first that discovered the existing of the various regions during fluid flow in gas condensate reservoirs. Fussell, (1973) proposed an Equation of State (EOS), for prediction of gas-condensate well productivity using compositional simulator. The simulator tracks the compositional changes below the dew point pressure. Fussell, (1973) showed that O'Dell and Miller, (1967) theory cannot predict the saturation profile in two-phase region correctly. He showed that the productivity of gas-condensate well is much higher than the results showed by O'Dell and Miller,

(1967). Then Jones and Raghavan, (1988) showed that pressure responses from gas-condensate drawdown test can be correlated with classical liquid solution, if pressures were transformed into two-phase pseudopressure. They also showed that steady-state two-phase pseudopressure integral can be used for estimation of reservoir flow capacity (kh) in equation 2.7. Similar results were developed for pressure build up test in gas-condensate wells by Jones et al., (1989). Using steady-state pseudopressure Raghavan et al., (1995) studied several gas-condensate field and concluded that their method is working best when the reservoir pressure is much higher than the saturation pressure. Aforementioned scholars utilized the concept of steady state (SS) pseudopressure method in interpreting and developing the results. The SS model assume fluid flow in the reservoir with two regions without the transition zone. These two regions are near wellbore region, where oil and gas are present and both are mobile toward the wellbore, and an outer region containing only gas phase where the oil saturation is zero. Fevang, (1995) added another region known as transition zone where both gas and oil present, but oil (condensate) is not moving towards the wellbore. In his well deliverability study Fevang, (1995) divided the pseudopressure integral into three parts representing three flow regions. Xu and Lee, (1999) showed that using three regions pseudopressure integral of Fevang, (1995) is more accurate than previous steady-state concept for estimation of flow capacity (kh). Fevang, (1995) pseudopressure integral required prior knowledge of relative permeability curves as a function of saturation, correct fluid properties and accurate knowledge of producing gas to oil ratio (R_p). One of the difficulties of Fevang's pseudopressure integral is its dependency on using simulator for accurate estimation of producing gas to oil ratio (R_p).

To tackle this issue Mott, (2002) proposed simpler technique for calculating R_p based on growing of region 1 as a function of time. His method does not need simulator software for estimation of R_p and can be implemented in spreadsheet format. Similar concept was applied by Raghavan and Jones, (1996), where the size of two-phase region for gas-condensate reservoir calculated for deliverability of the well. Chowdhury et al., (2004) proposed a semi-analytical model similar to Mott, (2002) with the effect of capillary number and non-Darcy flow that was missed in previous analytical approaches. Their method provides accurate results in prediction of lean/rich gas-condensate well deliverability, verified by compositional numerical simulation.

Jokhio and Tiab, (2002) also used Fevang, (1995) method for gas-condensate well pressure transient test and predict well deliverability. They used effective permeability concept in using the pseudopressure integral, which eliminates prior knowledge of relative permeability curves.

The analytical method (e.g., three regions pseudopressure method) are the efficient and quick way to analyse the impact of the various factor such as viscosity, compressibility or rock properties on gas-condensate well deliverability modelling (Dake, 2001; Fan *et al.*, 2005). Many scholars have used three regions pseudopressure approach as a predictive tool and modelled well deliverability of gas-condensate reservoirs (Raghavan and Jones, 1996; Dehane, Tiab and Osisanya, 2000; Guehria, 2000; Jokhio, Tiab and Escobar, 2002; Maravi, 2003; Penula, 2003; Xiao and Al-Muraikhi, 2004; Wheaton and Zhang, 2007; Vo, 2010; Bonyadi, Rahimpour and Esmaeilzadeh, 2012; Al-Shawaf, Aramco and Kelkar, 2014; Arabloo, Heidari Sureshjani and Gerami, 2014; Behmanesh, Hamdi and Clarkson, 2015, 2017; Rahimzadeh *et al.*, 2016; Khanal, Khoshghadam and Lee, 2016; Hekmatzadeh and Gerami, 2018). Hence, also in this study analogy of three-flow regions pseudopressure approach is employed for well deliverability modelling of gas-condensate reservoirs. Fevang, (1995) pseudopressure integral for estimation of total gas flow rate in terms of black oil PVT properties is as follow.

$$q_{g,total} = C \int_{P_{wf}}^{P_R} \frac{k_{rg}}{B_g \mu_g} + \frac{k_{ro}}{B_o \mu_o} R_s dp \quad 2.12$$

Where C is defined in equation 2.3; K_{rg} and K_{ro} are representing gas and oil (condensate) relative permeabilities respectively; B_g and B_o are gas and oil formation volume factor (both are function of compressibility factor); μ_g and μ_o are gas and condensate (oil) viscosity; R_s is solution gas to oil ratio.

If the bottom-hole flowing pressure (P_{wf}) falls below the saturation pressure then the reservoir contains three flow regions as suggested by Fevang, (1995), shown in Figure 1.4. To represent these flow regions the pseudopressure integral in equation 2.12 splits into three parts, representing three flow regions as previously explained in 1.1. Existence of the three flow regions are solely function of pressure and will be discussed in details in the following.

Region 1: is near wellbore region and the main source of well deliverability reduction due to condensate blockage. In this region both gas and oil (condensate) flow simultaneously toward the wellbore at different velocity rate. If bottom-hole flowing pressure (P_{wf}) is less than the dew point pressure ($P_{wf} < P_{dew}$), region 1 will always exist and can be represented by the following integral.

$$q_{g,region\ 1} = C \int_{P_{wf}}^{P^*} \frac{k_{rg}}{B_g \mu_g} + \frac{k_{ro}}{B_o \mu_o} R_s dp \quad 2.13$$

Where P^* is the pressure in the interface between region 1 and region 2.

Condensate build up Region 2: in this region condensate is dropping out of the gas but the mobility ratio is zero or very low, which is not enough for the condensate phase to flow toward the wellbore. The first droplet of the liquid dropped out from the original gas at the outer edge of region 2 (at the boundary with region 3). Hence, the pressure at the boundary of the region 2 with region 3 is equal to the dew point pressure. Since in this region only gas flows the pressure integral with the pressure limits between dew point pressure (P_{dew}) and pressure at the interface between region 1 and region 2 (P^*) is as follow.

$$q_{g,region\ 2} = C \int_{P^*}^{P_{dew}} \frac{k_{rg}}{B_g \mu_g} dp \quad 2.14$$

Roussennac, (2001) in his experimental study observed that region 2 is initially expands from the well outwards as soon as the bottom-hole flowing pressure drops to below the dew point pressure. Then region 2 moved away from the wellbore and region 1 developed next to the wellbore.

Single – phase gas Region 3: this region exist when bottom-hole flowing pressure (P_{wf}) is above the dew point pressure (P_{dew}). If $P_{wf} > P_{dew}$ then the whole reservoir is in single dry gas phase and equation 2.12 turns back to standard gas rate equation, where $K_{ro} = 0$ and K_{rg} is function of irreducible water saturation (S_{wi}) as follow.

$$q_{g,region\ 1} = C \int_{P_{dew}}^{P_R} \frac{k_{rg}(S_{wi})}{B_g \mu_g} dp \quad 2.15$$

It should be noted if the pressure interface between region 1 and 2 (P^*) is bigger than average reservoir pressure (P_R) [$P^* > P_R$], then integration of region 1 pressure function should be only from P_{wf} to P_R . In this case region 2 and 3 don't exist (Fevang, 1995; Fevang and Whitson, 1996). This is the case in highly saturated gas-condensate reservoirs (Fevang, 1995; Fevang and Whitson, 1996; Jokhio and Tiab, 2002).

Adding up all three-flow region pressure integrals yield an equation for estimating total gas flow rate in gas-condensate reservoirs as follow.

$$q_{g,total} = C \left(\int_{P_{wf}}^{P^*} \frac{k_{rg}}{B_g \mu_g} + \frac{k_{ro}}{B_o \mu_o} R_S dp + \int_{P^*}^{P_{dew}} \frac{k_{rg}}{B_g \mu_g} dp + \int_{P_{dew}}^{P_R} \frac{k_{rg}(S_{wi})}{B_g \mu_g} dp \right) \quad 2.16$$

Prior and accurate knowledge of phase and drawdown behaviour is essential for accurate estimation of well deliverability using three-flow regions pseudopressure approach. The knowledge of phase behaviour is essential for reservoir engineer to plan optimum production strategy for gas-condensate field development (Ugwu, 2011).

In concept of well deliverability modelling using equation 2.16, accurate estimation of fluid phase behaviour determines the reliability of the developed model. The phase behaviour of gas-condensate mixture is one of the most complex due to existing of 10 to 15% of heptane and heavier hydrocarbon components in the mixture. Estimating fluid properties of such system to develop phase envelope require advance knowledge of each composition as a function of pressure and temperature. A PVT model (e.g., equation of state or black oil) defines the relation between phase behaviour, compositional variation and fluid properties. To emphasise the importance of accurate PVT model for gas-condensate mixture, Whitson et al., (1999) highlighted that in engineering treatment of gas-condensate reservoirs, the extra issues that must be addressed are:

1. *“how yielding the condensate will change during the life of the reservoir;*
2. *how two-phase gas and oil (condensate) flow near the wellbore, effect the productivity”.*

They suggested both aforementioned issues are strongly related to PVT properties of the fluid. The knowledge of PVT properties and accurate estimation of each parameters is paramount factor for accurate well deliverability modelling of gas-condensate reservoirs.

Although the three-flow regions pseudopressure approach extensively used for deliverability modelling of gas-condensate reservoirs in recent decade, but there is a gap in current literature to show how inaccuracy in estimation of governing parameters including PVT properties and relative permeabilities will affect the performance of the equation. Main objective of this research is to identify the most important parameters that effect well-deliverability modelling of gas-condensate reservoirs with an emphasis to PVT properties. The effect of inaccurate estimation of PVT properties on performance of three regions pseudopressure approach in equation 2.16 will be investigated. Modified black oil (MBO) PVT properties were used in development of three-flow region pseudopressure integral in 2.16. Hence, our analysis is based on MBO approach and its parameters for estimation of three-flow regions pseudopressure method. In following section, first we introduce two main PVT modelling approach then the parameters that are contributing to three-flow regions pseudopressure approach in equation 2.16 is discussed in details.

2.3.1 Modelling Fluid Properties

Currently there are two PVT models including black oil (BO) approach and compositional approach. BO is based on simple interpolation of PVT properties as a function of pressure (Spivak and Dixon, 1973; Coats, 1985; Coats and Smart, 1986; Fevang and Whitson, 1996); and compositional model based on thermodynamically consistent model such as cubic equation of state (Coats et al., 1995; Gomes and Corrêa, 1992; Rubin and Buchanan, 1985).

BO PVT model is a fluid characterization formulation that represents multi-components reservoir hydrocarbons in only two pseudo-components; “surface gas” and stock tank oil (Fevang, Singh and Whitson, 2000; Walsh and Lake, 2003). Black oil model quantifies gas and oil phase from a reservoir condition to standard surface condition (pressure 14.69psia and temperature 60°F). The calculation is based on volumetric estimation (conversion) of gas and oil in the reservoir condition to the surface condition. This conversion also known as geologic condition of hydrocarbon fluid to sellable value at the surface. Schematic diagram in Figure 2.2 shows the traditional BO PVT formulation where the model accounts for surface gas and surface oil through reservoir to the surface.

In order to estimate the volumetric values using BO PVT, the knowledge of how much gas dissolved in oil phase at reservoir condition and how much of that oil would shrink at surface condition is necessary. In addition, the knowledge of expansion of free gas to several hundred times when it brought to the surface is required. To relate this surface volume to reservoir volume and vice versa several factors were defined in BO PVT formulation. Three main properties that serve the computations are wet gas formation volume factor (B_g), oil formation volume factor (B_o) and solution gas to oil ratio (R_s) shown in equation 2.17 to 2.19 respectively (Whitson and Brulé, 2000; Walsh and Lake, 2003).

$$B_g = \frac{\text{volume of reservoir gas}}{\text{volume of surface gas from reservoir gas}} \quad 2.17$$

$$B_o = \frac{\text{volume of reservoir oil}}{\text{volume of sock tank oil from reservoir oil}} \quad 2.18$$

$$R_s = \frac{\text{volume of surface gas dissolved in reservoir oil}}{\text{volume of sock tank oil from reservoir gas}} \quad 2.19$$

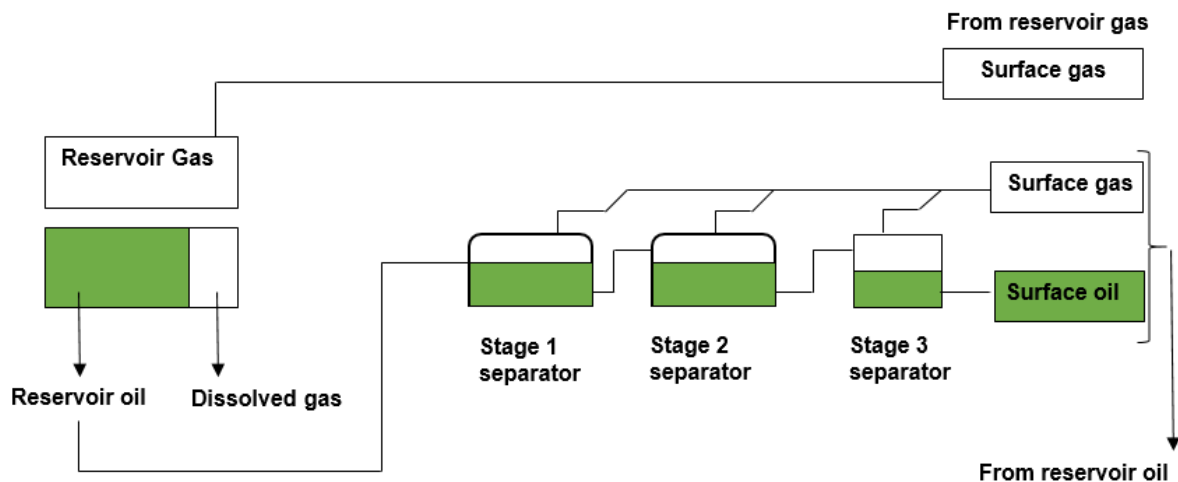


Figure 2.2. Schematic diagram of traditional black oil formulation of PVT model.

These three properties constitute of traditional black oil model and are developed based on the following assumptions.

- A. Reservoir oil consists of only two components of stock-tank oil and surface gas

- B. Reservoir gas does not yields liquid when brought to the surface (see diagram in Figure 2.2)
- C. The property of surface gas released from reservoir oil is the same as properties of reservoir gas
- D. Properties of oil and gas are constant during pressure depletion

For gas-condensate reservoirs the assumptions of A and B are implicit because they ignore the amount of oil (condensate) evolves from gas phase at the surface. Neglecting the amount of produced oil (condensate) cause severe underestimation of condensate recovery prediction at the surface. Therefore, to account for the amount of produced condensate from reservoir gas at the surface another term called solution oil to gas ratio (r_s) was added to the traditional black oil PVT formulation by Kniazeff and Naville, (1965).

Another assumption in BO PVT model is that the compositional variation is constant during pressure depletion. This is not the true for gas-condensate reservoirs as the composition of the mixture is changing with pressure depletion (Evinger and Muskat, 1942; Vo, 2010). Solution gas to oil ratio (r_s) that introduced by Kniazeff and Naville, (1965) also mimics the effect of the compositional variation on condensate properties in BO PVT model (ECLIPSE, 2014). Solution oil to gas ratio (r_s) various with respect to pressure change in the reservoir.

Additional modification of traditional black oil PVT is reformulation of gas formation volume factor to only include dry gas at the surface, which known as dry gas formation volume factor (B_{gd}). Dry gas formation volume factor (B_{gd}) is the ratio between volume of produced gas and volume of its gas components (Whitson, Da Silva and Soreide, 1988; Coats, Thomas and Pierson, 1995; Nassar, El-Banbi and Sayyoub, 2013). Adding two aforementioned terms to black oil PVT model introduced modified black oil model (MBO) PVT model. The schematic diagram of MBO PVT model is shown in Figure 2.3 where four hydrocarbon components can be quantified in terms of volume ratios defined in following.

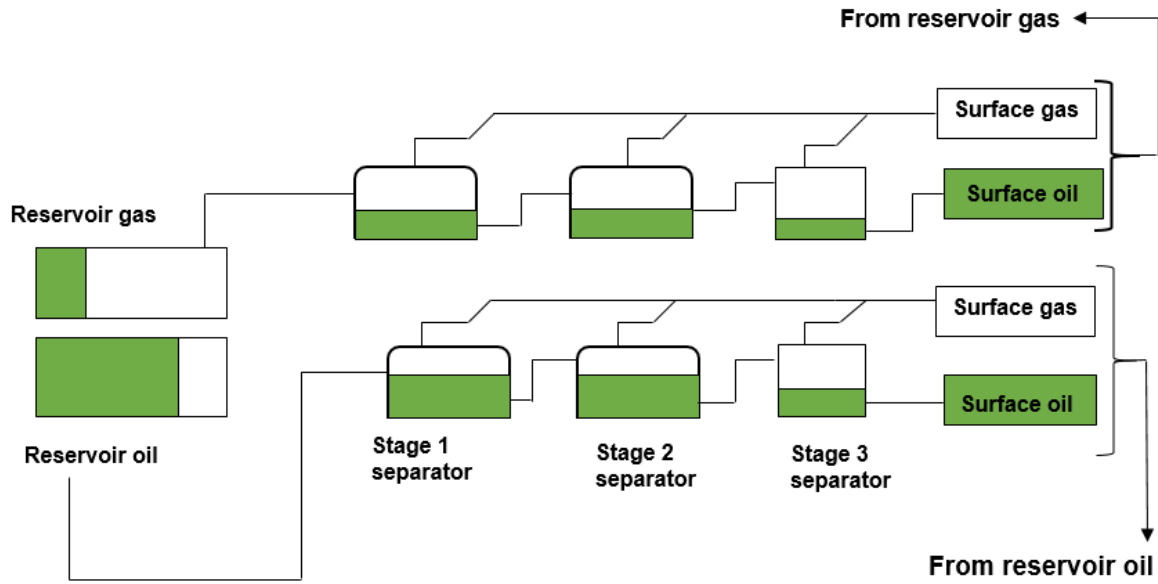


Figure 2.3 schematic diagram of modified black oil (MBO) model.

$$B_{gd} = \frac{\text{volume of reservoir gas}}{\text{volume of surface gas produced from reservoir gas}} = \frac{V_g}{V_{\bar{g}g}} \quad 2.20$$

$$B_o = \frac{\text{volume of reservoir oil}}{\text{volume of sock tank oil produced from reservoir oil}} = \frac{V_o}{V_{\bar{o}o}} \quad 2.21$$

$$R_s = \frac{\text{volume of surface gas produced from reservoir oil}}{\text{volume of sock tank oil produced from reservoir oil}} = \frac{V_{\bar{g}o}}{V_{\bar{o}o}} \quad 2.22$$

$$r_s = \frac{\text{condensate produced from reservoir gas}}{\text{volume of surface gas produced from reservoir gas}} = \frac{V_{\bar{o}g}}{V_{\bar{g}g}} \quad 2.23$$

MBO PVT mode successfully used for simulation of gas-condensate reservoirs PVT characterization below the saturation pressure in previous studies (Whitson and Torp, 1983; Fevang and Whitson, 1996; Fevang, Singh and Whitson, 2000; Jokhio and Tiab, 2002; Mott, 2002; Izgec and Barrufet, 2005; Nassar, El-Banbi and Sayyounh, 2013; Khamis and Fattah, 2019).

Fevang et al., (2000) in their simulation study compared MBO method with full compositional PVT model using 22 components. They showed there is no significant difference between MBO and compositional model in relation to 10 years of production

of a lean gas-condensate fluid. A comprehensive guideline for choosing compositional and black oil models for gas-condensate reservoirs is provided by Fevang et al., (2000). For the case of gas injection using MBO for PVT simulation is not recommended due to extra non-linearity that the injected gas (e.g., CO₂) can added to the mixture properties. Despite some deficiencies of the MBO PVT model, it is very popular in industry due to its simplicity and faster CPU running time in reservoir simulation studies.

Alternative approach for quantifying PVT properties of gas-condensate reservoirs are compositional simulation studies (Coats, Thomas and Pierson, 1995). The development of the compositional models is started due to increasing occurrence of gas-condensate and volatile oil reservoirs (Coats, 1985; Rubin and Buchanan, 1985). In compositional PVT model, the phase equilibrium and fluid properties such as compressibility, density, and viscosity are determined by equation of state (EOS). An equation of state presents a theoretical relationship between pressure, volume and temperature of each individual components at various pressure and temperature condition (Khanal, Khoshghadam and Lee, 2016). The cubic Peng and Robinson, (1976) and Soave- Redlich-Knowng (1972) equations of state are commonly used in the petroleum industry. In this technique, the phase composition is determined by flashing the fluid over wide range of conditions (pressure and temperature). During the computation process, the mass balance equation for each composition is used, where sum of the saturations should be 1 (100%). The number of mass balance equations increases as the number of compositions in the system increase, which require extra computation time. Recently, full compositional simulation become more feasible with advancement in computational techniques, however for large number of cells it is still impractical.

The main advantage of the compositional method over black oil is in determining and understanding relative effects of variable and parameters controlling/governing well deliverability. Despite advantages of the compositional modelling of PVT, it requires more computational effort than black oil model due to its great complexity. This can restrict the model application in reservoir studies where significant compositional variations occur (Gomes and Corrêa, 1992). Using either black oil or compositional model for simulating PVT properties the PVT quantities required by reservoir simulator are essentially the same (Whitson, 2006).

Well deliverability equation of 2.16 for gas-condensate reservoirs is presented in terms of MBO PVT model. In following sections, the detail calculation of each parameter in equation 2.16 is discussed. Some of the parameters like density and Z factor are not appear in equation 2.16, however they are required for generating PVT table.

2.3.2 Compressibility Factor (Z factor)

The properties of gas mixtures are well defined with many graphical charts and numerous equation of state in literature (Beggs and Brill, 1973; Standing, 1981; McCain and Cawley, 1991). The behaviour of the gases at lower pressure originally correlated based on experimental study of gases by Charles and Boyle, which is the basis for ideal gas law. Ideal gas law is a thermodynamic equation shown in 2.24 that allows correlating pressure, volume, temperature (PVT) and number of molecules (moles) that are present in a gas sample.

$$PV = nRT \quad 2.24$$

Where p is pressure in pound square inch absolute (psia), V is occupied volume by gas in cubic feet (ft³), n is mole of gas in pound-mole (lb-mole); T is temperature in Rankine (R) and R is universal gas constant, which in customary unit is $10.73146 \frac{\text{psi} \times \text{ft}^3}{\text{R lbm mole}}$. Using ideal gas equation of state is suitable for gases in very low pressure. However, in higher pressure it leads to about 500% error for establishing the PVT relationship. This is because ideal gas law assume no attraction or impulsive forces between the molecules and all collisions between the molecules are assumed perfectly elastic. Nevertheless, in reality, this is not the case for real gases and intermolecular forces between mixture components strongly affect volumetric behaviour. The deviation from ideal gas behaviour can be expressed as a factor. This factor expressed as compressibility factor, deviation factor or Z factor. Throughout this report, we used Z factor term.

Z factor is a dimensionless quantity and defined as actual volume of real gas to ideal volume at specific pressure and temperature $Z = V(\text{actual})/V(\text{ideal})$. Following is the

real gas law equation, which is standard description of volumetric behaviour of hydrocarbon gas.

$$PV = ZnRT \quad 2.25$$

The real gas equation is valid for engineering calculations of most reservoir gases. From real gas law in equation 2.25, all other volumetric PVT properties of gases can be derived. In following sections, PVT properties that required for estimation of gas and condensate production using three regions pseudopressure approach will be reviewed.

2.3.3 Density of the mixture

Density is defined as a mass per unit volume in a specified pressure and temperature (McCain and Cawley, 1991). In MBO PVT model the density of mixture gases is defined as a function of pressure, well stream gravity, Z factor, universal gas constant, temperature and some numerical constant as follow.

$$\rho_g = 28.97 \frac{P\gamma_w}{ZRT} \quad 2.26$$

Where pressure is in (psia), temperature in (R), density is in (lbm/ft³), γ_w is well stream gravity. In gas-condensate reservoirs, it is important to use well stream gravity in estimating density of the mixture. This is because well stream gravity represents the average molecular weight of the mixture (produced gas and condensate) at the surface condition (standard condition) and can be estimated from following equation proposed by Standing, (1974).

$$\gamma_w = \frac{\bar{\gamma}_g + 4580r_p\bar{\gamma}_o}{1 + 133,000r_s \left(\frac{Y}{M}\right)_o} \quad 2.27$$

Where r_p is total producing oil (condensate) to gas ratio at the surface in STB/scf; $\bar{\gamma}_g$ is average surface gas gravity; $\bar{\gamma}_o$ represents surface condensate gravity; M_o is surface condensate molecular weight. Average surface gas gravity can be calculated from the following equation:

$$\bar{\gamma}_g = \frac{\sum_{i=1}^N R_{pi} \gamma_{gi}}{\sum_{i=1}^N R_{pi}} \quad 2.28$$

Where R_{pi} is producing gas to oil ratio (GOR) at separator stage i in scf/STB and γ_{gi} is gas specific gravity at separator stage (Whitson and Brulé, 2000). The relation between surface specific gravity and condensate molecular weight $\left(\frac{\gamma}{M}\right)_{\bar{o}}$ in equation 2.27, is defined by following equation proposed by Eilerts, (1947), which is valid for all types of gas-condensate fluids (Whitson and Brulé, 2000).

$$\left(\frac{\gamma}{M}\right)_{\bar{o}} = 0.001892 + 0.0000735\gamma_{API} - (4.52 \times 10^{-8})\gamma_{API}^2 \quad 2.29$$

Surface condensate gravity $\bar{\gamma}_{\bar{o}}$ in 2.27 is ratio of density of condensate (oil) to density of water measured at standard conditions. $\bar{\gamma}_{\bar{o}}$ is dimensionless quantity and is calculated accurately by the following relation.

$$\bar{\gamma}_{\bar{o}} = \frac{141.5}{131.5 + \gamma_{API}} \quad 2.30$$

The major issue with engineering calculation of gas-condensate reservoirs are unavailability of all the data. In practice only first-stage separator data including solution gas to oil ratio (R_{s1}), gas specific gravity (γ_{g1}), stock tank oil gravity ($\bar{\gamma}_{\bar{o}}$), pressure (P_{sp1}) and temperature (T_{sp1}) are available (Gold, McCain and Jennings, 1989; Whitson, 2006). However, the total producing oil (condensate) to gas ratio (r_p) is still needed for calculation of well stream gravity using equation 2.27. This is inverse of solution gas to oil ratio (R_{s1}) and additional gas that is released from condensate phase at first-stage separator (R_{s+}).

$$r_p = \frac{1}{R_{s1} + R_{s+}} \quad 2.31$$

Where R_{s+} can be calculated from the following correlation proposed by (Whitson, 1989).

$$R_{s+} = \left[\left(\frac{P_{ps1}}{18.2} + 1.4 \right) \times 10^{(0.0125\gamma_{API} - 0.00091T_{sp1})} \right]^{1.205} \times \gamma_{g+} \quad 2.32$$

Where P_{ps1} is in psia, T_{sp1} is in °F and R_{s+} is in scf/STB. γ_{g+} is a gas gravity of additional solution (gas released from separator oil). γ_{g+} can be estimated from Katz, (1942) correlation as follow.

$$\gamma_{g+} = 0.25 + 0.02\gamma_{API} - (3.57 \times 10^{-6})\gamma_{API} \times R_{s+} \quad 2.33$$

Substituting equation 2.31 in 2.32 yields the R_{s+} in the following form.

$$R_{s+} = \frac{A_1 A_2}{(1 - A_1 A_3)} \quad 2.34$$

Computation of gas phase density from aforementioned procedure normally gives a reasonable estimation if accurate Z factor is provided in gas-condensate fluid. Gas density is used for estimation of gas viscosity in MBO PVT model.

To estimate condensate phase density, condensate formation volume factor is required. Hence, we discuss formation volume factor of gas-condensate mixture in next section.

2.3.4 Formation Volume Factor of Gas-Condensate Mixture

Formation volume factor is a PVT property of black oil model to convert volume of hydrocarbon mixture at elevated pressure and temperature to the volume of product phase at surface pressure and temperature. Surface pressure and temperature in standard condition is defined as pressure of 14.7 psia and temperature of 520 °Rankine or 60°Fahrenheit.

$$B_g = \frac{V_{mixture}(P, T)}{V_{product}(P_{sc}, T_{sc})} \quad 2.35$$

Where P_{sc} and T_{sc} are pressure and temperature at standard condition. For gas-condensate mixture, because reservoir fluid produce liquid (condensate) at the surface as shown in Figure 2.3, two forms of formation volume factor are used for PVT

calculation as discussed before in equations 2.17 and 2.20. These include wet gas formation volume factor (B_g) and dry gas formation volume factor (B_{gd}).

Using real gas law in equation 2.25, mathematically the wet gas formation volume factor in ft^3/scf is defined as follow.

$$B_g = \frac{\frac{ZnRT}{P}}{\frac{Z_{sc}nRT_{sc}}{P_{sc}}} = \frac{P_{sc}ZT}{T_{sc}P} \quad 2.36$$

Where Z factor at standard condition (Z_{sc}) is unity and substituting standard condition of 14.7 psia for P_{sc} and 520°Rankine for T_{sc} , following relationship yields for calculating wet gas formation volume factor.

$$B_g = 0.02827 \frac{ZT}{P} \quad 2.37$$

It should be noted that wet gas formation volume factor (B_g) is fully defined from real gas law as shown in equation 2.37, therefore no correlations are available in literature for computation of B_g .

In MBO PVT model for gas-condensate fluid, to take the phase change during depletion into consideration, dry gas formation volume factor is normally used.

The dry gas formation volume factor (B_{gd}) at standard pressure and temperature (14.7 psia and 520 °R or 60 °F) is defined as follow (Katz, 1942; Standing, 1974; Whitson and Brulé, 2000).

$$B_{gd} = \frac{P_{sc}ZT}{T_{sc}P} (1 + C_{\bar{o}g}r_s) = 0.02827 \frac{ZT}{P} (1 + C_{\bar{o}g}r_s) = B_g(1 + C_{\bar{o}g}r_s) \quad 2.38$$

Where temperature (T) is in °R, pressure (P) is in psia, solution oil to gas ratio (r_s) is in STB/scf and dry gas formation volume factor (B_{gd}) is in ft^3/scf . $C_{\bar{o}g}$ is conversion factor from surface oil volume in Stock Tank Barrel (STB) to equivalent surface gas in Standard Cubic Foot (scf) and estimated as follow.

$$C_{\bar{o}g} = 133000 \frac{\gamma_{\bar{o}g}}{M_{\bar{o}g}} \quad 2.39$$

Where $\frac{\gamma_{og}}{M_{og}}$ can be estimated from equation 2.29. If composition of the mixture is not available condensate phase molecular weight can be estimated from Cragoe, (1929) recommended by Whitson et al., (2000).

$$M_{og} = \frac{6084}{\gamma_{API} - 5.9} \quad 2.40$$

Because formation volume factor is inversely proportional to pressure, reciprocal of wet ($1/B_g$) and dry ($1/B_{gd}$) gas formation volume factors are used in reservoir simulation. The typical graph of ($1/B_g$) and ($1/B_{gd}$) against reservoir pressure is shown in Figure. 2.4 for gas-condensate reservoirs. Accurate estimation of wet and dry gas formation volume factor is directly affected by accurate determination of Z factor at desired pressure and temperature.

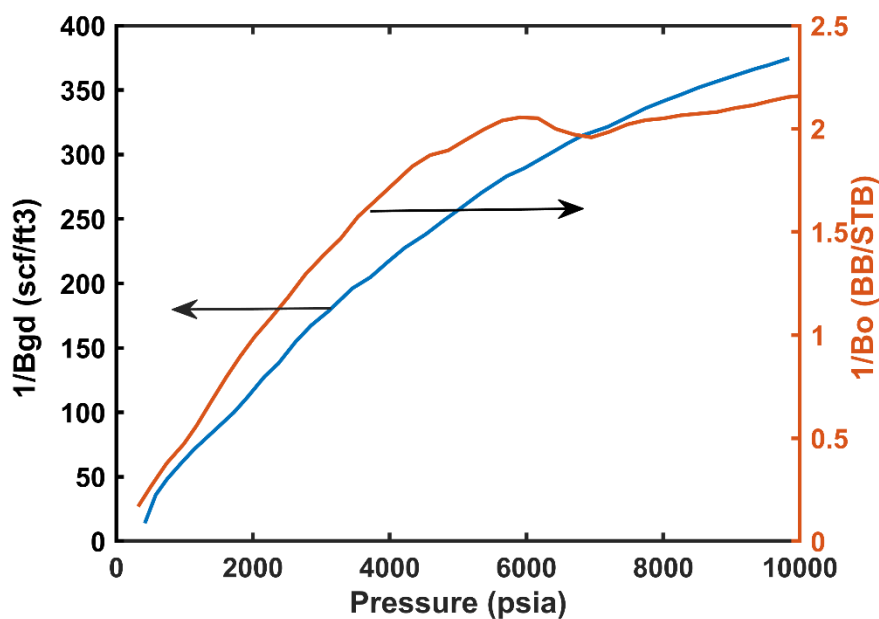


Figure 2.4. Typical gas-condensate formation volume factor as a function of pressure.

Condensate (oil) phase formation volume factor (B_o) is another PVT property that should be considered in computation of black oil PVT model. As shown in equation 2.21 the oil formation factor determines the volumetric ratio of oil (condensate) at reservoir pressure and temperature to standard (surface) pressure and temperature. Condensate (oil) formation volume factor is usually measured using constant volume depletion (CVD) test if the reservoir sample is available. However, in many cases, the samples are not always available and B_o is estimated using correlations. Developing accurate correlation for estimating B_o at various pressure and temperature has

received extensive attention among the researchers. As a result, many correlations are available for estimation of oil formation volume factor. Majority of the methods developed based on experimental data from reservoir samples or measurement of separator oil at the surface as a function of solution gas to oil ratio (R_s), specific gravity of gas (γ_g), oil specific gravity (γ_o) and temperature (T) (Ahmed, 2010, p. 96). To select the appropriate correlation for gas-condensate reservoirs the characteristics of condensate fluid should be considered. The gravity of produced oil (condensate) can be used as a selection criteria. Produced condensate is a very light oil with normally specific gravity between $40 \leq API \leq 60^\circ API$. Six popular methods that are valid within aforementioned API limit and frequently used in industry for estimation of B_o are discussed in following.

Standing, (1947) presented a graphical correlation that correlated oil formation volume factor as function of R_s , γ_o , γ_g , and T that later in 1981 its mathematical form presented as follow by the author (Standing, 1981).

$$B_o = 0.9759 + 0.000120 \left[R_s \left(\frac{\gamma_g}{\gamma_o} \right)^{0.5} + 1.25(T) \right]^{1.2} \quad 2.41$$

Where T is in °F, B_o is in bbl/STB and γ_o is specific gravity of stock tank oil. The above correlation is developed based on 105 experimental data points obtained from 22 Californian hydrocarbon reservoirs. Subsequently many other correlations have been developed based on original Standing method.

Vazquez and Beggs, (1980) developed an oil formation volume factor correlation based on 6000 data collected from world wide oil samples at various pressure. Using regression analysis their correlation is valid for light oils with $\gamma_{API} \geq 30$ and presented as follow.

$$B_o = 1 + 4.670 \times 10^{-4}(R_s) + 0.11 \times 10^{-4}(T - 60) \times \left(\frac{\gamma_{API}}{\gamma_{gc}} \right) - (1.8106 \times 10^{-8})R_s(T - 60) \times \left(\frac{\gamma_{API}}{\gamma_{gc}} \right) \quad 2.42$$

Where γ_{gc} is the corrected gas specific gravity, included for the effect of separator conditions and can be estimated from following correlation proposed by the same authors.

$$\gamma_{gc} = \gamma_g \left[1 + 5.912(10^{-5})\gamma_{API} (T_{Sep} - 460) \log \left(\frac{P_{Sep}}{114.7} \right) \right] \quad 2.43$$

Where T_{sep} is separator temperature in Rankine and P_{sep} stands for separator pressure in psia.

From studying 45 oil PVT data Glaso, (1980) proposed his oil formation volume factor, that can be used for saturated oil (condensate) B_o estimation. Comparative study of B_o correlations by Sutton and Farshad, (1990) indicates Glaso's correlation is accurate for $B_o \geq 1.4$. Glaso's correlation is presented in following form.

$$B_o = 1 + 10^{-6.58511+2.91329 \log B_{ob}^* - 0.27683 \log B_{ob}^{*2}} \quad 2.44$$

Where B_{ob}^* is a correlating parameter that can be estimated as follow.

$$B_{ob}^* = R_s \left(\frac{\gamma_g}{\gamma_o} \right)^{0.526} + 0.968(T - 460) \quad 2.45$$

In above equation T is in °F.

Based on 160 experimental data point of Middle Eastern oil reservoirs Al-Marhoun, (1990) developed his saturated formation oil factor correlation as a function of R_s , γ_o , γ_g and T. He recommended a linear relationship between R_s and B_o as follow.

$$B_o = 0.497069 + (0.8629 \times 10^{-3}T) + (0.18259 \times 10^{-2}F) + (0.31809 \times 10^{-5}F^2) \quad 2.46$$

Where F can be estimated as

$$F = R_s^{0.742390} \gamma_g^{0.323294} \gamma_o^{-1.202040} \quad 2.47$$

Different approach for estimation of oil formation volume factor is recently developed based on material balance relation (Ahmed, 2010, p. 97). The correlation is function

of solution gas to oil ratio (R_s), gas specific gravity (γ_g), oil specific gravity (γ_o) and oil density and presented as follow.

$$B_o = \frac{62.4\gamma_o + 0.0136R_s\gamma_g}{\rho_o} \quad 2.48$$

Where ρ_o is density of oil (condensate) at specified pressure and temperature in lb/ft³. Ahmed (2010) shows that using equation 2.48 for estimation of B_o is the best among aforementioned methods with the least average absolute error. More comprehensive review on validity of oil formation volume factor correlations by Al-Shammasi, (2001) and Aamir Mahmood and Ali Al-Marhoun, (1996) showed that the studied methods return the measured B_o with less than 2% error for large data bank. The accuracy of above B_o correlations are acceptable for PVT modelling of gas-condensate fluid in three-flow region pseudopressure integral of 2.16. Accurate determination of B_o is also important for reliable estimation of condensate density.

Condensate (oil) density is mass of a unit volume at specified pressure and temperature usually estimated from the following relation proposed by Standing, (1981).

$$\rho_o = \frac{62.4\gamma_o + 0.0136R_s\gamma_g}{B_o} \quad 2.49$$

Substituting equation 2.41 for B_o in above correlation yields the following relation that is widely used in industry for estimation of density of oil at or below the bubble-point pressure.

$$\rho_o = \frac{62.4\gamma_o + 0.0136R_s\gamma_g}{0.9759 + 0.000120 \left[R_s \left(\frac{\gamma_g}{\gamma_o} \right)^{0.5} + 1.25(T) \right]^{1.2}} \quad 2.50$$

For gas-condensate mixture, gas specific gravity γ_g should be gravity of gas released from separator oil (condensate). Standing correlation for density of the oil is superior to other methods as it does not require correction term for pressure and temperature (Whitson and Brulé, 2000; Ahmed, 2010). In a recent comparative study by Mmata and Onyekonwu, (2014) it has been shown that using Standing correlation of 2.50 for

estimation oil density return the experimental values with reasonable accuracy of 2.4% average absolute error.

2.3.5 Solution Gas to Oil Ratio (R_s)

Another important PVT property that needs accurate estimation in MBO PVT model is solution gas to oil ratio (R_s). R_s defined as the number of standard cubic feet (scf) of gas that dissolved in one stock tank barrel (STB) of oil at certain pressure and temperature. This ratio also known as gas solubility (Ahmad, 2020). R_s is an important volumetric property of MBO, normally measured using laboratory tests of constant volume depletion (CVD) or constant composition expansion (CCE). Initial value of R_s remains constant until the reservoir pressure drops to below the dew point pressure and increases afterward. The relationship between R_s and reservoir pressure is demonstrated for a North Sea gas-condensate sample in following figure.

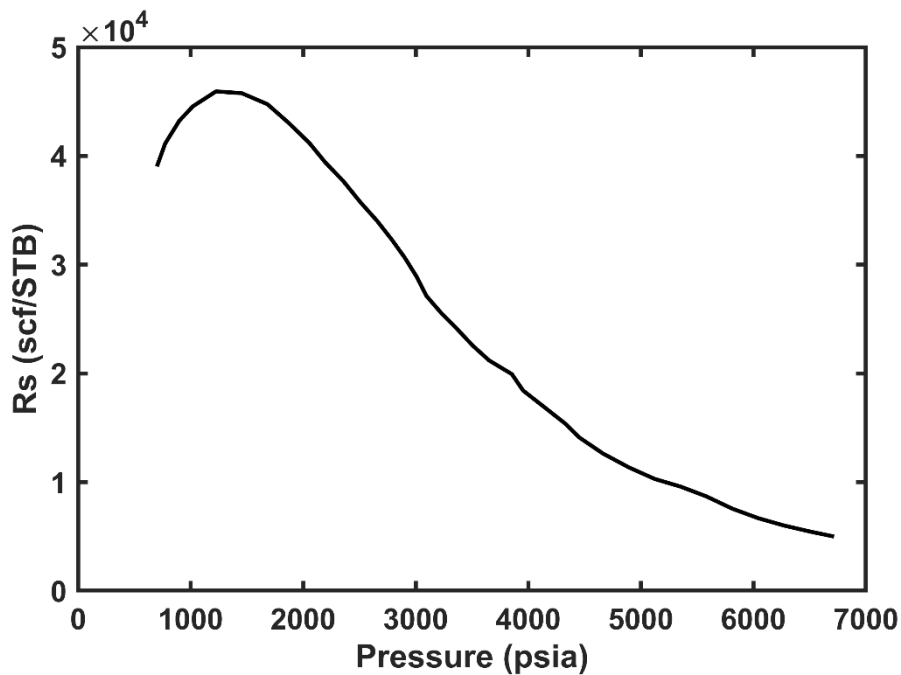


Figure 2.5. Solution gas to oil ratio (R_s) for North Sea gas-condensate sample at $T=280^\circ\text{F}$ (Modified from Whitson and Torp, 1983).

Accurate estimation of R_s is important and directly affect accuracy of other PVT properties such as formation volume factor (B_o), density (ρ_o) and well stream gravity (γ_w). If compositional data of the gas-condensate fluid is available solution gas to oil

ratio can be estimated through material balance method of Whitson and Torp, (1983) or more complicated cubic equation of state (e.g., Peng and Robinsons).

There are also many empirical correlations for estimating R_s when composition of the mixture is not available. Different authors developed their correlations based on the data of certain localities, hence their applications are limited. Many comparative studies are also conducted to see the superiority of these correlations (Ostermann and Owolabi, 1983; McCain and Cawley, 1991; De Ghetto *et al.*, 1994; Sutton, 2007). A few more widely accepted correlations for estimation of R_s is discussed in following.

Standing, (1947) proposed a graphical correlation for solution gas to oil ratio as a function of pressure, temperature, API gravity and specific gravity. Standing used same oil samples discussed previously (105 Californian oil samples) in developing following correlation for estimating R_s . The correlation is valid in the range of 20 – 1425 scf/STB (Danesh, 1998).

$$R_s = \bar{\gamma}_g \left[\left(\frac{P}{18.2} + 1.4 \right) \times 10^{0.0125API - 0.00091(T-460)} \right]^{1.2048} \quad 2.51$$

Where temperature is in Rankine and pressure is in psia. The Standing correlation return the experimental solution gas to oil ratio with 4.8% error.

Following Standing's method Vazquez and Beggs, (1980) developed a correlation for estimating solution gas to oil ratio based on 5008 measured data points. The correlation is valid for oil gravity of larger than 30 API and presented in the following fashion.

$$R_s = 0.178 \gamma_{gc} P^{1.1870} \exp \left[23.931 \left(\frac{\gamma_{API}}{T} \right) \right] \quad 2.52$$

To adjust the gravity to reference separator pressure corrected gas specific gravity should be used. This is because specific gravity of gas depends on the conditions that gas separated from the oil phase. Corrected gas specific gravity (γ_{gc}) in equation 2.43 can be used in Vazquez and Beggs, (1980) solution gas to oil ratio correlation. Sutton and Farshad, (1990) showed that using Vazquez and Beggs, (1980) for estimating R_s , predicts the experimental measurements with 12.7% error within the range of 0 – 2199 scf/STB.

To improve accuracy of previous models Glaso, (1980) proposed another solution gas to oil ratio correlation based on 45 oil samples from North Sea, which is valid for R_s in the range of 90 – 2637 scf/STB. The correlation reported as follow.

$$R_s = \bar{\gamma}_g \left[\left(\frac{\gamma_{API}^{0.989}}{(T - 460)^{0.712}} \right) 10^{2.8869 - [14.1811 - 3.3093 \log(P)]^{0.5}} \right]^{1.2255} \quad 2.53$$

The author stated an average error of 1.28% for estimating solution gas to oil ratio. Other correlations are also available in literature for computation of R_s , however most of them followed Standing, (1947)'s correlation in their development process.

Another well received correlation was proposed by Petrosky and Farshad, (1998) for estimation of R_s . They used 81 oil samples obtained from Gulf of Mexico in developing their correlation. Petrosky and Farshad, (1998) proposed the following expression for R_s .

$$\left\{ \begin{array}{l} R_s = \left[\left(\frac{P}{112.727} + 12.340 \right) \bar{\gamma}_g^{0.8439} 10^X \right]^{1.73184} \\ X = 7.916 \times 10^{-4} \gamma_{API}^{1.5410} - 4.561 \times 10^{-5} T^{1.3911} \end{array} \right\} \quad 2.54$$

The above R_s correlation is valid within the range of $217 \leq R_s \leq 1406 \text{scf/STB}$. The authors reported that their correlation predicts the experimental R_s in specified range with -0.05 average relative error.

Modelling solution gas to oil ratio (R_s) has received extensive attention among the research community in recent decades. Many correlations are available that can be used for accurate estimation of R_s in gas-condensate reservoirs. For instance Petrosky and Farshad, (1998) predicts R_s with absolute error of -0.05. Also De Ghetto *et al.*, (1994) showed that Rollins, McCain and Creeger, (1990) solution gas to oil ratio correlation predicts the experimental R_s with 4.3% error for light oil with API >31°.

2.3.6 Viscosity (Gas/Condensate)

Two types of viscosities are usually applied for engineering calculation of hydrocarbon reservoirs including dynamic viscosity (μ) and kinematic viscosity (ν). Dynamic viscosity is defined as measuring resisting of fluid (gas and liquid) to flow under external forces with the unit of centipoise (cp). However, kinematic viscosity is resistance to flow of a fluid under gravitational affect (weight of fluid due to gravity

effect) with the unit of centistokes (cSt). Two viscosities are related by density of the fluid ($\mu = \nu\rho$).

Most petroleum engineering applications are using dynamic viscosity, which is for Newtonian fluid (fluid that flows regardless of external forces with predictable viscosity when pressure and temperature changes) mathematically defined as follow.

$$\mu = \frac{\tau g_c}{du/dy} \quad 2.55$$

Where τ is shear stress per unit area in a shear plane parallel to the direction of flow, du/dy is velocity gradient perpendicular to plane of shear and g_c is a unit conversion from mass to force.

Developing condensate phase below the saturation pressure in gas–condensate reservoirs necessitate calculation of gas and condensate phase separately. Gas viscosities of hydrocarbon reservoirs are generally within the range of 0.01 – 0.03cp at standard reservoir conditions, increasing to 0.1cp for near critical gas-condensate systems (Lohrenz, Bray and Clark, 1964; Whitson and Brulé, 2000). Measurement of gas viscosities are rare because most of laboratories do not have the facility to conduct the experiments and the prediction is normally through using correlations. Viscosity of gases are usually correlated as a function of pressure, temperature and mixture composition [$\mu_g = f(P, T, y_i)$]. Based on this relationship many empirical and semi-empirical correlations have been developed for estimating of gas viscosity. The fundamental principle of using any gas viscosity correlations are as follow:

- Low pressure gas viscosity (μ_{gsc}) at standard pressure and temperature condition should be estimated
- Corresponding state principle should be used to estimate actual value of viscosity (μ_g)

This would relate the actual gas viscosity (μ_g) at P and T to low pressure viscosity by a ratio of μ_g / μ_{gsc} as a function of pseudoreduced properties (P_{pr}) and (T_{pr}) or as a function of pseudoreduced density (ρ_{pr}). In following a few existing literature correlations that are using this principles reviewed.

Carr et al., (1954) developed a graphical chart for estimation of gas viscosity using the relationship of $\mu_g / \mu_{gsc} = f(T_{pr}, P_{pr})$. Later Dempsey, (1965), presented polynomial

relation of Carr et al., (1954) viscosity method with 15 constants. Dempsey, (1965) is valid in the range of $1.2 \leq Tr \leq 3$ and $1 \leq Pr \leq 20$. In 1962, Jossi et al., (1962) developed an empirical viscosity correlation for estimation of pure component. Then Lohrenz et al., (1964) extended Jossi et al., (1962) correlation for estimation of mixture viscosity. Lohrenz et al., (1964) mixture viscosity correlation usually referred to Lohrenz – Bray – Clark (LBC) method. The LBC become standard compositional reservoir simulator correlation for estimating gas/liquid viscosities. The LBC method is very sensitive to the value of reduced density as the viscosity is estimated based on fourth degree polynomial reduced density.

Lucas, (1981) used μ_g/μ_{gsc} relationship similar to Carr et al., (1954) and developed his gas viscosity correlation that is valid for wider range of $1 \leq Tr \leq 40$ and $0 \leq Pr \leq 100$.

Using corresponding state principle Pedersen and Fredenslund, (1987) developed a viscosity model where the methane was reference fluid based on work of Christensen and Fredenslund, (1980). In this method, viscosity of reference fluid (gas, liquid) is estimated based on pressure, temperature, molecular size and density effect. Last two parameters can be estimated empirically from fluid molar mass and reduced density. The Pedersen and Fredenslund, (1987) is one of the fundamental viscosity methods used in reservoir simulators such as Eclipse (Schlumberger) and Landmark's Nexus (Halliburton). Baled et al., (2018) in their review study showed that using Pedersen and Fredenslund, (1987) correlation return the mixture viscosities with 5 – 15% error and 15 – 30% for heavy alkane and binary mixtures.

Later in 1966 the authors Lee – Gonzalez – Eakin (LGE) (Lee, Gonzalez and Eakin, 1966) proposed simpler semi-empirical viscosity correlation irrespective the knowledge of pseudo critical properties (T_{pr} and P_{pr}). The correlation is based on density, molecular weight for estimation of gas viscosity. The correlation developed as a function of pressure, gas density, temperature and molecular weight. Since its publication, LGE become very popular due to its simplicity for estimating gas viscosity in compare to corresponding state based methods. The LGE correlation is used by most PVT laboratories for estimating gas viscosity and its application extended for reservoirs simulators. Following LGE correlation, many other correlations have been developed in similar fashion (Elsharkawy, 2006; Londono et al., 2002; Sutton, 2005).

These correlations are computationally simple and effective for quick estimation of gas viscosity. For lower range of gas viscosities (0.01 – 0.03cp) the accuracy of gas viscosity correlations are within 5 – 10% error, which is adequate for most applications (e.g., dry gas, black oil reservoirs). However, in higher range of gas viscosities (0.03 – 0.1cp) the error of 20 – 30% may be expected (McCain and Cawley, 1991; Whitson, 2006). This error would proportionally effect the production forecast and well deliverability estimation for gas-condensate reservoirs.

The difficulty of viscosity estimation even become harder for condensate phase. The developed condensate inside the reservoir is a form of light oil with API gravity between 40 – 60 (0.74 – 0.82 condensate specific gravity). The viscosity of condensate fluid almost never measured or very rare because of several reasons highlighted in flowing. Measurement of condensate viscosities are very difficult to obtain due to unavailability of the samples, lack of high pressure high temperature (HPHT) facilities, small volume cell viscometers and time and cost required for the measurements (Whitson, Fevang and Yang, 1999; Al-Meshari *et al.*, 2007; Hemmati-Sarapardeh *et al.*, 2014).

Therefore using correlations for estimation of condensate viscosity is become a norm in industry. Nevertheless, using correlations for estimation of condensate viscosity are exceedingly inaccurate. The best performance of the prevalent existing correlations are within 10 – 30% error, and often increase to 50% (Whitson, 2006; Yang *et al.*, 2007).

Unacceptable accuracy of condensate viscosity may cause a serious problem in developing a reliable well deliverability model, especially when condensate blockage has significant impact on well deliverability (e.g., rich gas-condensate fluid in tight formation) (Fevang, Singh and Whitson, 2000; Whitson, 2006). Previous studies show 1% error in reservoir fluid viscosity resulted in a 1% error in cumulative production (total production of gas and oil) (Whitson, Fevang and Yang, 1999; Al-Meshari, 2004; Yang *et al.*, 2007).

Sutton, (2005) further investigate using existing literature models for estimation of gas-condensate viscosity below the saturation pressure and highlights the following drawbacks of existing literature models:

- They have a limited range of application.

- Smooth transition near critical point cannot be achieved.
- Accuracy of many viscosity models are function of accurate density estimation, in other word they are density dependant.
- Many correlations are required heavy tuning of their constants to match the experimental data.
- The performance of almost all viscosity correlations are notorious for estimation of condensate phase viscosity.

Among the MBO PVT properties that associated with three regions pseudopressure approach in 2.16 for estimation of well deliverability, viscosities (gas/condensate) has highest prediction error as mentioned in this section. The aforementioned challenges for viscosity (gas/condensate) prediction and gap in current literature motivated this study to further focus on developing new approaches for estimation of this important PVT parameter. The detail description of each viscosity model along with current modelling approaches is discussed in chapter 4.

2.3.7 Drawdown Behaviour on modelling

The drawdown behaviour of gas-condensate reservoirs undergoing depletion discussed in 1.3.2. This behaviour is directly affect permeability of the developed phases as a results of pressure depletion inside the reservoir. Gas rate equation in 2.4 includes absolute permeability (k), which is the capacity and ability of the formation to transmit fluid in a porous medium (Ahmed, 2010). In a single phase system using absolute permeability is enough for well deliverability modelling. However, when several phases (e.g., gas, condensate, water) flow simultaneously in a porous structure like a hydrocarbon reservoirs, the permeability of the formation to each phase should be estimated. Respective permeability of each phase known as relative permeability (K_r). Relative permeability is one of the governing parameters that influence gas and condensate flow rate at the surface using pseudopressure approach in equation 2.16.

The flow in gas-condensate below the dew point is a combination of several phases (at least two phases of gas and condensate), moving towards the wellbore region simultaneously. Relative permeability characterizes how easily each fluid phase flows through a porous medium in a multi-phase system. Fevang and Whitson, (1996)

investigated the effect of condensate banking on well deliverability by introducing relative permeability into pseudopressure integral in equation 2.16.

Laboratory measurements are most common methods in determination of gas-condensate relative permeabilities (Sumnu-Dindoruk and Jones, 1998). The data obtained from measurements are the base of constructing relative permeability curves as a function of phase saturation. Conceptual modelling of gas-condensate systems suggests that relative permeability curves dictate the magnitude of gas productivity loss (Afidick, Kaczorowski and Bette, 1994; Bourbiaux, 1994; Altug, Mo-Yuen Chen and Trussell, 1999; Behmanesh, Hamdi and Clarkson, 2017). The use of inaccurate relative permeability curves may result in over or underestimation of gas-condensate reservoir performance prediction. Although laboratory measurements are standard methods for estimating gas and condensate relative permeabilities using core flood experiment, they involved several challenges as follow:

- The laboratory measurements of relative permeabilities are very expensive.
- The experiment is very difficult to conduct due to complexity of the gas-condensate fluid below the dew point pressure.
- Limitation of core samples makes the obtained data from the experiments limited where the whole saturation range cannot be determined (Sumnu-Dindoruk and Jones, 1998).

Deficiencies of experimental procedure motivate engineers to rely on available existing relative permeability correlations. Many empirical relative permeability methods have been developed in past several decades to predict relative permeability under different conditions. Some of these correlations are Brooks and Corey, (1964), Chierici, (1984); Corey et al., (1956), Stone, (1973, 1970) and Wyllie, (1951).

In gas-condensate reservoirs when multi-phase flow occurs complex surface tension (effect of the forces on the interface), and flow velocity effect near wellbore region, makes relative permeability estimation even more difficult. This would influence the accuracy of the correlational approach in estimating relative permeability.

The aforementioned difficulties of laboratory measurements make relative permeability curves scarce and contradictory. Therefore, other approaches have been proposed in literature for determination of relative permeabilities based on field performance and or well pressure test data. Fetkovich et al., (1986) proposed a

method to determine relative permeabilities for solution gas drive reservoirs using oil and gas flow rate time data. Al-Khalifa et al., (1987) proposed in-situ method to estimate three-phase relative permeabilities using pressure transient analysis. Hatzignatiou and Reynolds, (1996) proposed a procedure to estimate the effective permeability (absolute permeability multiply by relative permeability) curve from drawdown well test pressure data. Serra et al., (1990) introduced a procedure to estimate effective permeability from transient radial drawdown data.

Sumnu-Dindoruk and Jones, (1998) modified Fetkovich et al., (1986) for estimation of gas-condensate relative permeabilities. Their method require gas and condensate production rate, PVT properties, calculated initial gas in place (IGIP) from material balance, average reservoir pressure and critical water saturation. Jokhio, (2002) and Jokhio and Tiab, (2002) developed a scheme to estimate gas and condensate effective permeabilities from well pressure buildup test for gas-condensate reservoirs.

In this study mathematical manipulation of three regions pseudopressure approach developed by Jokhio, (2002) is used for estimation of effective permeability of each phase. The method relies on actual well test data during pressure build up/drawdown. This would eliminate uncertainty of the correlational approach in generating relative permeability curve, which is one of the main factors for inaccurate estimation of three-flow regions pseudopressure approach in 2.16. The method is further discussed in chapter 6 of this study.

2.4 Summary

Gas-condensate wells undergoing depletion are experiencing substantial productivity lose at the surface due to condensate blockage near wellbore region. Condensate blockage is a result of condensate drop out (heavy hydrocarbon drop out from gas phase) below the saturation pressure. Condensate drop out effect phase and drawdown behaviour of such system significantly. A model that accurately predict the phase and drawdown behaviour with the effect of condensate blockage in gas-condensate reservoirs are highly desirable. Such model require accurate estimation of PVT properties and reliable treatment of phase permeabilities. The emphasis of this study is on accurate estimation of gas and condensate PVT properties. Among the PVT properties, accurate estimation of Z factor is the key because almost all other

PVT properties such as gas density, gas and oil formation volume factor (B_g and B_o), well stream gravity are function of Z factor (Whitson and Brulé, 2000). Although there are extensive research on accurate estimation of Z factor for natural gas systems (Chamkalani et al., 2013; Elsharkawy, 2006; Rostami et al., 2018; Standing and Katz, 1942), however investigations for developing accurate Z factor models of gas-condensate systems have not received enough attention.

Viscosity is another PVT property that need accurate prediction, yet it has highest uncertainty as highlighted in 2.3.6 among the PVT properties. This is highlight the fact that current literature approaches for estimation of gas-condensate viscosity are not adequate in various conditions. The fundamental PVT properties of any PVT models are Z factor and viscosity. The two properties of viscosity and Z factor are strongly dependant on pressure and temperature. The performance of almost all existing viscosity models are with very high error between 10 – 50% for gas-condensate reservoirs (Whitson, 2006). Z factor is another crucial PVT property that always should be estimated with high accuracy. Nevertheless previous studies (Elsharkawy, Hashem and Alikhan, 2000; Ghiasi *et al.*, 2014; Saghafi and Arabloo, 2018) showed that using different mixing rules and hydrocarbon plus characterization the accuracy of current existing methods for prediction of Z factor is with deviation of 8 – 56% from actual values.

Hence, throughout the remaining of the thesis, the focus is on accurate modelling of Z factor and viscosity for better PVT representation of gas-condensate fluid below the saturation pressure. The effect of accurate determination of gas and condensate viscosities and Z factor on well production profile is ultimate interest of this study. For this purpose, three regions pseudopressure integral in equation 2.16 incorporated with volumetric material balance to generate the production profile of studied gas-condensate reservoir. The result of this study will be compared with actual field data as well as compositional reservoir simulator.

CHAPTER 3

METHODOLOGY AND CONCEPTUAL FRAMEWORKM

3.1 Introduction

This chapter introduces the methodologies and framework that have been taken to conduct this research study. First, a brief discussion of the existing literature approaches for characterizing PVT models is provided. Then various well deliverability models are discussed, where the advantages and drawbacks of each method are highlighted. The justification behind the selected approach is also provided.

3.2 Pressure – Volume –Temperature (PVT) modelling

Traditionally PVT properties of hydrocarbon mixtures are estimated using black oil (two components) model and compositional (several components) model. The later fluid modelling provides better accuracy for gas-condensate reservoirs, as it has the ability to monitor each component's saturation at all reservoir pressure and temperature stages (Khanal, Khoshghadam and Lee, 2016). However, the computational procedure is more complex and require more time to run in compare to black oil PVT model.

The development of the compositional models are started due to increasing occurrence of gas-condensate and volatile oil reservoirs. The phase equilibrium and fluid properties such as compressibility, density, and viscosity are determined by equation of state (EOS). An equation of state represents a theoretical relationship between pressure, volume and temperature. The cubic Peng and Robinson, (1976) and Soave - Redlich - Knowng (1972) equations of state are commonly used in the petroleum industry.

In this technique, the phase composition is determined by flashing the fluid over wide range of pressures. During the computation process, the mass balance equation for each composition is used, where sum of the saturations should be 1 (100%). The phase behaviour of the fluid has to be consistent with pressure, temperature and composition in each grid cell in reservoir simulations.

The number of mass balance equations increase as the number of compositions in the system increase. This would add extra computation time in simulation studies. Recently, full compositional simulation become more feasible with advancement in computational techniques, however for large number of cells it is still impractical.

Despite advantages of the compositional modelling of PVT properties, it requires more computational effort than black oil model due to its great complexity. The prediction accuracy of equation of state in compositional simulation is deteriorate in near critical regions (e.g., rich gas-condensate fluid and highly volatile oil) (Elsharkawy, 2006). This can restrict the model application in reservoir studies where significant compositional variations occur (Gomes and Corrêa, 1992).

To attempt for modifying black oil PVT model an approach was developed known as modified black oil (MBO), where the knowledge of expansion of gas and shrinkage of oil in the surface due to the amount of dissolved gas is added to the MBO (Izgec and Barrufet, 2005; Nassar, El-Banbi and Sayyouh, 2013). MBO is discussed in details in 2.3.1. Many studies show excellent agreement of MBO with compositional models (EOS) for simulating gas-condensate fluid (Whitson and Torp, 1983; Coats, Thomas and Pierson, 1995; Mott, 2002; Chowdhury *et al.*, 2004; Fan *et al.*, 2005; Behmanesh, Hamdi and Clarkson, 2017). MBO is much simpler than compositional formulation using EOS. Three-flow regions pseudopressure equation in 2.16 proposed by Fevang, (1995) written in terms of MBO PVT model. Therefore, in this study MBO PVT approach also adopted to generate PVT properties of gas-condensate fluid.

3.3 Approaches of Well Deliverability Modelling

Existing of condensate liquid below the saturation pressure in gas-condensate reservoir is making well deliverability modelling of such reservoir a challenging task. This is because a comprehensive model that account for condensate blockage and effect of capillary, viscous and inertial forces is a significant task for reservoir engineers to implement.

Two fundamental approaches to study fluid flow in any hydrocarbon reservoirs are including “classical” and “modern” techniques. Classical approach based on utilizing analytical solutions of linear differential equations while modern methods consist of numerical simulation models. Use of analytical technique can be regarded as more

specialized and difficult to apply, since it requires considerable knowledge to use in particular equation to describe a physical situation in a reservoir (Dake, 2001).

The most common approach of modelling well deliverability of gas-condensate reservoir and predicting well performance is through reservoir simulation studies. The simulation models incorporate the rock and fluid properties to predict the dynamic influence of condensate blockage over gas and condensate production (Fan *et al.*, 2005). The standard compositional industry simulator is Eclipse – 300 that enables better prediction of well deliverability by using small grids near wellbore region, where condensate blockage is exist (Fan et al. 2005). The small grids can be constructed using Local Grid Refinement (LGR). The disadvantage of LGR for modelling near wellbore region is a significant increase in computation time especially for reservoirs with tight formation. One of the major issues of gas-condensate resevoirs undergoing depletion is compositional changes during depletion. Compositional simulation studies enable engineers to detect compositional changes below the saturation pressure using advanced cubic equation of state (EOS).

Although compositional simulation studies are very popular in industry, however there are many applications that these type of analysis is not justifiable (Mott, 2002; Fan *et al.*, 2005; Bonyadi, Rahimpour and Esmaeilzadeh, 2012). This is due to their computational efficiency and considerable data required to start the study. The typical problem with engineering calculation of gas-condensate reservoirs is unavailability of all the data to run the simulation (Whitson, 2006). Therefore, other techniques so called analytical methods (e.g., steady-state pseudopressure or three-flow regions pseudopressure approach) are currently exist in literature that allow such studies with good accuracy comparable to compositional simulation studies (Fevang and Whitson, 1996; Mott, 2002; Chowdhury *et al.*, 2004; Fan *et al.*, 2005). The

For gas-condensate well deliverability modelling, three-flow regions pseudopressure approach, introduced in 2.16, has become a standard choice in recent years. This method can be implemented in spreadsheet and its very useful for quick estimation of well deliverability where many sensitivity runs are required (Fan et al., 2005).

Comparison of fully compositional simulation and local grid refinement with pseudopressure approach of equation 2.16 incorporated with non-Darcy flow show that pseudopressure method captured all near wellbore condensate blockage effect accurately (Mott, 2002; Chowdhury *et al.*, 2004; Fan *et al.*, 2005; Behmanesh, Hamdi

and Clarkson, 2017). The main advantage of pseudopressure approach is easy to implement and there is no increase in computational time (Mott, 2002; Chowdhury *et al.*, 2004; Fan *et al.*, 2005). To successfully implement three-flow regions pseudopressure approach reliable relative permeability curves, accurate estimation of GOR and accurate determination of PVT properties are required (Fevang and Whitson, 1996; Roussennac, 2001). The aim of this study is to investigate the accuracy of three-flow regions pseudopressure approach for gas-condensate performance modelling with an emphasis on accurate estimation of PVT properties including gas/condensate viscosity and Z factor.

3.4 Current Study Approach

One of the major issues in modelling of well deliverability in gas-condensate reservoirs using any discussed approaches is accurate determination of PVT properties. In relation to MBO PVT, used in three-flow regions pseudopressure integral in equation 2.16, the main PVT properties are gas and oil formation volume factor (B_g , B_o) (they are function of two-phase Z factor), gas and condensate viscosities (μ_g , μ_o) and solution gas to oil ratio (R_s). The estimation of MBO PVT properties mainly rely on correlations when the compositional data is not available. The problems and limitation of existing literature correlations for estimating different PVT parameters (B_g , B_o , R_s , μ_g , μ_o) are reviewed in 2.3.

In this research, extensive attempt has been made to eliminate some of the difficulties that PVT systems encounter for modelling gas-condensate fluid properties below the saturation pressure. In doing so for better and more accurate PVT representation of gas-condensate fluid the Artificial Intelligent (AI) or known as machine learning techniques were utilized. This approach was taken due to availability of the data in recent years for gas-condensate reservoirs. The AI methods are data driven techniques, that making prediction based on the real data rather than physics of the problem. There are many successful applications of AI techniques for reservoir modelling in recent years. Some of the examples of the machine learning techniques for different aspect of reservoir modelling in literature can be found in (Ahmadi *et al.*, 2014; Ghiasi *et al.*, 2014; Hemmati-Sarapardeh *et al.*, 2014; Kamari *et al.*, 2013; Naderi and Khomehchi, 2019; Shokir, 2008).

Various algorithms of Artificial Intelligent manipulated for better modelling of gas-condensate PVT properties. The AI methods applied in this study listed as follow.

- Artificial Neural Network (Feed Forward Neural Network, Cascade Forward Neural Network)
- Support Vector Machine (SVM)
- Fuzzy Logic [including Takagi – Sugeno – Kang (TSK) and Mamdani]
- Adaptive Neuro Fuzzy Inference System (ANFIS)

Based on the above AI methods several models have been developed, which offer accuracy, mathematical efficiency and simplicity in compare to existing literature correlations for estimation of viscosity and Z factor of gas-condensate reservoirs.

In order to see the effectiveness of the developed viscosity and Z factor models in relation to well deliverability of gas-condensate reservoirs; three regions pseudopressure method also was employed. Three regions pseudopressure method, incorporated with results of PVT properties (gas/condensate viscosity, Z factor) for calculation of well inflow performance. The ultimate interest of this study is to improve gas-condensate well production performance modelling. Hence, the results obtained from pseudopressure method incorporated with volumetric material balance to generate production profile of gas and condensate on the surface.

Our approach for computation of well inflow performance and generating production profile is similar to previous study performed by (Fevang and Whitson, 1996; Jokhio and Tiab, 2002; Mott, 2002; Chowdhury *et al.*, 2004; Arukhe and Mason, 2012; Bonyadi, Rahimpour and Esmaeilzadeh, 2012; Behmanesh, Hamdi and Clarkson, 2015, 2017; Hekmatzadeh and Gerami, 2018). However, the advantage of the current approach is that the properties that require for computing three-flow regions pseudopressure integral estimated using AI techniques to ensure better accuracy of the model is achieved.

3.5 Major Work Steps

The conceptual framework of this investigation can be summarized and major work steps that have been taken are highlighted as follow.

- i. Critical review of the relevant literature was carried out and the gaps and shortfalls in current literature are identified. This literature review assisted to

shape aims and objectives of the study in improving well deliverability modelling of gas-condensate reservoirs.

- ii. Extensive published literature used to develop a data bank to improve PVT modelling of gas-condensate reservoir through accurate modelling of gas/condensate viscosity and two-phase Z factor.
- iii. Several dynamic gas/condensate viscosity models have been developed using regression and AI methods including ANN, SVM and Fuzzy Logic.
- iv. Several two-phase Z factor models have been developed using smart AI methods including Cascade-Forward Neural Network (CFNN), Feed-Forward Neural Network (FFNN) and Adaptive Neuro Fuzzy Inference System (ANFIS).
- v. A dynamic Inflow Performance Relationship (IPR) curve has been developed using two-phase pseudopressure integral for high temperature gas-condensate reservoirs in tight formation.
- vi. The developed models in this study (viscosity, Z factor) were combined with well deliverability equation of pseudopressure integral and material balance equation to establish production profile of a single gas-condensate well.

3.6 Data Acquisition and Validation

Practical application of the developed models were verified by using several case studies. Required data for this study was sourced from published open literature. PVT reports, experimental studies, published papers were source of our data bank. An extensive data bank for each phase of the study was collected and utilized in developing data driven (AI) methods. Availability of the data to some extent in recent years motivated using the current approach in this study.

The gathered data covered wide range of gas-condensate reservoir conditions (pressure, temperature and compositional differences). An example of this data bank shown in Appendix A.

To ensure the validity and accuracy of the data used for this study the following steps were taken,

- The statistical and graphical analysis of the gathered data against current methods in literature were performed in order to verify the data bank.
- The physical trend of the data were performed and the consistency of the data sets have been confirmed.

3.7 Summary

The methodologies in this chapter have been implemented to ensure accurate well deliverability modelling for gas-condensate reservoir below the dew point pressure is achieved. The data bank for development of models in this study is from published literature. This data source partially used for development, testing and validating of each model. To ensure robustness of the developed models the random selection of the data in each step has been implemented. The current chapter provides a road map of the methodologies that have been adopted in this study.

CHAPTER 4

IMPROVEMENT OF GAS-CONDENSATE FLUID VISCOSITY PREDICTION

4.1 Introduction

Viscosity is one of the governing parameters for modelling gas-condensate well deliverability (Whitson, Fevang and Yang, 1999; Hernandez; *et al.*, 2002; Yang *et al.*, 2007; Arukhe and Mason, 2012). To emphasise the importance of viscosity on production the research shows 1% error in calculating reservoir fluid viscosity resulted in 1% error in cumulative production (Al-Meshari *et al.*, 2007; Fevang and Whitson, 1996; Hernandez; *et al.*, 2002; Sutton, 2005; Whitson *et al.*, 1999). Davani *et al.*, (2013) also showed that small error in viscosity prediction would have big impact on production forecast. This lead to significant error in financial evaluation of the project. Although the accurate estimation of viscosity is critical for well deliverability modelling, yet it has highest uncertainty prediction using existing literature models.

Behmanesh *et al.*, (2017) found that using single dry gas viscosity and Z factor effect the performance prediction of gas-condensate reservoirs. Using single-phase viscosity models for estimation of gas-condensate viscosity are valid above saturation pressure, as condensate liquid yet to develop. However, below the saturation pressure using single-phase viscosity models are not valid as the fluid become two phases of gas and condensate. The developed phases of gas-condensate mixture should be computed individually for modelling purposes due to gravity segregation of the phases. The aim of this chapter is to improve several models for better prediction of gas-condensate fluid viscosity below the saturation pressure.

This chapter provides the detail modelling of gas-condensate fluid viscosity below the saturation pressure. Initially the viscosity of gas phase in gas-condensate reservoirs is studied using existing viscosity models in literature. The actual gas phase viscosity data is used to optimize a well-known viscosity model using non-linear regression. Several models have been developed for better and accurate prediction of condensate viscosity in gas-condensate reservoirs using ANN, SVM and Fuzzy Logic approaches.

4.2 Assessment of gas phase viscosity models

Gas viscosity models in literature are categorized to two types based on availability of the data and other reservoir information. First type are semi-empirical correlations that correlate gas viscosity as a function of pressure, temperature and mixture composition. These type of correlations initially are estimating the fluid (gas & liquid) viscosity at lower pressure (μ_{gsc}) and relate this value to actual viscosity (μ_g) using corresponding state principles (CSP). The CSP states that two substances at the same conditions of critical pressure and critical temperature will have similar properties. These conditions are known as reduced temperature (T_r) and reduced pressure (P_r) (Katz, 1959).

To name a few of these correlations such as (Carr, Kobayashi and Burrows, 1954; Jossi, Stiel and Thodos, 1962; Lohrenz, Bray and Clark, 1964; Lucas, 1981; Pedersen and Fredenslund, 1987). In compositional reservoir simulators (e.g., Eclipse), (Pedersen and Fredenslund, 1987) and Lohrenz et al., (1964) known as LBC are very popular for estimating viscosity of hydrocarbon fluid (gas/liquid).

Second category of the correlations are less computationally intensive and they are very popular for reservoir engineering PVT calculations. Some of these methods specifically developed to address gas-condensate issues in estimating viscosity.

The applicability of the most popular literature methods in prediction of gas viscosity will be assessed in following using actual viscosity data obtained from the open literature.

4.2.1 Lohrenz – Bray – Clark (LBC), 1964

Jossi et al., (1962) proposed a correlation for estimating viscosity of gas and liquid pure components. Later Lohrenz et al., (1964) used same equation of Jossi et al., (1962) for estimating hydrocarbon mixture viscosity. The equation usually referred to Lohrenz – Bray – Clark (LBC) correlation and originally developed based on residual viscosity concept and the theory of corresponding state principle (CSP). LBC correlation shown in following relates mixture viscosity (μ) to fourth degree polynomial of the reduced density.

$$\frac{[(\mu - \mu^*)\zeta + 10^{-4}]^{\frac{1}{4}}}{A_3\rho_r^3 + A_4\rho_r^4} = A_0 + A_1\rho_r + A_2\rho_r^2 - \quad 4.1$$

Where ζ , ρ_{pr} and μ^* represent viscosity reducing parameter, reduced density and low pressure gas mixture viscosity respectively, $A_0 - 4$ are LBC coefficients of 0.1023, 0.023364, 0.058523, -0.040758 and 0.0093324 respectively.

$$\left\{ \begin{array}{l} \zeta = 5.35 \left(\frac{T_{pc}}{M_i^3 P_{pc}^4} \right)^{1/6} \\ \rho_{pr} = \frac{\rho}{\rho_{pc}} = \frac{\rho}{M} v_{pc} \\ \mu^* = \frac{\sum_{i=1}^N z_i \mu_i}{\sum_{i=1}^N z_i \sqrt{M_i}} \end{array} \right. \quad 4.2$$

Where pseudocritical properties of temperature T_{pc} , pressure P_{pc} and volume v_{pc} can be calculated from Kay's mixing rule (Kay, 1936). In equation 4.2, z_i stands for mole fraction of each pure component i and M_i is molecular weight of each component. To establish special relation between C_{7+} fractions of gas-condensate mixture and critical volume, LBC suggested the following relationship.

$$v_{cC_{7+}} = 21.573 + 0.015122 M_{C_{7+}} - 27.65\gamma_{C_{7+}} + 0.070615 M_{C_{7+}}\gamma_{C_{7+}} \quad 4.3$$

Where $v_{cC_{7+}}$ is the critical molar volume, $M_{C_{7+}}$ is molecular weight of C_{7+} fraction and $\gamma_{C_{7+}}$ is specific gravity of C_{7+} fraction.

The low pressure, pure component gas viscosity for each composition μ_i^* , can be calculated using Stiel and Thodos, (1962) expression as follows.

$$\left\{ \begin{array}{ll} \mu_i^* \zeta_i = (34 \times 10^{-5}) Tr^{0.94} & \text{for } Tr \leq 1.5 \\ \mu_i^* \zeta_i = (17.78 \times 10^{-5})(4.58Tr - 1.67)^{5/8} & \text{for } Tr > 1.5 \end{array} \right\} \quad 4.4$$

In LBC mixture viscosity correlation ' μ ' is in centipoise (cp), viscosity reducing parameter ' ζ ' is in cp^{-1} , density ' ρ ' is in lbm/ft^3 , specific volume ' v_c ' is in $ft^3/lbm \text{ mol}$, temperature ' T ' is in Rankine ($^{\circ}R$), pressure ' P ' is in psia, and molecular weight of each component ' M_i ' is in $lbm/lbm \text{ mol}$. The accuracy of the LBC in predicting oil viscosity reported with average absolute deviation of 16 percent. They reported that their correlation is best performed in the range of 8.33 – 73.49 $^{\circ}F$ operating temperature and 4.94 – 7014psia reservoir pressure.

We selected LBC correlation for this study because it is widely implemented in compositional reservoir simulators and it is computationally simpler and faster than other CSP based viscosity correlations such as Pedersen and Fredenslund, (1987).

LBC method is sensitive to the density value since the method is developed with fourth degree polynomial of reduced density.

LBC can be used for estimating viscosity of gas and liquid at various reservoir pressure and temperature. However to match the measured viscosity values, the LBC coefficients are normally tuned. The tuning is generally through critical volume of C₇₊ components or LBC original constantans.

4.2.2 Lee – Gonzalez – Eakin (LGE)

Unlike the LBC correlation, which correlates low-pressure gas viscosity with temperature, molecular weight, pseudocritical temperature, and pseudocritical pressure, Lee et al., (1966) proposed a correlation that relates low-pressure gas viscosity with gas gravity (or molecular weight) and temperature. Lee et al., (1966) correlation commonly referred to Lee – Gonzalez – Eakin (LGE). In both LBC and LGE method gas viscosity is estimated by multiplying low pressure viscosity by a ratio. The ratio is correlated with density in LGE and reduced density in LBC. Sutton, (2007) showed that the performance of both corresponding state principle based correlations and LGE method is the same for estimation of gas viscosity.

In LGE method the authors modified theoretical viscosity expression of Starling and Ellington, (1964) and proposed a semi-empirical relation for estimation of viscosity of natural gas as a function of reservoir temperature, gas density (ρ) and fluid composition (y_i). The LGE correlation shown in 4.5 is based on measured data of pure component of 8 natural gases with specific gravity of less than 1.

$$\left\{ \begin{array}{l} \mu_g = 10^{-4}K \times \exp \left[X \left(\frac{\rho_g}{62.4} \right)^Y \right] \\ K = \frac{(9.379 + 0.016Ma)T^{1.5}}{209.2 + 19.26Ma + T} \\ X = 3.448 + \frac{986.4}{T} + 0.01009Ma \\ Y = 2.4 - 0.2X \end{array} \right. \quad 4.5$$

Where T is temperature in Rankine ($^{\circ}\text{R}$) and ρ_g is density at reservoir pressure and temperature in lb/ft^3 , M_a is apparent molecular weight. Apparent molecular weight is calculated as follow (Ahmed, 2010).

$$M_a = \sum_{i=1} y_i M_i \quad 4.6$$

Where M_i is molecular weight of each component in the mixture and can be obtained from property tables; y_i is mole fraction of each composition in the mixture. LGE is one of the main viscosity correlations in any compositional reservoir simulator for estimating of gas viscosity. In addition, the LGE method is very simple to use and is very popular for quick estimation of gas viscosity.

The method is limited for temperature range of $100 - 340^{\circ}\text{F}$ and pressure range between $100 - 8000\text{psia}$. The authors reported ± 2.7 error for estimating low pressure gas viscosity and 4% error for high pressure, provided density and molecular weight of compositions. The LGE correlation becomes less accurate for prediction of gas viscosity above the specific gravity of 1.

Success of LGE method for estimating gas viscosity motivated many researchers to present their viscosity correlations in similar fashion to LGE. Some of these methods will be discussed in following sections.

4.2.3 Londono – Archer – Blasingame (LAB)

Londono – Archer – Blasingame (LAB) (Londono, Archer and Blasingame, 2002) optimized LGE method to make it more accurate for estimating viscosity of pure component and light-natural gas mixture. LAB used large database of 4909 data points and cast the LGE method in the following form.

$$\left\{ \begin{array}{l} \mu_g = 10^{-4} K \exp[X \rho_g^Y] \\ K = \frac{(16.7175 + 0.0419188 M_w) T^{1.40256}}{212.209 + 18.1349 M_w + T} \\ Y = 1.09809 - 0.0392581 X \\ X = 2.12575 + \frac{2063.71}{T} + 0.011926 M_w \\ \rho_g = 1.601846 \times 10^{-2} \frac{M_w \cdot P}{RT} \end{array} \right. \quad 4.7$$

Where ρ_g is density (g/cm³); M_w is molecular weight of the gas, T is temperature, μ_g is gas viscosity, R is universal gas constant and P is reservoir pressure. The average absolute error (AAE) using optimized form of LGE in 4.7 was reported 2.29% for LAB data. The main difference between original and optimized form of LGE in 4.7 is that the original form of LGE generated using smaller database of mixture component, whether the optimized version used extensive database.

4.2.4 Sutton, (2005)

Sutton, (2005) used low pressure gas viscosity (μ_{gsc}) of Lucas, (1981) and modified original LGE correlation for estimating viscosity of gas and gas-condensate reservoirs. Sutton correlation is as follow,

$$\begin{cases} \mu_g = \mu_{gsc} \times \exp \left[X \left(\frac{\rho_g}{62.4} \right)^Y \right] \\ X = 3.47 + \frac{1588}{T} + 0.0009Ma \\ Y = 1.66378 - 0.04679 \end{cases} \quad 4.8$$

Where μ_{gsc} is defined as a function of pseudo critical properties of temperature (T_{pc}), pressure (P_{pc}) and can be estimated as follow.

$$\begin{cases} \mu_{gsc} \xi = 10^{-4} \left[\frac{0.807T_r^{0.618} - 0.357 \exp(-0.449T_r)}{0.34 \exp(-4.058T_r) + 0.018} + \right] \\ \xi = 0.9490 \left(\frac{T_{pc}}{M^3 P_{pc}^4} \right)^{1/6} \end{cases} \quad 4.9$$

The relationship between pseudo critical properties and reduced properties can be defined as follow.

$$\begin{cases} T_r = \frac{T}{T_{pc}} \\ P_r = \frac{P}{P_{pc}} \end{cases} \quad 4.10$$

The pseudo-critical properties of temperature and pressure related to the gas specific gravity (γ_g) and following two correlations were introduced by Sutton, (2005).

$$\begin{cases} T_{pc} = 164.3 + 357.7\gamma_g - 67.7\gamma_g^2 \\ P_{pc} = 744 + 125.4\gamma_g + 5.9\gamma_g^2 \end{cases} \quad 4.11$$

The above two correlations are based on 634 hydrocarbon sample compositions obtained from 275 constant volume depletion (CVD) report for gas-condensate and associate gas samples. Sutton, (2005) method is valid for gas specific gravity of between 0.554 – 2.819, temperature of 0 – 460°F and pressure of 12 – 17065psia. Sutton method is widely accepted among the research community for estimating gas viscosity using pseudocritical properties in 4.11 based on specific gravity of the mixture, knowing the compositions.

4.2.5 Elsharkawy (2006)

Elsharkawy, (2006) added calculation of non-hydrocarbon impurities including carbon dioxide (CO₂) and hydrogen sulphite (H₂S) to original LGE gas viscosity correlation. He also added another expression to LGE to account for existing of heptane plus fraction (C₇₊), which is particularly important in estimating viscosity of gas-condensate fluid. Existing of non-hydrocarbon impurities in natural gas and gas-condensate mixtures influence the accuracy of PVT properties such as viscosity and Z factor. Elsharkawy, (2006) used 2400 data point collected from experimental and published literature in developing his method. Elsharkawy, (2006) method is as follow.

$$\left\{ \begin{array}{l} \mu_{gc} = \mu_g + \Delta\mu_{C7+} + \Delta\mu_{CO2} + \Delta\mu_{H2S} \\ \mu_g = 10^{-4}K \times \exp \left[X \left(\frac{\rho_g}{62.4} \right)^Y \right] \\ K = \frac{(9.379 + 0.016Ma)T^{1.5}}{209.2 + 19.26Ma + T} \\ X = 3.448 + \frac{986.4}{T} + 0.01009Ma \\ Y = 2.4 - 0.2X \\ \Delta\mu_{C7+} = y_{C7+}(-3.2875 \times 10^{-1} \log \gamma_g + 1.2885 \times 10^{-1}) \\ \Delta\mu_{H2S} = y_{H2S}(-3.2268 \times 10^{-3} \log \gamma_g + 2.1479 \times 10^{-3}) \\ \Delta\mu_{CO2} = y_{CO2}(6.4366 \times 10^{-3} \log \gamma_g + 6.7255 \times 10^{-3}) \end{array} \right. \quad 4.12$$

Elsharkawy, (2006) was also optimized pseudo-critical properties of Sutton, (2005) shown in 4.13 based on 1200 data sets of gas-condensate mixtures compositions. Pseudo-critical properties recommended by Elsharkawy, (2006) is as follow.

$$\begin{cases} T_{pc} = 149.18 + 358.14\gamma_g - 66.976\gamma_g^2 \\ P_{pc} = 787.06 + 147.34\gamma_g + 7.916\gamma_g^2 \end{cases} \quad 4.13$$

Elsharkawy, (2006) viscosity and critical properties methods are valid for the temperature range of 94 to 327°F and pressure between 200 to 11,830psia. The author reported 8.9% absolute average deviation for estimating gas viscosity using his method.

In this study, the applicability of the above gas viscosity models for prediction of gas-condensate fluid is assessed. For this purpose two sets of viscosity experimental data by Al-Meshari et al., (2007) and Yang et al., (2007) have been selected. These studies carried out in elevated pressure and temperature in laboratory condition similar to the reservoir temperature and pressure condition. The fluids used in these experimental studies are from gas-condensate reservoirs in Saudi Arabia and North Sea. The collected fluids (gas and liquid) recombined in laboratory and gas viscosity measurements were made (Al-Meshari *et al.*, 2007; Yang *et al.*, 2007). Statistical accuracy of the existing literature models against experimental data examined using percentage of Absolute Average Relative Deviation (AARD%), presented in 4.14. Figure 4.1 illustrates the performance of each model in predicting gas phase viscosity.

The correlation proposed by Londono – Archer – Blasingame (LAB) provides best performance in predicting experimental viscosity data with lowest AARD%, hence it has been selected for further modification.

$$AARD\% = \frac{1}{Np} \sum_{i=1}^N \left| \frac{\mu_i^{Experiment} - \mu_i^{Calculated}}{\mu_i^{Experiment}} \right| \times 100 \quad 4.14$$

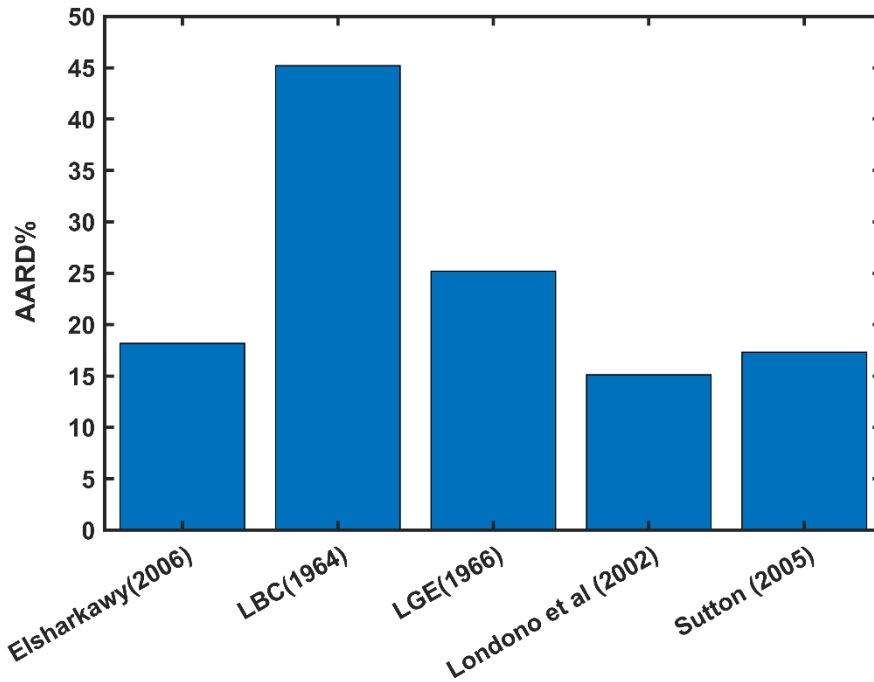


Figure 4.1. The prediction performance of existing literature models in estimating gas phase viscosity of gas-condensate reservoirs below the saturation pressure.

In an attempt to minimize the error between experimental data and the LAB correlation a non-linear regression model on MATLAB was employed. Then the LAB model was cast in the following form:

$$\left\{ \mu_g = 2.469 \times 10^{-4} K \exp \left[X \left(\frac{\rho_g}{27.6718} \right)^Y \right] \right. \quad 4.15$$

The parameters of K, Y and X are same as the original Lee – Gonzalez – Eakin (LGE) equation shown in 4.5. Half of the experimental data were used for optimizing LAB model and the other half used to test the performance of the model. The performance of proposed model in 4.15 plotted against the experimental data and shown in Figure 4.2. New optimized LAB model is predicting experimental data with 5.2% average absolute relative deviation (AARD%). This model will be used for prediction of gas phase viscosity of gas-condensate reservoirs, required for well deliverability modelling in chapter 6 of this study.

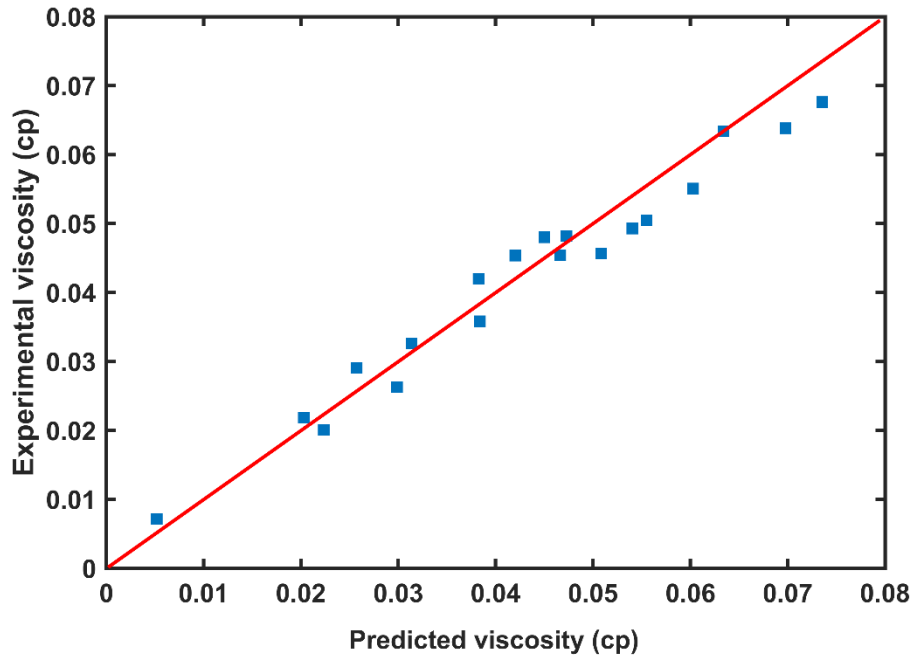


Figure 4.2. Plot of calculated viscosity using new developed model against measured viscosity data.

The viscosity of liquid phase (condensate) is another factor that need accurate determination for reliable modelling of gas-condensate reservoirs undergoing depletion. Next section focuses on studying condensate viscosity of gas-condensate reservoir below the saturation pressure.

4.3 Assessment of condensate (oil) phase viscosity models

Accurate and reliable estimation of condensate viscosity is required for reliable estimation of PVT properties using any available PVT modelling approaches (e.g., Modified black oil or equation of state). Less attention is given for accurate estimation of condensate viscosity in existing literature. Yet condensate viscosity has the highest prediction uncertainty (Whitson, 2006; Yang *et al.*, 2007).

In this section, initially the validity of the existing literature models for prediction of condensate viscosity is examined, and then several models will be proposed for prediction of this crucial PVT property.

The existing literature models are divided into two categories as follow:

- Corresponding state principle (CSP) based model (also known as compositional modelling)

- Gas-saturated oil viscosity based models (also known as live-oil viscosity correlations)

The example of compositional models are LBC (1964) introduced in 4.2.1 and Pedersen and Fredenslund, (1987). LBC is originally proposed for estimating viscosity of hydrocarbon mixture (gas/liquid). For estimating condensate viscosity in this study we employed LBC method due to its simplicity and its extensive use in numerical reservoir simulation. The compositional model of LBC is used when compositional data is available (see 4.2.1). However, the typical problem in engineering calculation of gas-condensate reservoirs are unavailability of all required data (Gold, McCain and Jennings, 1989; Whitson, 2006). In this case, to estimate condensate viscosity engineers rely on other purely empirical correlations known as live-oil or gas-saturated oil correlations.

These correlations are function of solution gas to oil ratio R_s , reservoir pressure, reservoir temperature, fluid API gravity, gas specific gravity (γ_{Gas}) and dead oil viscosity " μ_{od} " (viscosity that contain no dissolved gas and relatively thick oil).

There are many live-oil (oil contains dissolved gas) correlations in literature that can be used for prediction of condensate phase viscosity. We defined some standard criteria to pick the most adequate models for our purpose. It is known that condensate liquid is a light oil mixture with viscosity, ranging from 0.1 to 1cp, in the near wellbore region (Whitson, Fevang and Yang, 1999; Al-Nasser and Al-Marhoun, 2012) and also the API gravity between 40 – 60 °API. The aforementioned two conditions were our constraints in selecting existing live oil literature correlations that can be used for prediction of condensate viscosity in this study. These correlations are useful when compositional data of the gas mixture is not available. Five well-known live oil literature models have been selected for estimating condensate viscosity and will be discussed in this chapter.

Furthermore, in order to assess applicability of existing literature models for estimating condensate viscosity the compositional model of LBC which introduced in 4.2.1 is utilized.

4.3.1 Data acquisition

To assess the validity of existing literature models as well as developing AI models comprehensive published experimental data sets was collected. The source of the

data is from (Fevang, 1995; Guo *et al.*, 1997; Audonnet and Pádua, 2004; Gozalpour *et al.*, 2005; Al-Meshari *et al.*, 2007; Yang *et al.*, 2007; Thomas, Bennion and Andersen, 2009; Kariznovi, Nourozieh and Abedi, 2012; Kashefi *et al.*, 2013; Khorami *et al.*, 2017; Strand and Bjørkvik, 2019). In aforementioned studies, various methods of rolling ball viscometer, electromagnetic pulse technology viscometer, capillary viscometer and vibrating-wire sensor have been used for measurement of condensate phase viscosity. Binary mixtures of methane and n-decane in different temperature and pressure considered as gas-condensate fluid in most of previously mentioned experimental studies. This data bank consists of 335 data sets, which covers API gravity, gas specific gravity, reservoir fluid compositions, reservoir pressure, reservoir temperature and initial gas to oil ratio.

Statistical distribution of the data is summarized in Table 4.1. Complete description of the data bank is provided in Appendix A.

Table 4.1. Statistical information of the data bank.

Property	Minimum	Maximum	Average
Pressure, (MPa)	0.25	75.84	25.25
Reservoir Temperature, (°K)	303	443.15	353.15
Solution GOR, R_s , (scf/STB)	41.7	13496	3628
API gravity	39.7	65	57.3
Gas Specific gravity (γ_g)	0.57	1.49	0.89
Condensate viscosity, (cp)	0.0404	0.982	0.232

4.3.2 Beggs and Robinsons, (1975)

Almost all live oil (gas-saturated oil) viscosity correlations are in a similar form of original Chew and Connally, (1959). Live oil viscosity correlated by Chew and Connally, (1959) as a function of solution gas to oil ratio and dead oil viscosity at the reservoir condition. They showed that in fixed solution gas to oil ratio (R_s) the relation between the live oil and corresponding dead oil viscosity is a straight line with logarithmic scale (Chew and Connally, 1959). They propose this relationship in the following simple mathematical form.

$$\mu_{ob} = A(\mu_{od})^B \quad 4.16$$

Where A and B can be estimated from the original chart of Beal, (1946). Beggs and Robinson, (1975) developed a functional relation for A and B based on 2073 live oil viscosity measurements. The viscosity values measured with -1.83% uncertainty.

$$\begin{cases} A = \frac{10.715}{(R_s + 100)^{0.515}} \\ B = \frac{5.44}{(R_s + 150)^{0.338}} \end{cases} \quad 4.17$$

Using live oil viscosity relation shown in 4.16 along with Beggs and Robinsons correlation in 4.17 is limited to R_s within the range of 20 to 2070 scf/STB, oil gravity of 16 to 58°API, pressure range of 0 to 5250 and temperature of 70 to 295°F (Beggs and Robinson, 1975; Aily *et al.*, 2019).

4.3.3 De Ghetto et al., (1994)

De Ghetto et al., (1994) used similar form of Chew and Connally, (1959) live oil viscosity correlation and optimized the parameters of the A and B functions in 4.17, proposed originally by Beggs and Robinsons, (1975). They used 195 oil samples collected worldwide to optimize the values of A and B and indicate that the correlation is applicable to viscosity of live oil with API > 31.1. De Ghetto et al., (1994) present the following relation for A and B as a function of R_s .

$$\begin{cases} A = \frac{25.192}{(R_s + 100)^{0.6487}} \\ B = \frac{2.7516}{(R_s + 150)^{0.2135}} \end{cases} \quad 4.18$$

They showed that using above A and B values, the live oil viscosity can be estimated with less than 10% error within the temperature range of 80.6 to 334.6 °F, R_s of 8.61 to 3299scf/STB and $0.07 < \mu_{ob} < 295.9\text{cp}$ (De Ghetto *et al.*, 1994).

4.3.4 Elsharkawy and Alikhan (1999)

Elsharkawy and Alikhan, (1999) optimized the value of A and B to be used for estimation of live oil viscosity in 4.16 not similar to Beggs and Robinsons, (1975) and De Ghetto et al., (1994). They used 254 datasets from Middle Eastern oil samples and

proposed two new functions for A and B. They concluded that estimating A and B values using their proposed equation shown in 4.19, would predicts live oil viscosity with 18.6% average absolute relative error. Their correlation is valid for the range of 10 to 3600 for (R_s) and 0.05 to 20.89cp (μ_{ob}) (Elsharkawy and Alikhan, 1999).

$$\begin{cases} A = 1241.932(R_s + 641.026)^{-1.12410} \\ B = 1768.84(R_s + 1180.335)^{-1.06622} \end{cases} \quad 4.19$$

4.3.5 Bergman and Sutton, (2007)

Bergman and Sutton, (2007) used 2048 live oil measured viscosity data sets collected from worldwide and proposed equation 4.20 to estimate values of A and B. They showed that live oil viscosity can be estimated using their proposed equation in 4.20 incorporated with 4.16 with absolute average error of 9%. Their method best fit the value of live oil viscosity within the range of 5 to 2890scf/STB solution gas to oil ratio (R_s) and range of 0.125 to 123cp live oil viscosity (μ_{ob}).

$$\begin{cases} A = e^{[4.768 - 0.8359 \ln(R_s + 300)]} \\ B = 0.555 + \frac{133.5}{R_s + 300} \end{cases} \quad 4.20$$

4.3.6 Kartoatmodjo and Schmidt, (1991)

Kartoatmodjo and Schmidt, (1991) proposed a live oil viscosity correlation as a function of solution gas to oil ratio (R_s) and dead oil viscosity. Their correlation is slightly different from original live oil viscosity of Chew and Connally, (1959) shown in 4.16 as shown in 4.21. They used 5321 gas-saturated-oil samples collected globally to develop their live oil correlation. Their correlation can be applied to crude oils in the range of 14.4 to 59°API gravity, temperature range of 80 to 320°F, R_s range of 0 to 2890scf/STB and live oil viscosity range of 0.098 to 586cp (Kartoatmodjo and Schmidt, 1991).

$$\begin{cases} \mu_{ob} = -0.06821 + 0.9824X_1 + 4.034 \times 10^{-4}X_2^2 \\ X_1 = 0.43 + 0.5165 \times 10^{(-8.1 \times 10^{-4}R_s)} \\ X_2 = [0.2001 + 0.8428 \times 10^{(-8.1 \times 10^{-4}R_s)}] \mu_{od}^{X_1} \end{cases} \quad 4.21$$

All live oil viscosity methods in literature and seen above are function of solution gas to oil ratio (R_s) and dead oil viscosity (μ_{od}). Accurate estimation of R_s and μ_{od} is

required for reliable estimation of live oil viscosity. Measured values of R_s and μ_{od} are preferable for calculation; however, in the absence of experimental values, correlational estimation of viscosities are very popular (Chew and Connally, 1959; Beggs and Robinson, 1975). R_s is correlated with gas gravity, saturation pressure, stock tank oil gravity and temperature (Beal, 1946; Standing, 1947). Further discussion about important determination of R_s is given in 2.3.5. Among the most well-known methods for calculating R_s , we employed equation 2.50 proposed by Standing, (1947). This equation is still widely used in industry and recommended by Whitson et al., (2000) and Yang et al., (2007) as one of the most accurate correlation in literature. Considerable number of dead oil viscosity correlations are also exist in literature (Beal, 1946; Beggs and Robinson, 1975; Bergman and Sutton, 2007; Egbogah and Jack, 1990; Elsharkawy and Alikhan, 1999; Kartoatmodjo and Schmidt, 1994; Labedi, 1992; Naseri et al., 2005; Standing, 1981). Bergman and Sutton, (2007) reviewed the performance of 23 dead oil viscosity correlations with an extensive data bank. They found their proposed dead oil correlations is superior to all other techniques in literature. Whitson and Brulé, (2000, p. 36) also recommend Bergman and Sutton, (2007) for estimating dead oil viscosity for engineering calculation of gas-condensate reservoirs.

Therefore in this study Bergman and Sutton, (2007) is employed for estimation of dead oil viscosity. Bergman and Sutton, (2007) correlation is as follow.

$$\begin{cases} \ln \ln(\mu_{od} + 1) = A_0 + A_1 \ln(T + 310) \\ A_0 = 22.33 - 0.194\gamma_{API} + 0.00033\gamma_{API}^2 \\ A_1 = -3.20 + 0.0185\gamma_{API} \end{cases} \quad 4.22$$

Where γ_{API} is oil (condensate) stock tank gravity, T is temperature in Fahrenheit. All discussed live oil correlations as well as compositional model of LBC is applied for estimating experimental condensate viscosity. In following section the results of existing literature models are discussed.

4.3.7 Results of existing models

Three statistical metrics of coefficient of determination (R^2), root mean square error (RMSE) and absolute average relative deviation percentage (AARD%), shown in

equations 4.23 to 4.25 respectively, used for assessing the performance of existing literature models in prediction of condensate viscosity.

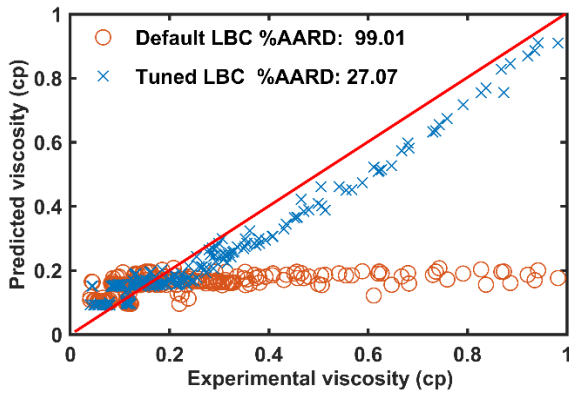
To visualise the accuracy of each model the graphical error analysis in a form of cross plot was employed. The results of statistical and graphical error analysis show that the performance of existing literature models in predicting condensate viscosity is very poor. Hence, to improve the accuracy of each models, non-linear regression was applied to refine the models. Table 1 depicts the original and tuned form of the utilized correlations for estimating condensate viscosity. Graphical error analysis of the original and refined literature correlations in predicting condensate viscosity are presented in Figure. 4.3a-f. The slope line of 45° in aforementioned figures representing zero error line in matching between measured and calculated values. The reason for poor performance of LBC viscosity models might be due to sensitivity of LBC method to mixture density and critical volumes of the heavy components (Whitson and Brulé, 2000; Yang *et al.*, 2007). Live oil viscosity correlations are function of deal oil viscosity and solution gas to oil ratio. It should be noted that dead oil viscosity is one of the most difficult properties to be estimated by correlations due to its dependency to paraffin, aromatic, naphthalene and asphaltene content (Whitson and Brulé, 2000; Hemmati-Sarapardeh *et al.*, 2014). This can be a reason for poor performance of live oil viscosity correlations for estimating condensate viscosity.

The procedure for tuning of the LBC, (1964) correlation recommended by Yang *et al.*, (2007) followed in this study, where coefficients of $A_0 - 4$ of the LBC correlation are optimized to match the experimental data. The new coefficients of LBC correlation are shown in Table 4.2. Coefficients of live oil viscosity models were also optimized using regression to match the experimental condensate viscosity data. The original and new tuned correlations of live oil viscosity are shown in Table 4.2.

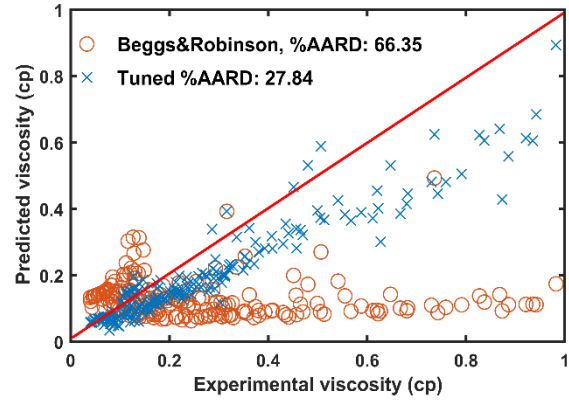
$$R^2 = 1 - \frac{\sum_i^N (cond\ vis_{Calculated(i)} - \widehat{cond\ vis_{Actual(i)}})^2}{\sum_i^N (cond\ vis_{Calculated(i)} - \overline{cond\ vis_{Actual(i)}})^2} \quad 4.23$$

$$RMSE = \left(\frac{\sum_i^N (cond\ vis_{Calculated(i)} - cond\ vis_{Actual(i)})^2}{N} \right)^{0.5} \quad 4.24$$

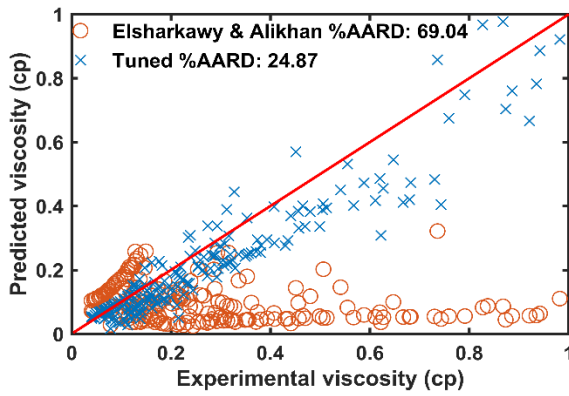
$$AARD\% = \frac{100}{N} \sum_i^N \frac{|(cond\ vis_{Calculated(i)} - cond\ vis_{Actual(i)})|}{cond\ vis_{Actual(i)}} \quad 4.25$$



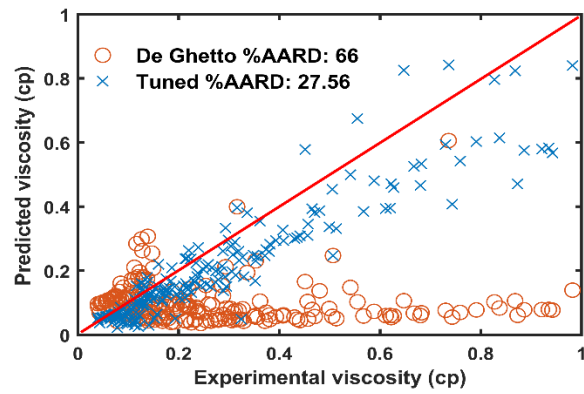
(a)



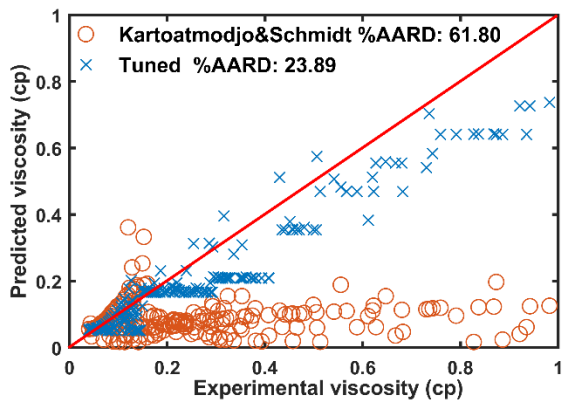
(b)



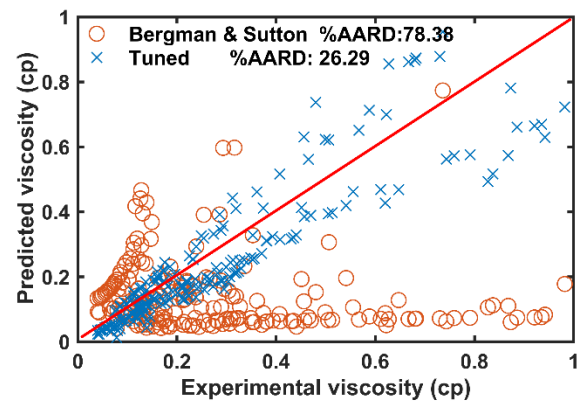
(c)



(d)



(e)



(f)

Figure 4.3. Cross plot of the experimental condensate viscosity versus predicted condensate viscosity using employed literature correlations and refined results.

Table 4.2. The original and tuned form of the utilized literature correlations.

Author	Original Correlation	Tuned Correlation
LBC, (1964)	$[(\mu - \mu^*)\zeta + 10^{-4}]^{\frac{1}{4}}$ $= 0.1023$ $+ 0.023364\rho_r$ $+ 0.058523\rho_r^2 -$ $0.040758\rho_r^3 + 0.0093324\rho_r^4$	$[(\mu - \mu^*)\zeta + 10^{-4}]^{\frac{1}{4}}$ $= 0.11364$ $+ 0.02173\rho_r$ $- 0.20666\rho_r^2$ $+ 0.06283\rho_r^3$ $+ 0.17139\rho_r^4$
Beggs & Robinson, (1975)	$\mu_{ob} = \frac{10.715}{(R_s + 100)^{0.515}} (\mu_{od})^{\frac{5.44}{(R_s+150)^{0.338}}}$	$\mu_c = \frac{17.99}{(R_s + 100)^{0.515}} (\mu_{od})^{\frac{4.056}{(R_s+150)^{0.338}}}$
Kartoatmodjo & Schmidt, (1991)	$\mu_{ob} = -0.06821 + 0.9824X_1 + 4.034 \times 10^{-4}X_2^2$ $X_1 = 0.43 + 0.5165 \times 10^{(-8.1 \times 10^{-4}R_s)}$ $X_2 = [0.2001 + 0.8428 \times 10^{(-8.1 \times 10^{-4}R_s)}] \mu_{od}^{X_1}$	$\mu_c = -0.30612 + 1.174X_1 + 4.034 \times 10^{-4}X_2^2$ $X_1 = 0.43 + 0.5165 \times 10^{(-8.1 \times 10^{-4}R_s)}$ $X_2 = [0.2001 + 0.8428 \times 10^{(-8.1 \times 10^{-4}R_s)}] \mu_{od}^{X_1}$
De Ghetto et al, (1994) For ($^{\circ}$ API > 31.1)	$\mu_{ob} = \frac{25.192}{(R_s + 100)^{0.6487}} (\mu_{od})^{\frac{2.7516}{(R_s+150)^{0.2135}}}$	$\mu_c = \frac{62.96}{(R_s + 100)^{0.6487}} (\mu_{od})^{\frac{2.1334}{(R_s+150)^{0.2135}}}$
Elsharkawy & Alikhan, (1999)	$\mu_{ob} = A(\mu_{od})^B$ $A = 1241.932(R_s + 641.026)^{-1.12410}$ $B = 1768.84(R_s + 1180.335)^{-1.06622}$	$\mu_c = A(\mu_{od})^B$ $A = 3978.167(R_s + 641.026)^{-1.12410}$ $B = 1361.93(R_s + 1180.335)^{-1.06622}$
Bergman & Sutton, (2000)	$\mu_{ob} = A(\mu_{od})^{0.555 + \frac{133.5}{R_s+300}}$ $A = e^{[4.768 - 0.8359 \ln(R_s+300)]}$	$\mu_c = A(\mu_{od})^{0.555 + \frac{133.5}{R_s+300}}$ $A = e^{[4.6792 - 0.7772 \ln(R_s+300)]}$

The accuracy of condensate viscosity using existing literature models depends on accurate estimation of many parameters (e.g., solution gas to oil ratio, reduced density, dead oil viscosity, well stream gravity for condensate). Although the attempt to improve the accuracy of the viscosity models were made by optimizing associated constants of each model, yet the accuracy is still less than satisfactory. Hence, in this study we took different approach known as Machine Learning (ML) for accurate estimation of condensate viscosity without going through tedious computational procedure of existing literature models. These methods are also known as Artificial Intelligent (AI) techniques. In next section, a brief overview of AI techniques for application of reservoir modelling is discussed.

4.4 Machine Learning (ML) Approach

In order to use computers for solving and processing applications, mathematical models are required (Forsyth, 1989). The fundamental approach to acquiring these models in natural sciences and engineering disciplines is by applying fundamental laws and theories in physics, chemistry and other related science to determine usually the relationships between variables (Forsyth, 1989). The input variables are called the independent variables, while the output variables are the dependant variables. For some tasks, however the relationship between dependant and independent variables are not defined and there are no governing mathematical equations between them. Therefore the transformation between the input and the output can not be done directly (Flach, 2012). For instance physics of gas-condensate fluid below the saturation pressure is becoming more thermodynamically complex, which makes it very difficult to establish a robust relationship between the input and the output variables for instance in the case of condensate viscosity.

Because of that lack of knowledge or complexities of the problems, alternative methods to build models have been introduced by scientists. These methods rely on using sets of measured input and output data that have been obtained during measurement process or from past saved data (Flach, 2012). The computer which is being trained uses certain algorithms and statistical analysis to build a model which can; for instance; predict the output values (condensate viscosity). This type of process is known as machine learning (ML).

Arthur Samuel has used the term machine learning for first time in 1959. He defined ML as “a field of study that gives computers the ability to learn without being explicitly programmed” (Samuel, 1959). Figure 4.4 shows the main structure of modelling by machine learning.

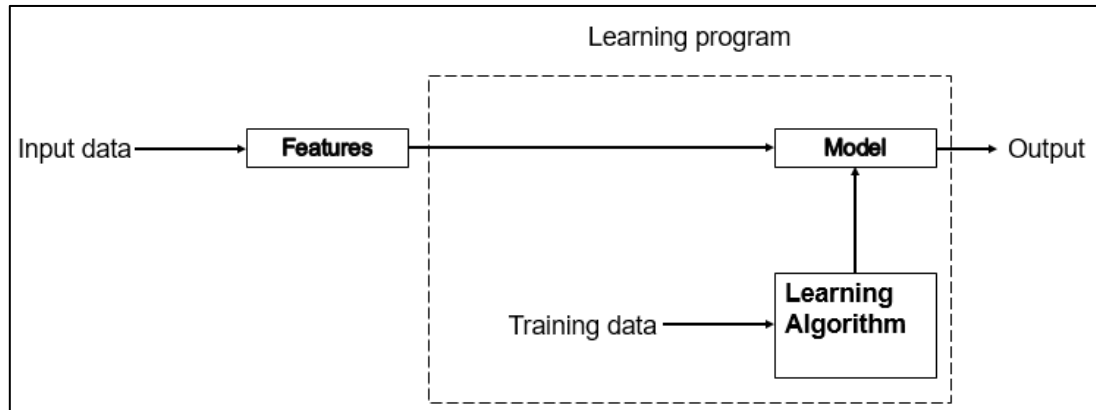


Figure 4.4 Machine Learning Block Diagram.

Based on the method selected to feed the input and output data for learning process, there are two main class of machine learnings known as supervised and unsupervised learning (Louridas and Ebert, 2016). In supervised machine learning, the nature and the label of the output are known. For example in this chapter using experimental database, we know the output is condensate viscosity. In the other word the data that provided for training of the network include sets of input and output parameters.

In unsupervised learning, the training set is containing the data but no solutions; and the computer must find the solution on its own by relating the pattern on the data set (Louridas and Ebert, 2016). Regardless of classes of ML (supervised or unsupervised) the process is that the computer first learns to perform a task by studying a training set. Then the computer performs the same task with the data it hasnot encountered before.

The recent development and success of machine learning (ML) techniques in solving complex engineering problems have drawn attention to their various application in petroleum industry. Shell recently announced using new artificial intelligence (AI) platform to drive its effort in predictive maintenance and spread AI-powered applications across the company. British Petroleum (BP) has invested heavily on using AI techniques aims at accelerating project lifecycle from exploration through reservoir modelling (Norton, 2018; BP, 2019). In modelling aspect, which is the scope of this research, availability of the data in recent years motivated to utilize the data driven techniques for reliable and accurate forecast of outputs (e.g., flow rate, Z factor and

GOR). Some of these example can be found in the literature include (Ahmadi et al., 2014; Ghiasi et al., 2014; Hemmati-Sarapardeh et al., 2014; Kamari et al., 2013; Naderi and Khamehchi, 2019; Shokir, 2008).

For gas-condensate reservoirs Ahmadi and Ebadi (2014), Elsharkawy and Foda (1998), Jalali et al. (2007) and Nowroozi et al. (2009) were using machine learning (ML) approaches for predicting dew point pressure. Zendehboudi et al. (2012) used ML approach to model condensate-to-gas ratio (CGR). Recently Ghiasi et al. (2014) employed least square support vector machine (LSSVM) to predict compressibility factor of gas-condensate reservoirs. Although the aforementioned studies utilized ML techniques for modelling gas-condensate reservoirs such as dew point pressure, CGR and compressibility factor, however there is still significant potential to use various approaches of ML for modelling this type of reservoir. There is not any models in current literature for prediction of condensate viscosity using any ML methods. Hence, the aim is to use ML based techniques to develop a robust and accurate models for prediction of condensate viscosity in gas-condensate reservoirs below the saturating pressure. For this purpose, three ML based techniques including Support Vector Machine (SVM), Artificial Neural Network (ANN) and Fuzzy logic methods employed and will be discussed in details in the following sections.

4.4.1 Support Vector Machine (SVM)

The support vector machine (SVM) has been identified as an efficient and powerful strategy developed from the machine-learning community (Cortes and Vapnik, 1995; Suykens et al., 2002). SVM is a tool for a set of related supervised learning methods that analyse data and recognize pattern using regression analysis and it is identified as a non-probabilistic binary linear classifier.

SVM method has many advantages over other machine learning techniques as follows: they are more likely to converge to the global optima, prior determination of the network is not required in this model and can be automatically determined as the training ends (Suykens *et al.*, 2002; Eslamimanesh *et al.*, 2012). Furthermore, the number of hidden layers and hidden nodes should not be determined and this algorithm has fewer adjustable parameters compared to ANN network (Ahmadi and Ebadi, 2014; Eslamimanesh et al., 2012; Hemmati-Sarapardeh et al., 2014; Kamari et

al., 2013). SVM is mapping the predictor's data using kernel function and initial formula indicates that any function can be regressed as follow:

$$f_x = w^T \varphi(x) + b \quad 4.26$$

Where w^T and $\varphi(x)$ and b are transposed output layer vector, kernel function and bias, respectively. The input of the model x is of a dimension of $N \times n$ in which N and n denotes to number of data points and number of inputs parameters, respectively. In order to calculate w in above function, Cortes and Vapnik, (1995) proposed minimization of the cost function, defined in 4.26 subject to some constraint shown in 4.27 (Ahmadi and Ebadi, 2014; Eslamimanesh et al., 2012, 2011; Hemmati-Sarapardeh et al., 2014; Suykens et al., 2002).

$$J = \frac{1}{2} w^T + C \sum_{k=1}^N (\xi_k - \xi_k^*) \quad 4.27$$

Where J is the cost function, c is the tuning parameter of the SVM and ξ_k and ξ_k^* are the slack variables.

$$\left\{ \begin{array}{l} y_k - w^T \varphi(x_k) - b \leq \varepsilon + \xi_k, \quad k = 1, 2, \dots, N \\ w^T \varphi(x_k) + b - y_k \leq \varepsilon + \xi_k^*, \quad k = 1, 2, \dots, N \\ \xi_k, \xi_k^* \leq 0 \quad k = 1, 2, \dots, N \end{array} \right\} \quad 4.28$$

Where x_k is input of k^{th} data point and y_k is output of k^{th} data points. ε is the fixed precision of the function approximation. Choosing a small ε leads to developing an accurate model, however some data points may be outside of ε precision, and may result in infeasible solution. Therefore, slack parameters can be used to define allowable margin error. C in equation 4.26 is one of the tuning parameters, which determine the amount of deviation of the model from the desired ε . The optimum value of cost function in SVM can be reached by minimization process, where Lagrangian approach can be used as follow.

$$\left\{ \begin{array}{l} L(a, a^*) = -\frac{1}{2} \sum_{k,l=1}^N (a_k - a^*_k)(a_l - a^*_l)K(x_k, x_l) - \varepsilon \sum_{k=1}^N (a_k - a^*_k) \dots \\ \dots + \sum_{k=1}^N y_k(a_k - a^*_k) \sum_{k=1}^N (a_k - a^*_k) = 0, a_k, a^*_k \in [0, c] \\ K(x_k, x_l) = \varphi(x_k)^T \varphi(x_l), k = 1, 2, \dots, N \end{array} \right\} \quad 4.29$$

Where a_k and a^*_k are Lagrangian multipliers, and the final form of least square SVM function is obtained as follow.

$$f(x) = \sum_{k,l=1}^N (a_k - a^*_k)K(x, x_k) + b \quad 4.30$$

To solve the above equation and find a_k , a^*_k and b , quadratic programming problem can be used which is very difficult to implement. Thus the least square modification proposed by Suykens and Vandewalle, (1999) to facilitate original SVM algorithm. They reformulated the SVM cost function J as follow.

$$J = \frac{1}{2} w^T w + \frac{1}{2} \gamma \sum_{k=1}^N e^2_k \quad 4.31$$

$$Y_k = [w^T \varphi(x_k) + b + e_k], \quad k = 1, \dots, N. \quad 4.32$$

Where γ is a tuning parameter, e_k is error variable, Y_k is constraint of the cost function (J). Equation 4.31 is new form of SVM equation known as least square SVM (LSSVM). The Lagrangian solution for this equation is calculated as follow.

$$L(w, b, e; a) = \frac{1}{2} w^T w + \frac{1}{2} \gamma \sum_{k=1}^N e^2_k - \sum_{k=1}^N a_k (w^T \varphi(x_k) + b + e_k - y_k) \quad 4.33$$

Where a_k denotes to the Lagrange multiplier, that may be either positive or negative, since LSSVM has equality restrictions. The above equation can be solved by equate the derivate of each parameter (w , b , e , and a) to 0 according to Karush Kuhn-Tucher's (KKT) conditions (Fletcher, 1987). These conditions are demonstrated in equation 4.34 for cost function to achieve optimum goal (Suykens and Vandewalle, 1999;

Pelckmans *et al.*, 2002; Suykens *et al.*, 2002). Hence, the following equations are obtained for optimal solution of the cost function.

$$\left\{ \begin{array}{l} \frac{\partial L}{\partial w} = 0 \Rightarrow w = \sum_{k=1}^N a_k \varphi(x_k) \\ \frac{\partial L}{\partial b} = 0 \Rightarrow \sum_{k=1}^N a_k = 0 \\ \frac{\partial L}{\partial e} = 0 \Rightarrow a_k = \gamma e_k, \quad k = 1, 2, \dots, N \\ \frac{\partial L}{\partial a} = 0 \Rightarrow w^T \varphi(x_k) + b + e_k - y_k = 0 \quad k = 1, 2, \dots, N \end{array} \right\} \quad 4.34$$

To turn the above equation to a linear form the following expression can be demonstrated.

$$\begin{bmatrix} 0 & -1^T \\ 1 & \Omega + \frac{1}{\gamma} I_N \end{bmatrix} \begin{bmatrix} b \\ \alpha \end{bmatrix} = \begin{bmatrix} 0 \\ y \end{bmatrix} \quad 4.35$$

while $y = (y_1, \dots, y_n)^T$, $1_n = (1, \dots, 1)^T$, $a = (a_1, \dots, a_n)^T$ and $\Omega_{il} = \varphi(x_i)^T \varphi(x_l)$ for $i, l = 1, \dots, n$. By Mercer's theorem, the resulting LSSVM model for function approximation turns to the following equation (Cortes and Vapnik, 1995; Suykens and Vandewalle, 1999).

$$f(x) = \sum_{k,l=1}^N \alpha_k K(x, x_k) + b \quad 4.36$$

Where α and b are the routes to equation 4.36 and can be determined as bellow:

$$\left\{ \begin{array}{l} b = \frac{1_n^T \left(\Omega + \frac{1}{\gamma} I_n \right)^{-1} y}{1_n^T \left(\Omega + \frac{1}{\gamma} I_n \right)^{-1} 1_n} \\ \alpha = \left(\Omega + \frac{1}{\gamma} I_n \right)^{-1} (y - 1_n b) \end{array} \right. \quad 4.37$$

Knowing a and b from 4.37, then $f(x)$ in 4.36 may be executed as choice of nonlinear regression and utilize the Kernel function. (Cortes and Vapnik, 1995; Suykens and Vandewalle, 1999; Suykens *et al.*, 2002; Eslamimanesh *et al.*, 2012; Fazeli *et al.*,

2013). In equation 4.35, $K(x, x_k)$ stands for dependency of Kernel function to the inner values of two vectors x and x_k in the feasible area referred to the inner products of vectors $\phi(x)^T \phi(x_k)$ as shown in below equation:

$$K(x, x_k) = \phi(x)^T \phi(x_k) \quad 4.38$$

Where the radial basis function (RBF) Kernel may executed as following formulation (Cortes and Vapnik, 1995; Eslamimanesh et al., 2012; Pelckmans et al., 2002; Suykens et al., 2002).

$$K(x, x_k) = \exp\left(-\frac{\|x_k - x\|^2}{\sigma^2}\right) \quad 4.39$$

Where γ and σ^2 are tuning parameters of LSSVM, that they can be indicated by performing of any optimization algorithm such as Simulated Annealing algorithm or Genetic Algorithm (GA). In order to achieve the optimum values of aforementioned parameters in LSSVM method, our objective function is root mean square error (RMSE) between the experimental values and the output of the LSSVM.

Our task in this chapter was to develop a smart model for prediction of condensate viscosity using LSSVM, explained in details earlier. To implement the LSSVM for prediction of condensate viscosity database, initially the data sets divided into three subsets of "Training", "Optimization" and "Testing". Training set is used for generating the model structure, optimization is used for minimization of the error in trained model and test data is used to investigate the prediction capability of the developed model. Optimization sets also known as the validation set. The database was randomly split into three sub data sets of 80% training, 10% testing and 10% validation. We also ensure the homogeneous accumulations distribution of the data for the domain of the three data sets (Eslamimanesh *et al.*, 2011; Gharagheizi *et al.*, 2014). The allocation percentage of the data is selected according to the recommendations by Ahmadi and Ebadi, (2014) and Eslamimanesh et al., (2012) to enhance the performance of the developed model.

During the training of the model cross validation has been performed where, the training data sets into several folds and accuracy of each fold was checked. The LSSVM implemented in MATLAB and powerful Simulated Annealing (SA) algorithm

was utilized to minimize the error between the experimental viscosity and predicted values by the model. The objective function of minimization procedure was root mean square error as defined as follow.

$$RMSE = \sqrt{\frac{\sum_{i=1}^n (Vis_{esti} - Vis_{expi})^2}{ns}} \quad 4.40$$

Where Vis represents condensate viscosity, subscripts est and exp represent the predicted and actual value, ns is number of data points from the initial assigned population of 144 data sets. The optimized values of γ and σ^2 using SA optimization method for predicting the condensate liquid viscosity presented in the following table.

Table 4.3. The optimum values of the LSSVM parameters.

LSSVM model	Input parameters	Model parameters	
		γ	σ^2
Condensate phase viscosity	Reservoir pressure, Temperature, API, gas SG, Rs	5625.256	23.65

The algorithm reduces the error between the experimental values of viscosity, and the model to reach the optimum solution. The input variables for this model are as pressure, temperature, API gravity, gas specific gravity and solution gas to oil ratio “Rs”.

The prediction capability of the trained model was tested for new data sets using the generated LSSVM code. The cross plot of in Figure. 4.5A-B illustrates the performance of developed LSSVM model in training stage and testing stage, respectively. The majority (73%) of the data points in this study are within lower viscosity range of 0 – 0.4cp. Therefore, the performance of the LSSVM in testing new data is toward lower viscosity region, which is more realistic characterisation of condensate viscosity below the dew point near wellbore region (Whitson, Fevang and Yang, 1999; Yang *et al.*, 2007). The viscosity of condensate liquid in near wellbore region (Region 1), where condensate liquid is mobile is very low. This is due to the existence of more lighter C₇₊ fractions in mobile condensate liquid composition in aforementioned region (Fevang, 1995, p. 44).

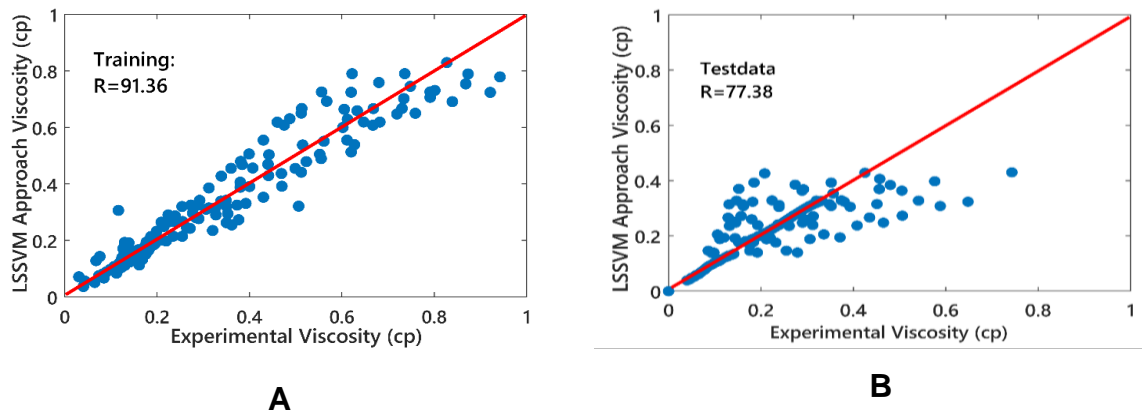


Figure 4.5. Performance of LSSVM in predicting condensate (oil) viscosity in training and testing stage.

Graphical representation of the error analysis of the LSSVM in predicting the condensate viscosity depicted in Figure. 4.6. Ability of the trained LSSVM in predicting new data sets are also analysed by presenting graph of standard deviation error in Figure. 4.6A and standard error from the mean in Figure. 4.6B.

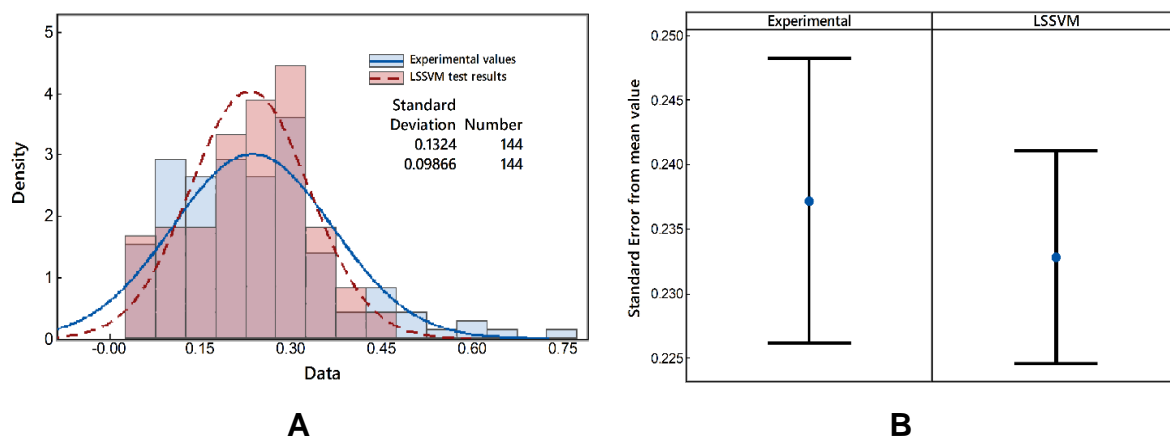


Figure 4.6. Graphical error analysis of LSSVM performance for predicting condensate (oil) viscosity.

Three statistical error analysis including coefficient of determination (R^2), root mean square error (RMSE) and average absolute relative deviation percentage (AARD%) shown in equations 4.22 to 4.24 respectively, were adapted for estimating the performance of the LSSVM. Table 4.4 shows the result of this analysis in training, validation and testing stage of the LSSVM.

Table 4.4. Statistical error performance of the LSSVM.

Stage of the process	R^2	RMSE	AARD%
Training set	0.9139	0.10845	13.96
Validation set	0.87256	0.111121	14.12
Testing set	0.7723	0.121037	14.25

The results obtained from LSSVM approach indicate a promising outcome for reliable and more accurate prediction of condensate viscosity. The results indicate that LSSVM is performing better than tuned literature correlations. However, the error is still high, approximately about 23% in testing stage, where the capability of the model assessed using new data sets. Therefore, to certify the effectiveness and accuracy of the suggested LSSVM model for estimation of condensate viscosity among smart approaches in another attempt an Artificial Neural Network (ANN) was developed, which is presented in following section.

4.4.2 Artificial Neural Network (ANN)

Artificial Neural Network (ANN) is a type of machine learning and artificial intelligence model that mimics human central nervous system, in particular the brain in human body (Bell, 2014). An ANN network consists of several organized layers containing hundreds or even more single units and artificial neurons that are connected through weight functions (Agatonovic-Kustrin and Beresford, 2000; Giri Nandagopal and Selvaraju, 2016). There are many types of neural networks but the main distinguish features between them are transfer functions of their neurons, learning rules and connection formula.

In ANN network complex computation system is performed for predicting the output responses. ANNs are inspired by biological networks, performing in a massive parallel connection between nonlinear, parametrized, and bounded functions called neurons (Cios and Shields, 1997; Mesbah, Soroush and Rostampour Kakroudi, 2017). Such a network is a massively parallel-distributed processor that has a natural tendency for storing experimental knowledge and making it available for future use. In ANN system knowledge is acquired by the network through a learning process and synaptic weights will store this knowledge (Haykin, 1994). Hence, mathematical interpretation of the problem does not required. Neurons in such system coordinate their work, and they

transfer information by using synapses “electromagnetic communications” (Ghaffari *et al.*, 2006a). Through a set of known input and output data the network will be trained. Through a learning process the network monitors the error between the predicted and desired outputs and continue to adjust the weights until the optimization criteria are reached. This process is usually carried out in two following stages:

- first the input variables are linearly combined
- the result is used as an argument of non-linear *activation function* (a)

The activation function must be non-decreasing and differentiable function; the most common choices are either the identity function ($y = x$), or bounded sigmoid (s-shaped) function, as the logistic [$y = 1/(1 + e^{-x})$] (Haykin, 1994; Hippert, Pedreira and Souza, 2001; Ghaffari *et al.*, 2006b; Eslamimanesh *et al.*, 2011).

The neurons are organized in a way that define the network architecture. In this chapter we applied multilayer perceptron (MLP) type, in which the neurons are organized in continuous layers.

In MLP architecture, the neurons in each layer may share same inputs, but they are not connected to each other. As shown in Figure 4.7, typical neural networks consist of hidden layers, output layer, inputs and bias units. Number of hidden layers and number of neuron of each layers can be arbitrary (Khosrojerdi *et al.*, 2016). However, increasing number of neurons may cause overfitting while decreasing their numbers may result on poor performance of the network. The main advantage of ANN is ability to process large amount of data sets (Ghaffari *et al.*, 2006; Khosrojerdi *et al.*, 2016; Mesbah *et al.*, 2017; Hippert *et al.*, 2001).

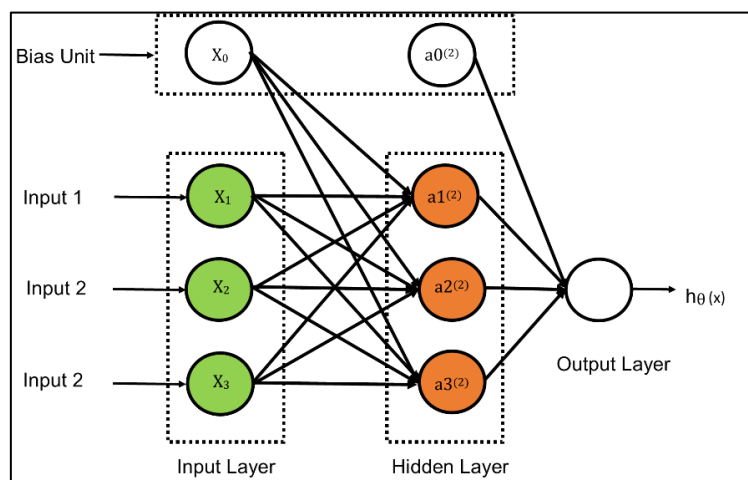


Figure 4.7. Schematic illustration of the ANN structure and computational steps to measure output.

The mathematical definition of the typical MLP neural network shown in Figure 4.7 is presented in the following section where superscripts are values associated with each layer.

In this mathematical definition $a_i^{(j)}$ = activation" of unit i in layer j and

$\theta^{(j)}$ = matrix of weights controlling function mapping from layer j to layer $j+1$. In order to calculate each *activation function* (a) a *sigmoid function* (g) is multiplied by sum of linear combination of inputs for each neuron; these inputs in Figure 4.7 include (x_1, x_2, x_3 and *bias unit* x_0) in hidden layer. The activation function (a) then can be calculated from the following equation.

$$\begin{cases} a_1^{(2)} = g(\theta_{10}^{(1)} x_0 + \theta_{11}^{(1)} x_1 + \theta_{12}^{(1)} x_2 + \theta_{13}^{(1)} x_3) \\ a_2^{(2)} = g(\theta_{20}^{(1)} x_0 + \theta_{21}^{(1)} x_1 + \theta_{22}^{(1)} x_2 + \theta_{23}^{(1)} x_3) \\ a_3^{(2)} = g(\theta_{30}^{(1)} x_0 + \theta_{31}^{(1)} x_1 + \theta_{32}^{(1)} x_2 + \theta_{33}^{(1)} x_3) \end{cases} \quad 4.41$$

Then the output function $h_\theta(x)$ in Figure 4.7, is sum of each neuron's weight multiplied by activation function of same neuron in layer 2 defined by equation 4.42. The neurons of the output layer have linear transfer functions.

$$h_\theta(x) = a_1^{(3)} = g(\theta_{10}^{(2)} a_0^{(2)} + \theta_{11}^{(2)} a_1^{(2)} + \theta_{12}^{(2)} a_2^{(2)} + \theta_{13}^{(2)} a_3^{(2)}) \quad 4.42$$

Where g is a sigmoid function can be evaluated from the following equation.

$$g(z) = \frac{1}{(1 + e^{-z})} \quad 4.43$$

In order for neural network to perform, the activation function of each neuron should be vectorised in a matrix form of z as follow.

$$\begin{cases} \theta_{10}^{(1)} x_0 + \theta_{11}^{(1)} x_1 + \theta_{12}^{(1)} x_2 + \theta_{13}^{(1)} x_3 = Z_1^{(2)} \\ \theta_{20}^{(1)} x_0 + \theta_{21}^{(1)} x_1 + \theta_{22}^{(1)} x_2 + \theta_{23}^{(1)} x_3 = Z_2^{(2)} \\ \theta_{30}^{(1)} x_0 + \theta_{31}^{(1)} x_1 + \theta_{32}^{(1)} x_2 + \theta_{33}^{(1)} x_3 = Z_3^{(2)} \end{cases} \quad 4.44$$

Substituting 4.44 into 4.42 transforms the activation function into the following form.

$$\begin{cases} a_1^{(2)} = g(z_1^{(2)}) \\ a_2^{(2)} = g(z_2^{(2)}) \\ a_3^{(2)} = g(z_3^{(2)}) \end{cases} \quad 4.45$$

And if x and z represented by the following two matrices,

$$\begin{cases} x = \begin{bmatrix} x_0 \\ x_1 \\ x_2 \\ x_3 \end{bmatrix} \\ z^{(2)} = \begin{bmatrix} z_1^{(2)} \\ z_2^{(2)} \\ z_3^{(2)} \end{bmatrix} \end{cases} \quad 4.46$$

The value of the output layer is a sigmoid function of $z^{(3)}$, and can be determined by the following equation.

$$h_{\theta}(x) = g(z^{(3)}) \quad 4.47$$

Where the value of x are considered as input of activation function. The above calculation procedure was implemented using MATLAB software in this study. The detailed computation procedure is for simple ANN network with only one hidden layer shown in Figure. 4.7. The complexity of a neural network is influenced by its size, i.e., the number of neurons and hidden layers as previously mentioned. However, the network should be designed with enough level of complexity, so that it does not start to over fit the data (Hagan *et al.*, 2014; Soroush *et al.*, 2015).

Figure 4.8 depicts the schematic diagram of ANN structure for prediction of condensate viscosity. This design has one input layer consists of five parameters, one hidden layer, two bias units and one output unit. This architecture recommended by Hagan *et al.* (2014), Hagan and Menhaj (1994) and Hippert *et al.* (2001) as an efficient and the most popular multilayer feed-forward architecture. Nevertheless, there are large number of other designs, which might be considered suitable for other applications. To select the best architecture in terms of number of neurons in a hidden layer a trial and error procedure was implemented. The performance of each structure was assessed by comparing coefficient of determination (R^2) and root mean square error (RMSE). We came up with the proposed structure shown in Figure 4.8, which

comprises of five neurons in layer two as the best topology. The input parameters are API gravity, solution gas to oil ratio (R_s), pressure, temperature and gas specific gravity (SG). The output layer is viscosity of condensate fluid calculated by the ANN network.

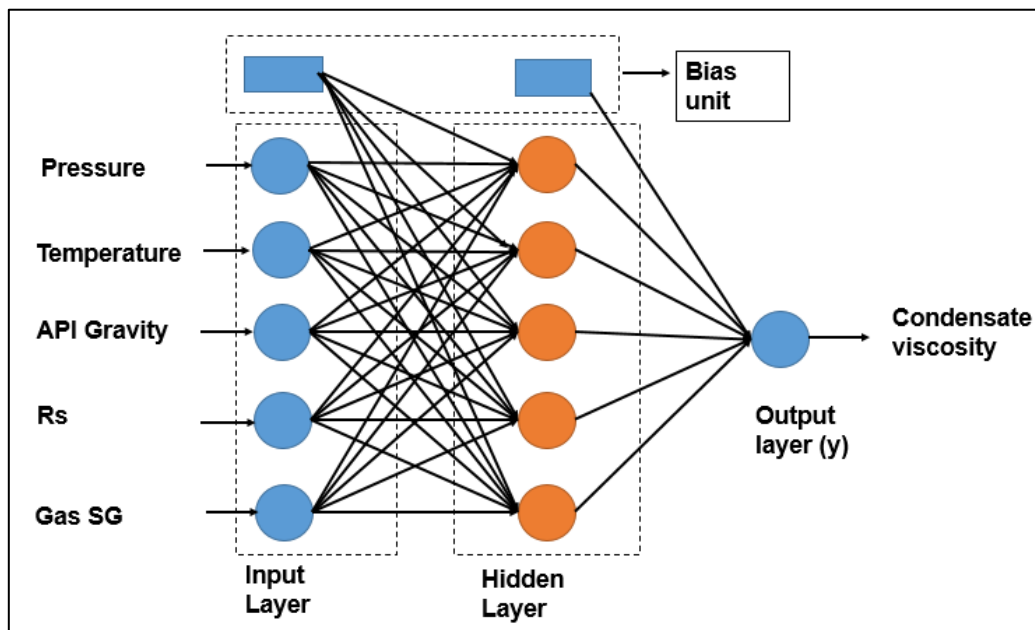


Figure 4.8. Developed ANN model architecture for prediction of condensate viscosity.

There are many algorithms available to train the network. The role of any algorithm is to minimize the error between the output of the network and target values (experimental condensate viscosity). This can be done by finding the optimum values of the weights and biases in an iterative procedure. The most well-known training algorithms are Levenberg–Marquardt (LM), scaled conjugate gradient (SCG), Bayesian Regularization (BP) and resilient back propagation (Hippert, Pedreira and Souza, 2001; Soroush *et al.*, 2015). The LM backpropagation algorithm introduced by Kenneth, (1944) and recommended by Behera and Chattopadhyay, (2012) as one of the fastest and most popular backpropagation algorithm was used for adjusting the weights in this study. The tangent sigmoid transfer functions selected as an activation function for the neurons in hidden layer. For training of the model 70% of whole data bank (210 data points) randomly selected and split into three subsets of 80% (168 data points) for training, 10% (21 data points) for validation and 10% (21 data points) for testing. The ANN network is trained to map input data by iterative adjustment of the weight functions. Information from the input layer feed forwarded through the network to optimize the weight between the neurons. Optimization of the weight function is carried out by back propagation of the error during training or learning stage.

The ANN reads the inputs and output values in training stage and changes the value of weight functions to minimise the difference in predicted and the target (observed) values. The error in prediction is minimized across training iterations (epochs) and training continues to the point that the network reaches a specified level of accuracy (Ghaffari *et al.*, 2006a). Once the model has reached satisfactory accuracy or the model is converged, the training will stop. The performance of the ANN network in predicting the condensate viscosity has been shown in following graphical figures.

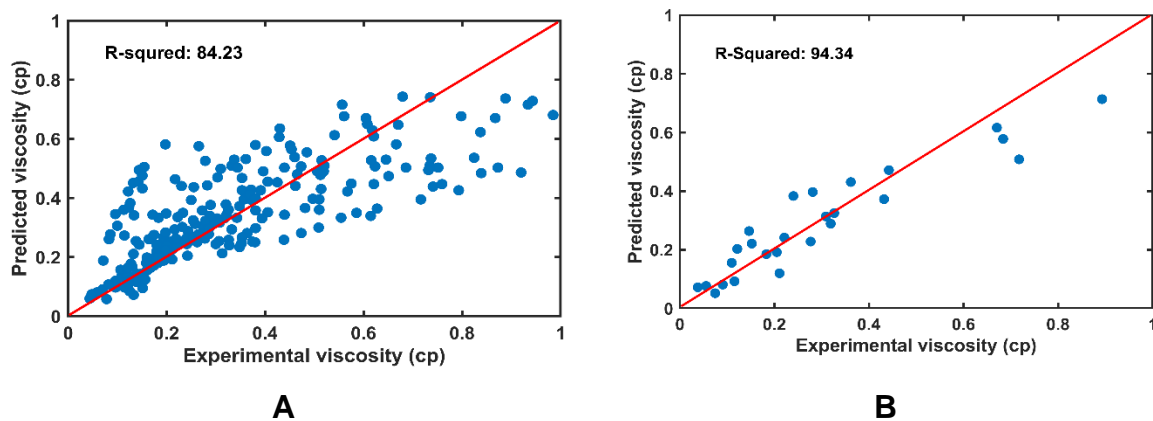


Figure 4.9. Prediction performance of developed ANN network for condensate liquid viscosity in training (A) and testing (B) stage.

To ensure that the developed model of LSSVM and ANN follow the physical trend of condensate viscosity as a function of pressure, their performance have been tested using three independent condensate viscosity samples adopted from the literature. These samples are binary fluids representing gas-condensate mixture that show liquid drop out below the saturation pressure. The samples are from (Al-Meshari *et al.*, 2007; Yang *et al.*, 2007; Kashefi *et al.*, 2013).

The results shown in Figure 4.10 and Figure 4.11 indicate that ANN and LSSVM are following physical trend of condensate viscosity as a function of pressure with good accuracy.

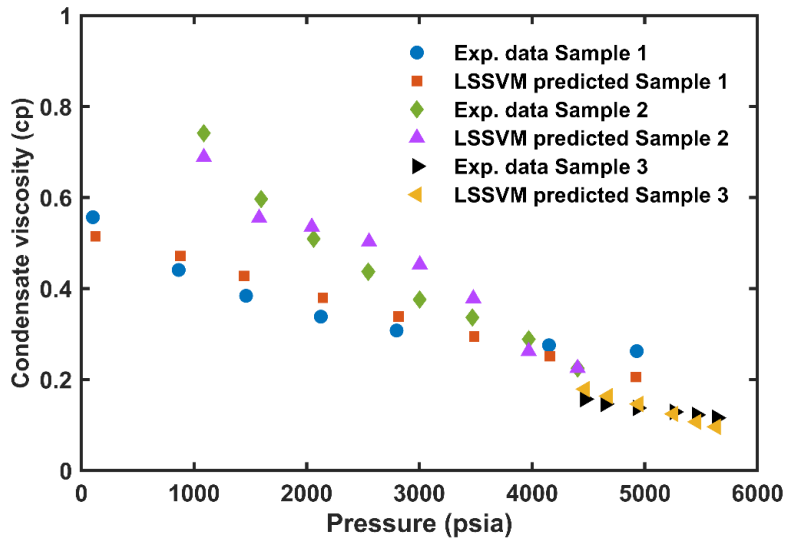


Figure 4.10. Prediction performance of the developed LSSVM condensate viscosity model as a function of pressure for three independent samples.

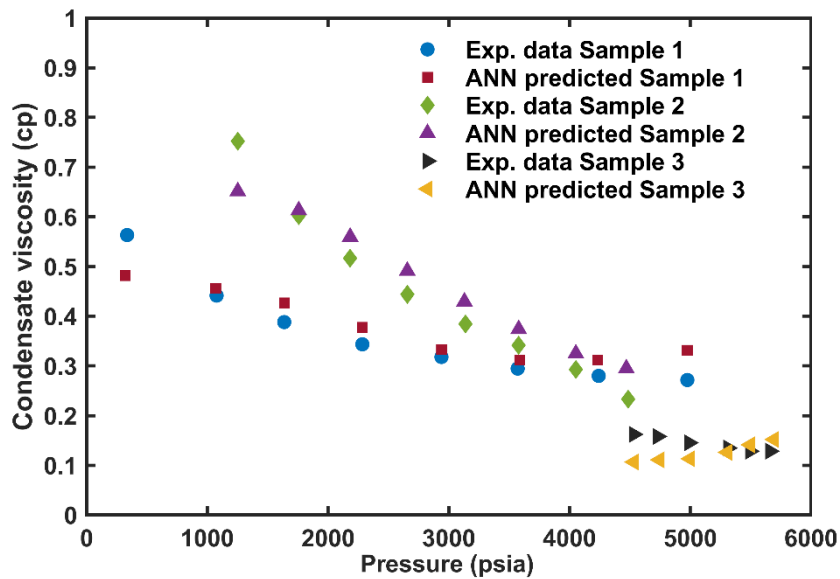


Figure 4.11. Prediction performance of developed ANN condensate viscosity model as a function of pressure for three independent samples.

4.4.3 Results and discussion

The prediction performance of several existing literature models against experimental condensate viscosity data were tested. All existing literature models failed to predict condensate viscosity with acceptable accuracy.

The cross plot of the results shown in Figure 4.3a confirms the poor performance of widely used compositional based LBC, (1964) model in prediction of condensate

viscosity. The reason for this is due to sensitivity of LBC method to mixture density and critical volumes of the heavy components. Hence, in this study the coefficients of the LBC correlation were optimized using least-square approach to match the experimental condensate viscosity data. The tuned LBC correlation shown on Table 4.1. Figure 4.3a represents the prediction performance of LBC, (1964) with default and adjusted coefficients.

Furthermore, the coefficients of five well-known live oil viscosity correlations were regressed to match the condensate experimental data. The results of these regressions presented in Figure 4.3b – f. These empirical correlations are function of dead oil viscosity and solution gas to oil ratio (R_s). It should be noted that dead oil viscosity is one of the most “difficult” properties to be estimated by correlations due to its dependency to paraffin, aromatic, naphthalene and asphaltene content (Whitson and Brulé, 2000; Hemmati-Sarapardeh *et al.*, 2014). This might be one of the reasons for poor performance of the default empirical live oil viscosity correlations. Moreover, these correlations were originally developed using crude oil samples, which its properties are fundamentally different from condensate liquid. The API gravity of crude oil sample is between 15 – 45°API while API gravity of condensate liquid is normally above 50°API.

Poor performance of the published literature correlations in predicting condensate viscosity, motivated to develop two machine learning models of LSSVM and ANN network in this study. The performance of the newly proposed models of LSSVM and ANN were compared against refined previously published correlations through graphical and statistical error analysis. The statistical error analysis carried out using coefficient of determination (R^2), root mean square error (RMSE) and average absolute relative deviation percentage (AARD%). The result of this error analysis is tabulated in the Table 4.5. Graphical representation of statistical analysis is provided in Figure 4.12 and Figure 4.13. The results indicate that ANN model outperformed other methods with AARD of 16.20%, R^2 of 0.8423 and RMSE of 0.1144. ANN followed by LSSVM, Kartoatmodjo and Schmidt (1994), Elsharkawy and Alikhan (1999), Bergman and Sutton (2007), LBC (1964), De Ghetto et al. (1994) and Beggs and Robinson (1975).

Table 4.5. Statistical parameters of developed ML based models and utilized correlations for prediction of condensate viscosity.

Method	R ²	RMSE	AARD%
LBC, (1964)	0.7241	0.1240	27.07
Bergman & Sutton, (2007)	0.7297	0.1236	26.29
Beggs & Robinson, (1975)	0.7207	0.1244	27.84
Elsharkawy & Alikhan, (1999)	0.7344	0.1228	24.87
De Ghetto et al, (1994)	0.7243	0.1240	27.56
Kartoatmodjo & Schmidt, (1994)	0.7412	0.1220	23.89
LSSVM	0.7738	0.1208	17.22
ANN	0.8423	0.1144	16.20

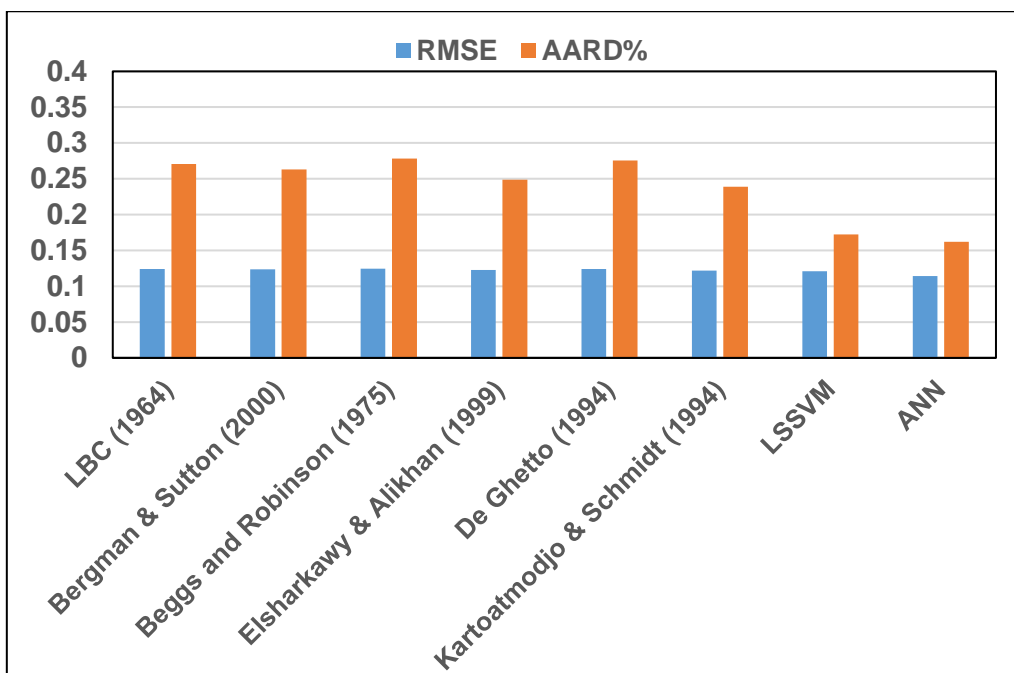


Figure 4.12. Statistical performance comparison of tuned literature models against developed ANN and LSSVM models (AARD% and RMSE) for prediction of condensate viscosity.

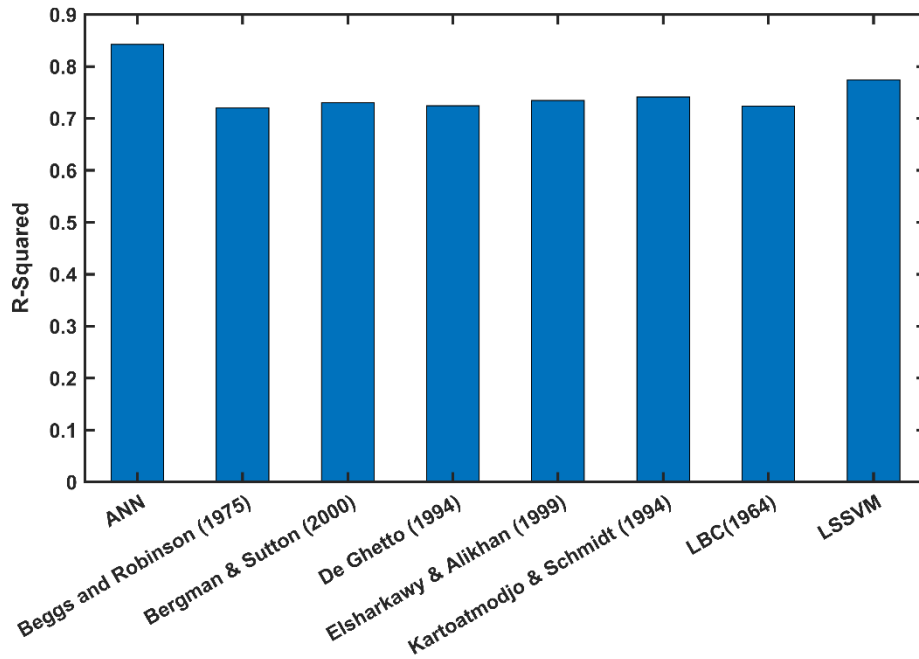


Figure 4.13. Statistical performance comparison of tuned literature models against developed ANN and LSSVM models (R^2) for prediction of condensate viscosity.

The results confirm using either compositional model of LBC or live oil viscosity correlations require significant tuning of coefficients for prediction of condensate viscosity of gas-condensate reservoirs below the saturation pressure. Whereas developed two intelligent approaches were able to monitor condensate viscosity with appropriate precision and integrity.

Non-linear relationship between the available experimental data and the desired outputs created using developed LSSVM model. The optimum values of two important tuning parameters of LSSVM include σ^2 and γ are presented in Table 4.3. Simulated Annealing optimization (SA) algorithm was applied to achieve these two optimum values.

The ability of proposed LSSVM and ANN models for calculating condensate liquid viscosity as a function of changing pressure have been investigated for three gas condensate samples from the literature. Figure 4.10 and Figure 4.11 are demonstrating experimental and predicted condensate viscosities using LSSVM and ANN models respectively. The results show that both models are able to forecast physical trend of experimental condensate viscosity. The accuracy of the models for predicting condensate viscosity of two independent samples determined by AARD%.

The error analysis show that both AI models perform well with acceptable level of accuracy.

From Figure 4.10 and Figure 4.11, it is evident that increasing pressure would decreases the condensate viscosity. The pressure changes due to depletion in gas-condensate reservoirs can have significant effect on condensate viscosity variation near wellbore region (Fevang and Whitson, 1996). These changes might due to the complex behaviour of gas-condensate reservoir below the dew points pressure, which violate thermodynamic laws. The developed LSSVM and ANN models successfully captured the trend of condensate viscosity while utilized correlations were not accurate enough in tracking these changes.

Although the prediction performance of the LSSVM was better than published literature correlations, however the error was still high with R^2 of 0.7738 and AARD of 17.22%. Therefore, Artificial Neural Network (ANN) method was used aiming to improve the accuracy. Performance prediction of ANN network is a function of number of neurons that is used in hidden layer. A trial and error approach were implemented to find the optimum number of neurons. For this study the ANN architecture with five neurons provides the most satisfying results with the least RMSE and the highest R^2 . Both machine learning models are providing promising results in prediction of condensate viscosity.

Although the developed ML based models are performing better than existing literature models, however the main deficiencies of both ML models is that they sacrifice the physics of the problem for accurate outcome. Hence, in another attempt of this study, different machine learning method known as Fuzzy Logic (FL) employed in order to compensate the neglected physics by ANN and LSSVM. The output of the TSK fuzzy logic is in a form of linear equation. This approach will be explained in the following sections of this chapter.

4.5 Fuzzy Logic Approach

In previous section of this chapter, it has been demonstrated that the accuracy of existing literature models for predicting condensate viscosity are inadequate. Hence, an alternative two soft computing approaches namely LSSVM and ANN models have been developed for better estimation of condensate viscosity. Although aforementioned approaches provide satisfactory estimation of condensate viscosity,

however the major criticism is that they are black box methods and visual relationship between input and output parameters cannot be established (AlQuraishi and Shokir, 2011; Fayazi *et al.*, 2014). These approaches are based on statistical truth of the utilized data rather than scientific relationship between the input/output parameters. As a result, not any meaningful correlation can be derived from these approaches. Our aim is to develop accurate yet mathematically efficient condensate viscosity correlation. The proposed correlation has to cope with nonlinearity of the condensate viscosity that occurs due to various stage of pressure depletion in gas-condensate reservoirs. For this purpose, another machine learning approach known as Fuzzy Logic was utilized. There are two typical Fuzzy Logic approaches in literature as follow:

- Takagi – Sugeno – Kang (TSK) rule based fuzzy logic
- Mamdani approach

The TSK fuzzy gives accuracy of the ML based method without compromising the physics of the problem.

Mamdani approach is purely linguistic; means interpret the mathematical problem in a language understandable to the human logic. Both approaches utilized for accurate modelling of condensate viscosity in gas-condensate reservoirs. In this section, first, we give background information to the fuzzy logic approach in general and then TSK and Mamdani techniques will be explained in details.

The science today is based on Aristotle's crisp logic, formed more than 2000 year ago. In Aristotle's logic, every problem has a bivalent manner, means black and white, yes or no and 0 and 1. The Aristotle's bivalent logic made accessible to modern science by German mathematician Cantor, who developed set theory for this purpose. In the Cantor's theory sets are defined as a collection of distinguishable objects. In 1937 the first paper published on the theory of vague sets by Black, (1937). The vague sets basically is similar to probability theory in mathematics. In vague sets, the objects no longer are distinguishable as introduced by Cantor's theory. In 1965, Zadeh continued the work on vague sets and he introduced well known theory of fuzzy sets, which we know it as fuzzy logic in today's science literature (Zadeh, 1965). He developed many, key concepts, including the idea of membership function and provide comprehensive framework to apply the theory for solving engineering and scientific problem.

Fuzzy theory deals with vagueness, imprecision and uncertainty in a system. Unlike the classical bivalent logic, that only admits (e.g., black and white, true (1) or false (0))

of an occurrence, fuzzy logic covers degree of truth of a factor between 0 and 1. In another word in contrast to the classical crisp set, where an object either belongs to a set or it does not, everything is a matter of degree in fuzzy set. The belonging of an object to a set can be done by the membership function. Fuzzy logic provides a linguistic solution for a problem, means it lifts the restriction of computer language (0 & 1) for a problem.

Fuzzy logic approach has been used in several petroleum engineering application including petro physics, reservoir characterization, enhanced oil recovery, drilling, decision-making analysis and well-stimulation (Chen *et al.*, 1993; Zhou, Wu and Cheng, 1993; Zhanggui *et al.*, 1998; Shokir, 2006, 2008; Ahmadi *et al.*, 2015; Zhao *et al.*, 2018; Khazali, Sharifi and Ahmadi, 2019). Shokir, (2006) used rule based fuzzy logic for modelling density and viscosity of natural gas reservoirs. Liao *et al.*, (2008) utilized fuzzy approach in separation process of oil; Khazali *et al.*, (2019) applied fuzzy decision tree for enhance oil recovery screening; Ahmadi and Ebadi, (2014) used fuzzy logic method for calculation of minimum miscible pressure of injected gas and reservoir oil.

Gas-condensate reservoirs modelling with condensate blockage effect, exhibits all characteristics that a fuzzy logic system proposed to deal with. For instance the well deliverability-modelling associate with inaccuracy in PVT and rock properties estimation. Some properties like condensate (oil) viscosity has the largest uncertainty both experimentally and in prediction (Fevang, 1995; Whitson, Fevang and Yang, 1999). Accurate determination of PVT properties is challenging task due to the complex fluid behaviour of gas-condensate reservoirs below the dew point that violate thermodynamic laws. The thermodynamic abnormality is because of the condensation of gas phase “become liquid hydrocarbon (condensate)” phase instead of vaporization as it is expected when pressure reduced and expansion induced in an isothermal system. After many years of research, this behaviour is still not understood accurately and we call it vague in this study. Such behaviour directly affect the accurate estimation of PVT properties (condensate viscosity, compressibility factor).

These vagueness behaviour and difficulties motivated us in this study to take fuzzy logic approach, hoping to tackle if not all some of these challenges.

Two most well-known methods of fuzzy logic in literature are Mamdani and Takagi – Sugeno – Kang (TSK) approach. In this study, both methods have been adopted for

developing intelligent models for prediction of condensate viscosity below the saturation pressure.

4.6 Takagi – Sugeno – Kang (TSK) Fuzzy approach

The most well know rule based fuzzy inference systems (FIS) are linguistic Mamdani-type and Takagi – Sugeno – Kang (TSK) (Mamdani and Assilian, 1975; Takagi and Sugeno, 1985). Both antecedents and consequence are fuzzy sets in Mamdani approach, whereas in TSK model antecedent contains of fuzzy sets and the consequence is a linear equation. Therefore, the outcome of TSK fuzzy model can be interpreted as a linear equation. This linear equation would benefit the accuracy of the intelligent model as well as representing the physics of the problem.

This linear relationship between input/output is defined by set of fuzzy so called IF – THEN rules as follow.

$$R_1: \text{if } x_i \text{ is } A_{i1} \text{ and } \dots \text{ and } x_m \text{ is } A_{im} \text{ then} \quad 4.48$$

$$y_i = a_{i1}x_1 + \dots + a_{im}x_m + a_{i0}$$

Where $R_1 = (1, 2, \dots, n)$ is number of fuzzy rules, $x_i = (1, 2, \dots, m)$ are the input variables, y_i are the output variables whose values are inferred, A_{i1}, \dots, A_{im} are membership functions of the fuzzy sets in the premises and $a_{i0}, a_{i1}, \dots, a_{im}$ are the model parameters in the consequence (Takagi and Sugeno, 1985). To determine these three items using input-output data of a respective system “gas-condensate viscosity data” the design procedure of TSK fuzzy model can be summarized in three steps as follow:

1. Fuzzy clustering
2. Setting the membership functions
3. Parameters estimation (Takagi and Sugeno, 1985; Passino and Yurkovich, 1998; Shokir, 2006, 2008).

Partitioning set of input variables into some fuzzy sub sets can be carried out in first two steps, while the relation of input/output of each fuzzy sub sets is defined in third step (Takagi and Sugeno, 1985). The outline of the TSK fuzzy algorithm is shown in Figure 4.14. From the diagram, it can be seen that TSK algorithm requires combination of input/output variable called premise variables, where in this study the input variables are pressure (P), temperature (T) and solution-gas to oil ratio (Rs), and the output

variable is condensate viscosity (μ_c). As previously mentioned temperature has a significant effect on viscosity and it has given a special attention in this study because, strictly speaking, according to Ahmed, (2010) and Whitson et al., (2000) gas condensate reservoirs are defined by only temperature. If temperature located between critical and cricondentherm temperature (326°K – 395°K) the reservoir classed as gas-condensate reservoir.

After preparing the dataset the partitioning of the data is required, which any clustering technique can be used for this step. Subsequently, the membership functions are defined by Gaussian distribution, which essentially relates the premise variables to each cluster with a certain degree of membership. Least square approach can be used to determine the value of constants in 4.42.

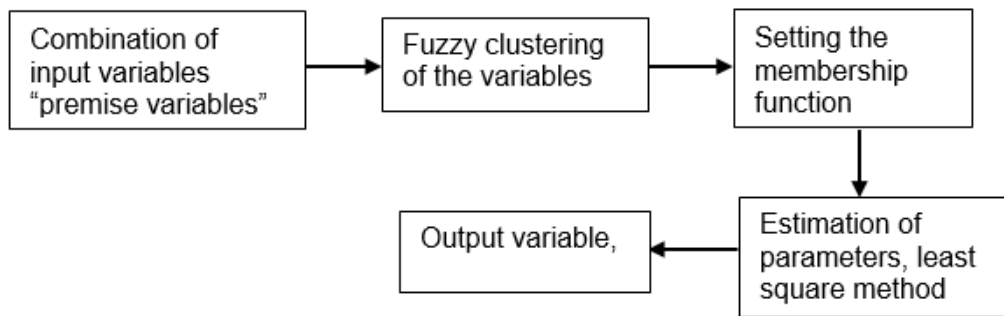


Figure 4.14. Outline of the TSK fuzzy algorithm.

The optimum number of clusters is fundamental for efficiency of the TSK algorithm. This also known as optimum number of rules for data sets. The optimum number of rules, for condensate viscosity utilized data were determined using Calinski and Harabasz, (1974) cluster evaluation method. The data bank introduced in 4.3.1 is used for developing the fuzzy models in this section. Having determine optimum number of clusters (rules), K-mean fuzzy clustering approach, as one of the most popular classification techniques (Bezdek and Pal, 1992; Klawonn et al., 2015) for partitioning set of data has been used to develop the TSK fuzzy model.

Then Gaussian membership function as an efficient technique over other methods such as triangular or trapezoidal function (Ahmadi and Ebadi, 2014) was utilized to determine the degree of membership of an object to a set. Hence, membership degree of input/output data in respect to each cluster has been defined (Zadeh, 1965; Ross, 2017). The details description of each step highlighted in Figure 4.14, is given in the following section.

4.6.1 Fuzzy Clustering

Partitioning set of data points ‘input/output’ into several groups (clusters) in a way that the points in the same group are highly similar and dissimilar from points of other clusters is the aim of fuzzy clustering (Bai *et al.*, 2017). In this study 250 data sets were selected as a training data sets and divided into several clusters and then interpreted as rules.

There are several fuzzy clustering methods in literature such as fuzzy c-means (FCM), Gustafson-Kessel (GK), K-means clustering and subtractive clustering. Comprehensive introduction to each clustering technique can be found in (Bezdek and Pal, 1992).

In this study K-means clustering method was used as one of the most popular classification algorithm for the data without any defined categories or unlabelled data. This algorithm, is an iterative, hill climbing data-partitioning algorithm, where “ N ” observations can be partitioned into “ c ” clusters. Each observation in the process belongs to a cluster with nearest mean. Each cluster is represented by a so-called prototype, which has to be in the centre of the corresponding cluster. K-means clustering algorithm is based on an objective function “ J ” that can be determined from the following equation (Klawonn, Kruse and Winkler, 2015).

$$J = \sum_{i=1}^c \sum_{j=1}^n u_{ij} d_{ij} \quad 4.49$$

J also known as cost function and should be minimized under the following constraints:

$$\sum_{i=1}^c u_{ij} = 1 \quad \text{for all } j \in \{1, \dots, n\} \quad 4.50$$

Where $u_{ij} \in \{0,1\}$ indicates whether data vector x_j is assigned to a cluster i ($u_{ij} = 1$) or not ($u_{ij} = 0$); $d_{ij} = \|x_j - v_i\|^2$ is squared Euclidean distance between data vector x_j and cluster prototype v_i . In this method the number of cluster “ c ” must be known in advance. Our criteria for assigning initial number of clusters is based on the assumption that nonlinearity in the data can be approximated by 12 clusters (Shokir, 2006, 2008).

In general, there is no specific rule for defining optimum number of clusters “ c ” however several number of techniques such as elbow method, the silhouette method G-means algorithm and Calinski-Harabasz are exist in literature. In this study Calinski-Harabasz cluster evaluation method was used as an efficient technique (Calinski and Harabasz, 1974). The criteria of Calinski-Harabasz also called variance ratio criterion (VRC) and its defined as follow.

$$VRC_c = \frac{SS_B}{SS_w} \times \frac{(N - c)}{(c - 1)} \quad 4.51$$

Where SS_B and SS_w are between and within overall cluster variance respectively, c stands for number of clusters, and N represents the data points. The SS_B and SS_w are defined as follow.

$$SS_B = \sum_{i=1}^c n_i \|m_i - m\|^2$$

$$SS_w = \sum_{i=1}^c \sum_{x \in c_j} \|x - m_i\|^2 \quad 4.52$$

Where n_i is number of observations in cluster i , m_i is centroid of cluster i , m stands for mean of the data, x is number of data samples, c_j is the i th cluster and $\|m_i - m\|^2$, $\|x - m_i\|^2$ is Euclidean distances between two vectors. Large SS_B and a smaller SS_w are representing well-grouped clusters, which means the larger VRC_c ratio, the better data partition (Calinski and Harabasz, 1974). Therefore to achieve the optimum number of clusters, the validity measure of VRC_c is maximized with respect to number of clusters c . Hence, highest Calinski-Harabasz index is the optimum number of clusters (Calinski and Harabasz, 1974; Bandyopadhyay and Maulik, 2002). Figure 4.15 illustrates the obtained results using validity criterion function VRC_c using equation 4.51 for training data set.

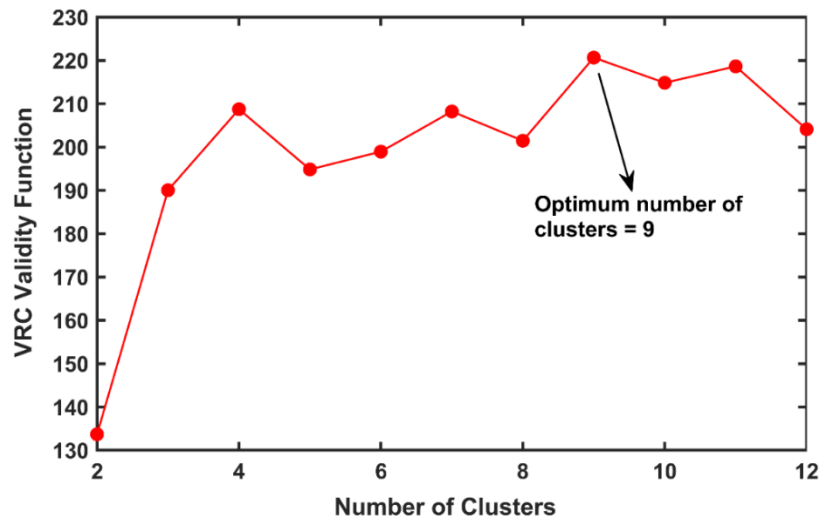


Figure 4.15. Optimum number of cluster for the training data sets using validity function (VRC), for condensate viscosity input data.

Having defined the optimum number of clusters for our training data, k-means algorithm, presented in equation 4.49 was proceed for assumed finite set of points $A = \{x_1, x_2 \dots, x_n\}$ in n-dimensional space \mathbb{R}^n as follow.

Step 1: Choose an initial cluster centres $z_1, z_2, z_3, \dots, z_K$ randomly from the n points $\{x_1, x_2 \dots, x_n\}$.

Step 2: assign data points $a = A$ to its closest centre and obtain k -partition of A .

Step 3: Recalculate centres for the new partition and go to step 2 until no more data, change their clusters, or the algorithm is converged.

K-means algorithm is minimizing distances of sum of point-to-centroid, over all defined clusters. This is an iterative procedure where centre of each cluster k , and membership values of each cluster (maximum and minimum) can be obtained at the end (Jain, Murty and Flynn, 1999; Bandyopadhyay and Maulik, 2002; Bagirov, 2008; Klawonn, Kruse and Winkler, 2015).

4.6.2 Setting the membership function

To determine membership degree of an object to a certain set, A_{i1}, \dots, A_{im} in equation 4.48 the membership function has to be set (Zadeh, 1965; Mohaghegh, 2000). The membership degree is usually between 0 and 1.

Mathematical expression in equation 4.53 states the membership (1) or non-membership (0) of a component x to a set (universe U). This is a binary issue, which state an object is either belong to a set or not (Zadeh, 1965).

$$\mu_A(x) = \begin{cases} 1, & x \in A \\ 0, & x \notin A \end{cases} \quad 4.53$$

Where $\mu_A(x)$ represents an ambiguous membership of component x in set A , and \in and \notin represent contained or not contained in set A , respectively. Zadeh, (1965) extended classical binary membership of only 0 and 1 to a real continuous intervals where the numbers between 0 and 1 can represent various degree of a membership of an object to a set. This mathematically can be represented as follow.

$$\mu_A: U \rightarrow [0,1] \quad 4.54$$

Where U represents a universal set defined for specific problem in fuzzy set A . For instance if $U = \{x_1, x_2, \dots, x_n\}$, then the degree of membership of x_1, x_2, \dots, x_n in U can be defined by the following equation.

$$A = \{(\mu_A(x_1)|x_1), (\mu_A(x_2)|x_2), \dots, (\mu_A(x_n)|x_n)\} \quad 4.55$$

The relation between the input/output are defined by fuzzy if/then rules, where conclusion can be achieved based on the hypothesis. This explain the principle of an inference mechanism that states if a fact of a hypothesis is known then another fact or conclusion can be reached (Shokir, 2008).

The information that how the data points are distributed in the input space would provide the guideline for creating number of fuzzy clusters and their detection. Cluster centres and eigenvalues of fuzzy covariant matrices can be used for capturing this information (Takagi and Sugeno, 1985; Shokir, 2006, 2008). For example if the input space of i th cluster centre is $v_{i1}, v_{i2}, \dots, v_{im}$, then the antecedent fuzzy sets of TSK model can be defined by any membership function. In this study gaussian membership function is employed to define the antecedent fuzzy sets as follow.

$$\mu_{Ai}(v_i) = \exp\left(-\frac{(v_i - c_i)^2}{2\sigma_i^2}\right) \quad 4.56$$

Where v_{ij} is scalar values of inputs, σ_i is standard deviation and c_i is the mean of the i th fuzzy set A_i . The centre c_i and variance σ_i of the membership function is shown in following figure.

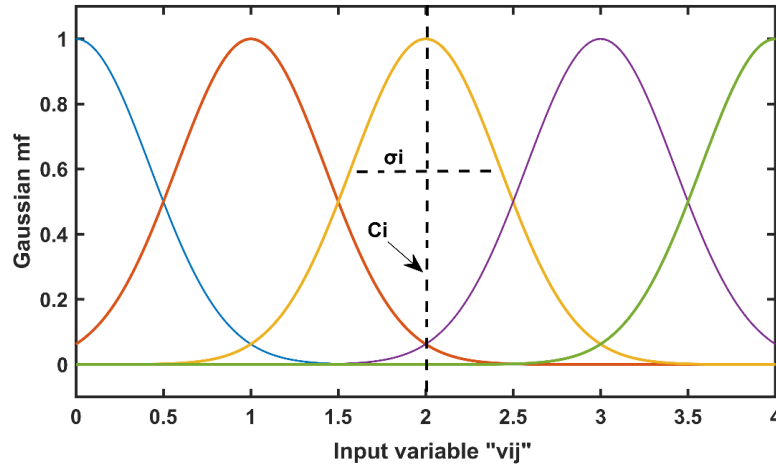


Figure 4.16. Gaussian membership function for detecting fuzzy clusters.

4.6.3 Determination of constants

In order to develop condensate viscosity correlation the data bank collected from open literature, divided to two parts, where 242 of these data sets randomly selected to build the TSK model and 84 data sets utilized to test the developed model. The data sets $N=1,2,\dots, 242$ have been organized in a matrix form with dimension of a 242×4 , as shown in equation 4.57. Having determined optimum number of clusters using Calinski and Harabasz, (1974) method, K-mean algorithm has been applied to define the range of each cluster. Gaussian membership function then used to determine how a data point belongs to a defined cluster by means of membership degree between 0 and 1. Figure 4.17 illustrates the output respond of Gaussian membership functions to one of the inputs (reservoir pressure).

$$N = \begin{bmatrix} P_1 & T_1 & RS_1 & \mu_{c1} \\ P_2 & T_2 & RS_2 & \mu_{c2} \\ \vdots & \vdots & \vdots & \vdots \\ P_N & T_N & RS_N & \mu_{cN} \end{bmatrix} \quad 4.57$$

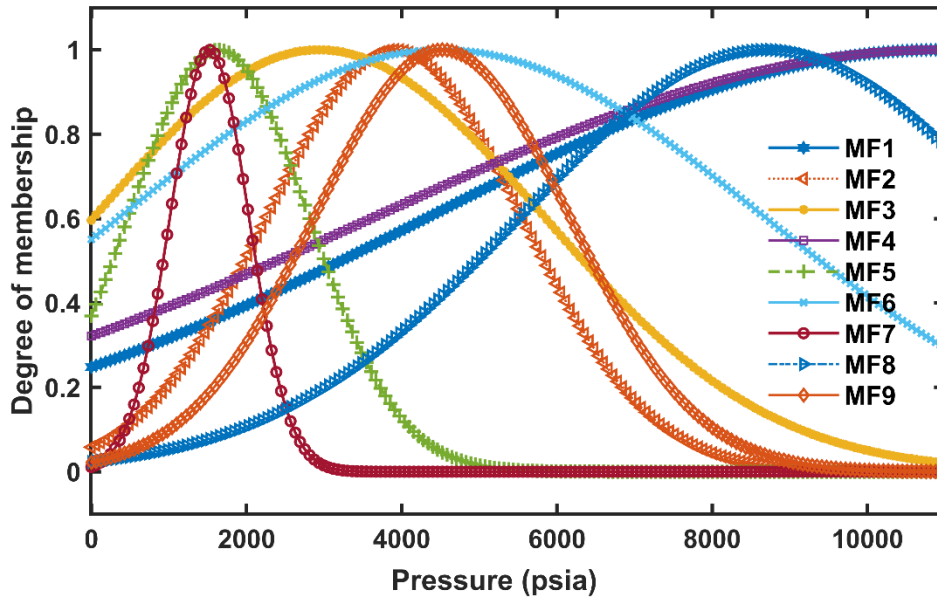


Figure 4.17. Gaussian membership function for input 1 “pressure”.

The consequent parameters of the TSK model $a_{i0}, a_{i1}, \dots, a_{im}$ term in equation 4.48 are computed using least-square approximation method in the following fashion.

If X denotes to a matrix having i th row in the input vector of x_i (inputs), Y represents a vector column with y_i (output) as its i th component and w_i denotes to $N \times N$ real matrix, then the degree of firing β_{ij} is defined by equation 4.57. The β_{ij} is j th diagonal of the real matrix. (Takagi and Sugeno, 1985; Shokir, 2008).

$$\beta_{ij} = \frac{\beta_i(x_i)}{\sum_{z=1}^c \beta_i(x_j)} \quad 4.58$$

And if $\theta_i = [a_{i1}, \dots, a_{im}, a_{i0}]$ represents consequent parameters of i th rule in each vector, in order to determine a_{i0} in θ_i , a unitary column I is added to the matrix X , $X_e = [X, I]$. This is an extended matrix for the input values, then θ_i is calculated by the following equation.

$$\theta_i = [X_e^T \cdot W_i \cdot X_e]^{-1} X_e^T \cdot W_i \cdot Y \quad 4.59$$

Where X_e^T is transpose of matrix X_e . The obtained parameters θ_i for each matrix, substituted in equation 4.60 to approximate output value Y .

$$Y \approx X \cdot \theta_i$$

4.60

Y represents condensate viscosity in this study, which can also be represented as a linear function that is explained in following section.

4.6.4 Development of new correlation

In this part of the study, a simple yet accurate correlation has been developed for prediction of condensate (oil) viscosity in gas-condensate reservoirs below the dew point pressure, using TSK fuzzy approach. The proposed correlation is function of pressure, temperature and solution gas to oil ratio. Our reasoning for aforementioned selection of the factors explained in following. Condensate viscosity is direct function of reservoir pressure as changing in pressure due to reservoir depletion has a major impact on this important property (Fevang, 1995; Whitson, 2000). The effect of pressure on condensate viscosity is demonstrated in Figure 4.10 and Figure 4.11. In many gas-condensate reservoirs, condensate liquid developed only when BHFP depleted below the dew point pressure. Moreover, it is well-known that temperature has a significant effect on hydrocarbon viscosity (Gozalpour *et al.*, 2005; Craft and Hawkin, 2015). Another factor that has been considered in developing the viscosity function is solution gas to oil ratio (R_s). Solution gas to oil ratio determine how much gas is dissolved in the liquid, which indicate if the mixture behave more like liquid or gas. This in return directly influence the viscosity of gas-condensate mixture. The recommended linear function in this study has the following form.

$$\mu_c = AP + BT + CR_s + D \quad 4.61$$

Where P, T and R_s stand for reservoir pressure, temperature and solution gas to oil ratio respectively and A, B, C and D are arbitrary constants of the model. Pressure and temperature are directly were imported from the data bank as an input. R_s is calculated from Standing and Katz, (1942) shown in 4.22.

The TSK fuzzy approach is employed to determine and optimize the parameters of A, B, C and D in 4.60. The architecture of fuzzy system using TSK fuzzy with Gaussian

MFs shown in Figure 4.18. Numerical value of 9, next to the inputs, are devoting to the number of rules.

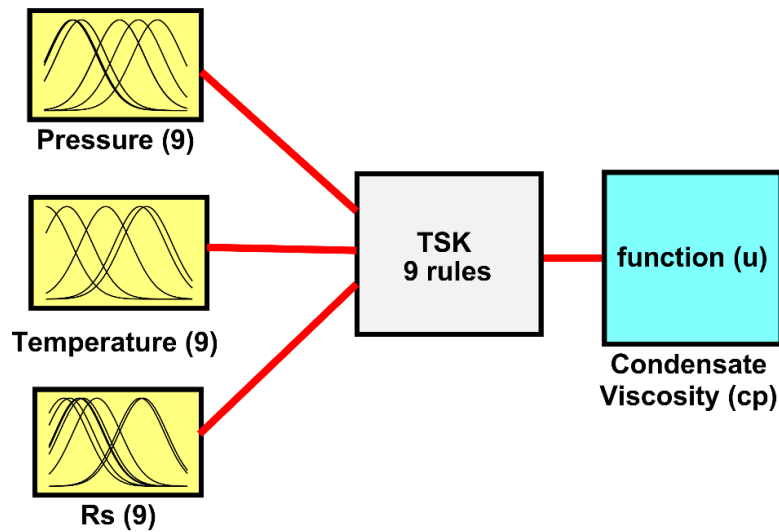


Figure 4.18. Architecture of constructed TSK fuzzy model for predicting condensate viscosity.

The range of each cluster for input variables (P , T , R_s) and the values of constants parameters (A , B , C , D) in equation 4.60 is presented in Table 4.6. For instance, the function introduced in 4.60 can be used in the following fashion:

$$\left\{ \begin{array}{l} \mu_c = AP + BT + CR_s + D \\ R1: \text{if } 44.99 < P < 75.15 \text{ and } 303.15 < T < 405.37 \text{ and } 5245 < R_s < 6101 \\ \text{Then } \mu_c = -0.0063P + 0.0025T + 0.0452R_s + 0.0032 \end{array} \right.$$

Table 4.6. The range of constants and input parameters of proposed condensate viscosity model.

Pressure (MPa)	Temperature (°K)	Rs (scf/STB)	A	B	C	D
44.99 – 75.15	303.15 – 405.37	5245 – 6101	-0.0063	0.0025	0.0452	0.0032
11.29 – 26.93	348 – 404.6	714 – 9732	0.0003	0.0025	-0.0123	-0.0063
19.91 – 20.24	390.72 – 393.15	1167 – 1465	0.0024	0.0022	0.000124	-7.007
50.07 – 75.44	303.15 – 315.92	971 – 3646	0.0011	-0.0056	-0.0017	23.84
7.99 – 11.29	348.15 – 353.92	1160 – 9869	0.0008	-0.0019	0.000012	-0.5807
28.52 – 31.16	323.15 – 353.15	4955 – 6267	0.0006	-0.0034	0.0001	-0.7915
3.55 – 10.49	255.37 – 303.15	4695 – 5425	0.0007	0.0014	0.0001	0.2219
21.90 – 60.08	315.28 – 405.37	1235 – 9186	0.0001	0.00004	-0.001	0.6126
11.29 – 31.16	323.15 – 443.15	2222 – 2618	0.00001	0.0036	-0.0053	13.97

4.6.5 Results and discussions

The new developed model was compared with well-known literature correlations of LBC (1964); Beggs and Robinsons, (1975); Kartoatmodjo and Schmidt, (1991), De Ghetto et al. (1999) and Elsharkawy and Alikhan, (1999). These existing literature

correlations were introduced previously in this chapter. The developed correlation was also compared with other two developed machine learning (ML) based models of ANN and LSSVM in this study. Statistical error parameters of root mean square error (RMSE), mean absolute error (MAE) and average absolute relative deviation percentage (AARD%) shown in Table 4.7, and were used for comparison of the results. RMSE and AARD% were estimated using equations 4.24 and 4.25 respectively. MAE is determined from the following equation.

$$MAE = \frac{1}{n} \sum_{j=1}^n |\mu_{experimental} - \mu_{calculated}| \quad 4.62$$

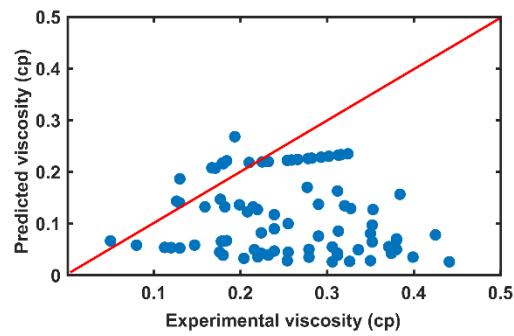
To visualize the performance of the new developed model against other methods graphical error analysis include error distribution and cross plot have been utilized. We tested the prediction performance of the developed correlation as well as other models for condensate viscosity in the range of (0 – 0.5cp). This is because the viscosity of condensate liquid is normally between 0 – 1cp (Fevang, 1995; Whitson and Brulé, 2000) and in lower range, this liquid can flow toward the wellbore along with the gas phase. In higher viscosity range the interfacial tension of the condensate liquid is high, which not allowed the liquid flow towards the wellbore. In higher viscosity range, most of the liquid drop out not able to flow simultaneously with gas phase and trapped inside the porous structure (become non-recoverable condensate). This is due to stronger intermolecular forces that imposed to the liquid droplets in lower viscosity region.

The results indicate that the developed condensate viscosity correlation yields good agreement between the predicted and measured condensate viscosity with the lowest RMSE of 0.0194, MAE of 0.0163, and AARD % of 7.123. The cross plot of estimated against experimental condensate viscosity is presented in Figure 4.19A-H. From the results we can see that Kartoatmodjo and Schmidt, (1994) has the highest scattering around zero error line while Beggs and Robinson, (1975) provides least spreading for prediction of condensate viscosity. The reason for the high error by utilized literature models is might due to individual limitation of each model and also different oil type (e.g., oil with lower API gravity) that was used in their development. Both ANN and LSSVM performance for prediction of condensate viscosity are good in lower range of (0 – 0.3cp) as it shown in Figure 4.19F and Figure 4.19G. However, in higher viscosity range between 0.3 – 0.5cp, the data scatter and their prediction performance

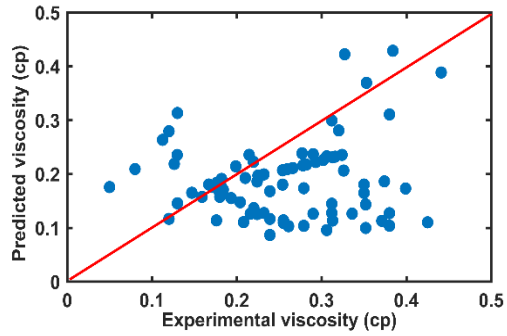
deteriorate. This is because the majority of the utilized data bank (73%) that used in development of ANN and LSSVM models are within the range of 0 – 0.4cp. Hence, their performance is better within aforementioned range are more accurate. Although the error is high in higher viscosity range, but still the performance of these two ML based models are better than existing literature correlations. This inconsistency of condensate viscosity prediction by ANN and LSSVM was tackled in this study using TSK fuzzy approach. Figure 4.19H depicts the performance of the developed condensate viscosity model using TSK fuzzy approach in the range of (0 – 0.5cp). The result confirms that TSK fuzzy model well predicts experimental viscosity in aforementioned range.

Table 4.7. Statistical accuracy of condensate phase viscosity models.

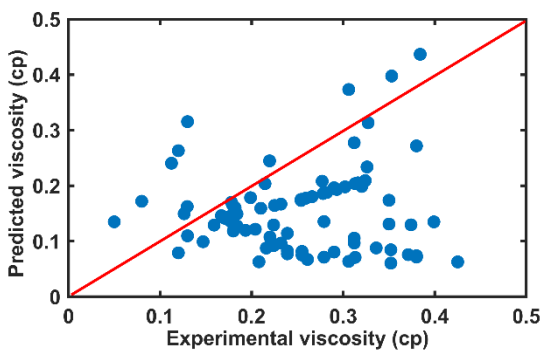
Method	RMSE	MAE	AARD%
Lohrenz-Bray-Clark (1964)	0.1826	0.1493	54.98
Beggs and Robinson (1975)	0.1205	0.0926	39.14
Elsharkawy and Alikhan (1999)	0.1468	0.1199	47.75
De Ghetto (1994))	0.1427	0.1149	45.19
Kartoatmodjo and Schmidt, (1994)	0.1865	0.1666	63.49
ANN	0.0656	0.0474	20.11
LSSVM	0.074	0.0631	26.50
TSK Fuzzy	0.0194	0.0163	7.123



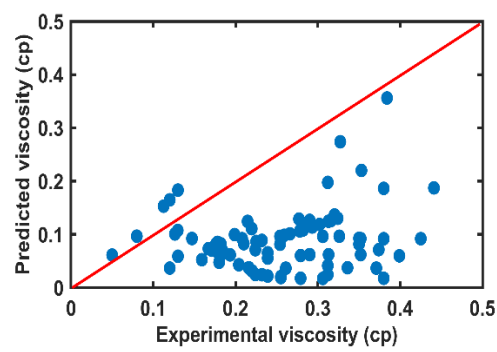
Lohrenz-Bray-Clark, (1964) [A]



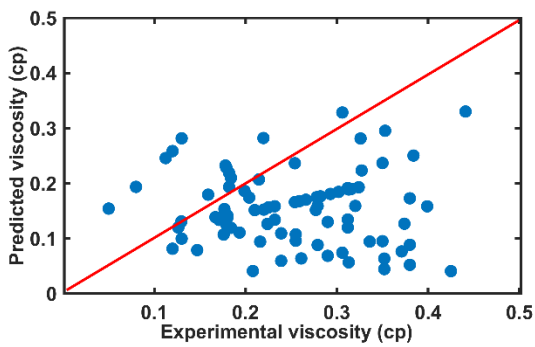
Beggs and Robinson, (1975) [B]



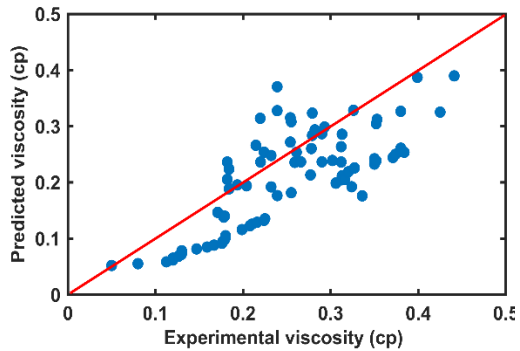
De Ghetto et al., (1994) [C]



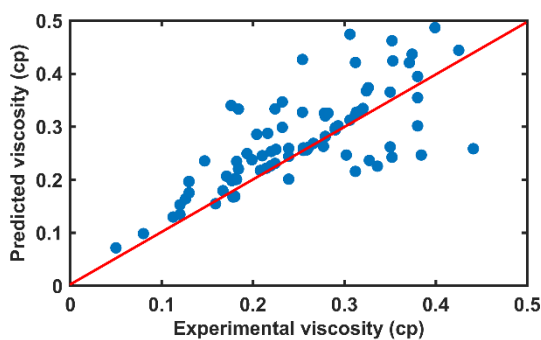
Kartoatmodjo and Schmidt, (1994) [D]



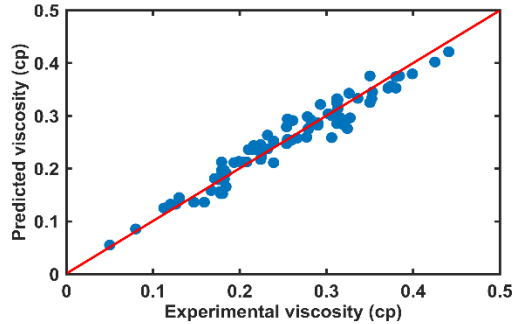
Elsharkawy and Alikhan, (1999) [E]



LSSVM [F]



ANN [G]

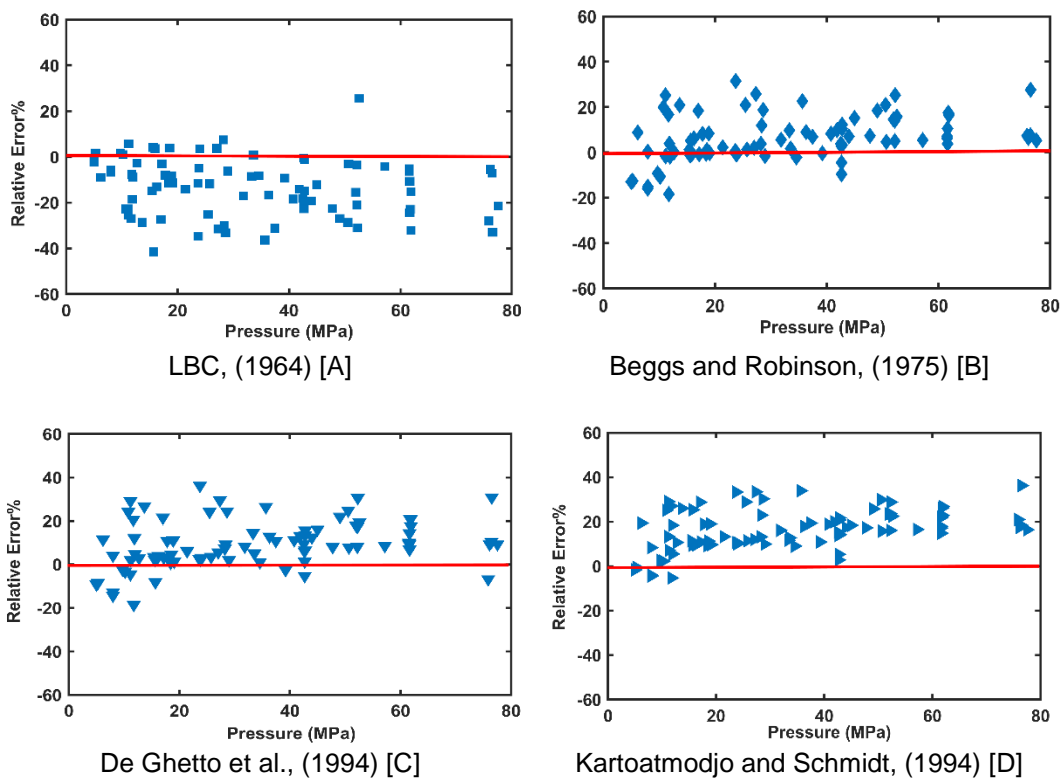


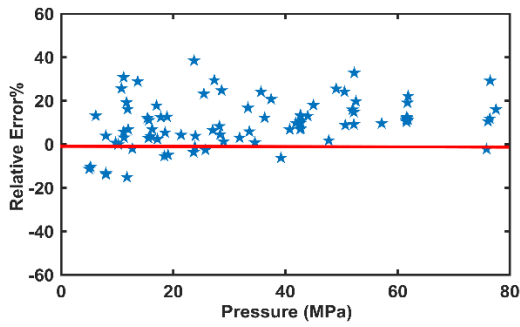
TSK Fuzzy method [H]

Figure 4.19. Cross plot of estimated against condensate viscosity measurements of existing literature correlation, ANN, LSSVM and TSK Fuzzy method.

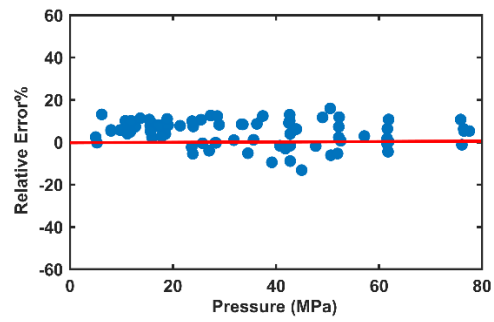
It is important to know how the developed models behave in prediction of condensate viscosity as a function of pressure and temperature. This is because condensate viscosity is strong function of pressure and temperature. Therefore, Figure 4.20A – H and Figure 4.21A – H were generated, which illustrate how each model performs in predicting condensate viscosity using relative errors percentage based on reservoir pressure and temperature. Both figures confirm that the developed correlation using TSK fuzzy approach scatter less than other models around the zero error line. In addition, the results show that compositional model of LBC, (1964) underestimates the condensate viscosity while other correlations are overestimating the condensate viscosity in specified pressure range of (0.25 – 75.84 MPa) and temperature range of (303 – 443.15°K).

Figure 4.20H and Figure 4.21H both are showing that the new condensate viscosity model is responding very well to the pressure and temperature change in prediction of condensate viscosity, while existing literature models cannot cope with non-linearity of the gas-condensate system due to pressure/temperature change in the system. This confirms by poor performance of the existing literature models depicted in Figure 4.20A – E.

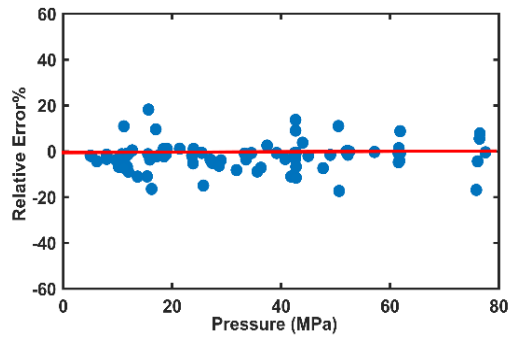




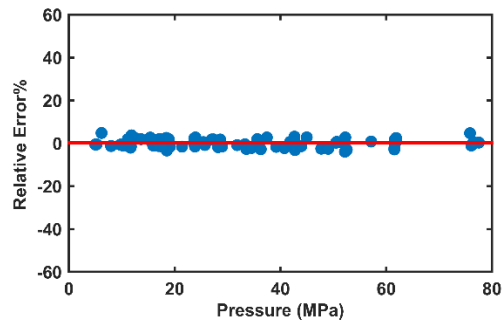
Elsharkawy and Alikhan, (1999) [E]



LSSVM [F]

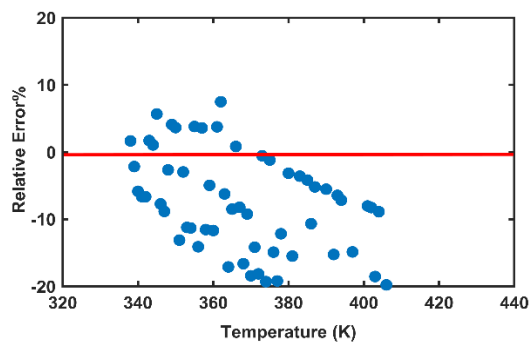


ANN [G]

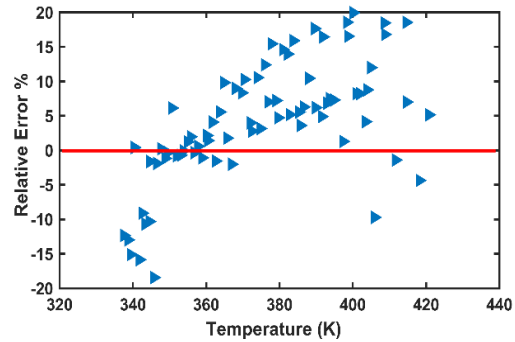


TSK Fuzzy [H]

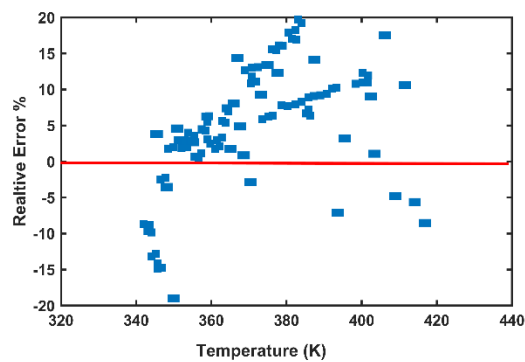
Figure 4.20. Residual plot of relative error percentage for different viscosity models as a function of reservoir pressure.



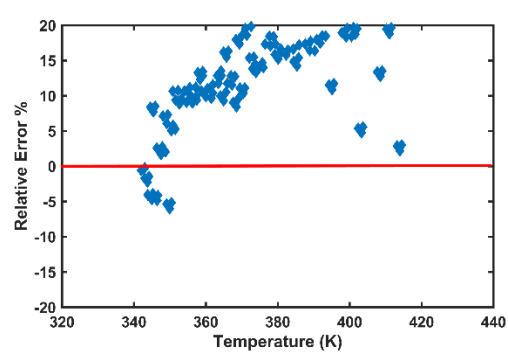
Lohrenz-Bray-Clark, (1964) [A]



Beggs and Robinson, (1975) [B]



De Ghetto et al., (1994) [C]



Kartoatmodjo and Schmidt, (1994) [D]

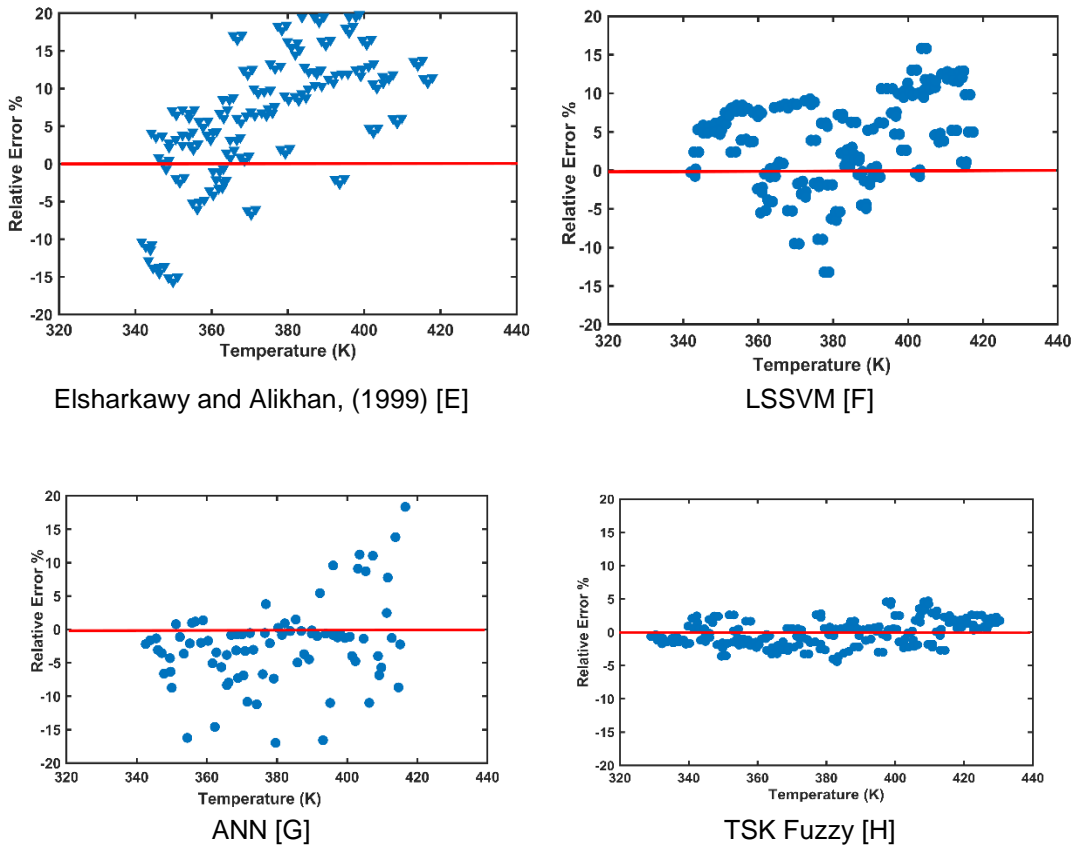


Figure 4.21. Residual plot of relative error percentage for different viscosity models as a function of reservoir temperature.

In order to see the effect of temperature, pressure and solution gas to oil ratio on condensate viscosity, the trend analysis of the developed model has also been studied. Figure 4.22A – C show the effect of reservoir pressure in the range of (0 – 78MPa) on condensate viscosity. As the pressure increases condensate oil viscosity is also increasing. The results also comply with the physics of the problem as explained in following.

In gas-condensate reservoirs with depletion mode of recovery in the beginning of the production, the initial reservoir pressure is high and condensate liquid behave like a gas phase, due to existing very high amount of (R_s) in the mixture. The relationship between R_s and reservoir pressure in this study is illustrated in Figure 4.23. As the reservoir pressure depleted, it reaches the dew point pressure where hydrocarbon liquid phase developed, the amount of dissolved gas (R_s) is decreasing proportionally with pressure reduction. Hence, in lower reservoir pressure there is less amount of dissolved gas, which in return increase the viscosity of the condensate liquid (Bergman and Sutton, 2007a; Hemmati-Sarapardeh *et al.*, 2014). The result in Figure 4.22B also

confirms the aforementioned criterion. As it can be seen from these Figure 4.22 and Figure 4.23, the developed condensate viscosity correlations are following the physical trend of the experimental data with very good accuracy.

The effect of temperature on condensate viscosity within the temperature range of (338 – 420°K) illustrated in Figure 4.22C. It is well known that increasing temperature will decrease the viscosity of the liquid either in isobaric condition or as saturated liquid condition (Craft and Hawkin, 2015, p. 511). According to the particle theory when temperature of a liquid increases this would increase distance between the molecules, which reduce the binding forces that hold the molecules of the liquid. This proportionally decrease the viscosity of the liquid. The result presented in Figure 4.22C satisfies the particle theory very well and confirms the validity of the developed TSK model for prediction of condensate viscosity as a function of temperature.

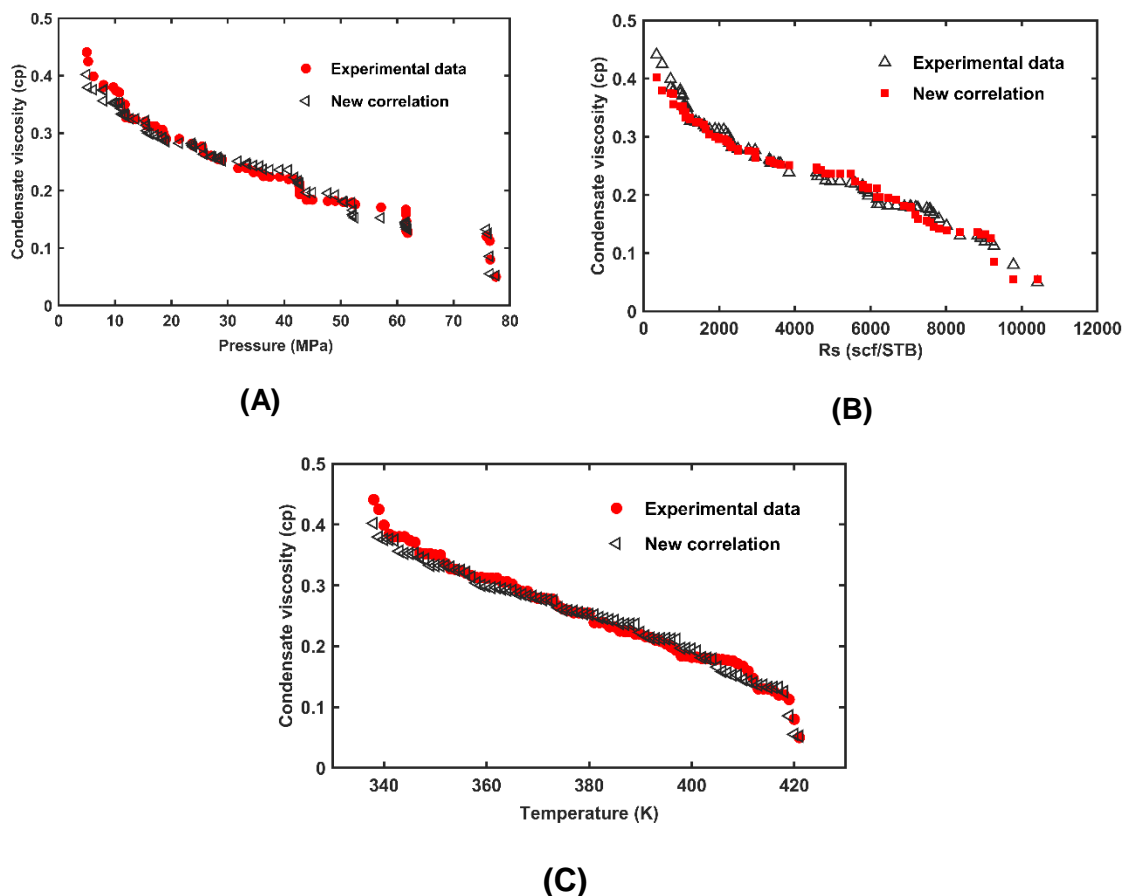


Figure 4.22. Experimental prediction capability of the developed TSK fuzzy model as a function pressure (A), solution gas to oil ratio (B) and temperature (C).

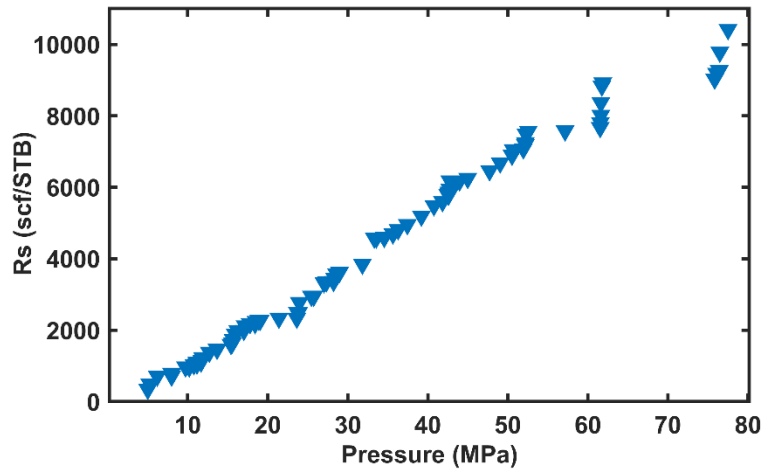


Figure 4.23. The relation between pressure and solution gas to oil ratio (R_s) for the utilized databank.

4.7 Mamdani Fuzzy Approach

In previous section, it has been observed that using TSK fuzzy approach given promising results for prediction of condensate viscosity. In this section another well known fuzzy logic approach known as Mamdani fuzzy is applied for better modelling of condensate viscosity in gas-condensate reservoirs.

Mamdani fuzzy approach has been applied for many engineering applications. The main reason for using this method was to use completely new methodology based on linguistic approach in modelling gas-condensate PVT property (condensate viscosity) and simplify the computational procedure.

In this section, first we introduce the nature of fuzzy algorithm and show how Mamdani method embedded in the algorithm. Then the detail description of Mamdani approach for modelling condensate viscosity will be provided.

4.7.1 Fuzzy Engine process

It is concluded by Biezma et al., (2018) that the fuzzy system introduced by Zadeh, (1973) has three main following features.

- Linguistic variables instead of or in addition to numerical variables
- An inference mechanism that uses approximate reasoning algorithms;
- Simple relations between the variables in terms of IF-THEN rules to formulate complex relationships.

These aforementioned characteristics of FL allow us to deal with any problem that has imprecise, ambiguous and vague information to be dealt with conventional binary logic. Figure 4.24 depicts the relationship between aforementioned three features introduced by Zadeh, (1973) in a typical fuzzy logic system.

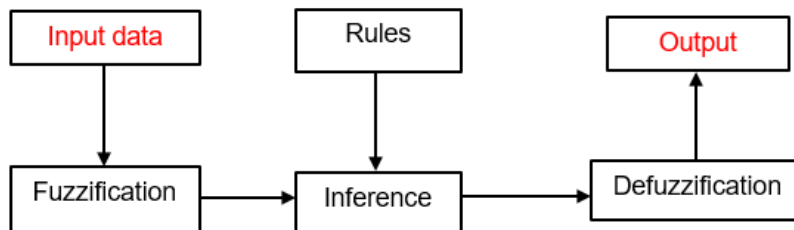


Figure 4.24. General architecture of a Fuzzy Logic System (FLS).

The input data is the condensate viscosity data including pressure, temperature and solution gas to oil ratio (R_s). The output of the system would be condensate viscosity. In the fuzzification step, the considered value of the input variables converted into grades of memberships of fuzzy sets. Fuzzy sets are defined by membership functions (e.g., Triangular, Gaussian, Trapezoid, etc.). These MFs utilizes the spectrum of logical values between 0 and 1. To achieve the spectrum membership functions are divided into certain number of subsets identified with linguistic terms (e.g., Very Low, Low, Medium, High and Very High).

In next step having generated number of fuzzy rules either manually or automatically, these so called IF-THEN rules transferred into the inference fuzzy engine for fuzzy reasoning and establishing input, output relationship. During the process several fuzzy rules are fired in parallel-rule firing to allow simultaneous consideration of all the information (Ahmadi and Ebadi, 2014; Mohaghegh, 2000; Ross, 2017). The information generated in fuzzy inference system should be defuzzified to be able to see a numerical values in the form of a crisp sets. Mathematically, the defuzzification of a fuzzy sets are the process of “rounding it off” from its location in the unit hypercube to the nearest. The last step is implementation of the defuzzified fuzzy sets to obtain the produced output from fuzzy inference system (FIS) in the form of crisp values.

The detail of each step for modelling condensate viscosity is explained in following sections.

4.7.2 Membership Functions (MFs) fuzzification

The role of MFs in any fuzzy inference system discussed in details in section 4.6.2, here the focus is on using different type of MFs in fuzzy inference systems.

All the information in fuzzy set is described by its membership function, which they can be symmetrical or asymmetrical. This can specify the degree of membership of input variables to different subsets (e.g., Very Low, Low, Medium, High, and Very High). Different kind of MFs with the variety of the detected advantages and disadvantages have been proposed in literature. It is very important to select right type of membership function suitable to the relevant problem as success of one MF in one problem cannot guarantee its applicability to another.

Several geometrical shapes proposed in literature for defining MFs. In this study we choose three most widely used MFs in literature include gaussian, triangular and trapezoidal due to their flexibility, transmissibility and eye catching ability (Ahmadi and Ebadi, 2014; Hameed, 2011; Khazali et al., 2019). In this part we examine the performance of these three well-known membership functions for determination of condensate viscosity in gas-condensate reservoirs.

Gaussian MFs, defined by equation 4.63, are suitable for problems that require continuously differentiable curves and smooth transition (Hameed, 2011). Gaussian MFs initially utilized to relate the three inputs (pressure, temperature and R_s) to one output (condensate viscosity) of FIS system.

$$f(x; \sigma, c) = e^{-\left(\frac{x-c}{2\sigma^2}\right)^2} \quad 4.63$$

Where c is the centre (i.e., mean) of i th fuzzy set and σ is the width (i.e., standard deviation) of the i th fuzzy set.

Based on the above formula the three inputs of pressure, temperature and solution gas to oil ratio (R_s) and one output of condensate viscosity were defined. Then several main linguistic subsets known as Very Low (VL), Low (L), Medium (M), High (H) and Very High (VH) used to interrelate the inputs and output. Figure 4.25A-D is illustrating the input and output parameters of Mamdani approach using Gaussian MF.

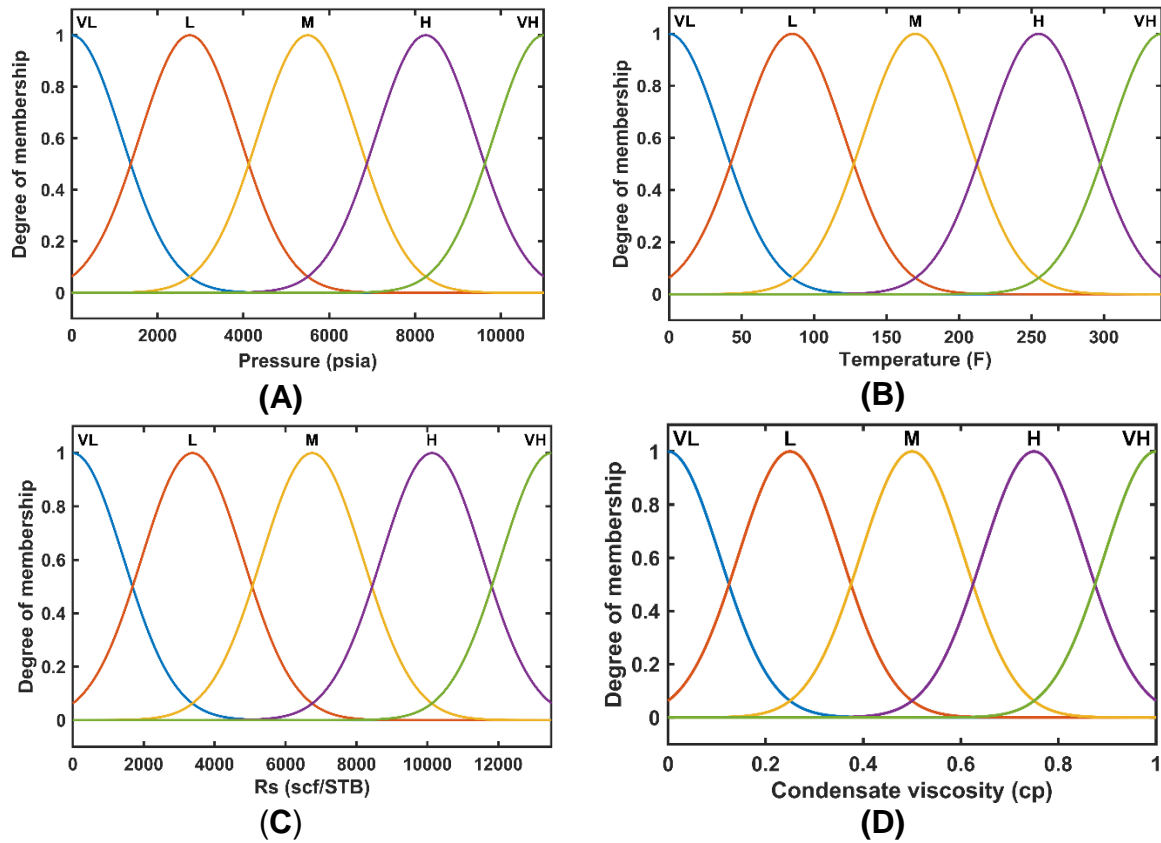


Figure 4.25. The constructed gaussian membership function representing (A) pressure (B) temperature (C) solution gas to oil ratio and (D) condensate viscosity.

The triangular shape MFs are the second most important and widely used function in fuzzy inference systems. The triangular shape is vector of x and depends on three scalar parameters a , b and c . The scalar parameters are basically representing the three sides of triangle. Mathematically triangular MFs are defined as follow.

$$f(x; a, b, c) = \left\{ \begin{array}{ll} 0, & x \leq a \\ \frac{x - a}{b - a}, & a \leq x \leq b \\ \frac{c - x}{c - b}, & b \leq x \leq c \\ 0, & x \geq c \end{array} \right\} \quad 4.64$$

Graphical representation of triangular MFs for condensate viscosity estimation depicted in following figure.

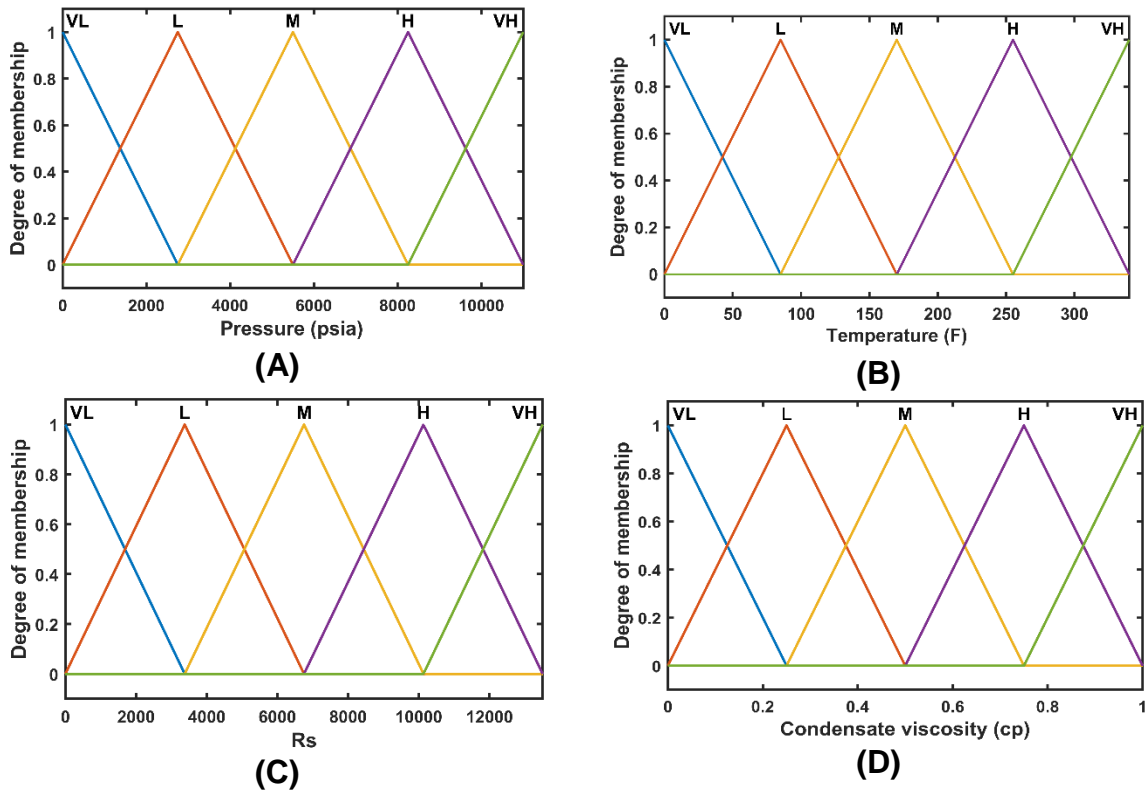


Figure 4.26. The constructed triangular membership function representing (a) pressure (b) temperature (c) solution gas to oil ratio and (d) condensate viscosity.

In the last step of this level to relate the inputs and output parameters of condensate viscosity within linguistic subintervals, trapezoidal membership functions have been utilized. Mathematical definition of trapezoidal MF is given in equation 4.65. The trapezoidal shape is a function of a vector, x , and four scalar parameters of a , b , c and d . The parameters of a and d represent the “feet” of the trapezoid and b and c represent the “shoulder” (MathWorks, 2019). Figure 27A-D illustrates the trapezoidal MFs for three inputs of pressure, temperature and solution gas to oil ratio and the output of condensate viscosity.

$$f(x; a, b, c, d) = \left\{ \begin{array}{ll} 0, & x \leq a \\ \frac{x-a}{b-a}, & a \leq x \leq b \\ 1, & b \leq x \leq c \\ \frac{d-x}{d-c}, & c \leq x \leq d \\ 0, & x \geq d \end{array} \right\} \quad 4.65$$

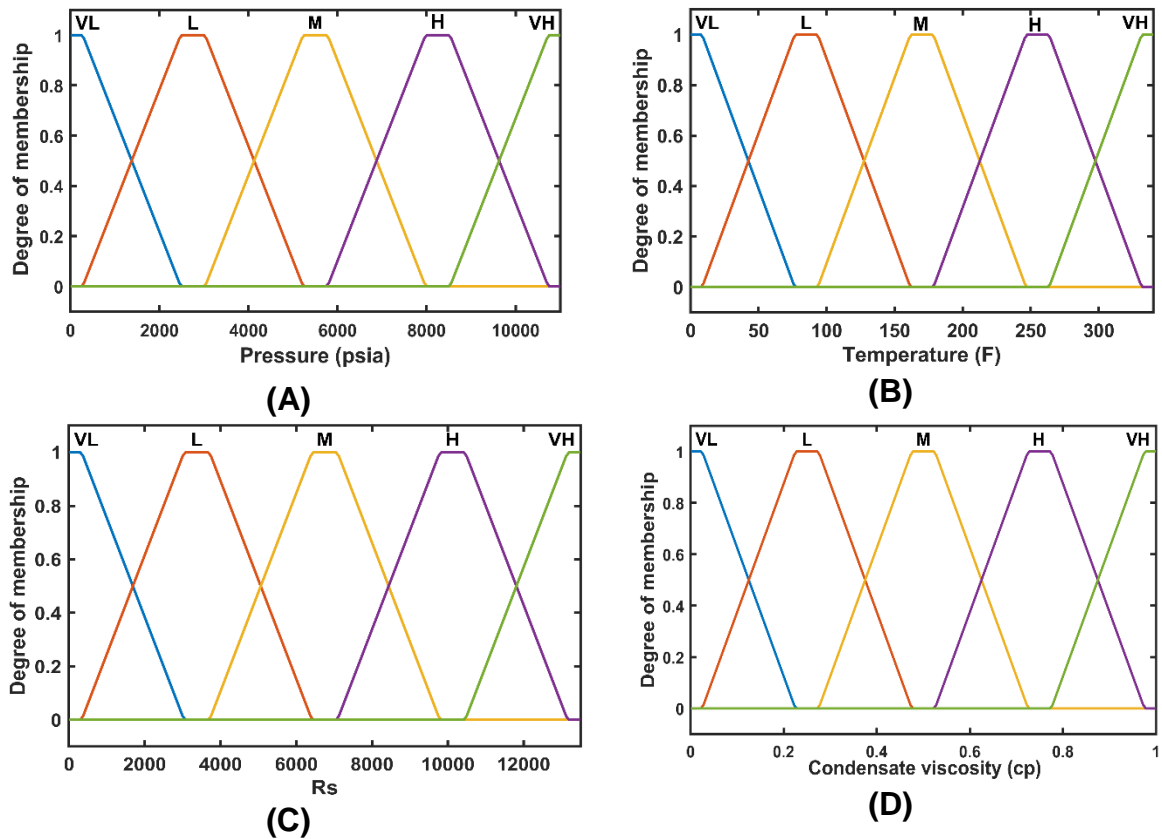


Figure 4.27. The constructed trapezoid membership functions (A) pressure (B) temperature (C) solution gas to oil ratio and (D) the condensate viscosity.

4.7.3 Mamdani Fuzzy Inference System

Having defined the MFs in previous section, the expert knowledge has been introduced into the fuzzy inference system, defining IF-THEN rules. The degree of membership in one fuzzy set is determined by IF portion of the rule and the consequence associated with system output is determined by THEN portion of the rule.

To implement IF-THEN rule procedure, Mamdani FIS is proposed by Mamdani and Assilian, (1975) and widely accepted among the fuzzy community due to the following advantages (Asklany *et al.*, 2011; MathWorks, 2019).

- Very fast computational procedure
- Easy to implement
- It is intuitive
- Well suited to human input

The applicability of Mamdani fuzzy approach for modelling condensate viscosity is examined by this study.

In this method the fuzzy sets from the consequent of each rule are combined through the aggregation operator and the resulting fuzzy set is defuzzified to yield the output of the system (Mamdani and Assilian, 1975; Asklany *et al.*, 2011). The typical IF-THEN rule of the Mamdani algorithm is shown in the following equation.

$$IF x_1 \text{ is } A_1 \text{ AND } x_2 \text{ is } A_2 \dots \text{ AND } x_n \text{ is } A_n \text{ THEN } y \text{ is } B \quad 4.66$$

Where: $x_{1,2,\dots,n}$ are input variables; $A_{1,2,\dots,n}$ are value of a certain linguistic input (VL, L, M, H or VH); y is output and B is value of the output (VL, L, M, H or VH).

In this study the parameters of pressure, temperature and solution gas to oil ratio (R_s) are input variables and condensate viscosity is the output variable. The relationship between considered input variables and condensate viscosity (μ_c) is defined by set of 15 rules shown in Table 4.8. These set of rules are including all input, output relationship possibilities.

This table is read from left to right for instance, rule no 1 can be read as follow:

IF *Pressure* is VL AND *Temperature* is VLLMHVH AND R_s is VLLMHVH THEN *Condensate Viscosity* is VL.

Where VLLMHVH = Very Low, Low, Medium, High or Very High.

Table 4.8. Fuzzy rules defined for estimation of condensate viscosity in gas-condensate reservoirs.

no	Pressure (psia)	Temperature (F)	R _s (scf/STB)	Condensate Viscosity (cp)
1	VL	VLLMHVH	VLLMHVH	VL
2	L	VLLMHVH	VLLMHVH	L
3	M	VLLMHVH	VLLMHVH	M
4	H	VLLMHVH	VLLMHVH	H
5	VH	VLLMHVH	VLLMHVH	VH
6	VLLMHVH	VL	VLLMHVH	VL
7	VLLMHVH	L	VLLMHVH	L
8	VLLMHVH	M	VLLMHVH	M
9	VLLMHVH	H	VLLMHVH	H
10	VLLMHVH	VH	VLLMHVH	VH
11	VLLMHVH	VLLMHVH	VL	VL
12	VLLMHVH	VLLMHVH	L	L
13	VLLMHVH	VLLMHVH	M	M
14	VLLMHVH	VLLMHVH	H	H
15	VLLMHVH	VLLMHVH	VH	VH

Maximum – minimum (max-min) composition method was utilized to implement Mamdani FIS model as one of the most common type in literature (Ross, 2017). The max-min method is initially used by Zadeh, (1965) in definition of approximate reasoning using natural language IF-THEN rules. In max-min method minimum operator is used to model the implication and the resulting output membership functions are combined by using maximum operator (Hameed, 2011; Ross, 2017; Biezma, Agudo and Barron, 2018).

4.7.4 Defuzzification in Mamdani approach

Defuzzification is required to convert the fuzzified quantity of inputs to a precise quantity of output. There are many methods in literature for defuzzification of FIS output. In this study we used Centroid or centre of gravity (COG) method as one of the most prevalent and physically attractive among all the defuzzification methods (Takagi and Sugeno, 1985; Leekwijck and Kerre, 1999; Ross, 2017, p. 121). Centroid

defuzzification returns the centre of area under the curve using integration technique as expressed by the following equation.

$$\mu_{centre} = \frac{\int x \cdot \mu(x) dx}{\int \mu(x) dx} \quad 4.67$$

Where $\mu(x)$ is representing values of membership functions obtained from output of FIS engine, μ_{centre} is the centre of the fuzzified membership functions. The integrals are taken over the entire range of the FIS output (condensate viscosity) and present the μ_{centre} as a crisp value.

This crisp value is the numerical value of condensate viscosity returned by the FIS system. All calculation procedure of the Mamdani approach carried out in MATLAB.

Three Mamdani fuzzy using the above discussed procedure was constructed with different membership functions for prediction of condensate viscosity. Figure 4.28 represents the constructed Mamdani fuzzy model using Gaussian MFs. Another two Mamdani fuzzy systems using Triangular and Trapezoidal membership function were constructed in similar fashion. Numerical values of 5 next to the inputs and output of the system represent utilized 5 linguistic terms of Very Low (VL), Low (L), Medium (M), High (H) and Very High (VH).

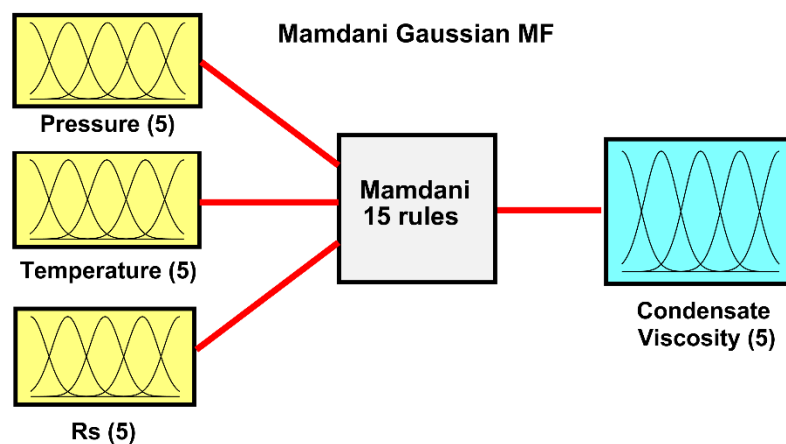


Figure 4.28. Architecture of the fuzzy inference (FIS) system for predicting condensate viscosity using Gaussian membership function.

4.7.5 Results and Discussion

The accuracy of the developed Mamdani fuzzy model using three types of MFs in prediction of condensate viscosity was quantified by metric quantifiers of root mean square error (RMSE), average absolute relative deviation percentage (AARD%) and

mean absolute error (MAE) shown in equations 4.24, 4.25 and 4.61 respectively. The performance of the developed models compared to four existing live oil viscosity models of Bergman and Sutton, (2007), De Ghetto et al., (1994), Elsharkawy and Alikhan, (1999) and Kartoatmodjo and Schmidt, (1994). Summary of the statistical error analysis is presented in Table 4.9.

Table 4.9. Statistical error comparison between Mamdani fuzzy approach with three MFs and existing literature models for prediction of condensate viscosity.

Method	RMSE	MAE	AARD%
Bergman (2000)	0.3287	0.2635	104.65
Elsharkawy and Alikhan (1999)	0.2744	0.1935	60.64
De Ghetto (1994)	0.2656	0.1842	57.47
Kartoatmodjo and Schmidt (1994)	0.2924	0.2185	62.92
Mamdani approach (Triangular MF)	0.3265	0.1389	73.99
Mamdani approach (Trapezoid MF)	0.2057	0.1644	46.45
Mamdani method (Gaussian MF)	0.0556	0.0443	17.22

To visualize the performance of the developed Mamdani fuzzy model for prediction of condensate viscosity, graphical representation of the results in terms of cross plot were generated. The aim of this graphical error analysis is to demonstrate how the prediction deviate from zero error line or 45°, the slope. This slope line is representing zero error and make perfect match between measured and calculated values (Mansour *et al.*, 2013; Aily *et al.*, 2019). Figure 4.29A, Figure 4.30A and 4.31A depict the cross plot of developed Mamdani fuzzy model with Gaussian, Triangular and Trapezoidal MFs for prediction of condensate viscosity. Mamdani fuzzy models with gaussian MFs, Figure 4.29A, predicted values of condensate viscosity close to the diagonal line (zero error line) for all condensate viscosity ranges between 0 – 1cp. This model outperformed other utilized techniques with lowest RMSE of 0.0556, MAE of 0.0443 and AARD% of 17.22%.

The statistical error analysis for implemented triangular based fuzzy model, shows that this model predicts condensate viscosity with RMSE of 0.3265, MAE of 0.1389 and AARD% of 73.99. As can be seen from Figure 4.30A cross plot of triangular based

Mamdani fuzzy model the estimated values are not in good match with diagonal line especially in higher condensate viscosity range ($\mu_{conde} \geq 0.35cp$).

Figure 4.31A demonstrates graphical error estimation of trapezoidal MF's based Mamdani fuzzy model for forecasting condensate viscosity. This model predicts condensate viscosity with RMSE of 0.2057, MAE of 0.1644 and AARD% of 46.45. Comparing the prediction performance of all three fuzzy models verify that using the developed Mamdani fuzzy models incorporated with triangular and trapezoidal MFs predict condensate viscosity with uncertainty. The large uncertainty of these two models is because the triangular and trapezoidal MFs are not able to include all ranges of condensate viscosity or all ranges of input variables (pressure, temperature and solution gas to ratio).

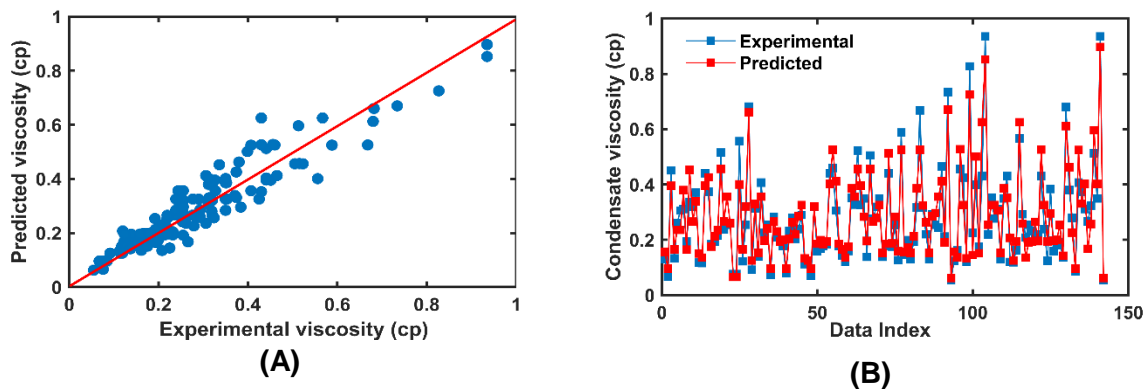


Figure 4.29. Performance prediction of Gaussian based MFs Mamdani fuzzy model in predicting condensate viscosity.

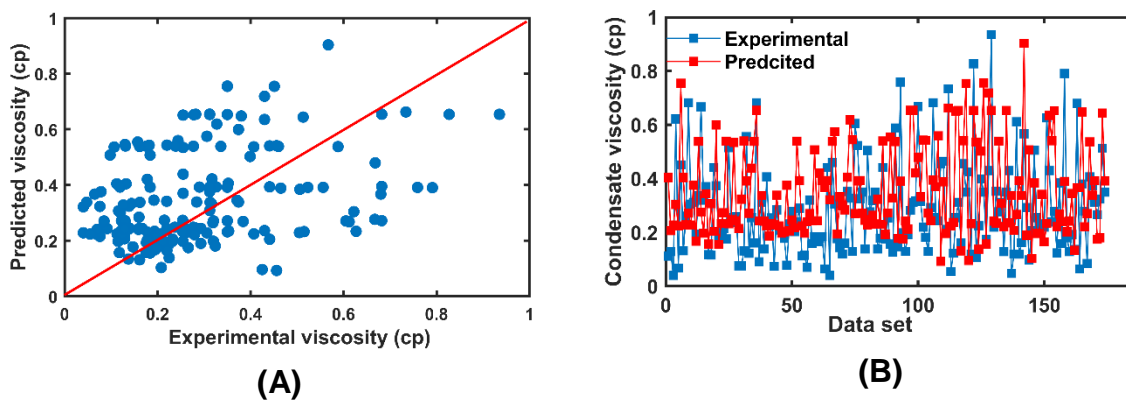


Figure 4.30. Performance prediction of triangular based MFs Mamdani fuzzy model in predicting condensate viscosity.

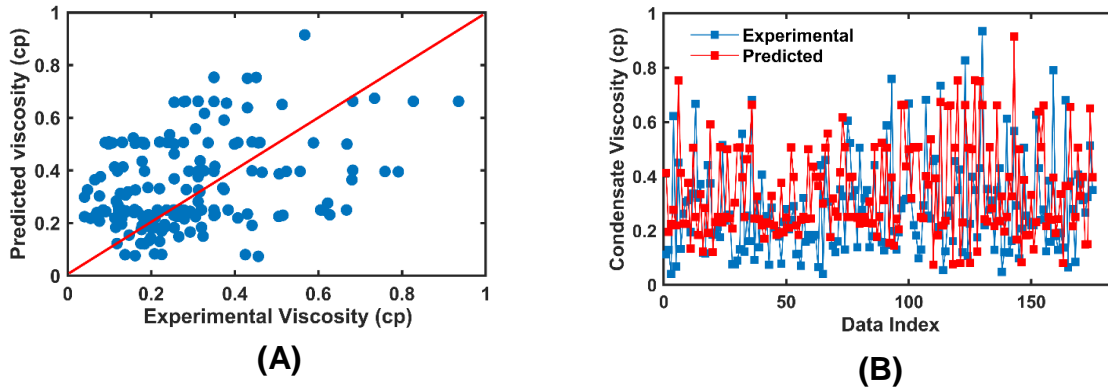


Figure 4.31. Performance prediction of trapezoidal based MFs Mamdani fuzzy model in predicting condensate viscosity.

To further illustrate the performance of the developed Mamdani fuzzy models for prediction of condensate viscosity the time series graphs are generated and shown in Figure 4.29B, Figure 4.30B and Figure 31B for gaussian, triangular and trapezoidal based Mamdani fuzzy models respectively. These graphs highlight the contrast between the developed Mamdani fuzzy model outputs and condensate viscosity measured experimental values versus relevant data index. From these figures, it can be seen that the Gaussian-based Mamdani fuzzy approach forecast the condensate viscosity in all data indexes while other two models deviate from the experimental data. From the graphical and statistical error analysis of this work, it can be concluded that the fuzzy model with Gaussian membership function can predict the condensate viscosity in depleted gas-condensate reservoirs with acceptable accuracy in compare to triangular and trapezoidal fuzzy models and also live oil literature correlations.

To make sure the developed Mamdani fuzzy models are physically following the trend of the condensate viscosity a set of data from Coats, (1986) was selected. The performance of the Mamdani fuzzy with gaussian MFs as well as existing literature correlations was tested using experimental data as a function of pressure. Figure 4.32 depicts this comparison and show satisfactory match that achieved between developed Gaussian MFs based fuzzy model and target condensate viscosity data. Variation of condensate viscosity with pressure can be observed from Figure 4.32, where reducing the reservoir pressure would decrease the condensate viscosity. This is a true characterization of condensate liquid viscosity, hence the developed fuzzy model is valid physically for prediction of condensate liquid viscosity.

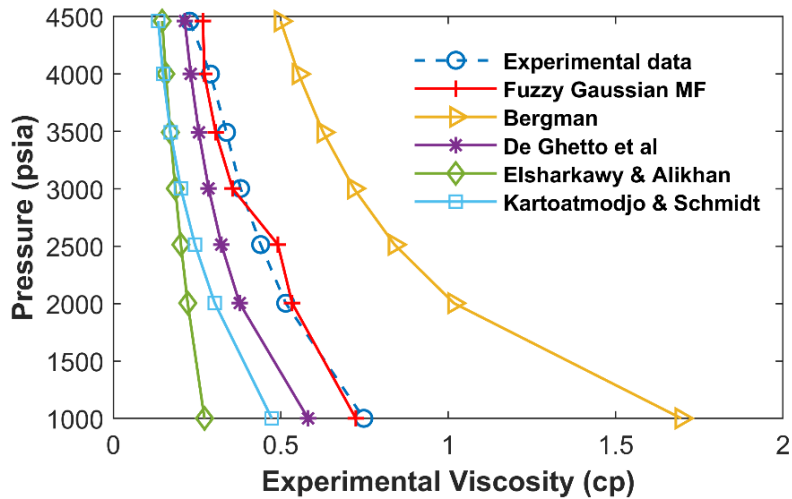


Figure 4.32. Performance of utilized literature correlations and Mamdani fuzzy model with gaussian MFs for predicting condensate viscosity as a function of pressure; sample from Coats, (1986).

The effect of solution gas to oil ratio (R_s) on condensate viscosity is also investigated and shown in Figure 4.33. Confirmed by the results of Figure 4.33, it can be concluded that R_s has negative impact on condensate viscosity in gas-condensate reservoirs, means increasing R_s , would decrease viscosity. This is also true characteristic of condensate liquid viscosity, as increasing solution gas to oil ratio would increase the amount of gas phase in liquid phase, which in return make the mixture lighter with lower viscosity. Both Figure 4.32 and Figure 4.33 indicate the validity of the developed condensate viscosity using Mamdani fuzzy approach in following physical trend of the experimental data as other literature correlations do.

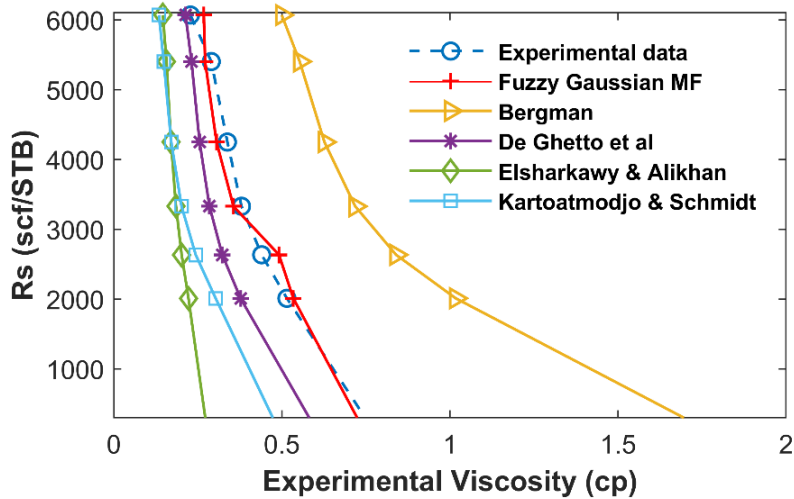


Figure 4.33. Performance of literature correlations along with gaussian fuzzy approach in predicting condensate viscosity as a function of solution gas to oil ratio R_s ; sample from Coats, (1986).

4.8 Computational efficiency of the developed models

The developed ML models in this chapter for prediction of condensate (oil) viscosity of gas-condensate reservoirs are favourable to the existing literature models as they require less parameters. ANN and LSSVM are only function of P , T , R_s , API gravity and Gas Specific gravity. Both developed TSK and Mamdani models are function of P , T and R_s . In terms of computational efficiency (the required time for each model to return the output), the developed AI models predict condensate viscosity very fast as shown in Figure 4.34. All developed AI methods predict the condensate viscosity with less than a minute. However, Mamdani fuzzy is faster than other AI techniques with only required 5 seconds to return the output values. Mamdani Fuzzy followed by ANN, TSK fuzzy and LSSVM.

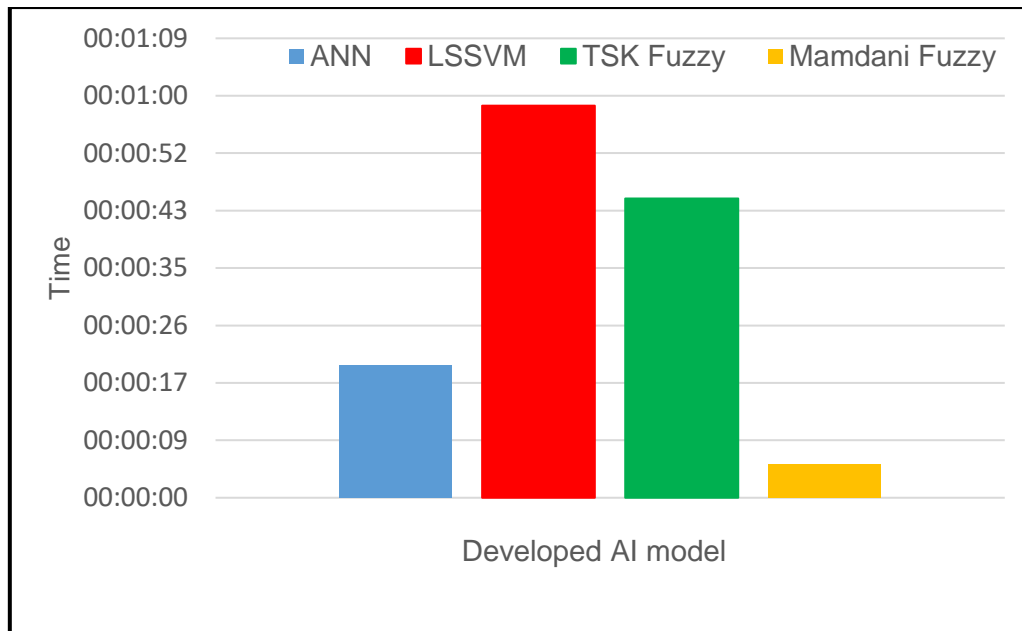


Figure. 4.34. Computational efficiency of the developed AI models (00:00:00 stands for Hour: Minute: Second).

4.9 Summary

Viscosity is one of the governing parameters that influence well deliverability modelling of gas-condensate reservoirs. This important PVT property should be treated separately and with high precision for both phases of gas and condensate (liquid) below the saturation pressure.

In this chapter, extensive effort has been made for accurate modelling of viscosity of both phases (gas and condensate). The applicability of existing literature models for prediction of viscosity of gas and condensate (oil) has been examined using published experimental data. The results show that the performance of existing literature models for prediction of gas and condensate (oil) viscosity are inadequate. In fact, for prediction of condensate (oil) viscosity existing literature models show significant error. To improve the performance of the existing literature models in prediction of gas phase viscosity non-linear regression was performed and a well-known method of Londono et al., (2002) was modified. New optimized Londono et al., (2002) model is predicting experimental data with 5.2% average absolute relative deviation (AARD%).

Variety of machine learning (ML) as well as non-linear regression approaches were utilized for better modelling of condensate viscosity.

Initially non-linear regression employed for optimizing several existing literature models of Beggs and Robinson, (1975); Bergman and Sutton, (2007); De Ghetto et al., (1994); Elsharkawy and Alikhan, (1999); Kartoatmodjo and Schmidt, (1991) and LBC, 1964). Then, several smart approaches including Support Vector Machine (SVM), Artificial Neural Network (ANN), TSK fuzzy logic, and Mamdani fuzzy logic were employed for better modelling of condensate viscosity in gas-condensate reservoirs.

Statistical and graphical error analysis confirmed the superiority of ML based approaches in prediction of condensate viscosity in comparison to the existing literature models. A unique condensate viscosity correlation as a function of pressure, temperature and solution gas to oil ratio was proposed using TSK fuzzy approach.

Physical accuracy of the developed machine learning models in this chapter for prediction of condensate viscosity is verified using trend analysis of independent data sets.

The results of present work could be utilized for quick estimation of the gas-condensate viscosity below the dew point pressure. These models offers computational efficiency, high accuracy and require less parameters for predicting condensate viscosity. The developed models can be embedded inside PVT packages and other simulation software currently in use in industry for better well deliverability modelling of gas-condensate reservoirs.

The developed ANN and LSSVM are predicting the experimental condensate viscosity with 0.1144 and 0.1208 RMSE, respectively as well as AARD% of 16.20 and 17.20.

CHAPTER 5

DEVELOPMENT OF TWO-PHASE Z FACTOR OF GAS-CONDENSATE MIXTURE

5.1 Introduction

The development and optimization of gas-condensate recovery and accurate well deliverability modelling require accurate determination of PVT properties. One of the most important factors that need accurate determination by engineers in calculation of well flow rate through reservoir rock, material balance calculations, evaluation of gas reserves, design of production equipment, and planning the development of a gas-condensate reservoir is the fluid Z factor (Elsharkawy and Foda, 1998; Sun *et al.*, 2012; Zendehboudi *et al.*, 2012). As explained in chapter 2, Z factor is one of the fundamental PVT properties in gas rate equations of 2.2 and 2.4. Furthermore, as described in chapter 2, Z factor is influencing the well deliverability calculation in gas condensate reservoirs.

In calculation of gas-condensate well deliverability accurate estimation of Z factor, is critical for the following reasons. Firstly, accurate and consistent estimation of initial hydrocarbon fluid in place require accurate estimation of compressibility factor. Secondly, correct estimation of Z factor dictates accurate prediction of recovery factor (gas and condensate liquid) as a function of pressure in depletion drive gas-condensate reservoirs (Whitson, Fevang and Yang, 1999).

Furthermore, at average reservoir pressure above the dew point condensate recovery is exactly equal to the gas recovery. Consequently, condensate recovery is strongly dependant on accurate description of Z factor both above and below the dew point pressure. To emphasise the important of accurate estimation of compressibility factor in gas-condensate well deliverability modelling Whitson *et al.*, (1999) quoted; “A “+5% error in initial compressibility factor and a –5% error in compressibility factor at the dewpoint will result in (a) a +5% error in initial gas and initial condensate in place, and (b) a +5 to +10% error in recovery of gas and condensate at the dewpoint”.

In this chapter, primarily the fundamental theories behind the Z factor will be discussed. Then the performance accuracy of existing literature models for estimation of gas-condensate Z factor will be reviewed. Finally, several Z factor models are proposed to ensure accurate estimation of gas-condensate reservoir Z factor below the saturation pressure.

5.2 Preliminary theory of Z factor calculation

In 1873, Johannes Diderik van der Waals recognized a unique relationship between Z factor, reduced pressure (P_r) and reduced temperature (T_r), which known as two parameters corresponding state principle. The corresponding state principle is generalization of properties of gases (pressure and temperature) and are related to the critical properties in universal way. It describes that the two substances at the same condition of reduced pressure (P_r) and reduced temperature (T_r) have similar properties. In other word Z factor of any pure gases at same P_r and T_r are the same. For mixture compositions such as gas-condensate fluid, the reduced properties replaced by pseudocritical properties and become pseudo-reduced pressure (P_{pr}) and pseudo-reduced temperature (T_{pr}). These values are serving as a correlating parameters for corresponding state principle and the way they are estimated effect the accuracy of the Z factor (Sutton, 2005).

Prior to discuss computation of Z factor, it is important to understand the calculation of pseudoreduced properties. The pseudo-reduced pressure and pseudo-reduced temperature are expressed by the following equations:

$$\begin{cases} P_{pr} = \frac{P}{P_{pc}} \\ T_{pr} = \frac{T}{T_{pc}} \end{cases} \quad 5.1$$

Where P_{pc} is pseudocritical pressure and T_{pc} stands for pseudocritical temperature. These pseudocritical properties can be estimated with gas compositions and mixing rules or from correlations based on gas gravity (Whitson and Brulé, 2000, pp. 23–24; Sutton, 2005b). Several correlations have been proposed in literature for calculation of pseudocritical properties (P_{pc} and T_{pc}) if the composition of the mixture is available (Kay, 1936; Stewart, Burkhardt and Voo, 1959; Sutton, 1985; Piper, McCain and Corredor, 1993; Elsharkawy, 2006). Based on gas specific gravity there are other correlations in literature for estimation of pseudocritical properties (Matthews and

Roland, 1942; Standing, 1981; Elsharkawy, Hashem and Alikhan, 2000; Elsharkawy and Elkamel, 2001; Londono, Archer and Blasingame, 2005; Sutton, 2007).

The Z factor data bank that is collected and used in this chapter include all compositional details of gas-condensate mixtures. This would allow us to use widely accepted Kay's mixing rule (Kay, 1936) shown in following equation for estimating critical properties of hydrocarbon components.

$$\left\{ \begin{array}{l} P_{pc} = \sum_{i=1,2,..}^N y_i P_{ci} \\ T_{pc} = \sum_{i=1,2,..}^N y_i T_{ci} \end{array} \right. \quad 5.2$$

Where y is mole fraction of component i in the mixture. Gas-condensate mixture frequently contains non-hydrocarbon impurities such as hydrogen sulphide (H_2S), nitrogen (N_2) and carbon dioxide (CO_2). These impurities influence the accuracy of the PVT properties including Z factor estimation and need to be considered in calculation of pseudocritical properties. Wichert and Aziz, (1972) proposed a correction to include non-hydrocarbon impurities for calculation of pseudocritical properties. Wichert and Aziz's correlation has widely been accepted in industry; hence, in this study we employed same method for estimating non-hydrocarbon impurities in gas-condensate mixture. Wichert and Aziz, (1972) presented their equation in following form.

$$\left\{ \begin{array}{l} T_{pc}^* = T_{pc} - \epsilon \\ P_{pc}^* = \frac{P_{pc}(T_{pc} - \epsilon)}{T_{pc}^* + y_{H_2S}(1 - y_{H_2S})\epsilon} \\ \epsilon = 120 \left[(y_{CO_2} + y_{H_2S})^{0.9} - (y_{CO_2} + y_{H_2S})^{1.6} \right] + 15(y_{CO_2}^{0.5} - y_{H_2S}^4) \end{array} \right. \quad 5.3$$

Where T_{pc} and P_{pc} are mixture pseudocritical properties based on Kay's mixing rule. In addition to non-hydrocarbon impurities one of the important properties that influence the calculation of Z factor in gas-condensate reservoirs below the saturation pressure, is accurate determination of hydrocarbon plus (C_{7+}) pseudocritical properties. Many correlations such as Lee and Kesler, (1975); Kesler and Lee, (1976); Rowe, (1978); Whitson, (1983); Pedersen, Thomassen and Fredenslund, (1984); Riazi and Daubert, (1987); Elsharkawy, Hashem and Alikhan, (2000); Sutton, (2005b) have been proposed for this purpose. Many of these methods are applicable for characterization

of C₇₊ fractions when compositional data is not available. If compositional data is available Matthews and Roland, (1942) is conventional method for estimating pseudocritical properties of C₇₊. This method is practical and widely used in industry for estimation of hydrocarbon plus pseudocritical properties (Sutton, 1985; Whitson and Brulé, 2000; Maravi, 2003).

Due to availability of compositional data in this study Matthews and Roland, (1942) shown in equation 5.4 utilized for estimating pseudocritical properties of C₇₊. Their method calculates hydrocarbon plus pseudocritical properties as a function of hydrocarbon plus specific gravity (γ_{C7+}) and molecular weight (M_{C7+}).

$$\begin{cases} T_{CC7+} = 608 + 364\log(M_{C7+} - 71.2) + (2450\log M_{C7+} - 3800)\log\gamma_{C7+} \\ P_{CC7+} = 1188 - 431\log(M_{C7+} - 61.1) + \dots \\ \dots [2319 - 852\log(M_{C7+} - 53.7)](\gamma_{C7+} - 0.8) \end{cases} \quad 5.4$$

5.3 Assessment of Z factor models

Based on the theory of corresponding state principle Standing and Katz, (1942) introduced a chart for estimating Z factor of natural dry and sweet gases as a function of pseudo reduced pressure (P_{pr}) and pseudo reduced temperature (T_{pr}). Standing and Katz (SK) chart is one of the most widely accepted practical correlation in petroleum engineering for calculating gas-phase Z factor. The data of binary mixture of methane with propane, ethane, butane and natural gases with wide range of composition was used in developing SK chart. The molecular weight of the mixtures used in SK chart not exceeding 40 (Elsharkawy, Hashem and Alikhan, 2000). The SK chart is suitable for estimating Z factor of dry gases. Several corrective methods introduced to SK chart to account for existence of high molecular weight gases and hydrocarbon plus fraction C₇₊ (Stewart, Burkhardt and Voo, 1959; Sutton, 1985, 2005b; Elsharkawy, Hashem and Alikhan, 2000). The importance of SK chart in industry motivated scholars to develop mathematical representation of the chart. Some of these methods are Dranchuk, Purvis and Robinson, (1973); Hall and Yarborough, (1973); Dranchuk and Abou-Kassem, (1974); Yarborough and Hall, (1974). Engineering community typically uses the published methods by Hall and Yarborough, (1973) and Dranchuk and Abou-Kassem, (1975) as they fit best the SK chart (Takacs, 1976). These methods are form of an equation of state that have been derived in an iterative procedure to estimate the Z factor as a function of P_{pr} and T_{pr} .

The P_{pr} and T_{pr} are determined using one of the available mixing rules for instance Kay, (1936).

Other scholars also tried to develop methods for direct calculation of SK chart, which using fitting techniques (e.g., regression). Some of these methods in literature are as follow (Papay, 1968; Beggs and Brill, 1973; Gopal, 1977; Azizi, Behbahani and Isazadeh, 2010; Heidaryan, Moghadasi and Rahimi, 2010; Sanjari and Lay, 2012). These correlations are explicit, which means they don't need numerical iterative procedure. These correlations recently become popular and they have been utilized by many researchers in the field for calculation of Z factor due to their simplicity and acceptable accuracy in wide range of pressure and temperature condition.

Another methodology for estimation of Z factor is through implementation of cubic equation of state (EOS). Cubic EOS are simple computation procedure that define relationship between pressure, volume and temperature of pure hydrocarbon components and mixtures components. First cubic EOS proposed by Van der Waals, (1873). Many equations of state after Van der Waals have been proposed in literature to model reservoir fluid phase behaviour and Z factor (Carnahan and Starling, 1969; Fuller, 1976; Lawal, 1999; Nasrifar and Moshfeghian, 2001). Redlich and Kwong, (1949) improved initial Van der Waals EOS for more accurate calculation of vapour phase Z factor. Evolutionary path of van der Waals EOS lead to proposing an excellent form of EOS by Soave-Redlich and Kwong (SRK) in 1972. SRK and later Peng and Robinson, (1976) EOSs become the industry leader for calculation of PVT properties (e.g., Z factor). Generally performance of EOS are good for simple hydrocarbon systems like natural gas and black oil reservoirs, however their performance deteriorates for more complex systems like volatile oil and gas-condensate reservoirs (Sarkar, Danesh and Todd, 1991; Elsharkawy and Foda, 1998; Ghiasi *et al.*, 2014). This is because the interaction between the gas and liquid molecules is not well simulated in critical conditions.

Availability and accessibility of the data in oil and gas industry motivated many scholars to use different approach so called intelligent models for prediction of various fluid properties. Recently giant oil and gas companies such as British Petroleum (BP) and Shell have supported using artificial intelligent (AI) techniques in different area of their operations. Many researchers are also using AI techniques for prediction of PVT properties in recent years. A few examples are (Heidaryan, Moghadasi and Rahimi,

2010; Chamkalani *et al.*, 2013; Hatampour and Ghiasi-Freeez, 2013; Ghiasi *et al.*, 2014). The intelligent methods provide promising breakthrough in accurate prediction of PVT properties.

The core objectives of this chapter can be separated to two parts. Part 1 is to assess previously developed methods for estimation of two-phase Z factor in gas-condensate reservoirs. Second part is to develop smart, yet accurate models for prediction of gas-condensate two-phase Z factor for wide range of reduced pressure and temperature when composition of the mixture is available. An extensive data bank from the literature was collected to achieve the objective of this chapter. In the following sections, the most frequent methods in literature for computation of Z factor are briefly introduced.

5.3.1 Hall-Yarborough (1973)

Success of Standing and Katz (SK) chart in petroleum industry for estimating Z factor, motivated many scholars to reproduce the SK chart in a mathematical (equation) form. Hall and Yarborough, (1973) and Yarborough and Hall, (1974) were among the first researchers that start this journey. They modified Carnahan and Starling, (1969) equation of state that accurately describes SK Z factor chart. The coefficient of their equation estimated by fitting the data obtained from SK chart. Hall and Yarborough, (1973) and Yarborough and Hall, (1974) propose the following equation for estimating of Z factor.

$$Z = \left[\frac{0.06125P_{pr}t}{Y} \right] \exp[-1.2(1 - t^2)] \quad 5.5$$

Where P_{pr} is pseudo-reduced pressure; t is reciprocal of pseudo-reduced temperature (e.g., T_{pc}/T) and Y is the product of the Van der Walls co-volume and reduced-density and can be obtained by solving $F(Y)$ as follow.

$$F(Y) = X_1 + \frac{Y + Y^2 + Y^3 + Y^4}{(1 - Y)^3} - X_2Y^2 + X_3Y^{X_4} \quad 5.6$$

Where the parameters of X are determined as follow.

$$\begin{cases} X_1 = -0.01625P_{pr}t[-1.2(1 - t^2)] \\ X_2 = (14.76t - 9.76t^2 + 4.58t^3) \\ X_3 = (90.7t - 242.2t^2 + 42.48t^3) \\ X_4 = (2.18 + 2.82t) \end{cases} \quad 5.7$$

To solve function F(Y) an iterative technique of Newton-Raphson with the initial guess of Y=0.001 is used. The method returned the experimental Z factor within 3 to 10 iterations.

Hall – Yarborough method is representing SK chart Z factor with very good accuracy in wide range of pressure and temperature. This method is valid for the reduced temperature in the range of $1 \leq T_r \leq 3$ and reduced pressure in the range of $0.2 \leq P_r \leq 25 - 30$ (Yarborough and Hall, 1974; Whitson and Brulé, 2000; Ahmed, 2010).

5.3.2 Dranchuk – Abu – Kassem (1975)

Unlike Hall and Yarborough Z factor equation, which is only function of pseudoreduced pressure and temperature, Dranchuk and Abou-Kassem, (1975) or known as DAK proposed an equation of state for calculation of Z factor that also include reduced gas density. Reduced gas density (ρ_r) is a ratio of gas density at specific pressure and temperature over gas density at critical pressure and temperature. DAK used 1500 Z factor data points obtained from SK chart in developing their method. DAK proposed Z factor equation with 11 constants as follow.

$$\begin{cases} Z = \left[A_1 + \frac{A_2}{T_{pr}} + \frac{A_3}{T_{pr}^3} + \frac{A_4}{T_{pr}^4} + \frac{A_5}{T_{pr}^5} \right] \rho_r + \left[A_6 + \frac{A_7}{T_{pr}} + \frac{A_8}{T_{pr}^2} \right] \rho_r^2 \dots \\ \dots - A_9 \left[\frac{A_7}{T_{pr}} + \frac{A_8}{T_{pr}^2} \right] \rho_{pr}^5 + A_{10} (1 + A_{11} \rho_r^2) \frac{\rho_r^2}{T_{pr}^3} 3 \exp[-A_{11} \rho_r^2] + 1 \\ \rho_r = \frac{0.27 P_{pr}}{Z T_{pr}} \end{cases} \quad 5.8$$

Where the constants of A_1 to A_{11} are as follow, $A_1 = 0.3265$, $A_2 = -1.0700$, $A_3 = -0.5339$, $A_4 = 0.01569$, $A_5 = -0.05165$, $A_6 = 0.5475$, $A_7 = -0.7361$, $A_8 = 0.1844$, $A_9 = 0.1056$, $A_{10} = 0.6134$, $A_{11} = 0.7210$. ρ_r is the reduced density of the mixture.

A_1 to A_{11} constants obtained by the authors using non-linear regression using SK chart data points. In implementing DAK method for estimating Z factor, Newton – Raphson iterative technique has been used (Lee and Wattenbarger, 1995). For high-density gases DAK method estimates Z factor with high error. Hence the modification has

been introduced to the original DAK code by Borges, (1991), where he sets the reduced density from value of 2.2 to 3 or greater. The DAK method predicts Z factor for reduced temperature in the range of $1 \leq T_r \leq 3$ and reduced pressure range of $0.2 \leq P_r \leq 25 - 30$.

5.3.3 Beggs and Brill (1973)

Although Hall – Yarborough and DAK method simulate SK Z factor chart with good accuracy, however the computation procedure is tedious and iterative techniques are needed. For easing the computation of the Z factor without using iterative procedure Beggs and Brill, (1973) proposed a direct correlation. For many petroleum engineering applications Beggs and Brill, (1973) give satisfactory representation of the SK chart with 1 – 2% deviation in reduced temperature range of $1.2 < Tr < 2$. The main limitations of Beggs and Brill are that reduced temperature must be greater than 1.2 ($\approx 80^\circ\text{F}$) and less than 2.0 ($\approx 340^\circ\text{F}$) and reduced pressure should be less than 15 ($\approx 10,000\text{psia}$). The Beggs and Brill is presented as follow for calculation of Z factor.

$$Z = A + \frac{1 - A}{e^B} + CP_{pr}^D \quad 5.9$$

Where the parameters of A, B C and D can be determined as follow:

$$\left\{ \begin{array}{l} A = 1.39(T_{pr} - 0.92)^{0.5} - 0.36T_{pr} - 0.10 \\ B = (0.62 - 0.23T_{pr})P_{pr} + \left(\frac{0.066}{T_{pr} - 0.86} - 0.037 \right) P_{pr}^2 + \frac{0.32P_{pr}^6}{10^E} \\ C = 0.132 - 0.32\log(T_{pr}) \\ D = 10^F \\ E = 9(T_{pr} - 1) \\ F = 0.3106 - 0.49T_{pr} + 0.1824T_{pr}^2 \end{array} \right. \quad 5.10$$

The main advantage of Beggs and Brill is that the equation is explicit and easy to use in many engineering calculation.

5.3.4 Rayes et al., (1992)

SK chart and subsequent models of Hall – Yarbrough, DAK and Beggs and Brill, (1973) are good representation of Z factor as for natural gas with single-phase

behaviour. Gas-condensate reservoirs undergoing depletion are developing condensate phase, which make the flow at least two-phase or even more if connate water enter the pay zone. Therefore using single-phase Z factor for this type of reservoirs is arguable.

Evolving condensate (liquid) phase below the saturation pressure in gas-condensate reservoirs motivated Rayes et al., (1992) to develop a two-phase Z factor as a function of pseudocritical properties of temperature and pressure. They used 131 constant volume depletion (CVD) studies of gas-condensate reservoirs for developing their correlation. Their correlation is valid for reduced temperature range between $1.1 < Tr < 2.1$ and reduced pressure range of $0.7 < Pr < 20$. They propose the following equation for computation of two-phase Z factor.

$$Z_{2-phase} = A_0 + A_1(Pr) + A_2\left(\frac{1}{Tr}\right) + A_3(Pr)^2 + A_4\left(\frac{1}{Tr}\right)^2 + A_5\left(\frac{Pr}{Tr}\right) \quad 5.11$$

Where $A_0 = 2.24353$, $A_1 = -0.0375281$, $A_2 = -3.56539$, $A_3 = 0.000829231$, $A_4 = 1.53428$ and $A_5 = 0.131987$.

Rayes et al., (1992) is the only two-phase Z factor model that specifically developed for gas-condensate reservoirs. The equation can be calculated explicitly for determining two-phase Z factor. However, the equation is limited for high pressure and high temperature (HPHT) condition.

5.3.5 Azizi et al., (2010)

The methods that developed to representing SK chart such as DAK and Hall – Yarbrough were based on limited data from the original SK chart. In another attempt to simulate the SK chart by a mathematical equation, Azizi et al., (2010) used a large Z factor data bank of 3038 points obtained from SK chart and proposed a direct Z factor correlation. Their proposed method include 14 constants obtained from fitting with SK chart Z factor data. They proposed their Z factor correlation in the following fashion.

$$Z = A + \frac{B + C}{D + E} \quad 5.12$$

Where A, B, C and D are determined from the following equations.

$$\begin{cases} A = aT_r^{2.16} + bP_r^{1.028} + cP_r^{1.58}T_r^{-2.1} + d\ln(T_r)^{-0.5} \\ B = e + f(T_r)^{2.4} + gP_r^{1.56} + hP_r^{0.124}T_r^{3.033} \\ C = i\ln(T_r)^{-1.28} + j\ln(T_r)^{1.37} + k\ln(Pr) + l\ln(P_r)^2 + m\ln(P_r)\ln(T_r) \\ D = 1 + n(T_r)^{5.55} + o(P_r)^{0.68}(T_r)^{0.33} \\ E = p\ln(T_r)^{1.18} + q\ln(T_r)^{2.1} + r\ln(Pr) + s(P_r)^2 + t\ln(P_r)\ln(T_r) \end{cases} \quad 5.13$$

The tuned values of $a - t$ in equation 5.13 are given in following table.

Table 5.1. Coefficients of Azizi et al., (2010) Z factor correlation.

Coefficient	Value	Coefficient	Value
a	0.0373142485385592	k	-24449114791.15
b	-0.0140807151485369	l	19357955749.32
c	0.0163263245387186	m	-126354717916.60
d	-0.0307776478819813	n	623705678.38
e	13843575480.94	o	17997651104.33
e	-16799138540.76	p	151211393445.06
g	1624178942.649	Q	139474437997.17
h	13702270281.08	r	-24233012984.09
i	-41645509.89	s	18938047327.52
j	237249967625.01	t	-141401620722.68

The advantage of Azizi et al., (2010) method over other DAK and Hall-Yarborough for simulating SK chart is that it does not need an iterative computational method for estimating Z factor. It is a direct correlation that developed to represents SK chart as simple as possible. This model is valid for reduced pressure between $0.2 < Pr < 11$ and reduced temperature between $1.2 < Tr < 2$.

To assess the applicability of all studied literature model for estimating two-phase Z factor of gas-condensate fluid below the saturation pressure a large data bank has been collected, which is discussed in following section.

5.3.6 Data bank

To examine the performance of the discussed literature methods in prediction of gas-condensate Z factor and also developing new methods for this important PVT property,

a data bank was collected. The data bank include 1084 data sets (19518 data points). This is largest and one of the most comprehensive data bank to assess and improve accuracy of gas-condensate reservoirs Z factor. Experimental studies of gas-condensate fluids and also the PVT reports are source of our data bank. The following references is used in sourcing the Z factor data bank: (Olds, Sage and Lacey, 1945, 1949; Whitson and Torp, 1983; Coats, 1985; Coats and Smart, 1986; Moses, 1986; Kenyon and Behie, 1987; Drohm, Goldthorpe and Trengove, 1988; Yang, Chen and Guo, 1997; Elsharkawy and Foda, 1998; Sun *et al.*, 2012; Liu *et al.*, 2013; Bonyadi *et al.*, 2014). In most of these studies constant volume depletion (CVD) has been employed in order to estimate the phase behaviour of gas-condensate samples. The data bank includes hydrocarbon compositions, molecular weight of C₇₊, pressure, temperature, gas specific gravity and two-phase Z factor. The data covers wide range of reservoir conditions as well as reservoir compositions from lean gas-condensate to very rich obtained from worldwide. The statistical description of the data is provided in Table 5.2.

Table 5.2. Statistical description of the data used for development of two-phase Z factor.

Property	Minimum	Maximum	Average
Temperature, °F	86	351	207
Tpr	1.1631	4.261	2.901
Pressure, psia	200	23244	8305
Ppr, (mole %)	0.2878	33.525	11.917
H ₂ S, (mole %)	0.000	0.5137	0.0075
CO ₂ , (mole %)	0.0001	0.749	0.0472
N ₂ , (mole %)	0.000	0.525	0.0326
C1, (mole %)	0.0687	96.003	5.1115
C2, (mole %)	0.0024	2.101	0.1529
C3, (mole %)	0.0007	0.202	0.028
IC4, (mole %)	0.0002	0.0638	0.0065
NC4, (mole %)	0.00	0.0638	0.0084
IC5, (mole %)	0.00	0.06	0.0037
NC5, (mole %)	0.00	0.0431	0.0032
C6, (mole %)	0.0002	0.0592	0.0047
C7+, (mole %)	0.0004	0.228	0.0249
SG gas	0.046717	1.410137	0.26218
MW C7+	102.30	253.00	186.78
Two-phase Z-factor	0.553	2.162	1.287

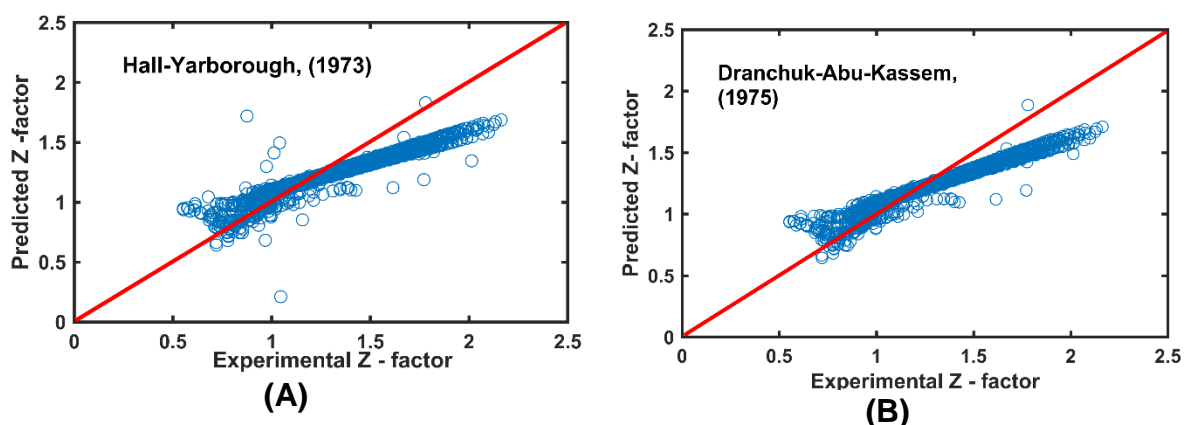
5.3.7 Results of literature models

Using the data bank shown in Table 5.2 applicability and accuracy of the existing literature models for prediction of gas-condensate Z factor is assessed. Statistical and graphical error analysis carried out to see the performance of the literature models in prediction of two-phase Z factor. The statistical parameters of mean average error (MAE), root mean square error (RMSE) and absolute average relative deviation percentage (AARD%) have been employed to see the accuracy of the utilized methods. The results of this statistical error analysis shown in Table 5.3. These analyses indicate DAK method best performed among existing literature models with MAE of 0.1300, RMSE of 0.1671 and AARD% of 2.4945. DAK method followed by Hall-Yarborough, (1973), Rayes et al., (1992), Beggs and Brill, (1973) and Azizi et al., (2010) for estimation of gas-condensate Z factor below the saturation pressure.

Table 5.3. Performance of employed literature models in predicting two-phase Z factor of gas-condensate systems.

Model	MAE	RMSE	AARD%
Hall-Yarborough, (1973)	0.1421	0.1846	3.0906
DAK, (1975)	0.1300	0.1671	2.4945
Beggs and Brill, (1973)	0.2047	0.2769	17.0566
Azizi et al., (2010)	0.3851	0.4822	28.6958
Rayas et al., (1992)	0.1516	0.1904	10.0522

In order to visualize the performance of literature models several graphical error analysis were performed. The graphs in Figure 5.1 are presenting cross plot of the obtained results against the experimental values of two-phase Z factor. The diagonal line is representing zero error line, means scattering the data over or under this line showing poor performance of the model. The results of cross plot show that DAK, (1975), Hall-Yarborough, (1973) and Rayes et al., (1992) predict the experimental values of two-phase Z factor with some level of accuracy while Beggs and Brill, (1973) and Azizi et al., (2010) performance is unsatisfactory.



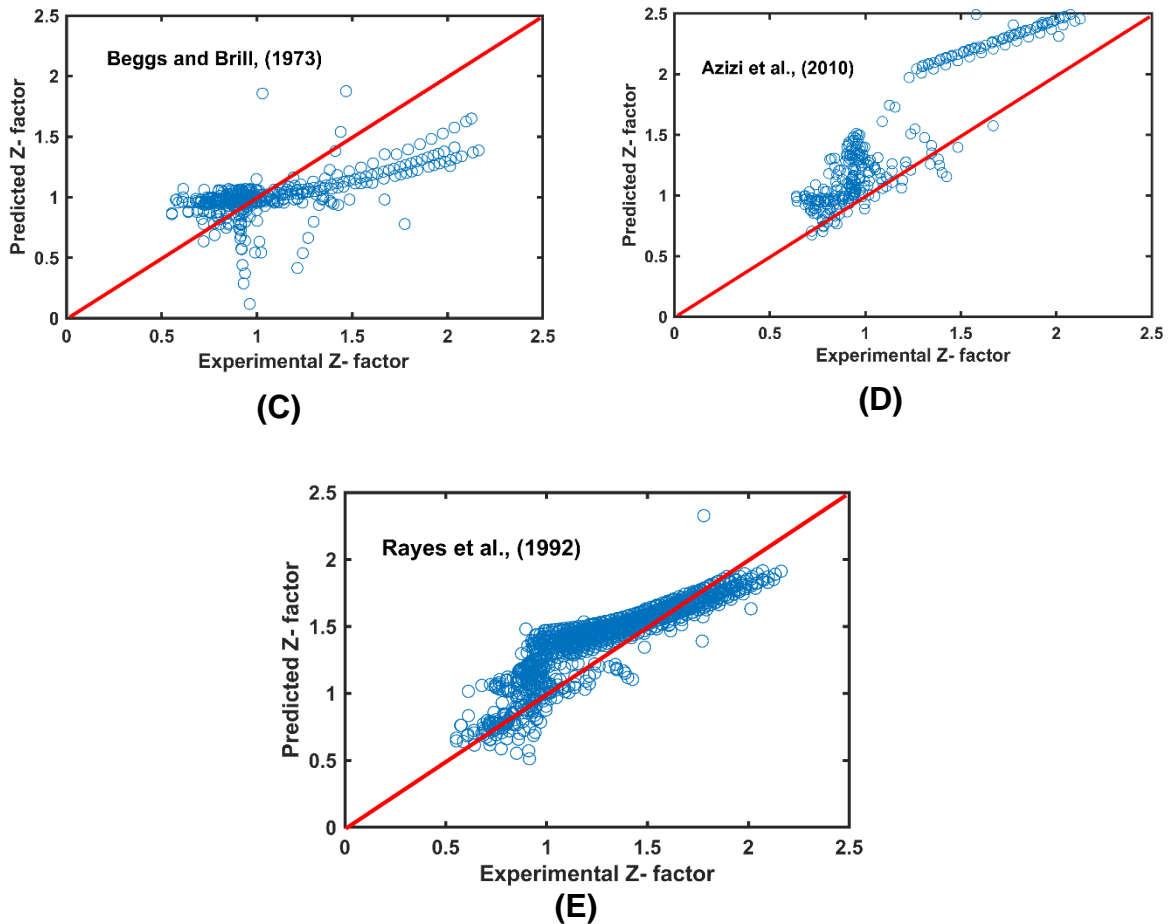


Figure 5.1. Scatter plot of five literature models in prediction of two-phase compressibility factor of gas condensate reservoirs below the saturation pressure.

To investigate the performance of each method in predicting various range of experimental gas-condensate two-phase Z factor the graph of relative error was generated and presented in Figure 5.2. As the graph shows prediction performance of DAK, (1975) and Hall-Yarborough, (1973) methods are poor especially in the specific range of $1.5 < Z_{two-phase} < 0.7$. The reasons for poor performance of both aforementioned methods in predicting gas-condensate two-phase Z factor could be behind their initial development. Hall-Yarborough (HY), (1973) and DAK, (1975) are both iterative techniques that are representing mathematical description of well-known SK (Standing and Katz, 1942) Z factor chart. The associated constants in DAK and HY equations were tuned using the data obtained from SK chart. SK chart is suitable for prediction of single phase sweet and dry gas systems, nevertheless not for prediction of two-phase Z factor of gas-condensate fluid (Rayes *et al.*, 1992; Elsharkawy, Hashem and Alikhan, 2000). Both DAK and HY also shown similar

behaviour for prediction of two-phase Z factor, as they initially were developed to simulate the SK chart.

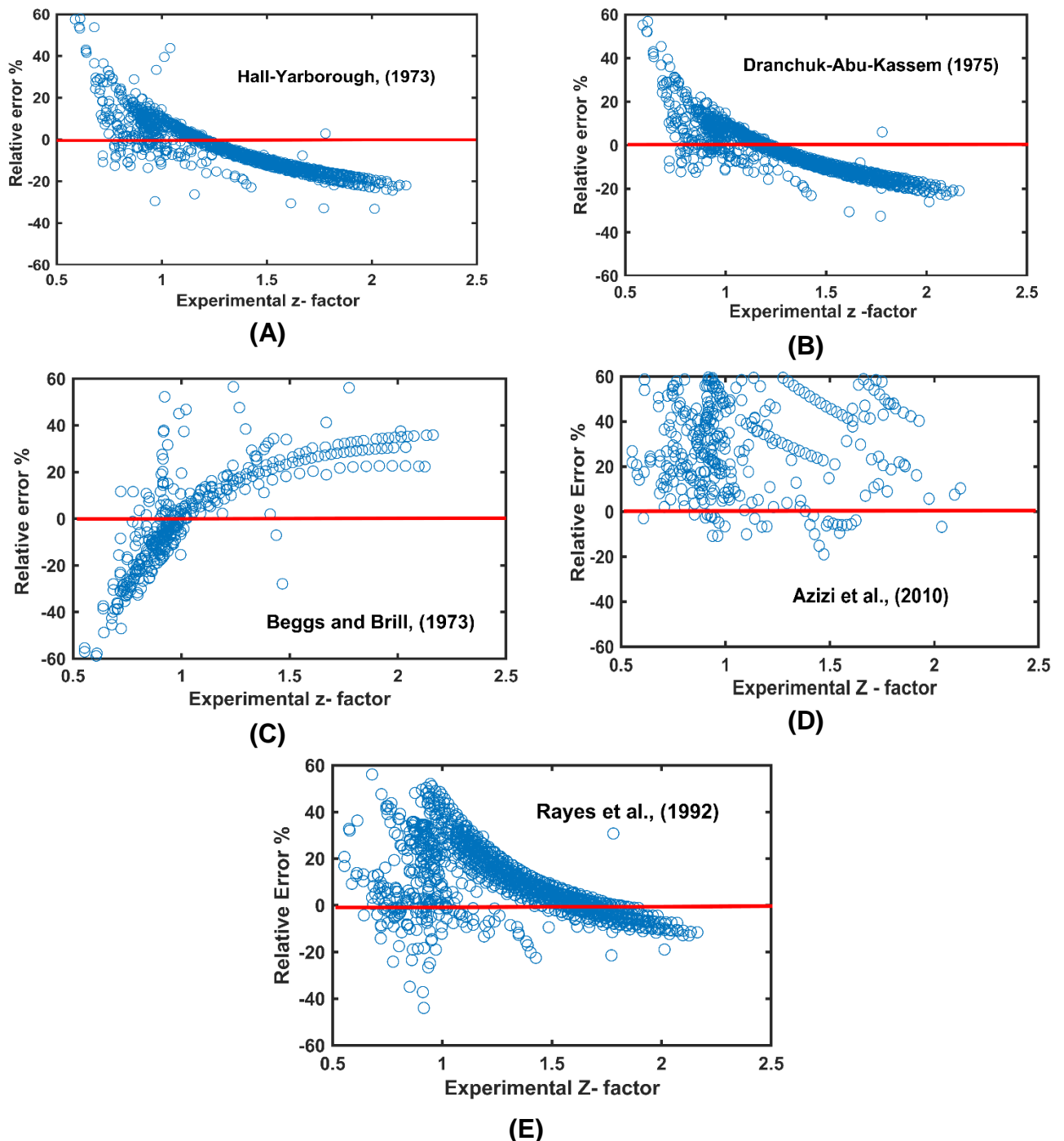


Figure 5.2. Graph of relative error utilizing literature models for prediction of two-phase Z factor.

Azizi et al., (2010) performance is also associated with high error as indicated by the results in Figure 5.1D and Figure 5.2D. In developing their correlation Azizi et al., (2010) used 3038 data points obtained from SK chart. The poor performance of this

correlation also indicates that SK chart is not applicable for estimating two-phase Z factor of gas-condensate reservoir below the saturation pressure (two-phase Z factor).

Beggs and Brill, (1973) correlation also predicts the experimental data with large error as can be seen from Figure 5.1C and Figure 5.2C. Rayes et al., (1992) method is the only method that specifically developed for prediction of gas-condensate Z factor below the dew point pressure. This method also return the experimental data with high error shown in Figure 5.1E and Figure 5.2E.

For fair evaluation of each literature models it should be highlighted that each method developed for specific range of T_{pr} and P_{pr} . Hence, the performance of the each method plotted against various range of T_{pr} and P_{pr} and shown in Figure 5.3 and Figure 5.4.

Hall-Yarborough and DAK methods well predict Z factor of reservoir gases (dry and sweet) within the range of $1 \leq T_{pr} \leq 3$ and $0.2 \leq P_{pr} \leq 25 - 30$ (Hall and Yarborough, 1973; Dranchuk and Abou-Kassem, 1974; Whitson and Brulé, 2000). The results in Figure (5.3A-B) and Figure (5.4A-B) show that even within aforementioned ranges of reduced pressure and temperature Hall-Yarbrough and DAK predict two-phase Z factor of gas-condensate reservoirs with high error.

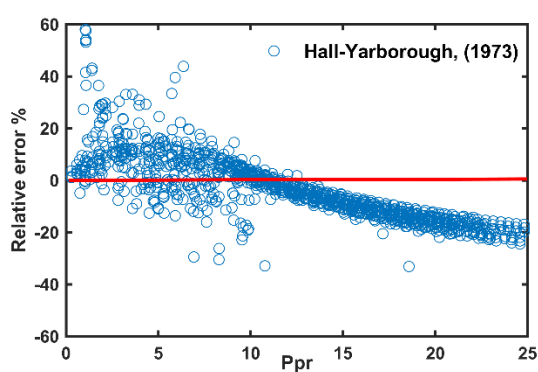
Beggs and Brill Z factor correlation is only valid for specific range of pseudo reduced temperature of $1.2 < T_{pr} < 2$ and pressure of $P_{pr} < 15$. This correlation forecasts the two-phase gas-condensate Z factor within the aforementioned T_{pr} and P_{pr} with large deviation as can be seen from Figure 5.3C and Figure 5.4C.

Azizi, et al, (2010) model is valid for reduced temperature between $0.2 < Pr < 11$ and reduced temperature between $1.2 < Tr < 2$. Looking at the results in Figure 5.12D and Figure 5.3D where performance of Azizi's model in specified reduced pressure and temperature depicted respectively, the two-phase Z factor experimental data is highly overestimated.

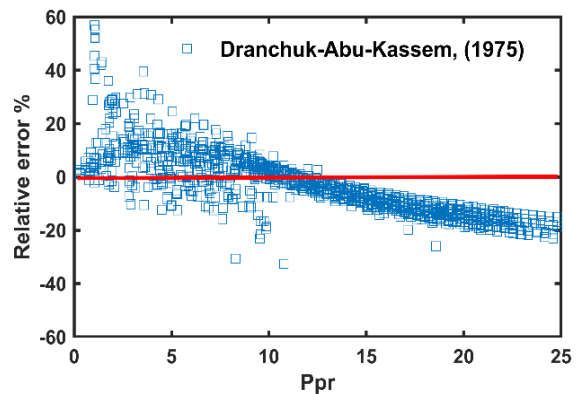
Rayes et al., (1992) performs very well if the Z factor is within the range of $0.704 < Z_{two-phase} < 1.775$, and deviate under and beyond these range. In terms of relative error as a function of T_{pr} and P_{pr} , Rayes et al., (1992) method returns two-phase

experimental Z factor with unsatisfactory accuracy, as illustrated by Figure 5.3E and Figure 5.4E for reduced pressure and reduced temperature respectively.

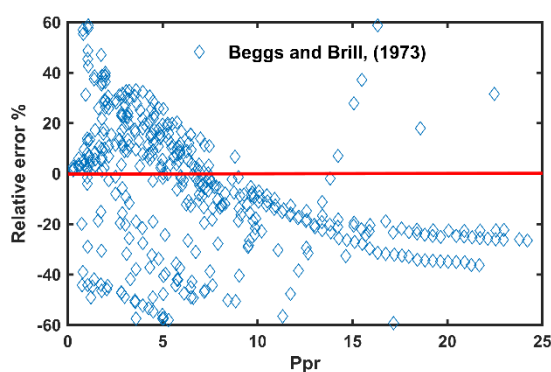
We should also highlight the fact that another reason for high error by utilized methods are using different reservoirs fluid samples in their development. Based on the presented results it can be concluded that using existing literature methods for calculation of two-phase Z factor of gas-condensate reservoirs are not adequate and associated with large error. The unsatisfactory performance and applicability to only limited range of data of literature models motivated to focus on developing methods for prediction of two-phase Z factor of gas-condensate reservoirs. There is a need for robust models that cope with non-linearity of gas-condensate systems below the saturation pressure in relation to prediction of Z factor. Availability of the data in literature and success of using machine learning techniques in recent years, motivated us to use several methods known as machine learning (ML) techniques. A comprehensive background information for ML techniques are provided in chapter 4.4 of this thesis.



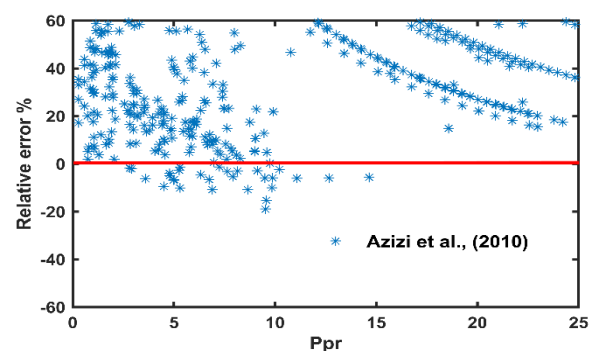
(A)



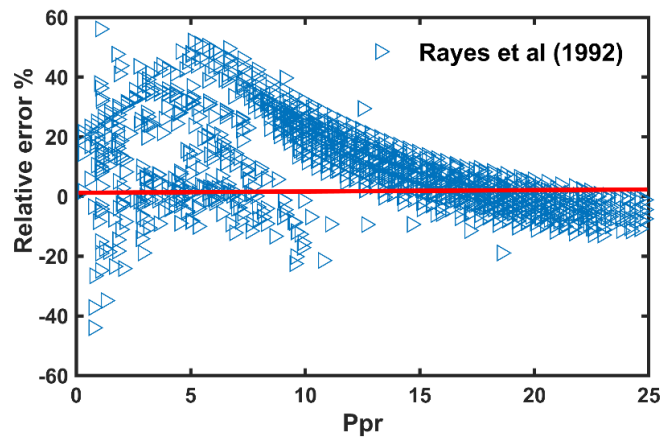
(B)



(C)

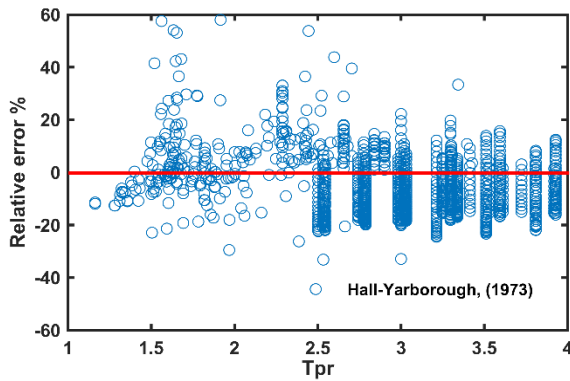


(D)

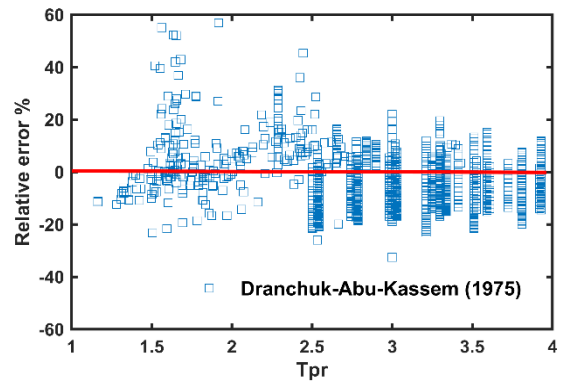


(E)

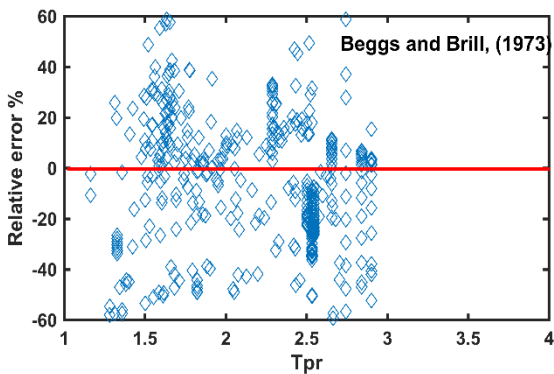
Figure 5.3. Residual plot of relative error percentage of utilized literature correlations in predicting gas-condensate two-phase Z factor as a function of pseudo reduced pressure (P_{pr}).



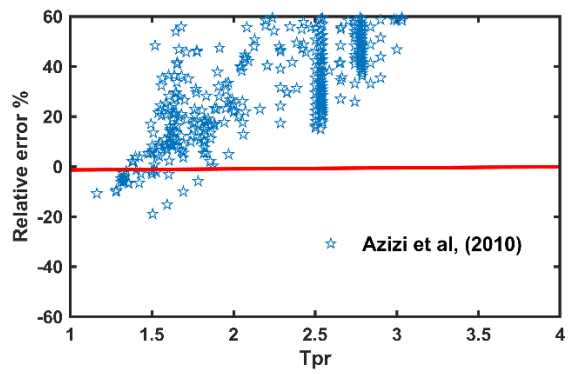
(A)



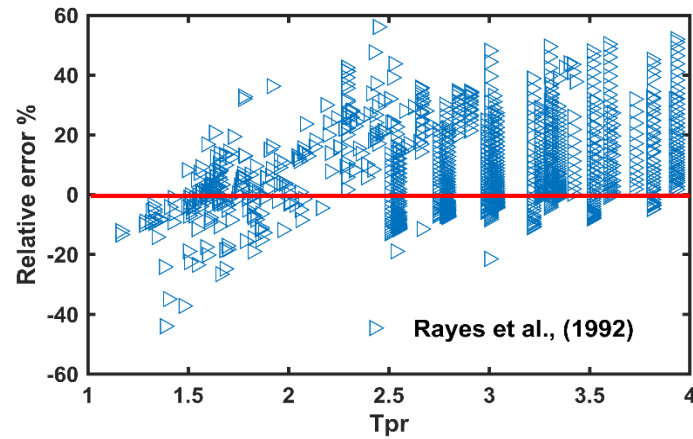
(B)



(C)



(D)



(E)

Figure 5.4. Residual plot of relative error percentage of literature models in predicting two-phase Z factor of gas-condensate systems as a function of pseudo reduced temperature (T_{pr}).

5.4 Development of new Z factor models

One of the primary aim of this study is to use innovative and different approach for modelling various aspect of gas-condensate well deliverability modelling. As it can be seen from chapter 4 of this thesis, a new modern numerical techniques known as machine learning (ML) extensively used to achieve our primary aim of the study. For modelling gas-condensate two-phase Z factor below the saturation pressure, various ML based techniques were implemented. The reason for implementing ML based approaches in estimating PVT properties are given as follow.

- The correlations for estimating properties such as Z factor are limited to various range of operational conditions (temperature and pressure).
- Based on the presented figures and plots in previous section it is concluded that using existing literature methods for calculating two-phase gas-condensate Z factor associated with large error.

The developed ML techniques should tackle the above mentioned challenges that exist using correlations for estimating Z factor. For this purpose two artificial neural networks models namely feed forward neural network (FFNN) and cascade forward neural network (CFNN) have been employed for better estimation of gas-condensate Z factor. Furthermore, another form of TSK fuzzy model known as adaptive neuro fuzzy inference system (ANFIS) also has been utilized. Based on ANFIS modelling a set of gas-condensate two-phase Z factor correlations were proposed. In this part the methodology of each utilized ML based approaches is discussed in details.

5.4.1 Cascade Forward Neural Network (CFNN)

One of the class of neural networks alongside feed forward neural network (FFNN), are cascade forward neural network (CFNN). This network also known as cascade forward back propagation (CFBP). CFBP algorithm resembles FFNN and the only different is that each individual neurons in input layer attached to each neuron in hidden layer and to each neuron in the output layer (Warsito, Santoso and Yasin, 2018). This means each subsequent neuron is bound to the previous one and training is performed accordingly. The typical CFNN for one input and one hidden layer is shown in Figure 5.5, where the neurons in input layer is connected to the output layer activation function. This additional connection of the input and output is the main difference between the conventional FFNN and CFNN.

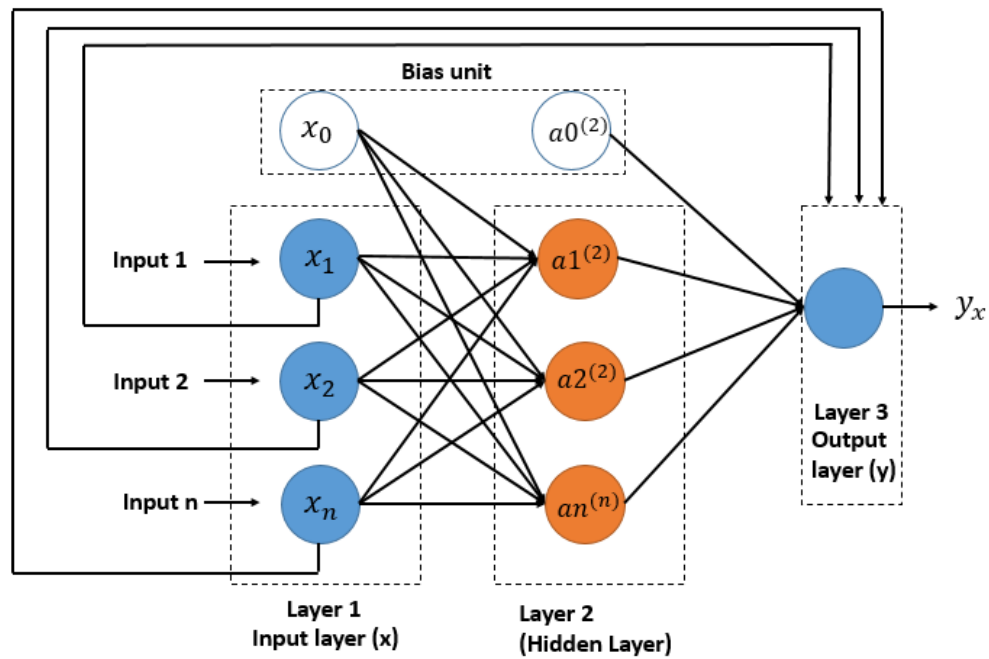


Figure 5.5. Architecture of the cascade forward (CFNN) neural network used in this study.

The relation between input and output layer of CFNN with one bias unit shown in Figure. 5.5 can be defined as follow.

$$y(x) = \sum_{i=1}^n g^i \theta_i^i x_i + g^o \left(\theta^b + \sum_{j=1}^k \theta_j^o g^h \left(\theta_j^b + \sum_{i=1}^n \theta_{ji}^h x_i \right) \right) \quad 5.14$$

Where x_i is representing inputs; $\theta_i(t)$ is connection weight function between input and output layer; g^i is the input activation function (usually sigmoid type), g^o is output

activation function, θ^b is the weight function of the bias unit, θ^h is the weight function of the hidden layer and g^h is hidden layer activation function.

The input layer of CFNN has 16 parameters include reservoir pressure (P), temperature (T), hydrogen sulphide (H₂S), nitrogen (N₂), carbon dioxide (CO₂), hydrocarbon compositions (C₁ – C₇), molecular weight of C₇₊ (MWC₇₊), specific gravity of gas on the surface (SG_g). The constructed network aims at predicting two-phase Z factor as output value. The inputs of the networks are independent variable and output is dependant. In another word gas-condensate two-phase Z factor is a function of all the inputs and can be written as follow.

$$Z_{2-phase} = f(P, T, H_2S, N_2, CO_2, C_1, C_2, C_3, IC_4, NC_4, IC_5, NC_5, C_6, C_{7+}, MWC_{7+}, SG_g)$$

In preparing the data, the data bank divided into three different data sets of training, validation and testing. The random selection of the data is employed, where 70% of the data bank assigned for training, 15% for validation and 15% for testing. Then several architecture of CFNN with various hidden layer in terms of size and combination of different neurons in each hidden layer examined. This is to ensure in developing a network with acceptable topology.

The objective for choosing the best CFNN network was the least mean square error (MSE) and highest coefficient of determination R (1). An example of the constructed CFNN in Matlab with three hidden layers and various neurons in each layer shown in following figure.

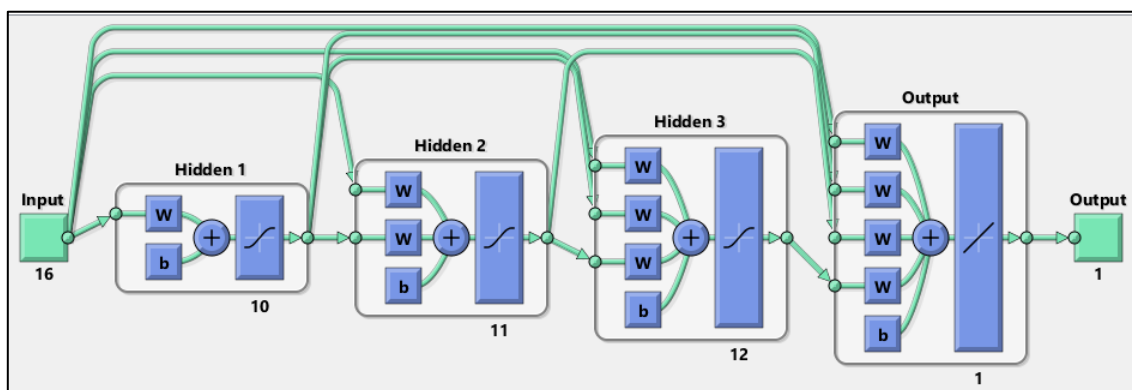


Figure 5.6. Cascade forward neural network with three hidden layer constructed in Matlab for prediction of two-phase Z factor.

Table 5.4 illustrates the results of this comparison for 1 hidden layer in constructed CFNN with different neurons. Same procedure was repeated to see the effect of number of hidden layers on improving the performance of the CFNN by means of increasing R. Among many algorithms available to train the network Levenberg –

Marquardt (LM) was used due to its stability and rapid convergence (Tanasa *et al.*, 2013; Mohamadi-Baghmolaei *et al.*, 2015; Rostami, Hemmati-Sarapardeh and Shamshirband, 2018). The LM algorithm is utilized for optimizing weights and biases of constructed CFNN, where the weights are computed as follow.

$$W_{k+1} = W_k - \left[J_{W_k}^T J_{W_k} - \eta I \right]^{-1} \times J_{W_k}^T e_{W_k} \quad 5.15$$

Where the weight matrix is W_{k+1} and W_k during $k + 1^{th}$ and k^{th} repetitions, J stands for Jacobian matrix, e is accumulated errors vector, I is the identity matrix and η is the parameter to express the ability of LM algorithm for altering the searching method (Hagan and Menhaj, 1994; Rostami, Hemmati-Sarapardeh and Shamshirband, 2018).

Table 5.4. The relation between the number of neurons and coefficient of determination for 1 hidden layer CFNN, using Levenberg – Marquardt (LM) as training algorithm.

No. Neurons	Training R	Validation R	Testing R	Convergence time
5	0.9931	0.9829	0.9919	00:00:00
10	0.9945	0.9953	0.9871	00:00:09
15	0.9951	0.9865	0.9744	00:00:00
20	0.9978	0.9926	0.9330	00:00:01
25	0.9972	0.9900	0.9778	00:00:02
30	0.9957	0.9931	0.9854	00:00:11
35	0.9965	0.9981	0.9869	00:00:04
40	0.9957	0.9953	0.9926	00:00:01
45	0.9943	0.9943	0.9686	00:00:02
50	0.9956	0.9923	0.9651	00:00:01
55	0.9967	0.9923	0.9651	00:00:02
60	0.9959	0.9962	0.9862	00:00:03
65	0.9973	0.9803	0.9974	00:00:13
70	0.9949	0.9858	0.9822	00:00:04

After attempting several trial and error to come up with the best CFNN network for prediction of gas-condensate two-phase Z factor, the topology of CFNN with one

hidden layer with only five neurons return the output with the lowest MSE and highest coefficient of determination (R). The developed code for this network provided in Appendix B.

5.4.2 Feed Forward Backpropagation Neural Networks

There are many different types of ANN networks that can be used for different applications. Feed-forward neural network is the first and simplest type of the neural network. In this type the information only moves in one direction forward from input to the hidden layer and then output (Giri Nandagopal and Selvaraju, 2016). In implementing ANN, it is important to recognize the difference between the network structure (the network's arrangement) and ANN algorithm (the computation that eventually produce the output of the network). Once the ANN is structured for prediction of particular application (in our case Z factor), the network is ready to be trained. Two approaches of supervised and unsupervised learning are currently exist in literature for training of the data. Supervised learning is working with a set of labelled data where an output response exist for each input data (training stage). In unsupervised learning the algorithm would find any hidden relations or pattern among the input and output data (Bell, 2014, p. 4).

The most widely used ANN architecture is fully connected, supervised network with backpropagation algorithm. Selecting the type of network depends on the nature of the data that is used for developing the network. Our data bank allows us to use supervised learning ANN method incorporated with backpropagation algorithm for training of the data. This type of networks are excellent for prediction task (Agatonovic-Kustrin and Beresford, 2000). The architecture of feedforward backpropagation ANN network that constructed for prediction of two-phase Z factor is shown in Figure 5.7. This architecture is for one hidden layer, the number of hidden layers are arbitrary and trial and error can be used to get the optimum structure to achieve the highest performance of the network.

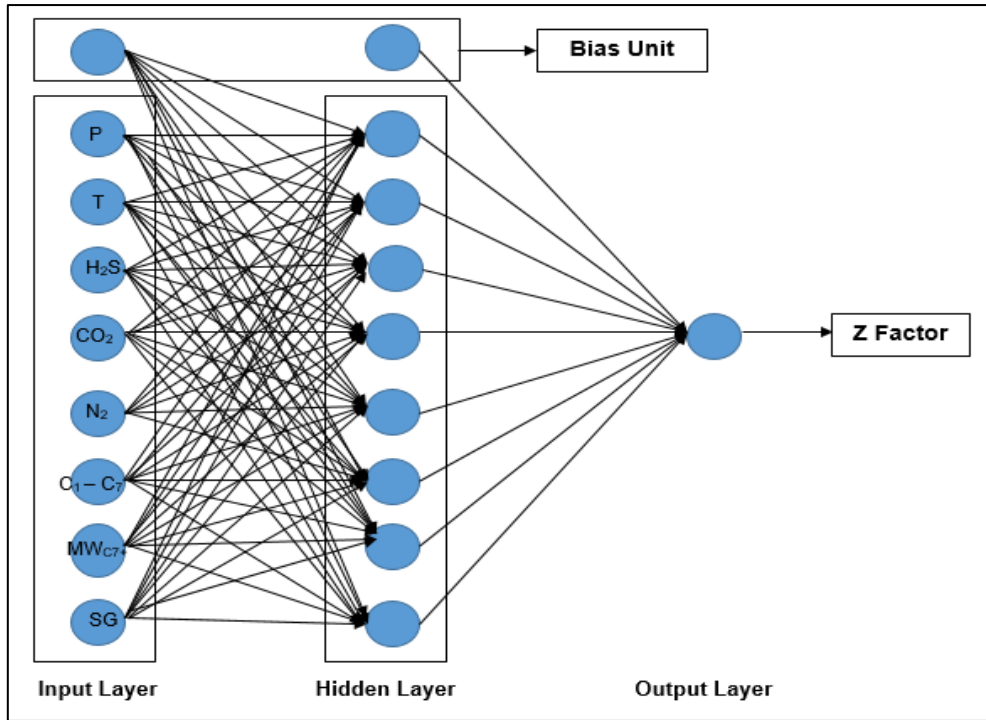


Figure 5.7. Feed Forward Artificial Neural Network structure used for prediction of Z factor.

In FFNN structure if x represents the input variables, ω represents weight function of each neuron and y stands for output of the network, the mathematical equation can be written as follow.

$$y = f^o \left(\omega^b + \sum_{j=1}^k \omega_j^o f^h \left(\omega_j^b + \sum_{i=1}^n \omega_{ji}^h x_i \right) \right) \quad 5.16$$

Where ω^b is the bias of input layer to output and ω_j^b is the weight from bias to hidden layer.

The accuracy of the neural network performance is influenced by network's architecture such as number of neurons, hidden layers and the training algorithm (Haykin, 1994; Gharagheizi *et al.*, 2014).

Despite high popularity of the FFNN, its main defect is correct determination of the neurons required in each layer. Using fewer neurons leads to poor performance of the model and higher number of neurons results in overfitting (Soroush *et al.*, 2015; Mesbah, Soroush and Rostampour Kakroudi, 2017). Defining the optimal architecture that simulate the actual behaviour of experimental two-phase Z factor is not an easy task. Hence, a trial and error scheme has been developed to find the size of hidden layers and magnitude of the neurons in each individual layer.

Initially the collected data bank 1084 data sets (19518 data points) were partitioned into three parts of training (70%) validation (15%) and testing (15%). The data selection for each developed networks is random, which means training, validation and testing in one network is not necessarily similar to other network. This gives high capability of the trained networks to predict the output with various input.

Furthermore, to train the network diverse algorithms can be used to minimise the error during the training. Some of these algorithms are including Levenberg–Marquardt (LM), Bayesian – Regularization (BR), Resilient Back Propagation (RBP) and Scaled Conjugate Gradient (SCG) (Majidi *et al.*, 2014). The most frequently used algorithms of Levenberg – Marquardt (LM) and Bayesian – Regularization (BR) have been implemented in our scheme to achieve the optimum network performance. LM algorithm is shown in equation 5.15. Here the formulation of BR algorithm is presented.

BR algorithm minimizes the combination of squared error and weights and then generalized the network by determination of correct weights and biases. The BR function uses Jacobian matrix, which performance of the network will be assessed by sum of mean square error (Mackay', 1992). BR takes place within LM algorithm, where backpropagation can be used to calculate Jacobian matrix with respect to the weights and biases of the network (Louridas and Ebert, 2016). The BR is formulated in the following.

$$W_{k+1} = - \left(\frac{[J_{W_k}^T J_{W_k} + \eta I]}{J_{W_k}^T e_{W_k}} \right) \quad 5.17$$

Both LM and BR algorithm are used in order to find the best neural network to perform for prediction of Z factor. Our criteria for selecting the best FFNN was chosen by monitoring network performance through mean square error (MSE) and coefficient of determination (R). The results of these comparisons for one hidden layer are given in Table 5.5 and Table 5.6 for FFNN with LM and FFNN with BR algorithm respectively. The networks are constructed in Matlab and the codes are presented at Appendix B.

Table 5.5. Statistical parameters and convergence time of FFNN with one hidden layer using LM algorithm.

No. Neurons	R ²	MSE	Convergence time (Second)
5	0.9864	0.0074	00:00:02
10	0.9891	0.0034	00:00:00
15	0.9892	0.0033	00:00:01
20	0.9605	0.0072	00:00:00
25	0.9914	0.0026	00:00:01
30	0.9947	0.0013	00:00:01
35	0.9854	0.0039	00:00:02
40	0.9922	0.0021	00:00:02
45	0.9953	0.0013	00:00:02
50	0.9741	0.0061	00:00:02
55	0.9917	0.0018	00:00:03
60	0.9537	0.0115	00:00:06
65	0.9861	0.0032	00:00:09
70	0.9503	0.0120	00:00:06

Table 5.6. Statistical parameters and convergence time of FFNN with one hidden layer using BR algorithm for training.

No. Neurons	R ²	MSE	Convergence time (Hours)
5	0.9756	0.0060	00:00:05
10	0.9895	0.0026	00:00:47
15	0.7559	0.0838	00:01:43
20	0.9909	0.0024	00:09:01
25	0.9965	0.0023	00:00:55
30	0.9726	0.0079	00:08:01
35	0.9746	0.00557	00:08:33
40	0.9956	0.00106	00:08:33
45	0.8411	0.0442	00:03:08
50	0.9877	0.0031	00:05:27
55	0.9834	0.00478	00:05:50
60	0.9876	0.003375	00:11:20
65	0.9872	0.003272	00:09:54
70	0.8442	0.004076	00:10:04

The performance of the FFNN in terms of MSE with two different algorithms of LM and BR is presented in Figure 5.8. As the results in Figure 5.8 shows the constructed FFNN incorporated with BR algorithm consists of 40 neurons returns the output values with the least MSE of 0.001062 than other networks. This followed by constructed network using LM algorithm with 30 neurons with the MSE of 0.001346. Taking the convergence time (computational efficiency) into consideration we propose the network with LM algorithm for prediction of gas-condensate two-phase Z factor as BR needs more time (00:08:30) than LM algorithm (00:00:01) in the training stage. The proposed FFNN is shown in Figure 5.9. This network consists of 16 inputs, one hidden layer with 30 neurons, one bias in each layer and one output (two-phase Z factor). This network is representation of the ANN structure in Figure 5.7. The FFNN will be used for prediction of gas-condensate two-phase Z factor below the saturation pressure.

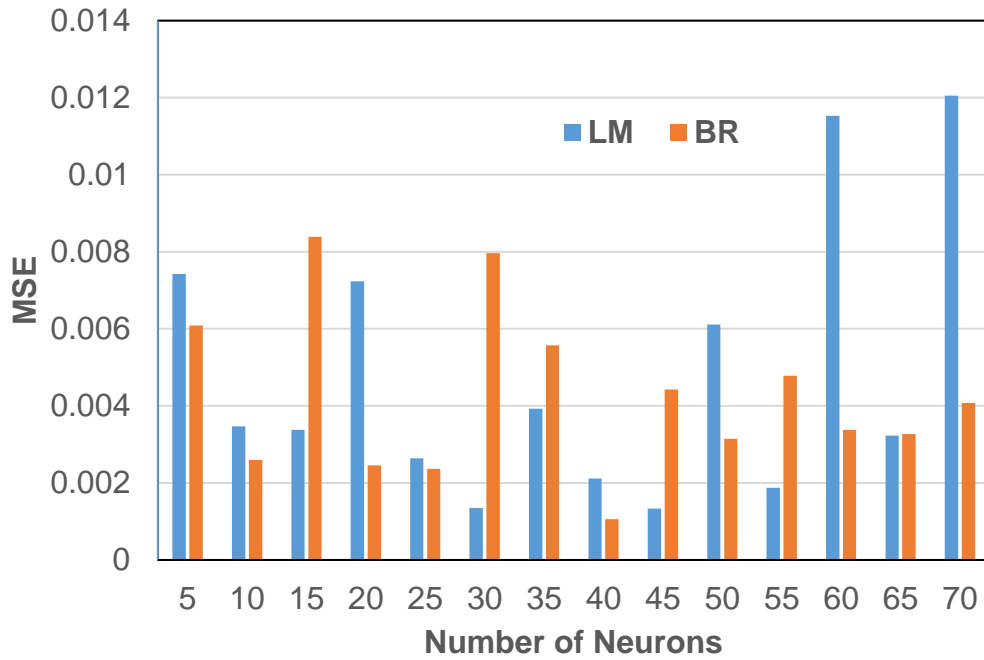


Figure 5.8. Comparison of constructed feed-forward neural network (FFNN) performance with different number of neurons in hidden layer.

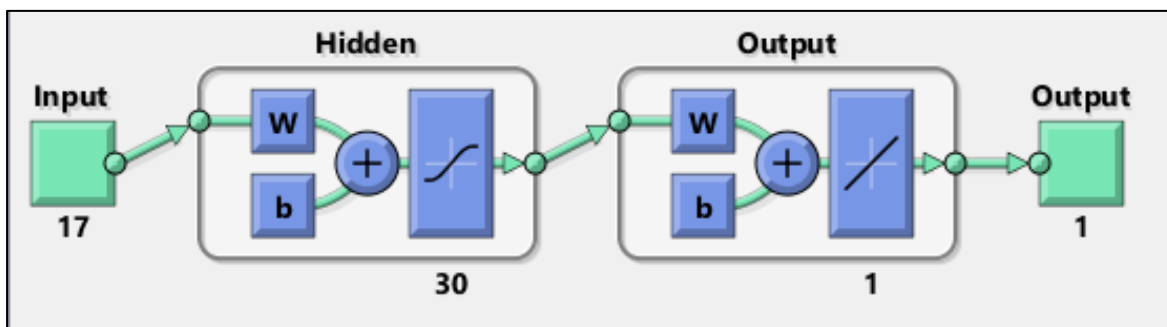


Figure 5.9. Proposed FFNN for prediction gas condensate two-phase compressibility factor.

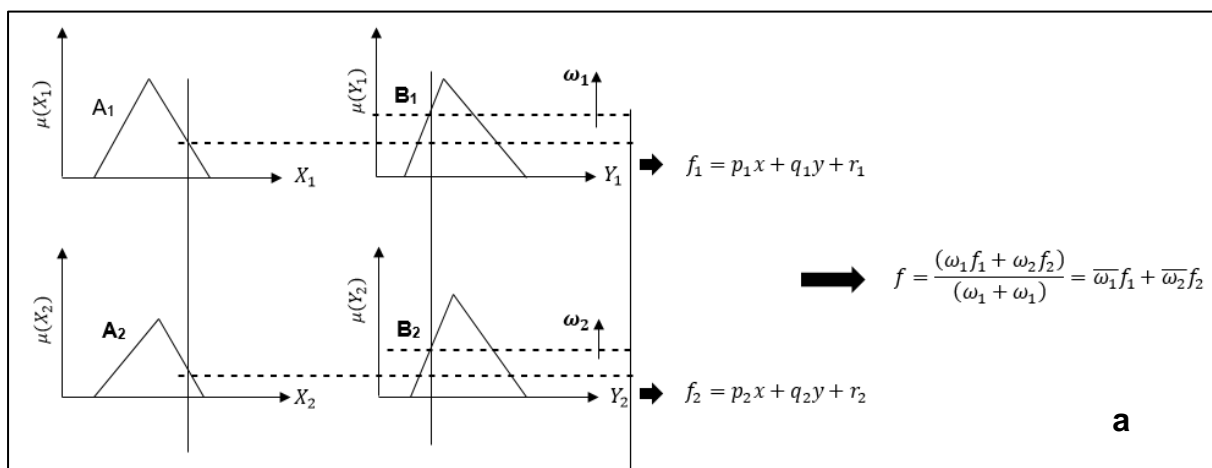
5.4.3 Adaptive Neuro Fuzzy Inference System (ANFIS)

Another intelligent technique that is utilized in this study for prediction of two-phase Z factor in gas-condensate reservoirs known as Adaptive Neuro Fuzzy Inference System (ANFIS). The method is another form of TSK fuzzy algorithm implemented in 4.6. The method is combination of artificial neural network and fuzzy rule based system. The main reason for adopting ANFIS to estimate two-phase Z factor is to have the benefits of artificial neural network as well as fuzzy reasoning.

As explained in section 4.5 and 4.6 fuzzy inference system is employing fuzzy IF-THEN rules that can model the qualitative aspects of human knowledge of a system

or process without any need of precise quantitative analysis. The ability of fuzzy sets for modelling and fuzzy identification initially was identified by Takagi and Sugeno, (1985). Although there has been numerous application of fuzzy system in various fields of engineering after Takagi and Sugeno, (1985) discovery, there was not any standard method for transforming human knowledge into rule base fuzzy inference system (FIS). Furthermore there was not an effective method available for tuning the membership function of Takagi and Sugeno, (1985) FIS system.

Adaptive Neuro Fuzzy Inference System (ANFIS) was developed following TSK fuzzy method to fulfil the aforementioned deficiencies of TSK fuzzy approach. In early development of TSK algorithm type 1 and type 2 of ANFIS were shaped. In these two types calculation of the errors in ANFIS algorithm was through using back-propagation gradient decent, which calculate the error signals from output layer backward to the input nodes. This learning rule is same as backpropagation gradient descent of feed-forward neural network. The difficulty with this approach is in tuning the membership functions through rigorous trial and error, which is not an easy task to implement. Furthermore, the gradient decent learning rule is notorious for slowness and has tendency to trap in local minima. Hence, Jang, (1993) introduced type – 3 Adaptive Neuro Fuzzy Inference System (ANFIS) in order to tackle the aforementioned deficiencies and enhance previous version of ANFIS model. He proposed an adaptive hybrid neural network based on combination of gradient decent algorithm and least square method for better optimization of the parameters of Takagi and Sugeno FIS system. This optimization of FIS system makes type 3 ANFIS a powerful tool for prediction and forecast of various applications. The architecture of type 3 fuzzy reasoning and ANFIS with two input variables of x and y is shown in Figure 5.10 and will be explained in following.



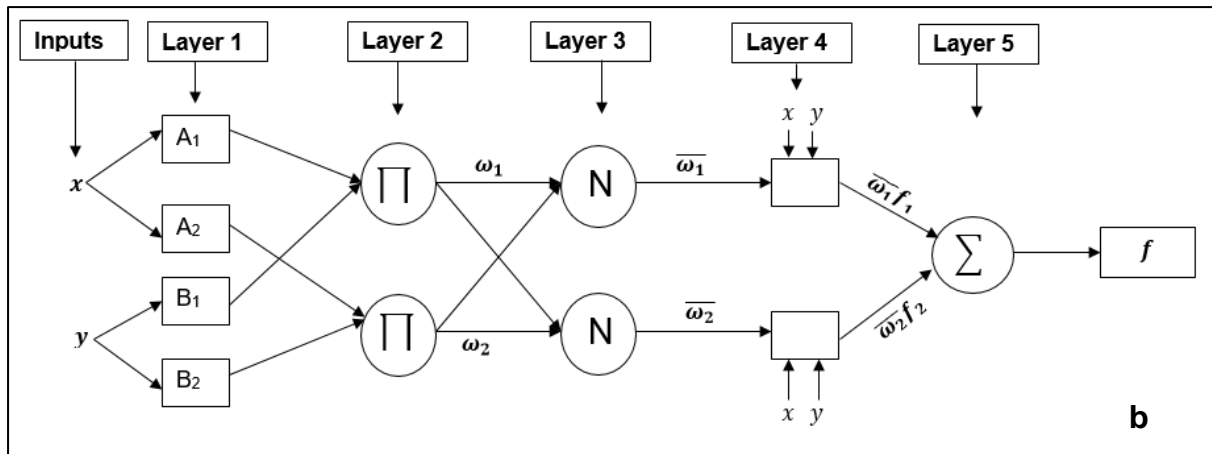


Figure 5.10. Schematic illustration of type – 3 fuzzy reasoning (a); ANFIS structure type – 3 (b).

Figure. 5.10a represents the fuzzy reasoning behind the ANFIS model with two input variables and triangular membership function. This is essentially explains Takagi and Sugeno’s fuzzy type with introducing number of rules in this case two as follow:

Rule 1: If x is A_1 and y is B_1 , then $f_1 = p_1x + q_1y + r_1$

Rule 2: If x is A_2 and y is B_2 , then $f_2 = p_2x + q_2y + r_2$

Where A_1, A_2, B_1 and B_2 are membership functions x and y are inputs, p_1, q_1 and r_1 are constant parameters of linear function.

The typical ANFIS structure shown in Figure 5.10b consists of five layers, each processing different operations in the structure. Two square and circular nodes have been proposed in Figure 5.10b, where square nodes reflect adaptive (having constant parameters) and circular nodes are fixed (without parameters) (Jang, 1993). The operation of ANFIS algorithm in each layer is as follow.

Layer 1: every node i in this layer represents by a function of square node as follow:

$$O_i^1 = \mu A_i(x) \quad 5.18$$

Where x is input of the node i , A_i is a linguistic term of fuzzy sets (very low, low, etc.,...) associated with the node function. The main role of this layer is to turn the raw data into linguistic terms based on previously selected membership functions (node functions). Many membership functions can be selected such as triangular, gaussian, trapezoidal, sigmoidal, s-shape and z-shape in this layer.

Layer 2: the nodes in this layer labelled with \square , where the results are calculated as multiplication of incoming signals from layer 1. Effectiveness of the network is determined by the results of this layer, as the outcome is a weight function. Following equation represents the network operation in layer 2.

$$\omega_i = \mu A_i(y) \times \mu B_i(y) = \omega_i, \quad i = 1,2 \quad 5.19$$

Where A_i and B_i are linguistic terms of y input in universe of μ . The output of the above equation is the firing weight of each node (ω_i).

Layer 3: Incoming weight's strengths calculated in layer 2 are normalized in this step to identify the difference between the firing strength of each rule from the total firing strength of entire rules. This normalization in layer 3 labelled by N and following equation can be used to determine each weight's strength.

$$\omega_i = \frac{\omega_i}{\omega_1/\omega_2} \quad 5.20$$

Layer 4: This layer characterizes the linguistic terms of the output model. This means the influence of each rule on output is determined in this layer with some degree. A square node with the following function carries out the computation in layer 4.

$$O_i^4 = \bar{\omega}_i f_i = \bar{\omega}_1(p_1x + q_1y + r_1) \quad 5.21$$

Where p_1 , q_1 and r_1 are linear variables. These variables are optimized by ANFIS algorithm to provide the accuracy between the model outcome and the target value.

Layer 5: A circular signal node in this layer is used to sum up all the incoming signals (rules) from previous layer. The computation transfers the rules to numeric values using weighted average sum approach as follow.

$$O_i^5 = \sum_i \bar{\omega}_i f_i = \bar{\omega}_1 f_1 + \bar{\omega}_2 f_2 = \frac{\sum_i \bar{\omega}_i f_i}{\sum_i \bar{\omega}_i} \quad 5.22$$

Where O_i^5 stands for output of the network, $f_{1,2}$ represent output functions of rule 1 and rule 2.

The above procedure also has been adopted for calculation and prediction of two-phase Z factor for gas-condensate reservoirs below the dew point pressure. For this purpose an ANFIS structure is proposed and will be explained in following section.

5.4.4 Proposed ANFIS structure

In this part a new ANFIS structure based on Jang, (1993) was developed for prediction of two-phase Z factor of gas-condensate reservoirs. A Matlab code has been developed and used for this purpose (refer to Appendix B for details of the developed code). The inputs variables consist of 16 parameters including, pressure (P), temperature (T), carbon dioxide (CO₂), hydrogen sulphide (H₂S), nitrogen (N₂), HCC₁, HCC₂, HCC₃, HCIC₄, HCNC₄, HCIC₅, HCNC₅, HCC₆, HCC₇₊, molecular weight of C₇₊ (MWC₇₊) and gas specific gravity (SG). To distinguish between the parameters of the fuzzy rule and English letters HC is added to each hydrocarbon components. The output parameter of the network is two-phase Z factor. To be consistent with other intelligent model CFNN and FFNN, the data bank divided to three parts of training (70%), validation (15%) testing (15%). These proportions were randomly selected to ensure suitable coverage of all the data ranges of the variables.

For simplicity if we assume the proposed structure with only two rules and using Takagi – Sugeno type FIS system, then the two-phase Z factor can be presented as follow.

Rule 1:

if T is A_1 , P is B_1 , CO_2 is C_1 , H_2S is D_1 , N_2 is E_1 , HCC_1 is F_1 , HCC_2 is G_1 , HCC_3 is H_1 , $HCIC_4$ is I_1 , $HCNC_4$ is J_1 , $HCIC_5$ is K_1 , $HCNC_5$ is L_1 , HCC_6 is M_1 , HCC_{7+} is N_1 , MWC_{7+} is O_1 SG is P_1 ; Then

$$\begin{aligned} \mathbf{function}_1 = & a_1T + b_1P + c_1CO_2 + d_1H_2S + e_1N_2 + f_1HCC_1 + g_1HCC_2 + h_1HCC_3 \\ & + i_1HCIC_4 + j_1HCNC_4 + k_1HCIC_5 + l_1HCNC_5 + m_1HCC_6 + n_1HCC_{7+} \\ & + o_1MWC_{7+} + p_1SG + q_1 \end{aligned}$$

Rule 2:

if T is A_2 , P is B_2 , CO_2 is C_2 , H_2S is D_2 , N_2 is E_2 , HCC_1 is F_2 , HCC_2 is G_2 , HCC_3 is H_2 , $HCIC_4$ is I_2 , $HCNC_4$ is J_2 , $HCIC_5$ is K_2 , $HCNC_5$ is L_2 , HCC_6 is M_2 , HCC_{7+} is N_2 , MWC_{7+} is O_2 SG is P_2 ; Then

$$\begin{aligned}
 \mathbf{function}_2 = & a_2T + b_2P + c_2CO_2 + d_2H_2S + e_2N_2 + f_2HCC_1 + g_2HCC_2 + h_2HCC_3 \\
 & + i_2HCIC_4 + j_2HCNC_4 + k_2HCIC_5 + l_2HCNC_5 + m_2HCC_6 + n_2HCC_7 + \\
 & + o_2MWC_7 + p_2SG + q_2
 \end{aligned}$$

In above rules T, P, CO₂, H₂S, N₂, HCC₁ – HCC₇₊, MWC₇₊ and SG are input parameters of the model, *A_i* to *P_i* is representing the membership function (gaussian, triangular, trapezoidal and etc.). In the developed functions, *a_i* to *q_i* are the constant parameters of the ANFIS model (optimized by training algorithm). In order to estimate these constant parameters, least square approach was used. The corresponding ANFIS architecture for prediction of gas-condensate two-phase Z factor is shown in Figure 5.11.

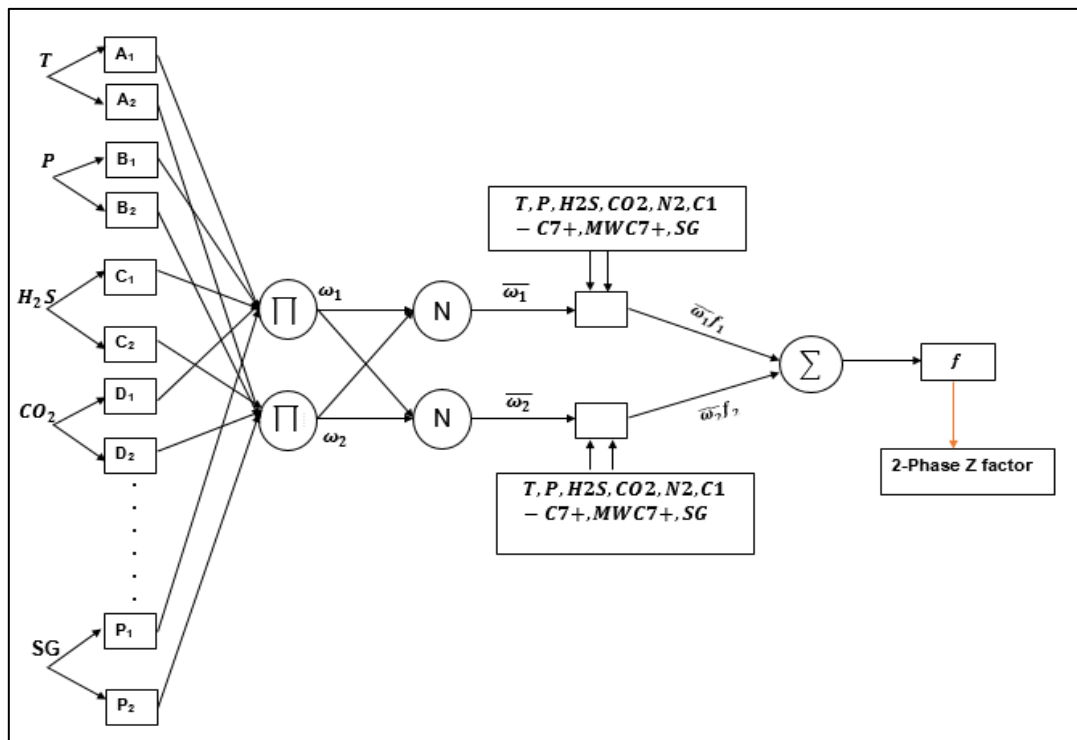
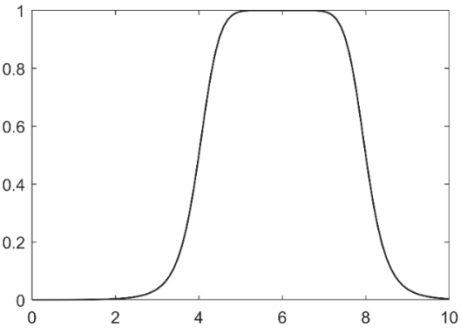


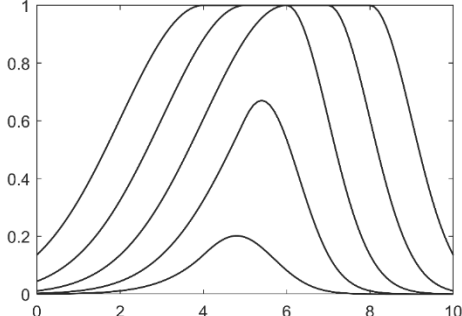
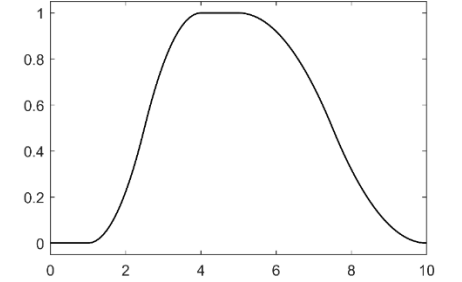
Figure 5.11. Proposed ANFIS architecture for prediction of gas condensate two-phase Z factor.

The effectiveness of the developed ANFIS model for prediction of two-phase Z factor influenced by the type of membership function, cluster range and number of fuzzy rules. Several membership functions are exist to relate the input variables to the output. The ability of 9 membership functions and their effectiveness in prediction of two-phase Z factor have been investigated. These membership functions are including gaussian, triangular, trapezoidal, generalized-bell shaped, gaussian combination

membership function, pi (Π) shaped, sigmoidal, S shaped and Z shaped membership functions. The description and mathematical representation of gaussian, triangular and trapezoidal membership functions previously given in section (4.7.2). The shape and mathematical formula of other studied membership functions presented in Table 5.7. Primarily the effectiveness of all membership functions have been studied using constant number of fuzzy rules (for instance 8 rules). The statistical parameters of mean square error (MSE) and coefficient of determination (R^2) have been recorded to see the best performance of the ANFIS using various membership functions. As the results in Table 5.8 shows gaussian membership function has the best performance for prediction of the output (two-phase Z factor). This is proven by lower mean square error (MSE) and highest coefficient of determination (R^2). Hence, gaussian membership function has been chosen to incorporate with ANFIS algorithm in this study for modelling gas-condensate two-phase Z factor.

Table 5.7. The description and details of the utilized membership functions for prediction of gas-condensate two-phase Z factor using ANFIS.

Name	Description	Shape
generalized-bell shaped	<p>The generalized-bell shaped membership function has three parameters of a, b and c. The parameter of c representing centre of the curve and a and b represent the feet of the shape. Parameter b is usually positive.</p> $f(x; a, b, c) = \frac{1}{1 + \left \frac{x - c}{a} \right ^{2b}}$	 <p><i>gblmf = f(x; 2, 4, 6)</i></p>

<p>Gaussian combination membership function</p>	<p>This membership function is a combination of sigmoid function and parameter; $y = gauss2mf(x; sig1, c1, sig2, c2)$.</p> <p>The first function sig1, c1 determine the shape of the most left curve.</p> <p>The second function sig2, c2 represents the shape of the most right curve shape. The function can be written mathematically as follow.</p> $f(x; \sigma, c) = e^{-\frac{(x-c)^2}{2\sigma^2}}$	 <p>$gauss2mf = f(x; 0.1, 10)$</p>
<p>pi (Π) shaped</p>	<p>The name of this membership function is because of its pi (Π) shape. Four parameters of a, b, c and d is used in construction of the shape. The parameters of a and d locate the feet of the curve, while b and c locate its shoulders.</p> $f(x; a, b, c, d) = \begin{cases} 0, & x \leq a \\ 2 \left(\frac{x-a}{b-a} \right)^2, & a \leq x \leq \frac{a+b}{2} \\ 1 - 2 \left(\frac{x-b}{b-a} \right)^2, & \frac{a+b}{2} \leq x \leq b \\ 1, & b \leq x \leq c \\ 1 - 2 \left(\frac{x-c}{d-c} \right)^2, & c \leq x \leq \frac{c+d}{2} \\ 2 \left(\frac{x-c}{d-c} \right)^2, & \frac{c+d}{2} \leq x \leq d \\ 0, & x \geq d \end{cases}$	 <p>$pi mf = f(x; 1, 4, 5, 10)$</p>

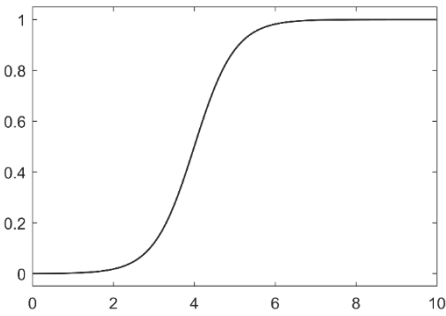
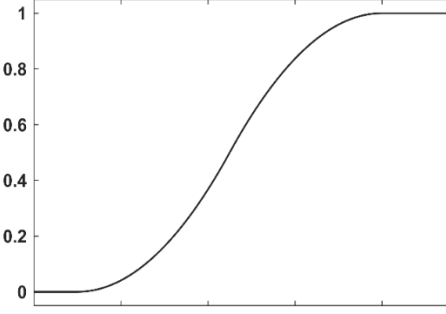
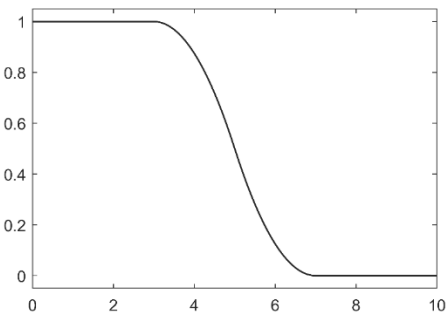
<p>Sigmoidal</p>	<p>The sigmoidal membership function is depending on two parameters of a and c. Depending on the sign of these parameters the sigmoidal membership function is open to the right or to the left. This would give this function ability to cover very large or very negative data points.</p> $f(x; a, c) = \frac{1}{1 + e^{-a(x-c)}}$	 <p>$sigmf = f(x; 2, 4)$</p>
<p>S shape</p>	<p>The S shape membership function is spline based curve on vector x. the parameters of a and b represents the extreme slope portion of the curve. The mathematical description of the function is:</p> $f(x; a, b) = \begin{cases} 0, & x \leq a \\ 2 \left(\frac{x-a}{b-a} \right)^2, & a \leq x \leq \frac{a+b}{2} \\ 1 - \left(\frac{x-a}{b-a} \right)^2, & \frac{a+b}{2} \leq x \leq b \\ 1, & x \geq b \end{cases}$	 <p>$smf = f(x; 1, 8)$</p>
<p>Z shape</p>	<p>The shao of this membership function is Z shape and it is function of two parameters of a and b. mathematically this function can be written as follow.</p> $f(x; a, b, c, d) = \begin{cases} 1, & x \leq a \\ 2 \left(\frac{x-a}{b-a} \right)^2, & a \leq x \leq \frac{a+b}{2} \\ 2 \left(\frac{x-a}{b-a} \right), & \frac{a+b}{2} \leq x \leq b \\ 0, & x \geq b \end{cases}$	 <p>$Zmf = f(x; 3, 7)$</p>

Table 5.8. Performance of the developed ANFIS model using various membership function.

Membership function	No. IF-THEN rules	R ²		MSE	
		Training	Testing	Training	Testing
Gaussian	8	0.9956	0.8454	0.001057	0.0486
Triangular	8	0.9265	0.76672	0.00253	0.1163
Trapezoidal	8	0.9512	0.8077	0.00105	0.0482
generalized-bell shaped	8	0.9365	0.79521	0.001253	0.0576
Gaussian combination	8	0.9486	0.80549	0.001059	0.0486
pi (Π) shaped	8	0.87562	0.74372	0.002365	0.01087
sigmoidal	8	0.86256	0.73243	0.002563	0.11784
S shape	8	0.85236	0.72376	0.002623	0.12060
Z shape	8	0.86325	0.73301	0.002585	0.11886

5.4.5 Clustering (Partitioning) of the data

Prior selection of adequate membership functions for ANFIS modelling need partitioning of the training data set to certain number of clusters. For partitioning of the data to number of clusters several clustering methods are available in literature. The examples are look up table method, fuzzy c-means (FCM), Gustafson-Kessel (GK), K-means clustering and subtractive clustering (SC). Using the look up table method is not recommended for the large scale problem due to increasing the parameters of the model and number of MFs, which consequently leads to the complexity of the model (Lee, 2005; Safari *et al.*, 2014) . Further details about different clustering techniques is given in section 4.6.1. FCM and SC are two methods that have been used extensively in the literature for data organization and also data compressions in ANFIS modelling. Both methods shown high efficiency over wide range of data for various applications, however many studies preferred SC over FCM due to its simplicity in calculation procedure and also its independency of problem dimensionality (Jang, Sun and Mizutani, 1997; Nikravesh, Zadeh and Aminzadeh, 2003; Lee, 2005).

FCM clustering algorithm determines the degree of belonging of each data point to each cluster. The centre of each cluster is found in an iterative procedure by minimizing an objective function called mountain function. If the data is highly non-linear and multidimensional the computation time is growing exponentially. This is because the algorithm needs to evaluate the mountain function over all of the grid points (Bezdek and Pal, 1992; Jang, Sun and Mizutani, 1997). Nevertheless, subtractive clustering is more adaptable to non-linear more dimensional data and

return the number of clusters quickly and efficiently in a simple computational procedure. SC is an appropriate choice for the data sets without knowing how many clusters are required (Chiu, 1994). Hence, in this study we utilized SC method proposed by Chiu, (1994) for partitioning two-phase Z factor training data bank. SC assumes that each data point is a potential cluster centroid. The results of SC can be used for initializing centroid of the FCM algorithm. The SC proposed by Chiu, (1994) is an extension of mountain clustering method of Yager and Filev, (1994). Based on density index (D_i) of potential centroid data, the SC algorithm evaluates the density index of each data point x_i as follow (Chiu, 1994; Chen *et al.*, 2015).

$$D_i = \sum_k^n \exp \left[-\frac{\|x_i - x_k\|^2}{(r_a/2)^2} \right] \quad 5.23$$

Where x_i and x_k are data points, r_a is clustering radius and can be determined by the following equation.

$$r_a = 0.5 \min\{\max\|x_i - x_k\|\} \quad 5.24$$

The data beyond the radius has little or no effect on the density index (D_i). To implement equation 5.24, first, the data index of cluster 1 (x_{c1}) should be selected. This data index has the highest density index (D_{c1}) at the first cluster centroid. Then the data in the radius r_a is removed from potential centroid data set, and the neighbourhood with lower density index is defined by the following equation.

$$D_i = D_i - D_{c1} \exp \left[-\frac{\|x_i - x_k\|^2}{(r_b/2)^2} \right] \quad 5.25$$

Where $r_b > r_a$, this would distinguish between two clusters. The above mathematical procedure of SC can be summarized in five steps as follow:

1. Using equation 5.23 based on the density of surrounding data points; calculate the likelihood that each data point would define a cluster centre.
2. Choose the data points with the highest potential to be the first cluster centre.
3. Using equation 5.24 remove all data points near the first cluster centre.
4. Choose the remaining points with the highest potential as the next cluster centre using equation 5.25.

5. Repeat steps 3 and 4 until all data points are within the influence range (r_a) of a cluster centre.

Accurate determination of clustering radius (r_a) using above procedure is directly influence the performance of the developed ANFIS model. Changing the value of r_a would change the number of membership functions, consequently number of IF-THEN fuzzy rules. To obtain optimum number of rules the value of clustering radius changed between $0 < r_a < 1$. The performance of the ANFIS system evaluated by the statistical metric of RMSE in the training and testing stage.

In this study a new iterative technique is developed and carried out to find the optimum number of fuzzy rules and determine the optimum number of clusters. The implementation of the method is as follow:

1. Calculate r_a values between $0 < r_a < 1$ in ten intervals using equation 5.24; and record the RMSE of training and testing of ANFIS model.
2. Select two intervals with lowest RMSE (for example 5 and 6 in table 15), and eliminate other clustering radius with high error.
3. Calculate r_a values for two new selected intervals ($0.45 < r_a < 0.5$); and record RMSE of the ANFIS model.
4. Repeat step 2 to 3 until the RMSE reduced to the point where number of IF-THEN rules converged or no longer changes.
5. Use the calculated clustering radius (r_a) value as an optimum choice for developing number of rules in ANFIS model.

The results in Table 5.9 and 5.10 illustrate the values of RMSE for training and testing data sets using the above procedure. As it can be seen from Table 5.9 the number of IF-THEN rules is converged at 11, with the cluster radius of ($r_a \approx 0.45$). Therefore, the proposed ANFIS model for prediction of gas-condensate two-phase Z factor consists of 11 fuzzy IF-THEN rules.

Table 5.9. Effect of clustering radius on number of fuzzy rules and the performance of the model (1st iteration).

No. ANFIS	Clustering radius (r_a)	No. IF-THEN rules	RMSE	
			Training	Testing
1	0.25	35	852	4451
2	0.30	23	3.60	277
3	0.35	17	43	1286
4	0.40	12	0.07252	1.13
5	0.45	11	0.04224	0.08657
6	0.50	9	0.04773	0.12197
7	0.55	8	0.04734	0.07299
8	0.60	6	0.05029	0.26412
9	0.65	4	0.05077	0.49331
10	0.70	4	0.049461	0.39360
11	0.75	4	0.05025	0.28450
12	0.80	3	0.05869	0.09796
13	0.85	2	0.06338	0.05266
14	0.90	2	0.06289	0.05207
15	0.95	2	0.06228	0.05146
16	1	2	0.06224	0.05696

Table 5.10. Effect of clustering radius on number of fuzzy rules and the performance of the model (2st iteration).

No. ANFIS	Clustering radius (r_a)	No. IF-THEN rules	RMSE	
			Training	Testing
1	0.45	11	0.04224	0.08657
2	0.451	11	0.04158	0.09991
3	0.4515	11	0.04121	0.14248
4	0.452	11	0.03984	0.11151
5	0.4525	11	0.04085	0.15212
6	0.453	11	0.03980	0.10294
7	0.4535	11	0.04201	0.10277
8	0.454	11	0.04206	0.09990
9	0.4545	11	0.04203	0.20143
10	0.455	11	0.039483	0.20952
11	0.4555	11	0.04198	0.18015
12	0.4560	11	0.04206	0.18578
13	0.4565	11	0.04055	0.12805
14	0.457	11	0.04199	0.15657
15	0.4575	11	0.04209	0.10474
16	0.4580	11	0.04209	0.18251
17	0.4585	11	0.04037	0.15201
18	0.4590	11	0.04007	0.09991
19	0.4595	11	0.03979	0.10813
20	0.46	11	0.03953	0.09709

The ANFIS structure with 11 fuzzy IF-THEN rules constructed in Matlab and shown in Figure 5.12. The output of ANFIS is a linear function with several optimized parameters for each rule. More clear graphical visualization of constructed type 3 ANFIS for prediction of gas-condensate two-phase Z factor is presented in Figure 5.13.

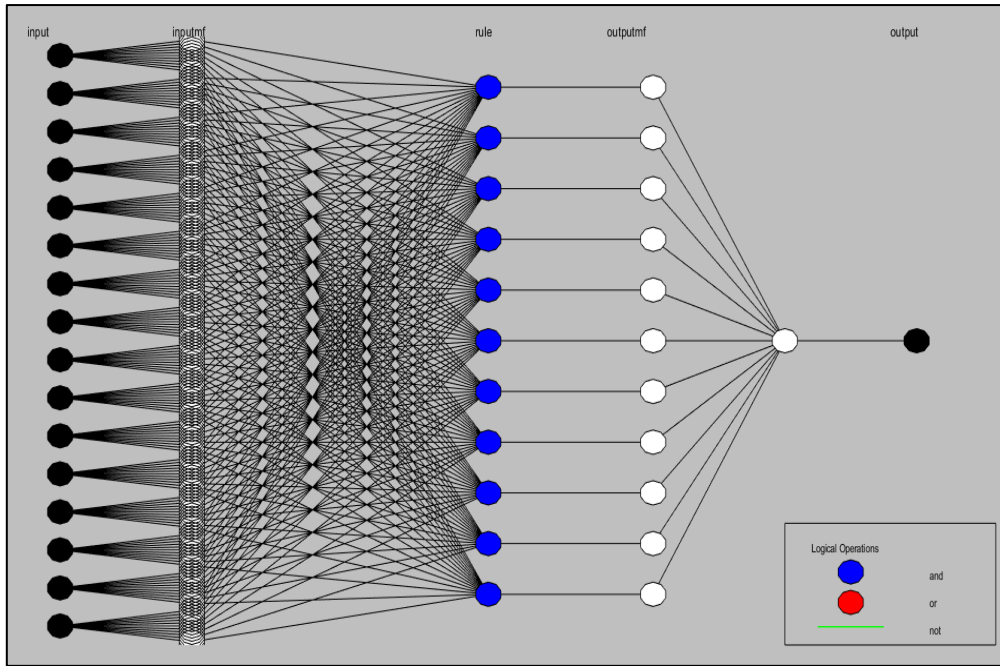


Figure 5.12. Structure of proposed ANFIS model for prediction of two-phase Z factor of gas condensate reservoirs.

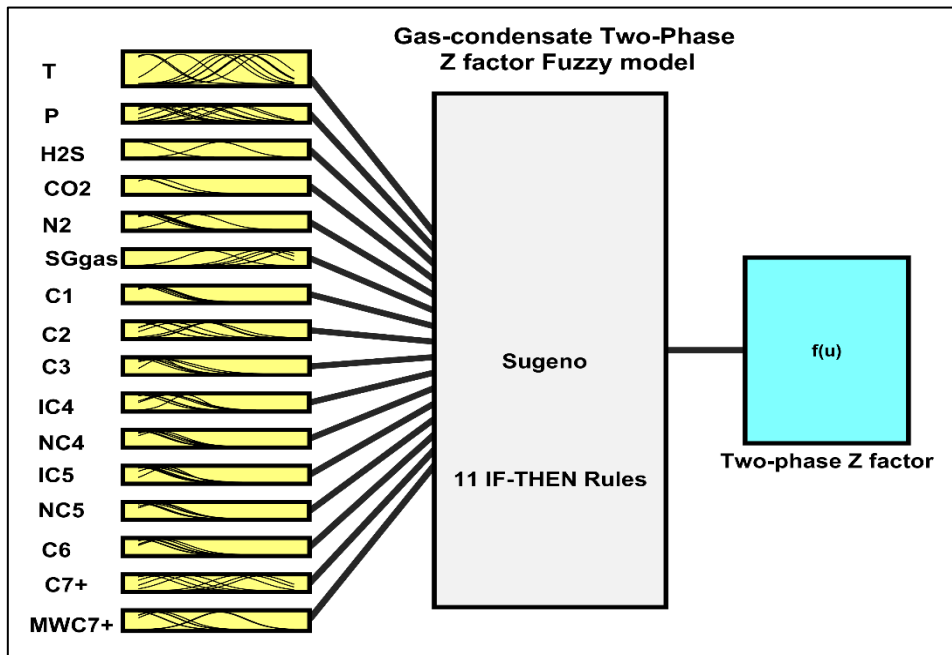


Figure 5.13. Architecture of Takagi – Sugeno fuzzy model for prediction of gas condensate two-phase Z factor.

5.4.6 Results and discussion

Z factor of gas-condensate reservoirs is one of the most important PVT properties that its accurate determination leads to accurate well deliverability modelling of such reservoirs below the saturation pressure. In this study extensive data bank from various published sources have been collected to investigate the accuracy of the current literature models for prediction of two-phase Z factor.

Five literature correlations of Hall-Yarborough (1973) and Dranchuk-Abu-Kassem (1975), Beggs and Brill (1973), Azizi et al., (2010) and Rayes et al., (1992) have been utilized for this purpose.

In utilizing the existing literature models initially pseudo critical properties of temperature (T_{pc}) and pressure (P_{pc}) of each gas-condensate system were computed, using mixture composition and Kay's mixing rule. For computing critical properties of hydrocarbon plus fraction because of availability of compositional data the method of Matthews and Roland, (1942) was used. To include non-hydrocarbon impurities in computation of pseudocritical properties Wichert and Aziz, (1972) correlation was employed. From calculated T_{pc} and P_{pc} , pseudo reduced temperature (T_{pr}) and pressure (P_{pr}) were calculated. Finally, two-phase Z factor of each gas-condensate system was estimated. The prediction accuracy of existing literature models for estimating gas-condensate two-phase Z factor were not acceptable and associated with high error. Therefore other techniques known as machine learning based models have been utilized for the prediction of gas-condensate two-phase Z factor.

Accuracy and robustness of any ML based method is depending on the diversity of the data bank that is used for their development (Ahmadi and Ebadi, 2014; Hajirezaie et al., 2015; Hemmati-Sarapardeh et al., 2020; Kamari et al., 2019). The detail statistical description of the data bank is presented in 5.3.6 of this chapter. Two neural network based models known as feed forward neural network (FFNN) and cascade forward neural network (CFNN) and one fuzzy logic based model know as adaptive neuro fuzzy inference system (ANFIS) adopted for prediction of two-phase Z factor in gas-condensate reservoirs. The data divided into three parts of training (70%), validation (15%) and testing (15%). Consistent proportion of the data used for all three models. The random selection of the data was performed to ensure homogeneous distribution of the data bank. These models consist of 16 inputs of T, P, H₂S, CO₂, N₂,

$C_1 - C_{7+}$, $MW_{C_{7+}}$ and gas specific gravity (SG), and a single output of gas-condensate two-phase Z factor.

Statistical error analysis of the developed machine learning methods were performed using metrics of MAE, RMSE and AARD% and illustrated in Table 5.11. This table shows the error measurements of all data sets at training, validation and testing stage for three developed ML based techniques. The results confirms very good performance of all three ML based models. ANFIS model outperforms the CFNN and FFNN with lowest MAE of 0.0025124, RMSE of 0.0025367 and AARD% of 0.2191478 followed by FFNN and CFNN for prediction of tow-phase Z factor of gas-condensate reservoirs. Furthermore, computational efficiency of all three developed models are demonstrated in table 5.11. As the results indicate the developed ML based models predicts the two-phase Z factor very fast with almost 0 seconds, nevertheless the CFNN is slightly perform better than FFNN and ANFIS.

Table 5.11. Statistical error computation of the developed models in prediction of gas-condensate's two-phase Z factor below the saturation pressure.

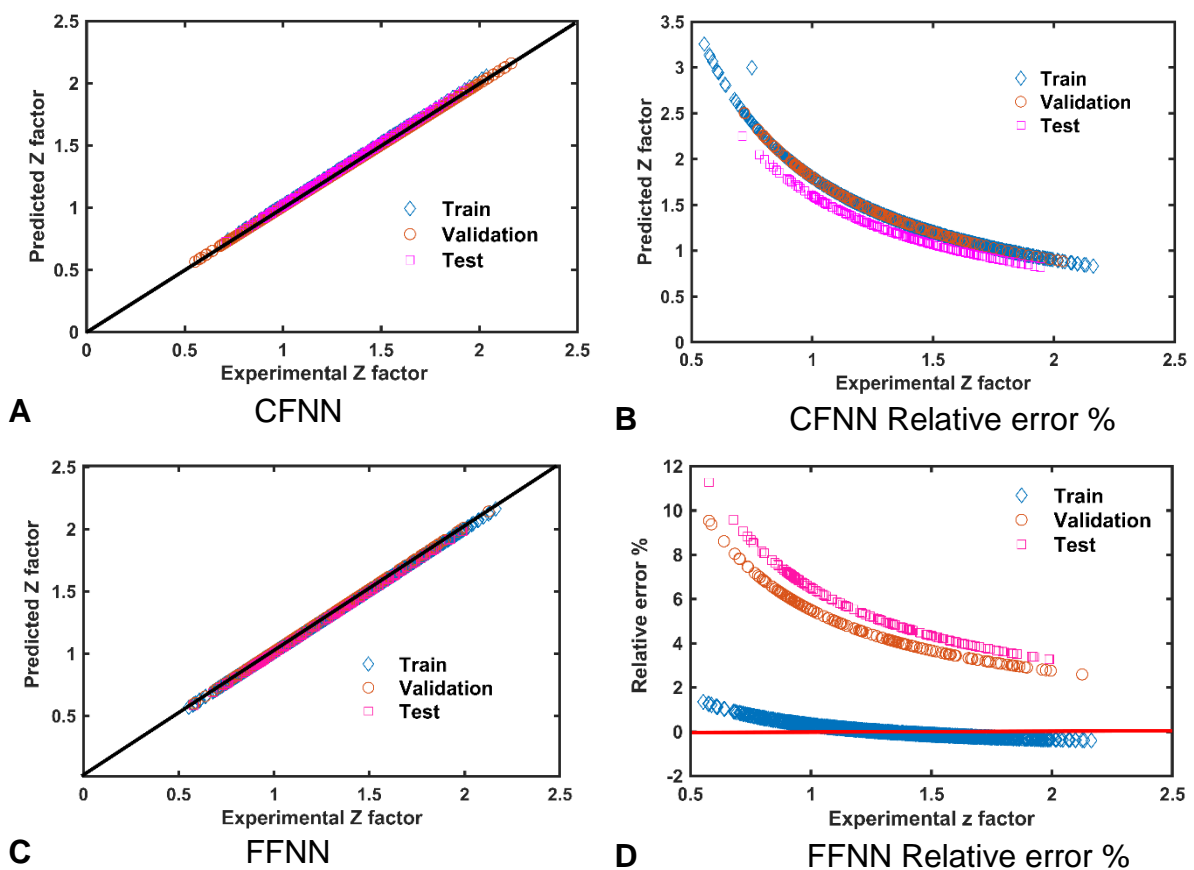
Model	MAE	RMSE	AARD%	Convergence time (hour,minute,second)
FFNN	0.0047	0.0058	0.3029	00:00:00
CFNN	0.0053	0.0062	0.5117	00:00:01
ANFIS	0.0025	0.0025	0.2191	00:01:25

To visualize the performance of ML based models Figure 5.14 shows the cross plot and the graph of relative error percentage of three models. The results of the cross plot show all three ML models predict experimental two-phase Z factor with high accuracy in all three stages of training, validation and testing. The statistical metrics in Table 5.11 and the results of cross plots/relative error in Figure 5.14E-F indicate that the ANFIS model has the best performance among other two utilized ML based methods for prediction of two-phase Z factor. This confirms high capability of ANFIS

for relating non-linear inputs and outputs of a problem, once correct optimization of its membership functions have obtained.

In order to see the performance of the ML based models as a function of T_{pr} and P_{pr} for prediction of two-phase Z factor, the graph of relative error against T_{pr} and P_{pr} were generated and presented in Figure 5.15 and Figure 5.16. The results show an excellent agreement between the obtained values of ML based models and experimental two-phase Z factor as a function of T_{pr} and P_{pr} .

Comparison of statistical error metrics of MAE, RMSE and AARD% of all utilized literature models and the developed ML based approaches presented in Figure 5.17 and Figure 5.18. The results show that ANFIS model has superiority over all other techniques with the least MAE, RMSE and AARD% of 0.00251, 0.00254 and 0.219 respectively.



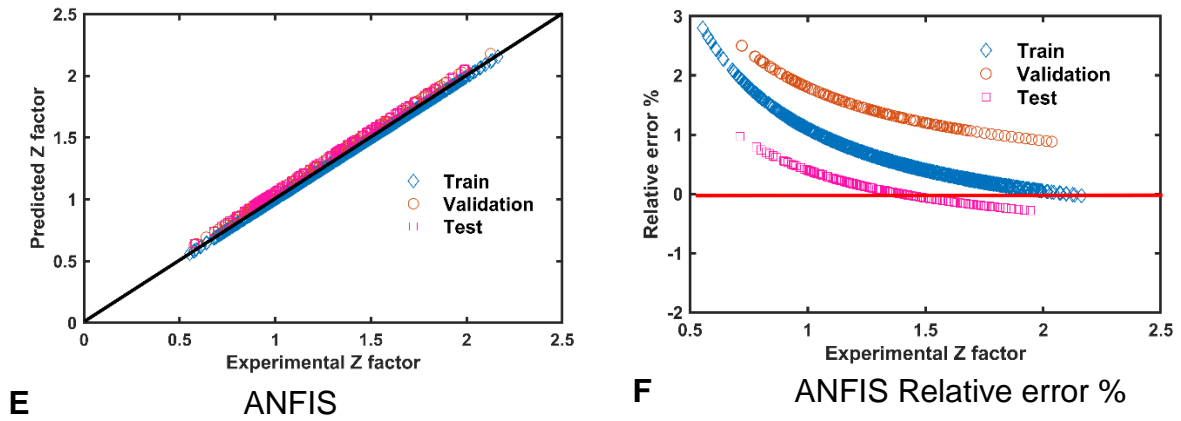


Figure 5.14. Cross plot and relative error of utilized three machine learning models in predicting two-phase Z factor at training, validation and testing stage.

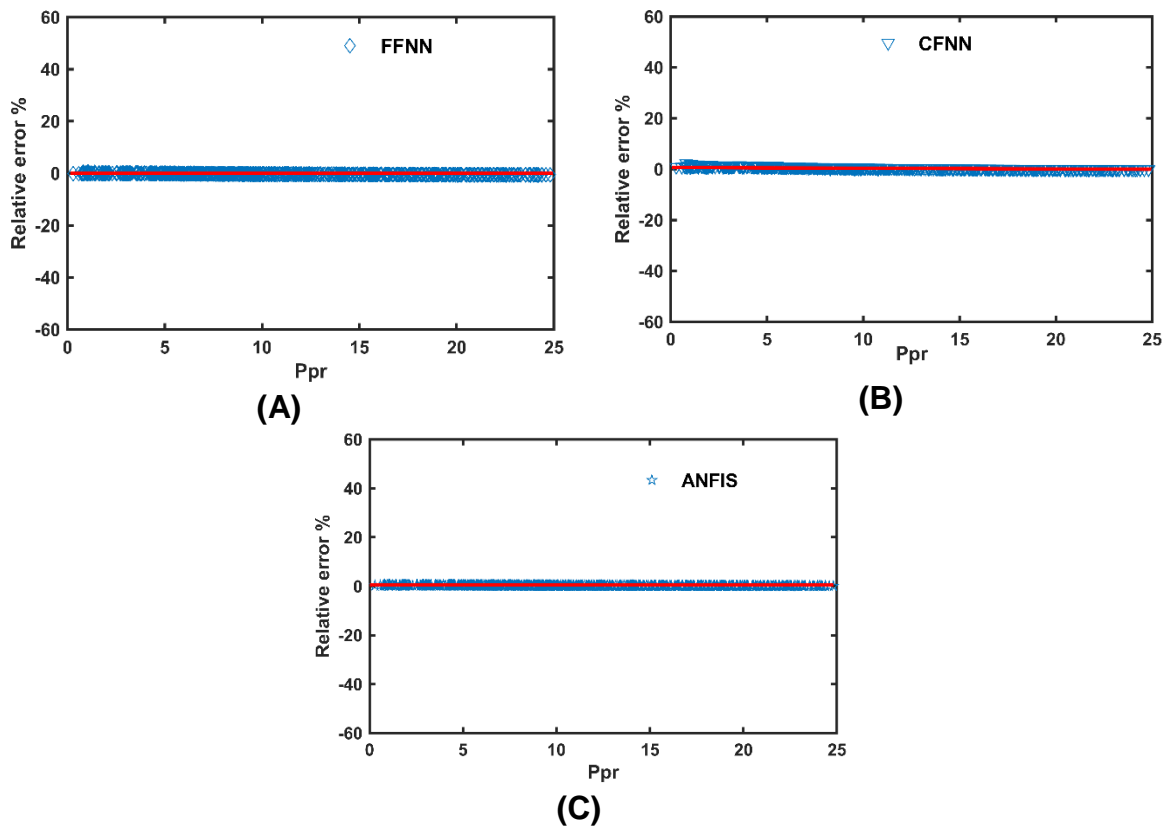


Figure 5.15. Residual plot of relative error percentage of intelligent models in predicting two-phase Z factor as a function of pseudo reduced pressure (P_{pr}).

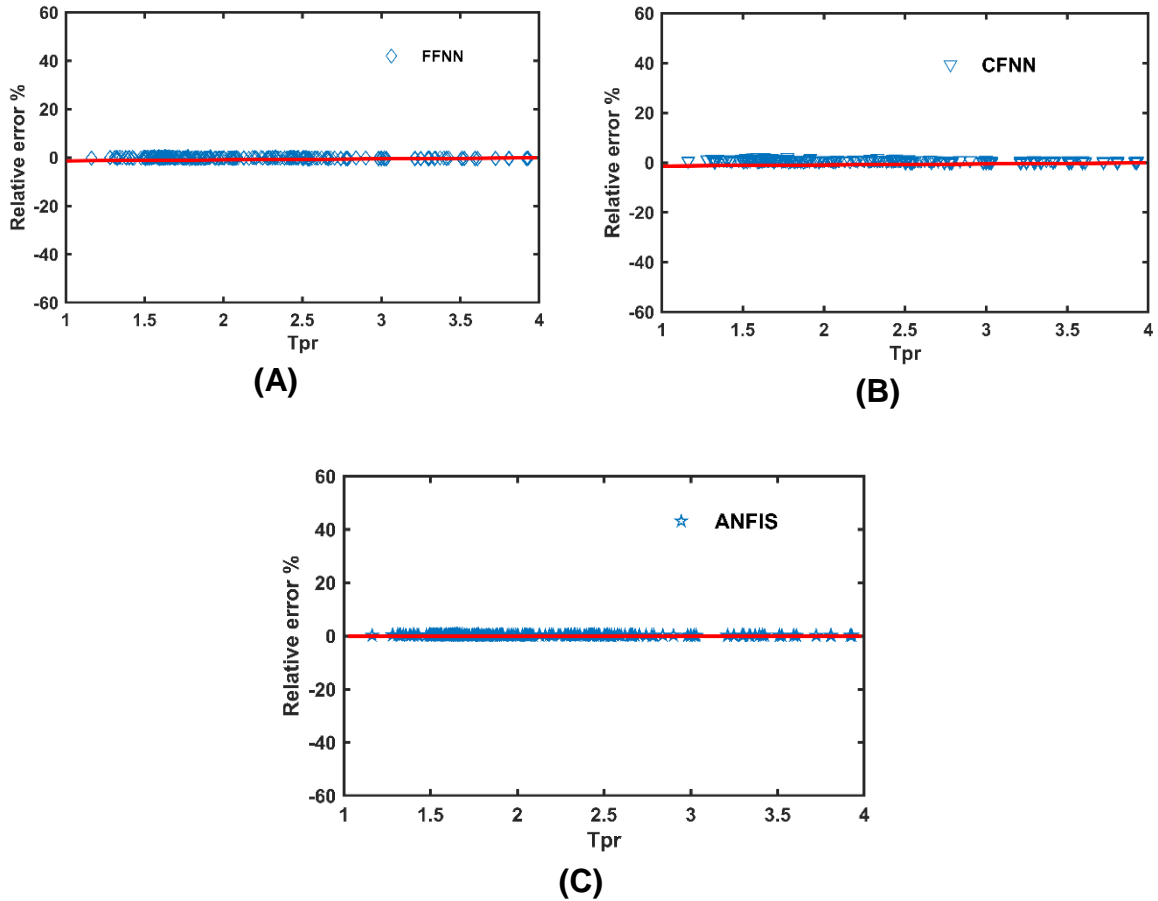


Figure 5.16. Residual plot of relative error percentage of intelligent models in predicting two-phase Z factor as a function of pseudo reduced temperature (T_{pr}).

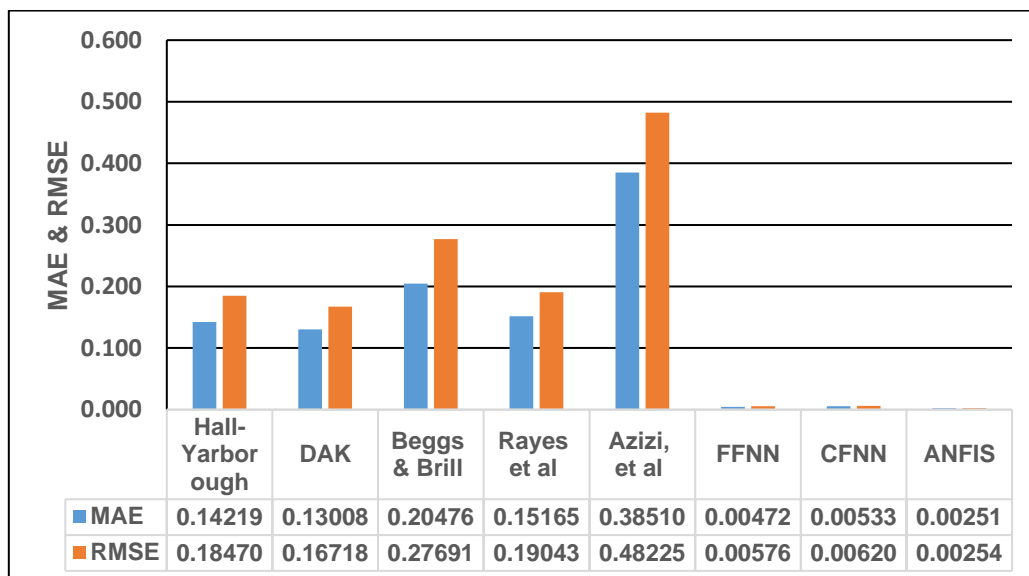


Figure 5.17. Error comparison of all utilized literature models and the developed ML based approached in prediction of gas-condensate two-phase Z factor.

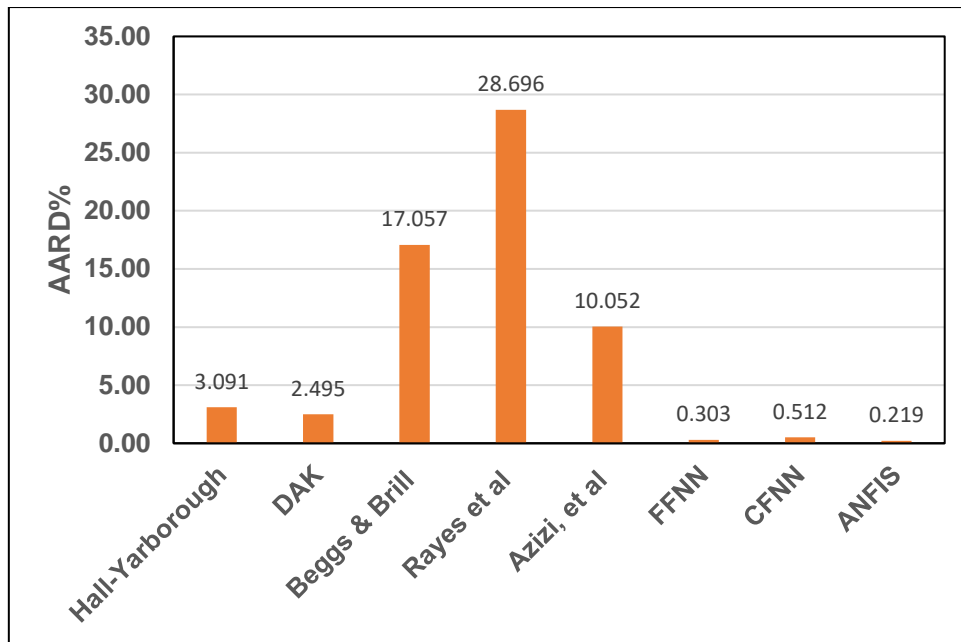


Figure 5.18. Error comparison of all utilized literature models and the developed ML based approaches in prediction of two-phase Z factor.

The ability of the developed ML based models in following the physical trend of the two-phase Z factor of gas-condensate reservoirs as a function of pressure and temperature has to be tested. This is important to ensure the developed ML based models are following physical trend of two-phase Z factor similar to literature correlations. For this purpose, two independent samples of gas-condensate fluids from literature were collected. First sample is from a rich gas-condensate reservoir in North Sea obtained from Danesh, (1998, pp. 53–56). This sample is from sweet gas-condensate with no hydrogen sulphide (H_2S) content. Constant Volume Depletion (CVD) test was performed and compositional changes of each components were detected with pressure depletion. The result of CVD test for this sample is provided in Table 5.12.

Second sample obtained from Elsharkawy, (2002), is a very rich sour gas-condensate reservoir contain considerable amount of hydrogen sulphide ($H_2S=28.16\%$ at the dew point pressure). CVD test also was performed on this sample, where the compositional changes of the sample during the CVD test was recorded as shown in Table 5.13.

Estimation of Z factor using literature models requires determination of pseudocritical properties (P_{pc} and T_{pc}). Kay, (1936) mixing rule is used for calculation of critical

properties. For characterization of hydrocarbon plus (C_{7+}) properties and determination of pseudocritical properties (P_{pc7+} , T_{pc7+}) the method proposed by Matthews and Roland, (1942) is used. Non – hydrocarbon properties were also determined by utilizing the method of Wichert and Aziz, (1972).

Performance of utilized literature models and also the developed ML based techniques in prediction of aforementioned independent samples examined by means of statistical parameters of MAE, RMSE and AARD%. These statistical parameters are determined for each model as a function of pseudo reduced pressure (P_{pr}). The results of this error analysis shown in Table 5.14 for both gas-condensate fluid samples.

Graphical performance of all methods for prediction of rich sour gas-condensate sample is plotted as a function of P_{pr} and shown in Figure 5.19. As the result in Figure 5.19 shows, among the literature models only Rayes et al., (1992) is close to the experimental two-phase Z factor in the range of ($P_{pr} \leq 4$). Other literature techniques of Azizi et al., (2010); Beggs and Robinson, (1975); DAK, (1973) and Hall and Yarborough, (1973) estimate the experimental two-phase Z factor with high error below ($P_{pr} \leq 4$).

The graph of experimental Z factor in Figure 5.19 also indicates that below the saturation pressure the Z factor has a direct correlation with reservoir pressure. As the pressure increases, the magnitude of two-phase Z factor also increases. The result show that the conventional methods cannot follow the physical trend of the change in Z factor of gas-condensate reservoirs below the saturation pressure. Statistical measurements of different approach as well as the developed models are illustrated in Table 5.14. The results of statistical error metrics show that the developed methods predict experimental two-phase Z factor with very good accuracy in compare to conventional techniques.

In sample 1, that high content of hydrogen sulphide (H_2S) exist, the conventional techniques return the experimental two-phase Z factor with very high error as shown in Figure 5.19 and Table 5.14. ANFIS outperforms other methods with MAE of 0.01764 and RMSE of 0.02994 followed by FFNN, CFNN, Rayes et al., (1992), Beggs and Brill, (1973), DAK, (1974), Hall and Yarborough, (1973) and Azizi et al., (2010). The results show reliability and robustness of the developed models for prediction of two-phase Z factor in critical gas-condensate fluid below the saturation pressure. The developed

ML based methods follow the physical trend of the experimental Z factor with minimum deviation.

For the second sample which the H₂S content is zero, although the conventional methods perform well in terms of MAE and RMSE, however the ANFIS model retuened the experimental Z factor with the least AARD% of 0.4506 followd by CFNN, FFNN, Beggs and Brill, (1975), DAK, (1975), Hall and Yarborough, (1973), Rayes et al., (1992) and Azizi et al., (2010). Figure 5.20 depicts the trend of experimental two-phase Z factor of sample 2 as a function of pressure and the performance of utilized literature methods and developed ML based models. As can be seen the ML based models are following the physical trend of the two-phase Z factor with very good accuracy.

The problem with conventional methods is that their accuracy are limited for specific range and their performance depends on the type of mixing rule that has been used in the calculation of critical properties (P_{pr} and T_{pr}). The ML based approaches developed in this study don't have aformentioned limitations. Their performance is highly accurate for prediction of two-phase Z factor of gas-condensate reservoirs regradless of the compositional variation that occurs in such reservoirs below the saturation pressure.

Table 5.12. Constant Volume Depletion (CVD) results on North Sea gas-condensate sample at temperature of 394K (Danesh, 1998, pp. 53–56).

T(F)	P (psia)	H ₂ S	N ₂	CO ₂	C ₁	C ₂	C ₃	IC ₄	NC ₄	IC ₅	NC ₅	C ₆	C ₇₊	MW C ₇₊	SG	Z 2-Phase
249.5	6822	0.0	0.30	1.72	79.17	7.48	3.29	0.52	1.25	0.36	0.55	0.62	3.74	231	0.943	1.1718
249.5	5800	0.0	0.30	1.71	79.93	7.44	3.22	0.51	1.23	0.35	0.54	0.58	4.19	207	0.889	1.0867
249.5	4930	0.0	0.31	1.71	80.77	7.41	3.21	0.50	1.21	0.34	0.52	0.55	3.47	202	0.845	1.0056
249.5	3915	0.0	0.32	1.72	81.61	7.46	3.20	0.50	1.18	0.33	0.50	0.52	2.66	190	0.797	0.9479
249.5	3045	0.0	0.32	1.73	82.33	7.54	3.19	0.49	1.15	0.32	0.48	0.49	1.96	180	0.760	0.9176
249.5	2030	0.0	0.33	1.75	82.71	7.64	3.22	0.49	1.15	0.32	0.48	0.46	1.45	174	0.737	0.9171

Table 5.13. Constant Volume Depletion (CVD) results on sour gas-condensate sample (Elsharkawy, 2002).

T(F)	P (psia)	H ₂ S	N ₂	CO ₂	C ₁	C ₂	C ₃	IC ₄	NC ₄	IC ₅	NC ₅	C ₆	C ₇₊	MW C ₇₊	SG	Z 2-Phase
250	4204	28.16	3.83	6.08	40.33	4.48	2.48	0.6	1.32	0.79	0.81	1.21	9.91	165	0.818	0.838
250	3614	27.67	4.55	6.44	43.82	4.71	2.43	0.55	1.2	0.68	0.69	0.96	6.3	121	0.778	0.788
250	3014	27.22	4.76	6.69	46.41	4.81	2.39	0.51	1.11	0.6	0.6	0.78	4.12	116	0.773	0.75
250	2414	26.95	4.73	6.85	48.07	4.87	2.37	0.49	1.06	0.55	0.54	0.66	2.86	112	0.768	0.718
250	1814	27.32	4.61	6.94	48.44	4.93	2.39	0.49	1.06	0.53	0.52	0.6	2.17	109	0.764	0.686
250	1214	28.92	4.34	6.99	46.88	4.96	2.52	0.55	1.14	0.58	0.57	0.63	1.92	107	0.762	0.639
250	714	31.82	3.94	6.79	43.31	4.94	2.77	0.67	1.4	0.74	0.71	0.77	2.14	107	0.762	0.553

Table 5.14. Statistical measurement of the developed models and literature models for prediction two-phase Z factor of two gas-condensate samples as a function of P_{pr} .

Sample 1	MAE	RMSE	AARD%
Hall-Yarborough, (1973)	0.1753	0.2154	24.04
DAK, (1974)	0.1681	0.2064	22.95
Beggs & Brill, (1975)	0.1680	0.2072	22.78
Azizi, et al, (2010)	0.2374	0.2720	34.36
Rayes et al., (1992)	0.0648	0.0707	6.91
FFNN	0.0271	0.0450	-2.25
CFNN	0.0420	0.0469	-0.0929
ANFIS	0.0176	0.0299	1.49
Sample 2	MAE	RMSE	AARD%
Hall-Yarborough, (1973)	0.0752	0.0861	7.41
DAK, (1974)	0.0640	0.0731	6.38
Beggs & Brill, (1975)	0.0299	0.0394	-2.75
Azizi, et al, (2010)	0.7888	0.7913	79.35
Rayes et al., (1992)	0.2176	0.2267	22.34
FFNN	0.0232	0.0384	-1.64
CFNN	0.0752	0.1014	-1.17
ANFIS	0.0116	0.0210	0.3764

The proposed approaches in this study are particularly of great interest for prediction of gas-condensate two-phase Z factor at high temperature and high pressure (HTHP) operational conditions $T_{pr} \geq 3$ and $P_{pr} \geq 30$.

In order to see the impact of each input variables on output of the developed models in this study, a sensitivity analysis has been carried out. The impact of all input variables, which are independent variables, (T, P, H₂S, CO₂, N₂, C₁ – C₇₊, MW_{C₇₊}, SG) on output parameter, which is dependant variable, (two-phase Z factor) was investigated. This sensitivity analysis also further reveals gas-condensate fluid

behaviour below the dew point pressure. To conduct sensitivity analysis, Pearson relevancy factor (r) was employed. In this method the relevance importance of each input variable will be detected by assigning a quantitative scale. The scale is a normalized values between -1 and 1, where the negative value show the negative effect of the input variable on output and positive show the positive effect (highly relevant). If the (r) is zero, it signifies that there is no relation between the input and output variable. The Pearson relation is defined by the following equation:

$$r(Inp_k, Z_{TP}) = \frac{\sum_{i=1}^n (Inp_{k,i} - Inp_{ave,k})(Z_{TP,i} - Z_{TP,ave})}{\sqrt{\sum_{i=1}^n (Inp_{k,i} - Inp_{ave,k})^2 \sum_{i=1}^n (Z_{TP,i} - Z_{TP,ave})^2}} \quad 5.26$$

Where, $Inp_{k,i}$ and $Inp_{ave,k}$ are i^{th} value and the average value of k^{th} input variables respectively ($k=T, P, H_2S, CO_2, N_2, C_1 - C_{7+}, MW_{C_{7+}}, SG$); $Z_{TP,i}$ represents i^{th} values of the predicted two-phase Z factor and $Z_{TP,ave}$ stands for average values of predicted two-phase Z factor. The relative impact of each parameter on two-phase Z factor presented in Figure 5.21. The result in Figure 5.21 shows that pressure (P) has the highest impact on two-phase Z factor of gas-condensate reservoirs below the dew point pressure. The positive impact of P on Z factor means increasing P would directly increase the Z factor. Physical law of gas-condensate fluid supports the positive impact of pressure on Z factor. It is well known from real gas law equation of state for mixture gases ($Z = PV/nRT$), that pressure (P) has positive impact on Z factor and temperature should have negative impact. These relationships can be explained further in following and the obtained results are related to the physics of the problem.

The intermolecular connection of a gas mixture diminishes with rising temperature (T) and cause the gas behaves more like an ideal gas. According to ideal gas law the temperature should have negative impact on Z factor, means increasing (T) should decrease the Z factor. The result in Figure 5.21 for temperature impact is against the aforementioned theory, as the temperature (T) has a positive impact on Z factor of gas-condensate fluid. The theory is correct as long as the mixture remains as a single-phase gas. However, below the saturation pressure, the liquid phase evolved from the gas phase and gas-condensate mixture is no longer single phase. Hence, the mixture behaves more like a liquid rather than gas especially for rich gas-condensate

reservoirs with high amount of condensate (oil) developed inside the pores in the reservoirs. Hence increasing (T) like pressure contributes to higher Z factor.

The compositional contents of C_1 to C_{7+} has different influence on Z factor. C_1 , C_2 and C_3 do not have considerable effect on Z factor, whereas C_4 to C_{7+} have positive impact on Z factor. It is interesting to relate the molecular weight of each composition to the relevancy factor. For heavier hydrocarbon fraction with higher molecular weight, the impact is greater in positive direction. C_4 to C_{7+} have higher molecular weight than $C_1 - C_3$, hence they have a higher positive impact on Z factor. This can be concluded that the higher amount of heavy hydrocarbon (IC_4 , NC_4 , IC_5 , NC_5 , C_6 and C_{7+}) would results in higher Z factor in the modelling.

Non-hydrocarbon components of H_2S , CO_2 and N_2 , all have negative impact on Z factor. Increasing the molar fraction of H_2S , CO_2 and N_2 would result in decreasing Z factor.

After pressure the molecular weight of C_{7+} (MWC_{7+}) has a highest positive impact on Z factor. This property causes gas-condensate mixture behave like a liquid (oil) phase, below the saturation pressure. This would increase the deviation from ideal gas behaviour, which results in larger Z factor.

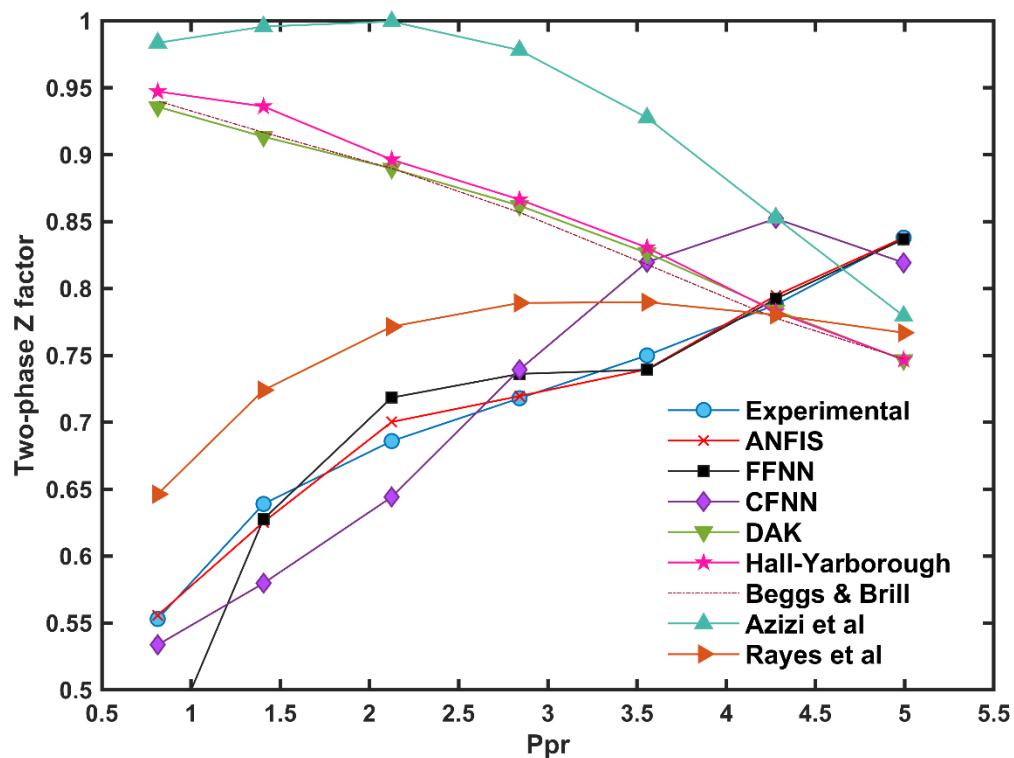


Figure 5.19. Testing different methods in predicting experimental Z factor as a function of Ppr for sour gas-condensate sample.

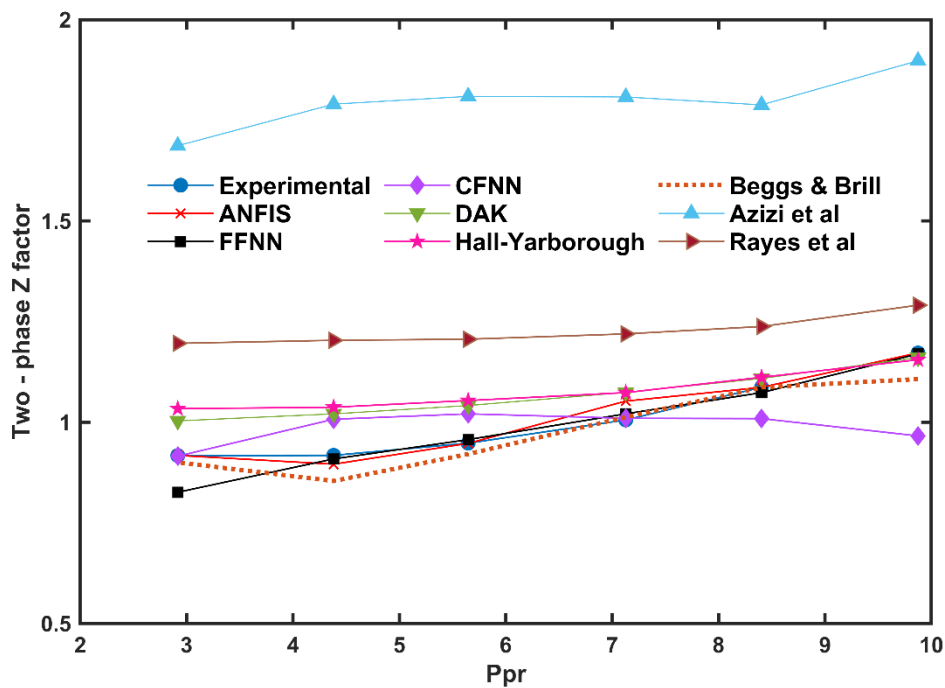


Figure 5.20. Prediction of Z factor as a function of P_{pr} for sweet gas condensate sample.

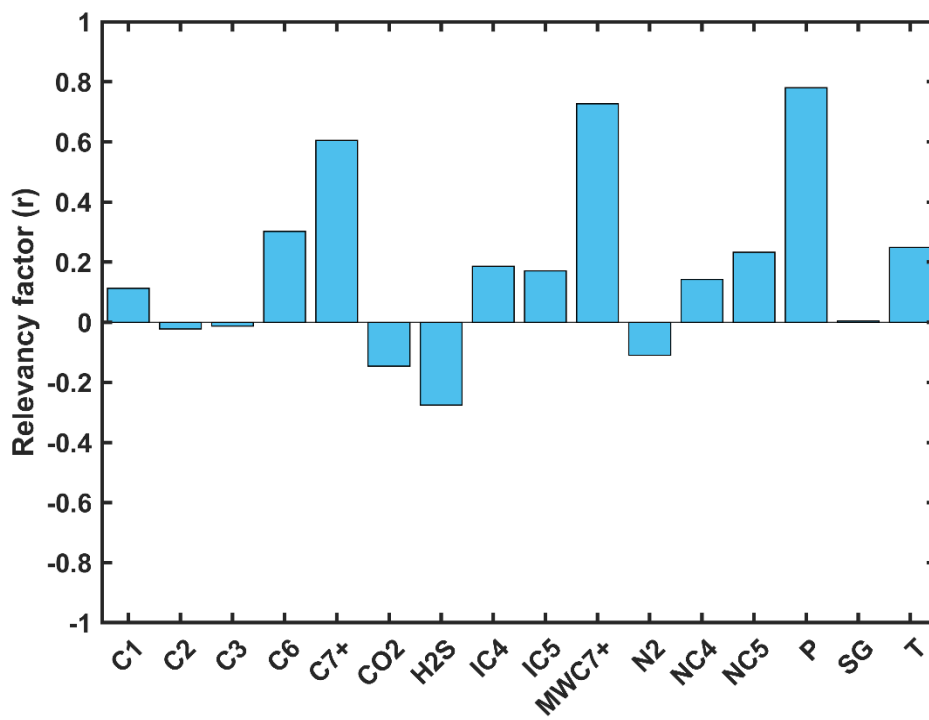


Figure 5.21. Relevancy factor (r) for each input variables.

5.5 Summary

Compressibility factor (Z factor) is one of the most important PVT properties that its accurate determination is required for reliable well deliverability modelling of gas-condensate reservoirs above and below the saturation pressure. In this chapter reliability and accuracy of existing literature models for prediction of two-phase Z factor below the dew point pressure is initially examined using extensive data bank obtained from open literature. The data bank is mainly from Constant Volume Depletion (CVD) tests performed on lean/rich gas-condensate fluids worldwide.

Two iterative techniques of Hall and Yarborough, (1973) and DAK, (1975) as well as three direct methods of Beggs and Brill, (1973), Rayes et al., (1992), and Azizi et al., (2010) utilized for prediction of Z factor below the dew point. Graphical and statistical error measurements have been carried out and indicate that DAK, (1975) best performed among literature models with MAE of 0.1300, RMSE of 0.1671 and AARD% of 2.4945 for estimating gas-condensate two-phase Z factor. DAK method followed by Hall-Yarborough, (1973), Rayes et al., (1992), Beggs and Brill, (1973) and Azizi et al., (2010). The problem with the current literature approaches is that they are not representing all range of operational conditions and limited to specific range of pseudo-reduced pressure (P_{pr}) and pseudo-reduced temperature (T_{pr}). Almost all literature models are limited for determination of two-phase Z factor in high pressure high temperature (HPHT) conditions.

In this study different approach was taken for modelling two-phase Z factor of gas-condensate reservoirs below the saturation pressure. Three machine learning (ML) based models including FFNN, CFNN and ANFIS were implemented for accurate modelling of two-phase Z factor. Various optimization algorithms such as Levenberg – Marquardt (LM) and Bayesian regularization (BR) coupled with different number of hidden layers and neurons have been adopted to achieve best optimum performance of FFNN and CFNN. Integrity and robustness of FFNN and CFNN examined using independent data sets. The statistical and graphical error measurements of the obtained results show high accuracy of both methods for prediction of two-phase Z factor. Another ML based approach known as ANFIS was also utilized for prediction of two-phase Z factor of gas-condensate reservoirs below the saturation pressure. Subtractive clustering technique was utilized and an iterative scheme was developed for determination of optimum number of IF–THEN fuzzy rules in ANFIS modelling.

ANFIS is predicting two-phase Z factor with the best accuracy among other intelligent models and literature correlations. The developed ANFIS model returned the experimental values of two-phase Z factor with MAE of 0.00251, RMSE of 0.00254 and AARD% of 0.5119. The developed MA based models overcome the limitation of existing literature models and they can be used for prediction of gas-condensate two-phase Z factor below the dew point in all ranges of pressure and temperature operational conditions. Furthermore the ML based models has an excellent computational efficiency.

The developed ML based models can be used as an alternative tools instead of existing literature models in reservoir simulation packages. This would ensure accuracy and reliability of the production forecast for gas-condensate reservoirs experiencing condensate drop out.

CHAPTER 6

PRODUCTION PROFILE FORECAST USING WELL TEST DATA

6.1 Introduction

Accurate and reliable well production forecast of gas-condensate reservoirs are very important for field development planning, projection of cash flow and future hydrocarbon recoveries.

Reliable modelling of this type of reservoirs require understanding the effect of condensate blockage and other contributing factors. Among many factors phase behaviour, absolute/relative permeability and how the well is being produced are the most important (Fevang and Whitson, 1996; Shi, 2009).

Phase behaviour of gas-condensate below the saturation pressure is related to variations in fluid properties (e.g., viscosity, Z factor). These variations would influence modelling of well deliverability and also production profile forecast. From gas rate equations of 2.1, 2.2 and 2.16, it is apparent that the cumulative production (G_p) and flow rate (q) are direct function of permeability, viscosity, solution gas to oil ratio (R_s), and Z factor. Hence, accurate determination of the aforementioned parameters will affect the estimation of gas and condensate production rate at the surface. Many studies in literature have shown that root cause of the unreliable modelling of gas-condensate well deliverability is due to inaccurate estimation of PVT properties. Some of these studies are as follow (Rayes *et al.*, 1992; Fevang and Whitson, 1996; Whitson, Fevang and Yang, 1999; Elsharkawy, Hashem and Alikhan, 2000; Mott, 2002; Sutton, 2005b, 2007; Arukhe and Mason, 2012; Yan *et al.*, 2013; Ghiasi *et al.*, 2014; Behmanesh, Hamdi and Clarkson, 2017; Khazali, Sharifi and Ahmadi, 2019).

Hence, to address the PVT issues in gas-condensate reservoirs, Artificial Intelligent algorithms were manipulated extensively in chapter 4 and 5. Several Artificial Intelligence (AI) or known as machine learning approaches were developed for better prediction of gas-condensate viscosity and two-phase Z factor. Although the machine

learning based models in chapter 4 and 5 predict PVT properties (viscosity and Z factor) very well, the reliability of the developed models in relation to production profile of gas-condensate reservoirs is unclear. Therefore, the aim of this chapter is to investigate the reliability of the developed PVT models in computation of production profile of gas-condensate wells, which is ultimate aim of this study. In doing so three regions pseudopressure integral has been utilized and coupled with material balance equation to generate production profile of a gas-condensate well. To verify the effectiveness of the developed PVT properties (e.g., viscosity and two-phase Z factor) in computation of production profile compositional simulation of the studied well performed using Eclipse 300.

Permeability is another important parameter that would influence the accuracy of well deliverability modelling in gas-condensate reservoirs. In this chapter effective permeability of each phase (gas and condensate) will be used for computation of pseudopressure integral. The detail reservoir and fluid data has obtained from well pressure test data.

6.2 Pressure Transient Test (PTA) and two-phase pseudopressure approach

Detail reservoir information are essential for reservoir engineers to predict the current and future performance of the reservoir. Pressure transient analysis (PTA) test is available in industry to provide engineers with detail reservoir information required for the analysis. PTA is essentially measuring pressure changes in a well as a function of time (Lee and Wattenbarger, 1995, pp. 111–113). It is well known that pressure behaviour of the reservoir following a rate change reflect the geometry and flow properties of the reservoir. From PTA test the information such as effective permeability, formation damage/stimulation, volumetric average reservoir pressure, drainage pore volume, fracture properties and communication between wells can be obtained.

Classical interpretation of PTA test results for determination of the aforementioned parameters are based on linear diffusion equation. The combination of Darcy's law, continuity equation and equation of state forms the diffusivity equation. The equation is a differential equation that governs the transient flow of the fluid through a porous

medium (Sanni, 2018). The diffusivity equation determines variation of pressure with time and position in the reservoir as follow.

$$\nabla^2 p - \frac{\phi \mu c_t}{k} \frac{\partial p}{\partial t} = 0 \quad 6.1$$

Where ∇ devoted to gradient, P is pressure, ϕ is porosity of the medium, μ is viscosity of the fluid, c_t is total compressibility, k is permeability and $\frac{\partial p}{\partial t}$ is pressure rate of change with respect to time.

Equation 6.1 is derived using several assumption as follow (Horne, 1995; Stewart, 2011)

- Darcy's law apply
- Single-phase flow
- Porosity, permeabilities, viscosity and compressibility are constant
- Fluid compressibility is very low
- Pressure gradient $\frac{\partial p}{\partial t}$ in the reservoir is small
- Gravity and thermal effect are negligible

With the above assumptions equation 6.1 is applicable for single-phase slightly compressible flow (oil reservoir) when average reservoir pressure is above bubble point pressure ($P_r > P_{bubble}$). However, for gas-condensate reservoirs as liquid condensation may occurs in the reservoir and both gas and liquid phase coexist below the saturation pressure, equation 6.1 is no longer valid. Furthermore, the properties of gas-condensate fluid are strong function of pressure and they are changing with time. Hence, the flow equation for gas-condensate reservoir is non-linear and equation 6.1 is not applicable for such reservoir. A classical approach to account for this non-linearity is defining a variable known as pseudopressure function (m_p). Therefore, the governing pressure transmission for gas-condensate reservoirs is changing to the following equation.

$$\nabla^2 m_p - \frac{1}{\eta} \frac{\partial m_p}{\partial t} = 0 \quad 6.2$$

Where η is constant of diffusivity equation and it is function of pressure and time. Equation 6.2 can further be simplified using pseudotime. Computation of

pseudopressure and pseudotime allow all solutions (gas-condensate fluid) defined for standard well test analysis, using pseudopressure and pseudotime instead of pressure and time (Roussennac, 2001). In the case of multiphase flow for instance gas-condensate below the saturation pressure the pseudopressure function in 6.2 must take into account the relative permeability data, at reservoir condition, which is very difficult to obtain. In this situation, effective permeability can be calculated using pseudopressure function.

Pseudopressure function (m_p) is defined in chapter 2 by pressure integral in equation 2.2 after Al-Hussainy et al., (1966). For gas-condensate fluid flow, pseudopressure function can be combined with analogy of three flow regions introduced by Fevang, (1995), explained in 2.3 to estimate gas and condensate flow rates at the surface. Three-flow regions pseudopressure approach is very quick and easy to implement for well performance modelling of gas-condensate reservoirs. Using PTA data combined with three regions pseudopressure method resulted in estimating gas flow rate (q_g) as a function of pressures. The established relationship between pressure and flow rates resulted in generating Inflow Performance Relationship (IPR). IPRs are important element for reservoir engineers in the design of new wells and also for monitoring and optimizing existing wells. In this section we discuss how to establish IPRs for gas-condensate reservoirs using three regions pseudopressure approach when PTA data is available. Then generating production profile of gas-condensate reservoirs using results of pseudopressure integral combined with volumetric material balance will be discussed.

Gilbert, (1954) introduced Inflow Performance Relationship (IPR) for oil wells. IPRs are important tool in understanding the reservoir/well behaviour and quantifying production rate (Guo, Sun and Ghalambor, 2008; Fattah *et al.*, 2014). IPRs are essentially quantifying gas or condensate (oil) flow rates in respect to specific bottom-hole flowing pressure (P_{wf}). Rawlins and Schellhardt, (1936) proposed an equation to relate gas flow rate (q_g) to P_{wf} , their equation is known as back – pressure equation or deliverability equation and shown in 2.11. To account for non-linearity of the flow (e.g., variation of viscosity and Z factor) due to liquid drop out below the saturation pressure

in gas-condensate reservoirs, pseudopressure function (m_p) is added to well deliverability equation.

Substituting m_p in 2.11 yields equation 6.3. This equation is effectively gas-condensate well deliverability equation that can be used for construction of IPR curve.

$$\left\{ \begin{array}{l} q_{gt} = C (\Delta m_{p_{gt}})^n \\ \Delta m_{p_{gt}} = m_{p_{gavg}} - m_{p_{gwf}} \end{array} \right\} \quad 6.3$$

Where C is performance coefficient in Mscf/day/psi², $\Delta m_{p_{gt}}$ is total gas pseudopressure function in psi, $m_{p_{gavg}}$ is average pseudopressure function, $m_{p_{gwf}}$ pseudopressure function at the bottom-hole flowing pressure, n is an exponent and q_{gt} is total gas flow rate on the surface. Depending on flowing velocity, the exponent n can be vary between 1 for completely laminar flow and 0.5 for fully turbulent flow. The coefficient of C is depending on well and reservoir geometry, permeability and fluid properties and its mathematically has been defined in chapter 2 equation 2.3.

The coefficient values of C and n in equation 2.3 can also be determined using well test data.

By taking the logarithm of both sides of equation 6.3 and solving for logarithm of pseudopressure function, the expression can be rewritten as:

$$\log (\Delta m_{p_{gt}}) = \frac{1}{n} \log q_g - \frac{1}{n} \log C \quad 6.4$$

The above equation suggests that plotting $\Delta m_{p_{gt}}$ versus q_g in log-log scale should yield a straight line with slope of $1/n$ and intercept of C. The deliverability exponent n can be determined from any two points on a straight line as follow.

$$n = \frac{\Delta \log q_g}{\Delta \log (\Delta m_{p_{gt}})} \quad 6.5$$

Also coefficient C can be estimated by rearranging equation 6.3 when pressure test data is available as follow.

$$C = \frac{q_{gt}}{\Delta m_{p_g}^n} \quad 6.6$$

The above procedure is a conventional well deliverability estimation of any gas well in industry using PTA test data. Establishing Inflow Performance Relationship (IPR) curve using the above procedure and equation 6.3, require calculation of pseudopressure function $\Delta m_{p_{gt}}$.

In this study three-flow regions pseudopressure approach of Fevang, (1995) adopted for estimation of $\Delta m_{p_{gt}}$. $\Delta m_{p_{gt}}$ is calculated for three flow regions of gas-condensate reservoirs. Substitution of Fevang's approach in 6.3, yields the following expression in terms of gas and condensate effective permeabilities.

$$q_{gt} = C \left\{ \int_{P_{wf}}^{P^*} \left(\frac{k \cdot k_{rg}}{B_g \mu_g} + \frac{k \cdot k_{rc}}{B_c \mu_c} R_s \right) dp + \int_{P^*}^{P_{dew}} \left(\frac{k \cdot k_{rg}}{B_g \mu_g} \right) dp + \int_{P_{dew}}^{P_R} \left(\frac{k \cdot k_{rg}(S_{wi})}{B_g \mu_g} \right) dp \right\}^n \quad 6.7$$

This is true representation of gas-condensate flow below the saturation pressure. Equation 6.7 includes three pressure integrals representing three flow regions inside gas-condensate reservoirs as discussed in 1.3. Calculation of pressure integrals in 6.7 depends on co-existing of the regions in the reservoirs as explained in section 2.3.

Pressure integrals in 6.7 has written in terms of effective permeability instead of relative permeability as previously shown in 2.16. This is particularly useful if the well pressure transient test data is available, where the effective permeability can be calculated from the well test data. This analogy would be more explored by using a gas-condensate case study in this chapter.

Using equation 6.7 requires information of pressures, permeabilities, fluid properties and coefficients of n and C. Well pressure test analysis (PTA) are conventional method to obtain pressure and permeability of the formation. Several well pressure transient test methodologies exist in the literature such as pressure build up, pressure drawdown, multirate, pulse, interference, fall off, injectivity, step rate and fall off. Our intention is not to discuss different well test methods, as this is beyond the scope of

this study. Nevertheless, the aim is to introduce how effective permeability ($k.k_{rg}$) and skin factor and pressure information that are required for computation of 6.7 can be calculated from well test data.

Pressure build up test is usually used to provide the reservoir and other properties of the formation. This test describes the build up in wellbore as a function of time after the well shut-in for certain time. The general equation of the pressure build up and drawdown come from solution of diffusivity equation and principle of superposition theory. Pressure build up equation originally proposed by Horner, (1951) and modified by Earlougher, (1977). The pressure build up test in terms of pseudopressure function and surface flow rate for slightly compressible fluid is as follow.

$$m_{Pr} - m_{Pwf} = 162.6 \left(\frac{q_{g,meas}}{h} \right) \left(\log(t) + \log \left(\frac{k.k_{rg}(p)}{\phi \mu_g c_t r_w^2} \right) - 3.23 + 0.87 s_{total} \right) \quad 6.8$$

Where $q_{g,meas}$ is measured gas flow rate at surface during the test; t is recorded pressure test time; h is reservoir thickness; $k.k_{rg}$ is effective permeability of gas phase; ϕ is porosity of the media; μ_g is gas viscosity; c_t is total compressibility factor; r_w is wellbore radius; and s_{total} is total skin factor include the skin from formation damage and stimulation (Horner, 1951; Al-Hussainy and Ramey, 1966; Agarwal, 1979; Lee and Wattenbarger, 1995)

$$s_{total} = 1.153 \left[\frac{\Delta m_{p_{g,1hour}}}{q_{g,meas} m_{g,1hour}} - \log \left(\frac{k.k_{rg}}{\phi \mu_g c_t r_w^2} \right) + 3.227 \right] \quad 6.9$$

Where m is slope of the straight line. Rearranging 6.9 and comparing with straight-line equation of $y = mx + b$ suggests an analysis technique with the arrangement of the following terms.

$$\left\{ \begin{array}{l} y \sim m_{Pwf} \\ x \sim \log(t) \\ m \sim -162.6 \left(\frac{q_{g,meas}}{h} \right) \\ b \sim -162.6 \left(\frac{q_{g,meas}}{h} \right) \left(\log \left(\frac{k.k_{rg}(p)}{\phi \mu_g c_t r_w^2} \right) - 3.23 + 0.87 s_{total} \right) \end{array} \right\} \quad 6.10$$

Equation 6.8 indicates that the plot of bottom-hole flowing pressure (P_{wf}), against logarithm of time (t) exhibits a straight line with the slope of $m \sim -162.6 \left(\frac{q_{g,meas}}{h} \right)$ and intercept of $b \sim -162.6 \left(\frac{q_{g,meas}}{h} \right) \left(\log \left(\frac{k \cdot k_{rg}(p)}{\phi \mu_g c_t r_w^2} \right) - 3.23 + 0.87 s_{total} \right)$. The slope “m” allows us to calculate the permeability of the formation (k). The plot commonly known as Horner plot and the typical semi log plot of P_{wf} against logarithm of time (t) is shown in Figure 6.1.

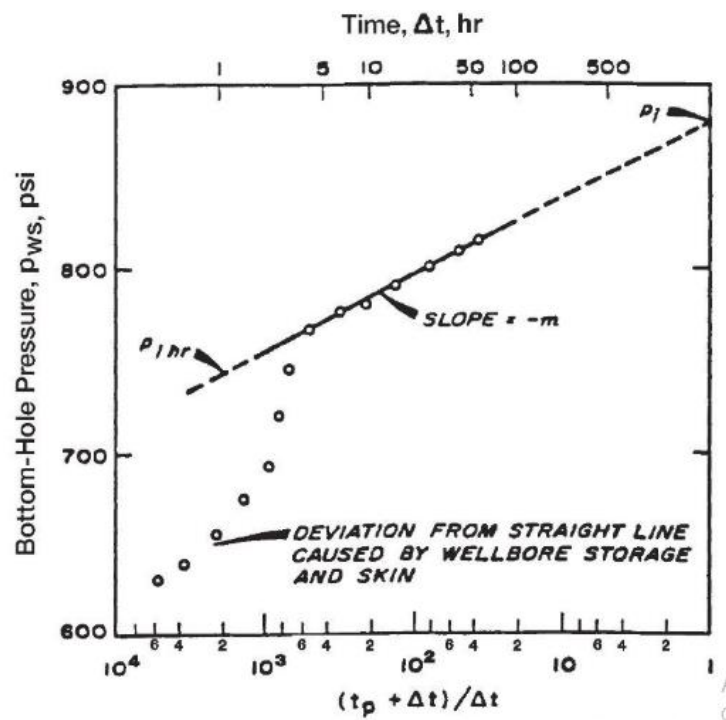


Figure 6.1. Horner plot for pressure build up test (Earlougher, 1977).

An early time deviation from the graph in Figure 6.1 is due to the wellbore storage effect and skin factor (Horner, 1951; Lee and Wattenbarger, 1995; Ahmed, 2010). This deviation is large if permeability is low and fluid compressibility is high. This is the case in heavy gas-condensate reservoir when the liquid build up starts from the beginning of the production.

In this study Horner plot type analysis also has been adopted for calculation of effective permeability when PTA data is available. Pseudopressure integral in 6.7 rewritten in terms of effective permeabilities of the phases instead of relative permeabilities. This is due to the fact that using relative permeability data, obtained from empirical models such as Corey et al., (1956) would produce misleading results for very low permeability gas-condensate reservoirs (Ojha et al., 2017; Hassan et al., 2019).

The detail computation of pseudopressure integral is given in following section through demonstration of a case study. Pressure-volume-temperature (PVT) properties (viscosity and Z factor) are also an important factors for estimating pseudopressure function. The objective of this chapter is to investigate how the production of gas (q_g) and condensate (q_c) are influenced using different PVT properties and two-phase Z factor models developed in chapter 4 and 5.

6.3 Computation of production profile in relation to gas/condensate viscosity and Z factor in HPHT gas-condensate well

The example that we analyse in this section is a vertical well known as (KAL – 5). The is in Yugoslavia and located in very high temperature and tight formation (365 °F at 11,500 ft [180°C at 3500m]. The compact formation makes the production impossible without stimulation. Pressure build up test was run in the well and bottom-hole flowing pressure (P_{wf}) was recorded against the shut in period (time in hours). The pressure test data, reservoir and fluid properties of the well is obtained from Economides et al., (1989) and presented in Table 6.1 and Table 6.2. The reservoir fluid contains high content of non-hydrocarbon impurities of 10.9% carbon dioxide (CO₂). Initial condition of the reservoir fluid coincides with most gas-condensate reservoirs with GOR of 9470 scf/STB (1706 std m³/stock-tank m³). The initial reservoir pressure (6750psi [46.5Mpa]) is identical to dew point pressure and condensation starts from the beginning of the production. This means the only region that developed during pressure depletion is region 1 ($P^* > P_R$). Hence, the pseudopressure integral with pressure limit between P_{wf} and P_R , shown in 2.12, can be used for calculation of well deliverability. The obtained data from pressure transient test indicate the well is located in a very tight formation with the permeability of 0.0035 millidarcy.

Table 6.1. Reservoir and fluid property of studied gas-condensate well after (Economides et al., (1989).

Well & Reservoir data		Fluid Data (%mole fraction)	
P _i , (psia)	6750	H ₂ S	0.006
P _{dew} (psia)	6750	N ₂	1.452
q _g , Mscf/day	75.4	CO ₂	10.931
q _c , STB/day	2.8	C ₁	72.613
GOR scf/STB	9470	C ₂	6.242
γ _g (to air)	0.94	C ₃	1.631
T, °F	354	i – C ₄	0.553
h, ft	216.5	n – C ₄	0.693
h _p ,ft	36	i – C ₅	0.442
∅	0.062	n – C ₅	0.379
r _w , ft	0.54	C ₆	0.516
S _w	0.3	C ₇	0.644
R _p ,scf/STB	9470	C ₈	0.541
API [Assumed]	50	C ₉	0.388
Skin	- 4.52	C ₁₀₊	2.979
K (md)	0.0035		

Table 6.2. Pressure build up data for (KAL – 5) obtained from (Economides et al., (1989).

Time (Hours)	Pressure (Psi)
0	1083.1
0.167	1174.5
0.333	1226.7
0.5	1303.6
1.0	1490.6
2.0	1751.6
3.0	2046.0
4.0	2279.4
6.0	2759.4
8.0	3246.5
12.0	4221.0
16.0	5162.0
22.0	6161.0
28.0	6336.0
34.0	6406.1
42.0	6452.5
50.0	6487.3
58.0	6507.6
68.0	6526.5
82.0	6556.9
97.0	6587.3
112.0	6587.3
141.0	6601.8

In order to calculate gas and oil maximum flow rates (q_g , q_o) using pseudopressure integral and construct the IPR curves the following data is needed.

- The PVT properties of each phase in region 1, (construction of PVT tables)
- Producing gas/oil ratio, R_P (obtained from well test data)
- Knowledge of pressure, P_{wf} and P_R (obtained from well test data)
- Effective permeabilities of each phase ($k.k_{rg}$) and ($k.k_{ro}$)

In the following section, first we discuss the construction of PVT tables and then mathematical solution of pseudopressure integral will be discussed. Effective permeability of each phase will be calculated using well pressure test data.

6.3.1 Construction of pressure – volume – temperature (PVT) relationship

To estimate maximum gas and oil (condensate) flow rate at the surface using pseudopressure approach, knowledge of PVT data such as formation volume factor, viscosity, Z factor and solution gas to oil ratio is required. Viscosity and Z factor are governing parameters in computation of pseudopressure integral and determining the performance of the well (Whitson, Fevang and Yang, 1999; Hernandez; *et al.*, 2002; Yang *et al.*, 2007; Arukhe and Mason, 2012). In chapter 4 and 5 accurate determination of viscosity and Z factor of gas-condensate reservoirs have been comprehensively discussed.

It also has been shown that using current literature approaches for modelling gas-condensate viscosity and Z factor resulted in high error. Subsequently several machine learning (ML) based models have been developed and presented in chapters 4 and 5. The developed ML based models were adopted for computation of fluid properties and constructing PVT tables for studied gas-condensate well. These models were developed to address the non-linearity of fluid flow below the saturation pressure in gas-condensate reservoirs undergoing depletion.

Other two PVT properties that have major influence for accurate determination of the pseudopressure integrals are solution GOR (R_s) and oil to gas ratio (r_s) (Fevang and Whitson, 1996; Mott, 2002). Whitson and Torp, (1983) MBO method proved to be one of the most accurate techniques for calculation of R_s and r_s for gas-condensate fluid

(Borthne, 1986; Coats and Smart, 1986; Guo, Du and School, 1989; Khamis and Fattah, 2019).

Therefore, Whitson and Torp, (1983) utilized for computation of R_s and r_s in region 1. The steps shown in following figure have been taken for construction of PVT table.

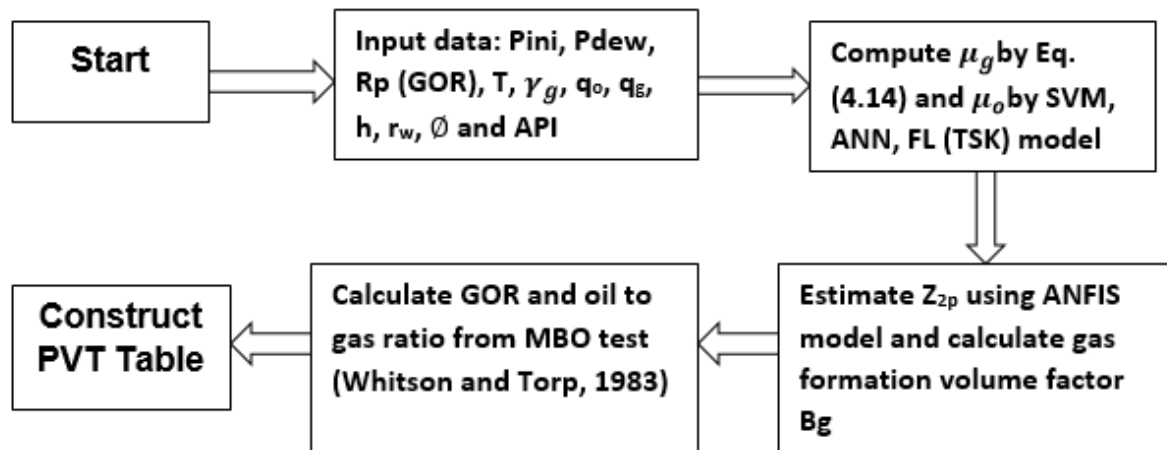


Figure 6.2. construction of PVT table for KAL – 5 gas-condensate well.

The constructed PVT table in this part will be used for computation of gas and condensate flow rates utilizing three regions pseudopressure approach.

6.3.2 Mathematical manipulation of pseudopressure integral

The well deliverability equation for this reservoir rewritten only for region 1 as described in 6.3 and depicted in 6.11 for gas phase and 6.12 for oil (condensate) phase.

$$q_g = C(\Delta m P_{g1})^n = C \left\{ \int_{P_{wf}}^{P_R} \left(\frac{k \cdot k_{rg}}{B_g \mu_g} + \frac{k \cdot k_{ro}}{B_o \mu_o} R_s \right) dp \right\}^n \quad 6.11$$

$$q_o = C(\Delta m P_{c1})^n = C \left\{ \int_{P_{wf}}^{P_R} \left(\frac{k \cdot k_{ro}}{B_o \mu_o} + \frac{k \cdot k_{rg}}{B_g \mu_g} R_o \right) dp \right\}^n \quad 6.12$$

Mathematical solution of pseudopressure integrals in 6.11 and 6.12 required producing gas to oil ratio, (R_p). R_p is a ratio of total gas production to total oil production

on the surface and can be estimated from following equation (Fetkovich *et al.*, 1986; Fevang and Whitson, 1996; Guehria, 2000; Jokhio and Tiab, 2002; Ahmed, 2010).

$$R_p = \frac{q_{gt}}{q_{ot}} = \frac{C \left[\left(\frac{k_{rg}}{B_g \mu_g} \right) + \left(\frac{k_{ro}}{B_o \mu_o} \right) R_s \right]}{C \left[\left(\frac{k_{rg}}{B_g \mu_g} \right) R_o + \left(\frac{k_{ro}}{B_o \mu_o} \right) \right]} \quad 6.13$$

Where, R_o is oil to gas ratio in (STB/scf), q_{gt} and q_{ot} are total gas flow rate and total oil flow rate at the surface respectively. Simplification of 6.13 yields the following equation.

$$R_p = R_s + \left(\frac{k_{rg}}{k_{ro}} \right) \left(\frac{B_o \mu_o}{B_g \mu_g} \right) (1 - R_o R_p) \quad 6.14$$

Fetkovich *et al.*, (1986), rearranged and solved 6.14 for relative permeabilities ratio (k_{rg}/k_{ro}) and proposed the following equation.

$$\frac{k_{rg}}{k_{ro}} (P) = \frac{(R_p - R_s)}{(1 - R_o R_p)} \left(\frac{B_g \mu_g}{B_o \mu_o} \right) \quad 6.15$$

Relative permeabilities K_{rg} and K_{ro} can be expressed directly as a function of ratio (K_{rg}/K_{ro}), when both phases are mobile (Evinger and Muskat, 1942). Using 6.15, for a given R_p , relative permeabilities of gas (K_{rg}) and condensate (K_{ro}) in region 1 can be evaluated directly as a function of pressure, $K_{rg}(p) = f[k_{rg}/k_{ro}(p)]$ and $K_{ro}(p) = f[k_{rg}/k_{ro}(p)]$. Presenting 6.14 in terms of effective permeabilities ($k.k_{rg}$) and ($k.k_{ro}$) and rearranging the equation allow us to calculate effective permeability of one phase as a function of other phase. The effective permeabilities of gas and oil phase in region 1, then can be calculated using following expressions.

$$k.k_{rg} = \frac{(R_p - R_s)}{(1 - R_p)} \left(\frac{B_g \mu_g \{k.k_{ro}\}}{B_o \mu_o} \right) \quad 6.16$$

$$k.k_{ro} = \frac{(1 - R_o R_p)}{(R_p - R_s)} \left(\frac{B_o \mu_o \{k.k_{rg}\}}{B_g \mu_g} \right) \quad 6.17$$

Substituting 6.16 in pseudopressure integral of 6.11 and simplifying yields pseudopressure integral in terms of gas effective permeability as follow (Fetkovich *et al.*, 1986; Fevang, 1995; Fevang and Whitson, 1996; Guehria, 2000; Jokhio, 2002).

$$\Delta m_{p_{g1}} = \int_{p_{wf}}^{P_R} \left(\frac{k \cdot k_{rg}}{B_g \mu_g} \right) \frac{R_p(1 - R_o R_s)}{(R_p - R_s)} (P) dp \quad 6.18$$

Pseudopressure integrals can now be computed if effective permeability integral as well as other properties of respective phase are known. Gas phase pseudopressure integral in 6.18 can be rewritten without effective permeability term (Jokhio, 2002) as shown in 6.19. This permits to estimate the effective permeability integral using Horner plot and theory of well testing.

$$\Delta m_{p_{g1}} = \left[\int_{p_{wf}}^{P_R} \left(\frac{1}{B_g \mu_g} \right) \frac{R_p(1 - R_o R_s)}{(R_p - R_s)} (P) dp \right] = \Delta m_{p_{g1}} / M_g \quad 6.19$$

The above integral is function of bottom hole flowing pressure (P_{wf}), average reservoir pressure (P_R) and other PVT properties. P_{wf} and P_R obtained from well test data and PVT properties were calculated as discussed in previous section. The integral is assumed to be equal to a term in right hand side ($\Delta m_{p_{g1}} / M_g$). The trapezoidal rule of integration is utilized for integration part of 6.19.

From theory of the well testing during pressure transient period for dimensionless *time* (t) > 50 gas phase effective permeability integral is determined from the following equation. The effective permeability integral is also assumed to be equal to a special term known as M_g .

$$\int_{P_{wf}}^{P_R} k \cdot k_{rg}(P) dp = 162.6 \frac{q_{g,meas}}{h \left(\frac{d\Delta m_{p_{g1}}}{d\ln(t)} \right)} = M_g \quad 6.20$$

The above equation indicates that $(K \cdot K_{rg})$ integral in two-phase system is inversely proportional to the derivate of gas pseudopressure (m_{p_g}) with natural logarithmic of time (Horner, 1951; Serra, Peres and Reynolds, 1990, 2007; Dake, 2001; Jokhio,

2002). On semi log plot of time against pseudopressure, the rate of change of pseudopressure is a slope of straight line. The plot of pseudopressure (m_p) against the recorded time during well test for (KAL – 5) is shown in Figure 6.3. This is a Horner plot, where the straight portion of the line represents the effective permeability of the formation defined by 6.20. This equation is valid for fully developed flow where pressure waves have crossed the skin and the wellbore storage effect. This means the enough time should be devoted to the pressure transient test to allow pressure waves are fully developed.

Where, $d\Delta mP/d\ln(t)$ is the derivative function of each phase that can be estimated from 6.21 (Jokhio, 2002; Jokhio, Tiab and Escobar, 2002).

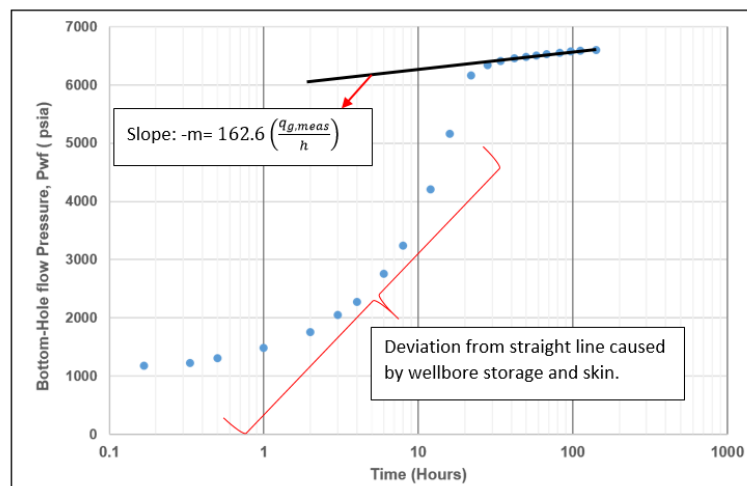


Figure 6.3. Horner plot for KAL – 5 gas-condensate well.

$$\left(\frac{d\Delta mP}{d\ln(t)}\right)_i = \frac{\left(\frac{d\Delta mP_{i-1}}{d\ln(t)_{i-1}}\right) \Delta\ln(t)_{i+1} + \left(\frac{d\Delta mP_{i+1}}{d\ln(t)_{i+1}}\right) \Delta\ln(t)_{i-1}}{[\Delta\ln(t)_{i+1} + \Delta\ln(t)_{i-1}]} \quad 6.21$$

The point i in above equation is the point, where the derivative is calculated and point $(i-1)$ is the point before it and $(i+1)$ is the point after it. Pseudopressure difference ($d\Delta mP$) is the difference between the (m_p) at each pressure and initial (m_p) at zero

hour ($d\Delta m_p = m_p - m_{p(t=0)}$). This is the difference in pseudopressure of any given pressure and pseudopressure at the beginning of the pressure build up test.

Computing pseudopressure function and effective permeability by the above procedure allow us to estimate the accurate value of ΔmPg in region 1 as follow.

$$\Delta mP_{g1} = \left(\frac{\Delta m_{p_{g1}}}{Mg} \right) \times Mg \quad 6.22$$

For modelling condensate (oil) phase in KAL – 5, gas-condensate well similar approach as explained for gas phase is employed. Condensate (oil) phase flow rate is determined from the following equation (Penula, 2003).

$$q_{ot} = C(\Delta mP_{o1})^n = C \left\{ \int_{P_{wf}}^{P_R} \left(\frac{k \cdot k_{ro}}{B_o \mu_o} + \frac{k \cdot k_{rg}}{B_g \mu_g} R_o \right) dp \right\}^n \quad 6.23$$

Where q_{ot} is the total condensate flow rate at the surface in (STB/day); $\Delta m_{p_{o1}}$ is two-phase pseudopressure function in psi²/cp; $k \cdot k_{ro}$ is effective permeability to oil in Darcy unit; $k \cdot k_{rg}$ is effective permeability to gas in Darcy unit; B_o is condensate (oil) formation volume factor in Barrel/ STB; μ_o is condensate (oil) viscosity in centipoise; B_g is gas formation volume factor in cubic feet (ft³)/standard cubic feet (scf); μ_g is gas viscosity in centipoise and R_o is oil to gas ratio in (STB/scf).

Effective permeability to condensate (oil) phase in Region 1 has previously defined in 6.17. Substituting 6.17 into 6.23 and simplifying yields $\Delta m_{p_{o1}}$, which represents condensate (oil) phase pseudopressure function in terms of effective permeability (Evinger and Muskat, 1942; Fetkovich *et al.*, 1986; Fevang, 1995; Guehria, 2000; Penula, 2003).

$$\Delta m_{p_{o1}} = \int_{p_{wf}}^{P_R} \left(\frac{k \cdot k_{ro}}{B_o \mu_o} \right) \frac{(1 - R_o R_s)}{(1 - R_o R_p)} (P) dp \quad 6.24$$

Oil phase pseudopressure integral can be rewritten without oil effective permeability term in the following form (Jokhio, 2002).

$$\Delta m_{p_{o1}} = \left[\int_{p_{wf}}^{P_R} \left(\frac{1}{B_o \mu_o} \right) \frac{(1 - R_o R_s)}{(1 - R_o R_p)} (P) dp \right] = \Delta m_{p_{o1}} / M_o \quad 6.25$$

The above pseudopressure integral is assumed to be equal to a special term $\Delta m_{p_{o1}} / M_o$, that later can be used to simplify and determine $\Delta m_{p_{o1}}$.

Oil effective permeability integral can be defined according to well test theory. Oil phase effective permeability integral in two-phase system is inversely proportional to the derivative of oil phase pseudopressure (m_{po}) with natural logarithmic of time and can be defined as follow.

$$\int_{p_{wf}}^{P_R} k \cdot k_{ro}(P) dp = 162.6 \frac{q_{o,meas}}{h \left(\frac{d\Delta m_{p_{o1}}}{d\ln(t)} \right)} = M_o \quad 6.26$$

Where pseudopressure function and its derivative $\left(\frac{d\Delta m_{p_{o1}}}{d\ln(t)} \right)$ in above equation can also be calculated by utilizing 6.21. M_o is a special term that used for simplifying the equation. Using special terms at the right hand side of equations 6.25 and 6.26, the oil (condensate) phase pseudopressure integral is determined as follow.

$$\Delta m_{p_{o1}} = \left(\frac{\Delta m_{p_{o1}}}{M_g} \right) \times M_g \quad 6.27$$

The production rate for well in low permeability formation is usually low that pressure drop caused by non-Darcy flow can be neglected. Reservoirs in compacted formation with very low permeability are usually stimulated (fractured), which eliminates the effect of non-Darcy flow (Fevang, 1995). Hence, the effect of non-Darcy flow on production rate has been excluded and the effect of condensate blockage on well production is our primary concern. Another assumption in our calculations is steady

state flow in the reservoir, meaning mass flow rate would be constant and there is no net accumulation of any fluid in the reservoir.

Estimation of pseudopressure functions ($\Delta m_{p_{g1}}$) and ($\Delta m_{p_{o1}}$) in region 1 by above procedure, permits to calculate total gas and condensate (oil) flow rate on the surface using 6.11 and 6.12 respectively. The coefficients of n and C in aforementioned equations can be estimated using semi-log plot of $\Delta m_{p_{o1}}$ versus measured surface flow rates (gas and oil). The semi-log plot is a straight line with the slope of ' n ' and intercept of ' C '. These relationships demonstrated in 6.4 to 6.6 (Forchheimer, 1901; Rawlins and Schellhardt, 1936). The graph in Figure 6.4 depicts plot of measured gas flow rate against total gas pseudopressure function. Using straight portion of the line on the graph, n is 0.8 and coefficient C is 0.0948. Consequently maximum gas flow rate can be calculated using 6.11 for gas phase and 6.12 for condensate (oil) phase and IPR curves can be established.

Our ultimate goal in this study is to see the effect of variation in viscosity and two-phase Z factor estimation using various approaches on computation of production profile of gas-condensate wells. In order to generate production profile of the well, pseudopressure approach incorporated with volumetric material balance equation. Production profile is forecasting expected flow rate of wells as a function of time. This is very important for assessing economic attractiveness of any reservoir engineering projects. Moreover it is a reflection of gas-condensate reservoir performance modelling.

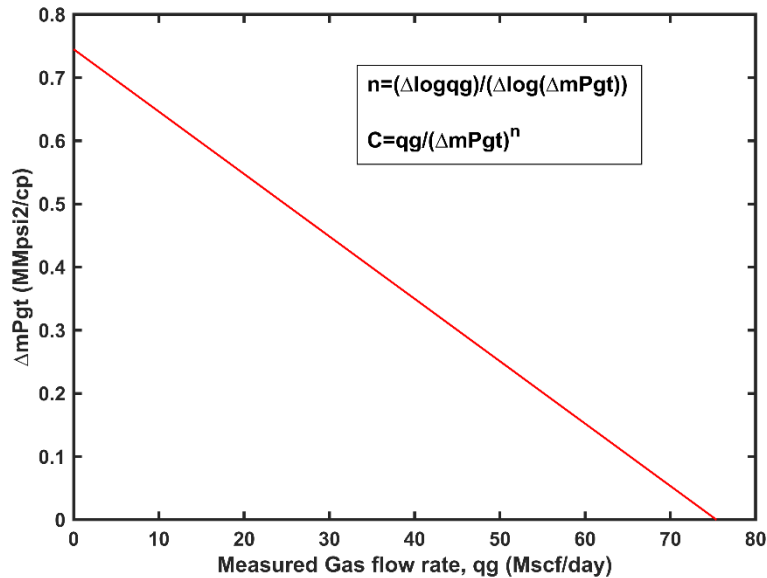


Figure 6.4. Plot of gas flow rate vs total ΔmP_{gt} for KAL – 5.

6.3.3 Material balance calculation

To relate production rate, calculated from pseudopressure integral, to time the volumetric material balance equation can be used (Guehria, 2000; Mott, 2002). Volumetric material balance provides estimation of hydrocarbon reserves in any stage of a reservoir depletion based on conservation of mass. It is also a tool to indicate cumulative gas and oil production from a reservoir with a stepwise pressure depletion. Tarner, (1944) developed a volumetric material balance that originally proposed for solution – gas drive reservoirs. Tarner volumetric material balance is utilized to relate the rate of production to time. This method is an iterative technique to find the acceptable value of producing gas to oil ratio ' R_p ' during pressure depletion process (Tarner, 1944). The method adhere the following assumptions (Standing, 1979).

- The reservoir formation is homogeneous with respect to permeability, porosity, fluid saturation and relative permeability.
- Gravity forces affecting fluid flow are negligible.
- Pressure is uniform throughout the reservoir.
- Equilibrium exists at all time between the saturated gas and the liquid drop out that has been evolved from saturated gas.
- Reservoir hydrocarbon pore volume remains constant.

Original form of Turner's material balance method simplified by Dake, (1978, pp. 81–82) as shown in following.

$$N = \frac{N_p[(B_o - R_s B_g) + G_p B_g]}{(B_o - B_{oi}) + (R_{si} - R_s)B_g} \quad 6.28$$

Where N is cumulative production, N_p is oil cumulative production and G_p stands for gas cumulative production. Multiplying components in 6.28 are groups of thermodynamic variables (defined in pseudopressure integral) that they can be summarized by two distinct multipliers for condensate (oil) production ϕ_c and gas ϕ_g .

$$\left\{ \begin{array}{l} \phi_c = \frac{B_o - R_s B_g}{(B_o - B_{oi}) + (R_{si} - R_s)B_g} \\ \phi_g = \frac{B_g}{(B_o - B_{oi}) + (R_{si} - R_s)B_g} \end{array} \right\} \quad 6.29$$

Substituting ϕ_c and ϕ_g in 6.28 yields the following equation.

$$N = N_p \phi_n + G_p \phi_g \quad 6.30$$

Where N_p is condensate (oil) cumulative production and G_p is cumulative gas production. The instantaneous, producing gas-oil ratio, R_p , given as

$$R_p = \frac{\Delta G_p}{\Delta N_p} \quad 6.31$$

The value of R_p is the average of produced gas to oil ratio " $R_{p,average}$ " within each pressure interval. In a stepwise pressure reduction between pressure intervals i and $i + 1$, the $\Delta N_{pi \rightarrow i+1}$ for cumulative production of 1STB oil can be calculated as follow.

$$\Delta N_{pi \rightarrow i+1} = \frac{1 - N_{pi} \phi_{n,ave} - G_{pi} \phi_{g,ave}}{\phi_{n,ave} - R_{p,av} \phi_{g,ave}} \quad 6.32$$

For each subsequent pressure intervals, the calculation steps is summarized in following steps:

1. Define the pressure intervals, ΔP (200psia – 500psia).
2. Determine ϕ_c and ϕ_g using 6.29 and updated PVT properties obtained for average pressure within each pressure intervals.

3. Assume a value of $R_p, average = R_p, guess$ in the interval (as an initial guess the R_p assumed between 9000 – 20000 scf/STB).
4. Calculate $\Delta N_{pi \rightarrow i+1}$ from 6.32.
5. Calculate cumulative gas production $G_{pi \rightarrow i+1}$ in each pressure intervals from ($\Delta G_{pi \rightarrow i+1} = \Delta N_{pi \rightarrow i+1} \times R_p, guess$).
6. Calculate the Condensate (oil) saturation from

$$S_o = \left(1 - \frac{N_p}{N}\right) \frac{B_o}{B_{oi}} (1 - S_w) \quad 6.33$$

7. Knowing absolute permeability (Table 6.1) and the effective permeability of each phase, the relative permeability of gas and condensate (oil) phase can be calculated from the following.

$$\begin{cases} krg = \frac{k \cdot krg}{k} \\ kro = \frac{k \cdot kro}{k} \end{cases} \quad 6.34$$

8. Estimate produced gas to oil ratio $R_{p,calc}$ from the following equation.

$$R_{p,calc} = R_s + \frac{Krg \mu_o B_o}{Krc \mu_g B_g} \quad 6.35$$

9. Compare two values of $R_{p,guess}$ in step 3 and $R_{p,calc}$ in step 8. If they do not converge, repeat steps 3 to 8 with a new value of the $R_{p,guess}$ until convergence occurs.
10. With average reservoir pressure (P_R) from each pressure intervals calculate gas/condensate flow rates from pseudopressure integral.
11. The gas production rates q_g and q_c then can be combined with obtained gas cumulative production (G_p) and condensate (oil) cumulative production (N_p).
12. Gas and condensate production profile can be calculated as a function of time.
13. The time of depletion for each pressure intervals is calculated from the following equation.

$$t = \frac{\Delta G_p}{q_g} \quad 6.36$$

The explained computation of material balance incorporated with well inflow performance calculation using pseudopressure approach to generate production

profile of the well. In computation of pseudopressure integral the viscosity and two-phase Z factor of gas and condensate phase were calculated using existing literature models and the developed AI models in chapter 4 and 5.

6.3.4 Validation of new production profile

To validate the gas and condensate production results, obtained from three-flow regions pseudopressure approach for the studied gas-condensate (KAL – 5) commercial numerical reservoir simulator *Eclipse 300* was performed.

Initially Constant – Volume – Depletion (CVD) test on reservoir fluid compositions (table 6.1) was performed using *PVTi* (Schlumberger) and Peng – Robinson cubic equation of state. The Peng – Robinson is industry standard choice for characterization of gas-condensate fluid properties. This is also known as full compositional simulation to ensure highest accuracy of the PVT properties.

The well (KAL – 5) is located in a compact formation with absolute permeability of 0.0035 millidarcy, which indicate without stimulation the production is impossible. Therefore, in our model multiple conductive fractures were created in two X and Y directions inside the reservoir. The conductivity of each fracture is 500 millidarcy per foot, which allow gas flows towards the wellbore.

Then a vertical well (KAL– 5) placed in middle of the created geometry. The reservoir and fluid details are obtained from Economides *et al.*, (1989) as shown in Table 6.1. This gas-condensate well is in a high temperature (354°F [179°C]) formation of Pannonian basin in Yugoslavia. The field covers a large area of 131234 ft² (40 km²). The outer well drainage area of the model is 2400 ft² (731.52m²) where a vertical well placed in the middle of the model with the pay zone of 36ft (10.97m). The schematic illustration of the created model is shown in Figure 6.5. The details of the developed Eclipse reservoir simulator code and created fractures can be found in Appendix D.

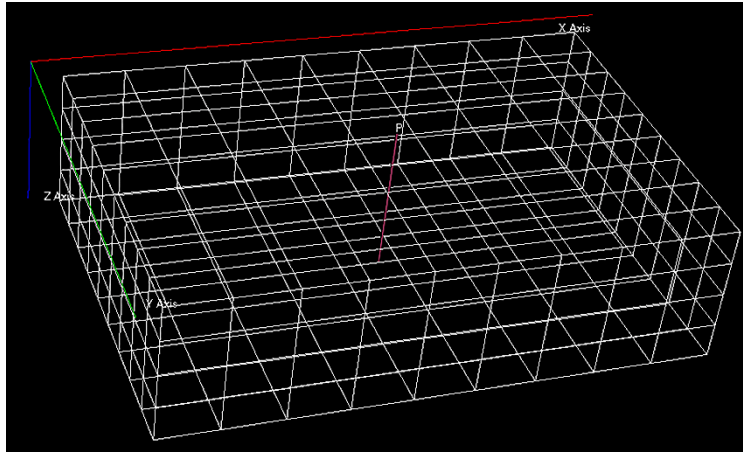


Figure 6.5. Schematic illustration of 3D created model in Eclipse 300.

Initial condition of the reservoir fluid coincides with most gas-condensate systems with producing GOR of 9470 scf/STB (1706 std m³/stock-tank m³). The initial reservoir pressure (6750psi [46.5M_{pa}]) is identical to dew point pressure and condensation starts from the beginning of the production. The result of CVD in Figure 6.6 indicates the reservoir fluid is a rich gas-condensate with maximum condensate saturation of 25.2%. Three parameters Peng – Robinson cubic equation of state utilized for full compositional simulation of the reservoir fluid properties. Multi-flash experiment of the reservoir fluid in standard condition of 14.696 psi and 60°F has been performed and fluid phase diagram was generated and shown in Figure 6.7. The simulation was run and generated results were recorded in terms of production profile. The production profile indicates how much gas or condensate is produced as a function of time.

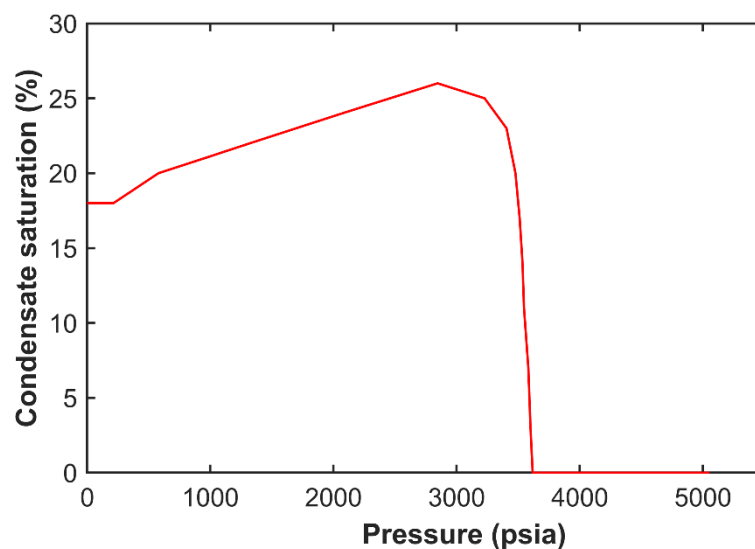


Figure 6.6. Condensate saturation curve a result of the CVD experiment of the reservoir fluid.

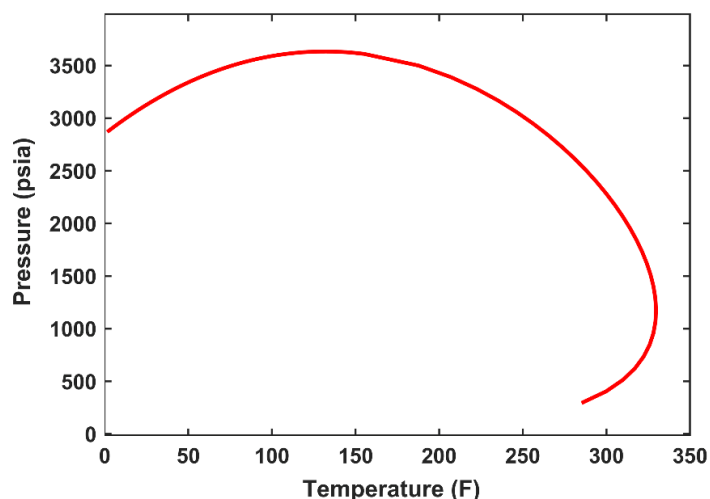


Figure 6.7. Phase diagram of the reservoir fluid in standard pressure and temperature.

The result of composition simulation will be compared to the results of three-flow regions pseudopressure approach using optimized MBO model and the developed viscosities and Z factor models.

In order to optimize MBO model, that can be used in three regions pseudopressure approach, several condensate viscosity models of optimized form of Beggs and Robinson, (1975); De Ghetto et al., (1994); Elsharkawy and Alikhan, (1999); Kartoatmodjo and Schmidt, (1991); LBC, (1964) and four machine learning based models of ANN, LSSVM, TSK fuzzy and Mamdani fuzzy developed in chapter 4 were used. Among the developed oil (condensate) viscosity methods TSK fuzzy approach, Artificial Neural Network (ANN) and least square support vector machine (LSSVM) outperformed other optimized methods. Therefore, aforementioned models have been used for prediction of oil (condensate) viscosity in generating MBO PVT table. In order to compute gas phase viscosity the optimized version of Londono et al., (2002) shown in equation 4.15 was used.

For better computation of two-phase Z factor three developed machine learning based models of cascade forward neural network (CFNN), feed forward neural network (FFNN) and adaptive neuro fuzzy inference system (ANFIS) in chapter 5 were considered. ANFIS model performed better than other two methods for prediction of two-phase Z factor. Hence, ANFIS was utilized for computation of two-phase Z factor of KAL – 5 gas-condensate well in MBO PVT table. Once the gas and condensate MBO PVT tables were generated, the results used for computation of gas and condensate flow rates using three regions pseudopressure integral. The results from

three regions pseudopressure integral were combined with material balance equation and production profile of gas and condensate were established. This would allow the comparison of the obtained results to compositional reservoir simulation results using Eclipse 300.

6.3.5 Results and discussion

In presenting the results first the behaviour of studied gas-condensate fluid in the reservoir will be explored and then the effect of inaccurate PVT data and two-phase Z factor in relation to production profile will be discussed.

The graph in Figure 6.8 shows how the fluid behaves in terms of viscosity variation as a function of pressure. Increasing reservoir pressure would proportionally increase the gas phase viscosity as intermolecular connection of the gas phase become stronger and the gas behave like a liquid in very high pressure. Contrary to the gas phase the liquid phase (condensate) viscosity is decreased with increasing the reservoir pressure as the liquid behave like a gas in very high temperature due to reduction in intermolecular forces (absorption and repulsion). The result of Figure 6.8 confirms the aforementioned criterion in regards to physical behaviour of the fluid as a function of pressure. It also shows that there is a strong relation between pressure and viscosity of gas/condensate and viscosity is extremely non-linear. Before analysing the affect of various gas/condensate viscosity and Z factor on the production results, we discuss permeability affect.

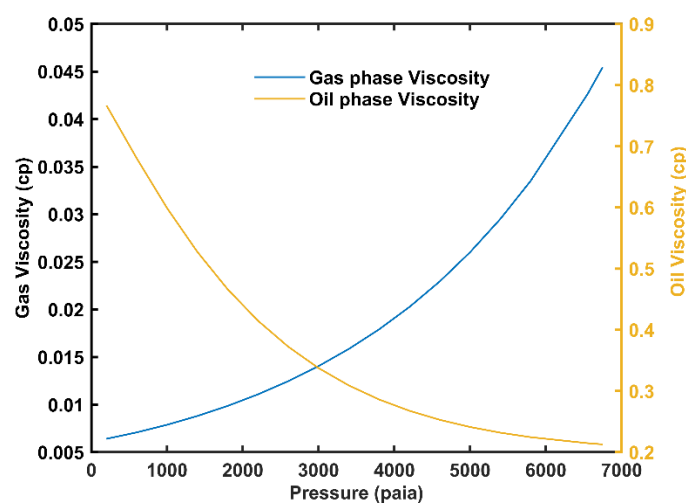


Figure 6.8. Variation of gas and oil (condensate) viscosity with pressure in KAL – 5.

Permeability alteration of the reservoir is a critical issue because of the condensate drop out. Figure 6.9 shows that gas effective permeability is sharply declined after the production begins. When reservoir pressure is reduced from initial reservoir pressure of 6750psia to 5850psia (the red line on the graph), the effective permeability of formation to the gas phase stabilized. The relative permeability of each phase calculated using equation 6.32 and the ratio of the k_{rg} to k_{ro} (k_{rg}/k_{ro}) is estimated and plotted against pressure in Figure 6.9. Changes in relative permeability of each phase due to the condensation drop out divided into five stages as it demonstrated in Figure 6.10. Each stage are discussed in following.

- Stage 1: The ratio of k_{rg} to k_{ro} (k_{rg}/k_{ro}) is high at the beginning of the production ($p_i=6750psia$), however as the production commence, severe decline in gas phase relative permeability occurs, where k_{rg} lost its ratio by 230 times to k_{ro} .
- Stage 2: The gas phase relative permeability continuous to decline further with a fast rate between $4200 psia < P < 6050psia$. This is due to further accumulation of liquid drop out in region 1.
- Stage 3: At this stage the gas relative permeability (k_{rg}) reduction would almost stabilizes. At the beginning of this stage, the liquid drop out might reaches its maximum saturation and after this point, it starts to decrease due to vaporization (this also known as retrograde behaviour). After vaporization condensate liquid produced as a gas form at the surface (Danesh, 1998, pp. 26–27).
- Stage 4: Further decline in pressure would increase the gas phase relative permeability. This means that the gas phase saturation inside the reservoir increases. This behaviour might imply the fact that the further reduction of reservoir pressure contributes to revaporization of the condensate phase that dropped out during pressure depletion.

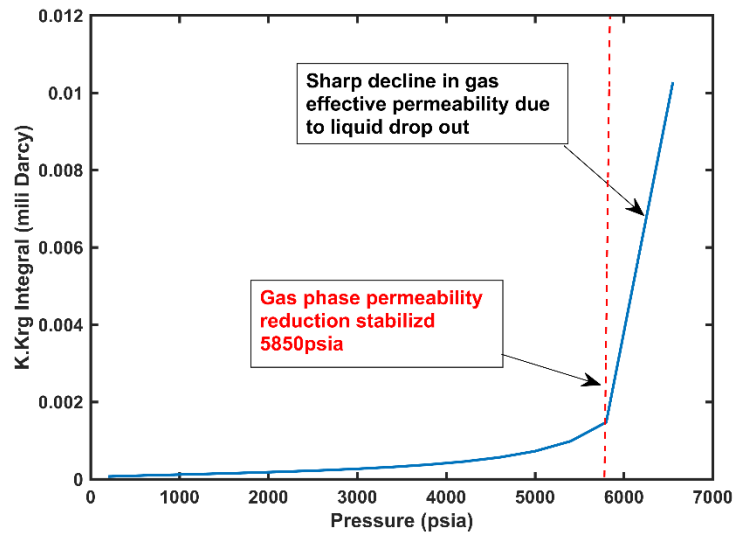


Figure 6.9. Gas phase effective permeability.

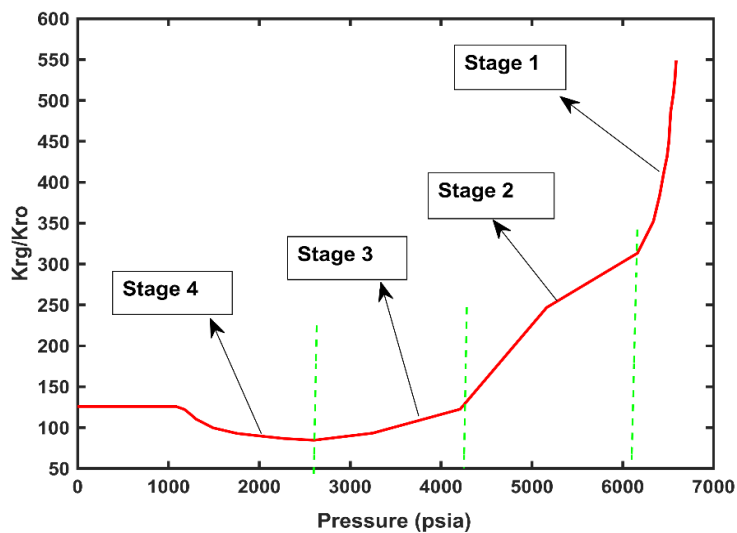


Figure 6.10. Relative permeability ratio (gas to oil) as a function of pressure for high temperature (354°F) gas condensate well.

Figure 6.11 and Figure 6.12 depict the generated production profile for gas and condensate rate of the studied well. From both graphs, it is evident that three-flow regions pseudopressure approach incorporated with optimized MBO PVT properties (e.g., TSK fuzzy for condensate viscosity and ANFIS for two-phase Z factor), is following the results of compositional simulation very well. In presenting production profiles, only various viscosity models have been labelled on the graphs for comparison, however in the computation process, the developed ANFIS used to generate two-phase Z factor in all models.

Statistical accuracy of the obtained results examined using two statistical metrics of average absolute relative deviation percentage (AARD %) and root mean square error (RMSE) shown in 6.37.

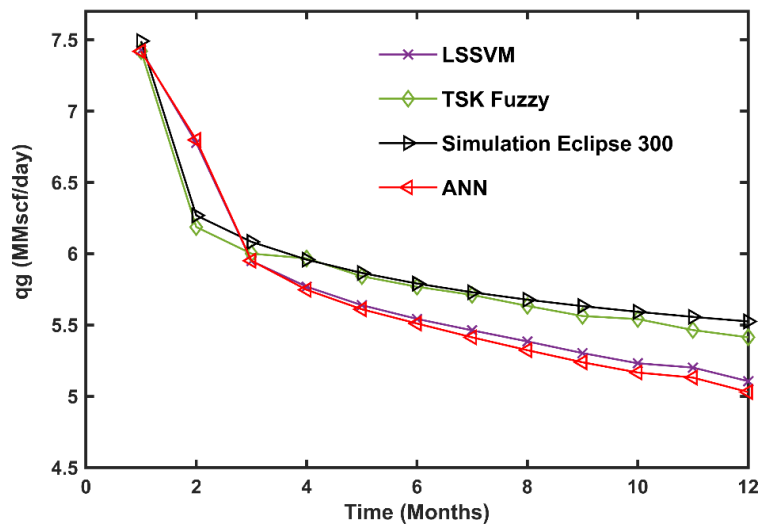


Figure 6.11. Gas production profile for KAL – 5 using analytical method incorporated with various ML techniques in generating PVT properties.

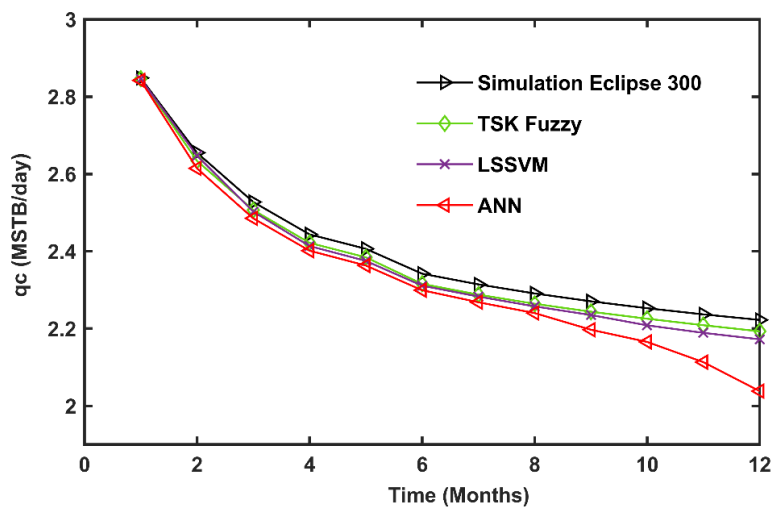


Figure 6.12. Gas production profile for KAL – 5 using analytical method incorporated with various ML techniques in generating PVT properties.

$$\left\{ \begin{array}{l} AARD\% = \frac{100}{N} \sum_{i=1}^N \frac{|(Simulation.(i) - Analytical.(i))|}{Simulation.(i)} \times 100 \\ RMSE = \left(\frac{\sum_i^N (Analytical.(i) - Simulation.(i))^2}{N} \right)^{0.5} \end{array} \right\} \quad 6.37$$

The results of statistical error analysis presented in Table 6.3, Figure 6.13 and Figure 6.14. From the results it has been observed that pseudopressure integral incorporated with TSK fuzzy condensate viscosity model and ANFIS model for calculating two-phase Z factor outperform other two methods with the least RMSE of 0.0224 and 0.1441 for gas phase and oil phase respectively in first 12 months of production forecast. In terms of AARD% the analytical model incorporated with TSK fuzzy approach condensate viscosity outperformed other methods with 0.856% for gas phase and 2.398% for condensate phase. The results confirm using accurate prediction of PVT properties (viscosity and two-phase Z factor) below the saturation pressure is critical for forecasting gas-condensate wells using three-flow regions pseudopressure integral and MBO model. The optimized MBO PVT model using intelligent methods ensure the accurate production profile of gas-condensate wells in compact formation.

Gas and condensate production from the studied well (KAL – 5) declined rapidly after 45 days. This is due to accumulation of the condensate liquid inside the reservoir, which directly effect the gas phase relative permeability (Figure 6.10 and Figure 6.11). This has a direct impact on forecast of the future performance of such reservoirs. Successful application of three regions pseudopressure integral is depending on reliable prediction of viscosity and two-phase Z factor in generating PVT tables. Machine learning based approaches provide a promising results for better prediction performance accuracy of gas-condensate wells in tight formation.

Table 6.3. Statistical error analysis of the developed analytical technique for predicting gas and condensate rates in (KAL – 5).

Method		RMSE	AARD%
Gas phase	Pseudopressure (ANN, ANFIS)	0.0829	2.358
	Pseudopressure (LSSVM, ANFIS)	0.0302	1.098
	Pseudopressure (TSK Fuzzy, ANFIS)	0.0224	0.856
Oil phase	Pseudopressure (ANN, ANFIS)	0.1945	3.375
	Pseudopressure (LSSVM, ANFIS)	0.1538	2.656
	Pseudopressure (TSK Fuzzy, ANFIS)	0.1441	2.398

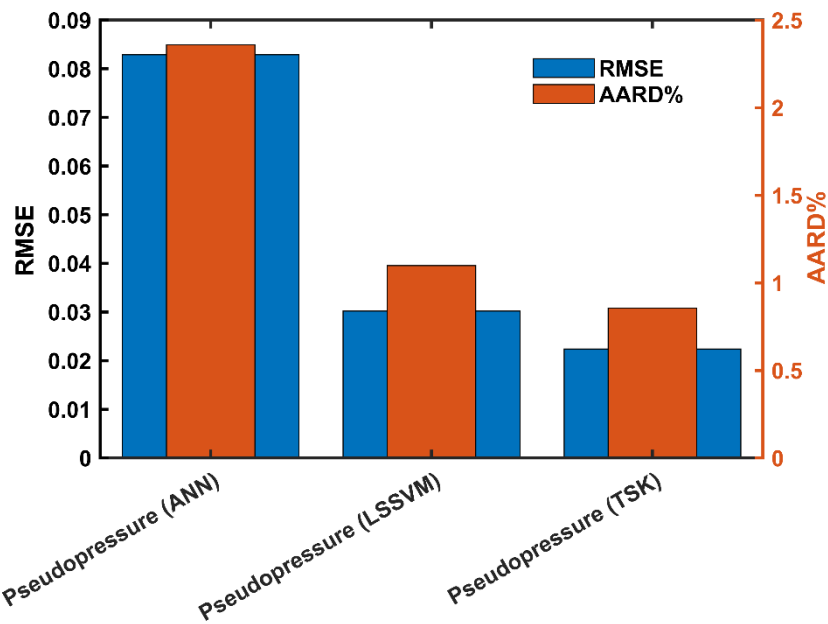


Figure 6.13. Statistical error results between analytical pseudopressure approach and compositional simulation results for perdition of gas phase production profile in KAL – 5.

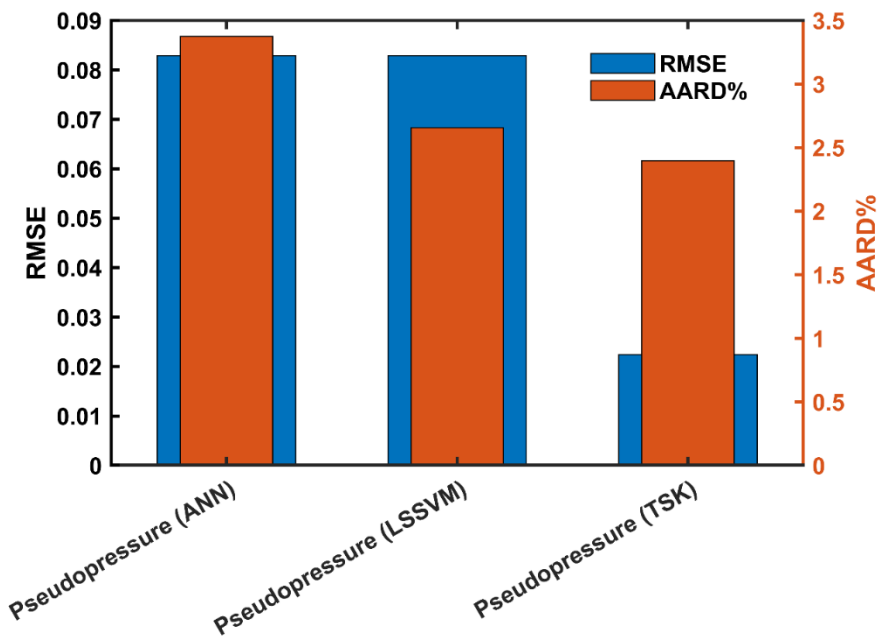


Figure 6.14. Statistical error results between analytical pseudopressure approach and compositional simulation results for perdition of oil phase production profile in KAL – 5.

Using analytical method of three-flow regions pseudopressure approach combined with developed MBO PVT models in this study has the following advantage over fully compositional simulation (Eclipse 300).

- The method is less data demanding in comparison to Eclipse reservoir simulation.

- Provide accurate and fast deliverability predictions when many sensitivity analyses are required particularly at the beginning of the production.
- The pseudopressure approach does not need knowledge of using reservoir simulators (e.g., Eclipse) and can be implemented in spreadsheet format.
- PVT properties required for computation of pseudopressure integral can be calculated using simple modified black oil model, where gas/condensate viscosity and two-phase Z factor can be estimated using developed smart models in this study.

The results of this chapter is very close to the existing literature work of Fevang, (1995), Mott, (2002), Jokhio, (2002), Chowdhury et al., (2004), Behmanesh et al., (2015) and Hekmatzadeh and Gerami, (2018). The major different between this work and aforementioned studies are in treating PVT properties. They mostly used modified black oil method (MBO) to generate and compute the PVT properties, then validate their result with compositional reservoir simulators, where EOS used for computing PVT properties. The highest error between two methods were related in uncertainty of gas/condensate viscosity and two-phase Z factor below the saturation pressure. In this study we bridge the gap between the results of MBO and EOS models in treating PVT properties by ensuring accurate estimation of gas/condensate viscosity and two-phase Z factor using AI techniques. The justification for our approach is with an improved viscosity and two-phase Z factor in PVT calculation, better accuracy of gas and condensate liquid can be achieved.

Our approach in this study is more efficient and assure a higher performance for computation of gas and oil flow rate of gas-condensate reservoirs. Inaccuracy of MBO model for establishing PVT properties of complex gas-condensate fluid in critical conditions was compensated by using AI techniques proposed in this study.

This has been confirmed by comparing the results of this study with compositional simulation of a HTHP gas-condensate well in compact formation.

6.4 Summary

Accurate prediction of production profile in gas-condensate wells are very important for financial evaluation and well production planning. The aim of this chapter was to investigate the effect of accurate estimation of gas/condensate viscosity and two-phase Z factor on reliable estimation of production profile. For this purpose, MBO PVT

model, where gas/condensate viscosity and two-phase Z factor were estimated using AI methods, incorporated with pseudopressure integral to calculate well inflow performance. Then to relate the results obtained from pseudopressure integral to time, volumetric material balance utilized and production profiles of a HTHP gas-condensate well were generated. The results show that pseudopressure integral incorporated with gas/condensate viscosity and two-phase Z factor using TSK fuzzy and ANFIS approach respectively has the best performance and predicts the production rate very close to compositional reservoir simulator. Gas phase flow rate at the surface is predicted using pseudopressure integral incorporated with TSK fuzzy and ANFIS for computation of gas viscosity and two-phase Z factor respectively with RMSE of 0.0224 and AARD% of 0.856 from compositional simulation results. Oil (condensate) phase flow rate at the surface is also estimated using pseudopressure integral combined with TSK fuzzy and ANFIS model in calculation of oil viscosity and two-phase Z factor respectively with RMSE of 0.1441 and AARD% of 2.398 in compare to simulator results.

Accurate prediction of PVT properties including viscosity and two-phase Z factor ensure accurate prediction of production profile. Using developed AI algorithms in this study for estimating governing parameters of PVT properties such as gas/condensate viscosity and Z factor is eliminating the uncertainty in prediction and ensure accurate gas-condensate reservoir performance modelling.

The generated production profile in this chapter is a simple analytical three-flow regions pseudopressure approach that can be used for quick and reliable estimation of gas-condensate wells. The method is an excellent alternative to fully compositional simulators, where considerable reservoir and fluid data is required to start the simulation.

CHAPTER 7

CONCLUSIONS AND RECOMMENDATIONS

7.1 Introduction

This chapter consists of two parts. In the first section, general conclusions and brief discussion of various methods utilized in this study are shown. Furthermore, it has been highlighted that the aim and objectives of the study have been achieved.

In the second part, the possible improvement of the current study is discussed. More conclusions that are specific were presented at the end of each chapter.

7.2 Improve accuracies of gas-condensate viscosity

One of the main achievement of this study is in developing several models for prediction of gas-condensate fluid viscosities through using numerical approaches.

The current methodology for estimation of gas-condensate viscosities below the saturation pressure is based on empirical and semi-empirical correlations. The correlations are embedded in black oil model or compositional model (equation of state) for computation of fluid viscosity.

Primarily in chapter 4, accuracy of the most frequently used methods of Lohrenz – Bray – Clark (1964), Lee – Gonzalez – Eakin, (1966), Londono – Archer – Blasingame (2002), Sutton, (2005), Elsharkawy, (2006), Beggs and Robinsons, (1975), Kartoatmodjo and Schmidt, (1991), De Ghetto et al., (1994), Elsharkawy and Alikhan (1999), Bergman and Sutton, (2007), for estimation of gas-condensate viscosities were assessed using experimental data. The results of the statistical error analysis show the performance of these models for estimating gas-condensate viscosity below the saturation pressure is as minimum as 15% and as high as 99% absolute average relative deviation. Both compositional and gas-saturated oil viscosity models were failed to predict the condensate viscosity of gas-condensate fluid below the saturation pressure. Non-linear regression was performed to optimize the coefficients of the existing models to be applicable for estimation of gas-condensate viscosities.

Several ML based approaches have been utilized for better estimation of condensate viscosity below the saturation pressure. Initially two ML based models including a

Least Square Support Vector Machine (LSSVM) and an Artificial Neural Network (ANN) were developed for estimation of condensate viscosity. The accuracy of the developed ML based models are compared with the tuned utilized literature viscosity models. The comparison of the results indicate that the developed ANN model predict condensate viscosity with coefficient of determination of 84.23 and root mean square error of 0.1144, which is superior to all other utilized viscosity models.

Furthermore, in this context two well-known fuzzy logic inference systems including Mamdani and TSK fuzzy logic were manipulated for modelling condensate phase viscosity. Mamdani based fuzzy approach performed to develop 15 IF-THEN rules to interrelate condensate viscosity to pressure, temperature and solution gas to oil ratio. Utilizing TSK fuzzy logic approach, an unique relationship between condensate viscosity, pressure, temperature and solution gas to oil ratio was established through proposing a linear correlation (equation 4.61). The superiority of the developed correlation in 4.61 over other methods was verified by root mean square error of 0.0194, mean average error of 0.0163 and absolute average relative deviation of 7.123%.

The main advantages of the developed viscosity models over existing literature models is that they are less data demanding, which make them particularly useful for prediction of condensate viscosity when the compositional data are not available. In addition, the developed models are computationally efficient and they can be used as an effective tool for quick and reliable determination of gas-condensate viscosities.

7.2.1 Improvement of two-phase gas-condensate Z factor

In the context of PVT modelling improvement of gas-condensate fluids, another major achievement of the study is in developing several smart approaches for determination of two-phase Z factor below the saturation pressure. Accurate prediction of two-phase Z factor is a critical importance for reliable deliverability modelling in gas-condensate reservoirs. This important PVT property determines how much gas-condensate deviate from ideal gas law and can be used for all engineering calculation of gas-condensate reservoirs. Comprehensive data bank was used to assess the accuracy and reliability of the existing two-phase Z factor models including Hall – Yarborough, (1973), Dranchuk – Abu –Kassem, (1975), Beggs and Brill, (1973), Rayes et al., (1973) and Azizi et al., (2010). The statistical and graphical error analysis indicate the

performance of employed literature models for prediction of gas-condensate two-phase Z factor below the saturation pressure are not satisfactory for various ranges of pseudoreduced pressure and pseudoreduced temperature especially for high pressure high temperature (HPHT) conditions.

Several machine-learning (ML) based approaches was developed for accurate estimation of gas-condensate two-phase Z factor. To this end, two types of neural networks known as cascade forward neural network (CFNN) and feed-forward neural network (FFNN) as well as Adaptive Neuro Fuzzy Inference System (ANFIS) were implemented. Performance of the developed machine-learning models are better than utilized existing models for prediction of gas-condensate two-phase Z factor, verified by statistical indicators of root mean square error (RMSE), mean average error (MAE) and average absolute relative deviation percentage (AARD%). ANFIS model outperformed all other Z factor models in various range of pseudoreduced pressure and pseudoreduced temperature with root mean square error of 0.0025 and absolute average relative deviation of 0.2191%. An iterative procedure was developed within ANFIS algorithm to ensure faster convergence of the algorithm for computation of two-phase Z factor. The developed ML based approaches in this study do not limit to certain range of P_{pr} and T_{pr} like existing literature models. The developed models are able to predict the gas-condensate reservoirs in highly critical conditions (HTHP) and with variety of non-hydrocarbon contents (e.g., CO_2 , H_2S and N_2). Another advantage of the developed models is that they are not limited within geographical location of the reservoirs (e.g., North Sea, Middle East etc.) like existing literature models.

Analysing the impact of each input variable used for development of the ML based models on two-phase Z factor using Pearson relevancy factor (r), revealed that pressure, molecular weight of C_{7+} and C_{7+} content, C_6 content and temperature have the highest positive impact on two-phase Z factor. This means increasing aforementioned parameters would directly increase the magnitude of two-phase Z factor.

Moreover, non-hydrocarbon components of H_2S , N_2 and CO_2 have negative impact on two-phase Z factor, which indicate increasing these variables resulted in decreasing two-phase Z factor.

The developed models in this study provide very good improvement in prediction of gas-condensate two-phase Z factor over previous correlations with broader applications in terms of pressure, temperature and compositional variations. These models can be implemented in any reservoir simulation software and provide superior accuracy and performance for prediction of two-phase gas-condensate Z factor. The limitation of the developed model is that the compositional data of gas-condensate reservoir should be available and insert into the models for prediction of Z factor.

7.2.2 Effectiveness of viscosities and two-phase Z factor models for producing accurate production profile

In chapter 6, the effect of the developed viscosity and two-phase Z factor models in this study for generating reliable production profile of a gas-condensate reservoir was investigated. The common industry approach for establishing production profile of gas-condensate reservoirs is through either implementing fully compositional reservoir simulations or analytical approach using pseudopressure integral.

The effectiveness of viscosities and two-phase Z factor models on production profile of gas-condensate wells have been investigated through implementing three-flow regions pseudopressure integral that combined with volumetric material balance. In order to calculate the PVT properties within three-flow regions pseudopressure integral optimized modified black oil (MBO) model was implemented. The novelty of the new approach in this study is to embed the developed viscosities and two-phase Z factor using machine – learning approaches for generating PVT table in MBO model. For computation of condensate viscosity and two-phase Z factor the developed TSK fuzzy model and developed ANFIS model were utilized respectively. The results show that the new developed production profile matched with fully compositional model using Eclipse 300 with RMSE of 0.0224 and AARD% of 0.856 for gas phase and RMSE of 0.1441 and AARD% of 2.398 for condensate (oil) phase.

The generated production profile is less data demanding and has an advantage over fully compositional simulations (Eclipse 300), which normally require extensive data to run. The developed analytical method is easy to implement in spreadsheet format and does not require knowledge of reservoir simulator. The results of the developed production profile indicate the dependency of gas-condensate reservoir performance modelling on accurate estimation of viscosities and two-phase Z factor.

The results of effective permeabilities of gas and condensate phase is calculated using pressure transient test data. The results of permeability indicate severe decline in gas permeability for the reservoirs where the condensation occurs from the beginning of the production.

The utilized computational procedure in chapter 6 is well able to predict single well production (gas and condensate) at the surface.

7.3 Recommendation for future work

In this study, the critical issues associated for accurate PVT properties of gas-condensate reservoirs, required for well deliverability modelling, have been investigated. Extensive attempt has been made for accurate modelling of gas-condensate reservoirs PVT properties including development of several smart modelling approaches for computation of gas-condensate viscosities and two-phase Z factor. The developed approaches in this study can be further improved as follow.

- The evolved ANN and LSSVM and Mamdani Fuzzy models that were used for prediction of condensate viscosity in this study can be further improved with other optimization algorithms such as Genetic Algorithm (GA) or Coupled Simulated Annealing (CSA).
- The developed intelligent models in this study for prediction of gas-condensate viscosities and two-phase Z factor can be embedded inside PVT packages such as Schlumberger PVTi in order to generate reliable fluid properties of such reservoirs.
- The intelligent models such as fuzzy approach can also be utilised for categorization of various type of gas-condensate fields around the world (e.g., low, medium, high and very high). This is to ensure better recovery planning and production optimization of such fields.
- The developed production profile in chapter 6 is applicable for single vertical well. The method can be applied to horizontal and inclined gas-condensate wells.

REFERENCES

Aamir Mahmood, M. and Ali Al-Marhoun, M. (1996) *Evaluation of empirically derived PVT properties for Pakistani crude oils*, *Journal of Petroleum Science and Engineering*.

Afidick, D., Kaczorowski, N. J. and Bette, S. (1994) 'Production performance of a retrograde gas reservoir: a case study of the Arun Field', in *SPE - Asia Pacific Oil & Gas Conference*. Melbourne: Society of Petroleum Engineers, pp. 73–80. doi: 10.2523/28749-ms.

Agarwal, R. G. (1979) "Real Gas Pseudo-Time" - A New Function For Pressure Buildup Analysis Of MHF Gas Wells', in *SPE Annual Technical Conference and Exhibition*. Las Vegas, Nevada: Society of Petroleum Engineers. doi: 10.2118/8279-MS.

Agatonovic-Kustrin and Beresford, R. (2000) 'Basic concepts of artificial neural network (ANN) modeling and its application in pharmaceutical research', *Journal of Pharmaceutical and Biomedical Analysis*, 22, pp. 717–727. Available at: <https://www.sciencedirect.com/science/article/abs/pii/S0731708599002721>.

Ahmadi, M. *et al.* (2015) 'Phase Equilibrium Modeling of Clathrate Hydrates of Carbon Dioxide + 1,4-Dioxine Using Intelligent Approaches', *Journal of Dispersion Science and Technology*, 36(2), pp. 236–244. doi: 10.1080/01932691.2014.904792.

Ahmadi, M. and Ebadi, M. (2014a) 'Evolving smart approach for determination dew point pressure through condensate gas reservoirs', *Fuel*. Elsevier, 117, pp. 1074–1084. doi: 10.1016/J.FUEL.2013.10.010.

Ahmadi, M. and Ebadi, M. (2014b) 'Fuzzy Modeling and Experimental Investigation of Minimum Miscible Pressure in Gas Injection Process', *Fluid Phase Equilibria*. Elsevier B.V., 378, pp. 1–12. doi: 10.1016/j.fluid.2014.06.022.

Ahmadi, M. and Ebadi, M. (2014c) 'Fuzzy Modeling and Experimental Investigation of Minimum Miscible Pressure in Gas Injection Process', *Fluid Phase Equilibria*. Elsevier, 378(2014), pp. 1–12. doi: 10.1016/J.FLUID.2014.06.022.

Ahmadi, M., Ebadi, M. and Hosseini, S. M. (2014) 'Prediction breakthrough time of water coning in the fractured reservoirs by implementing low parameter support vector machine approach', *Fuel*. Elsevier, 117(PART A), pp. 579–589. doi: 10.1016/j.fuel.2013.09.071.

Ahmed, T. H. (2010) *Reservoir engineering handbook*. 4th edn. Oxford: Gulf Professional Pub.

Aily, M. *et al.* (2019) 'Modeling viscosity of moderate and light dead oils in the presence of complex aromatic structure', *Journal of Petroleum Science and Engineering*. Elsevier, 173, pp. 426–433. doi: 10.1016/J.PETROL.2018.10.024.

Akhimiona, N. and Wiggins, M. L. (2005) 'An Inflow-Performance Relationship for Horizontal Gas Wells', in *SPE Eastern Regional Meeting*. Society of Petroleum Engineers. doi: 10.2118/97627-MS.

Al-Attar, H. and Al-Zuhair, S. (2009) 'Simplified approach for predicting gas well performance', *Journal of Petroleum Science and Engineering*, 65(1–2), pp. 51–61. doi: 10.1016/j.petrol.2008.12.016.

Al-Hussainy, R. and Ramey, H. J. (1966) 'Application of Real Gas Flow Theory to Well Testing and Deliverability Forecasting', *Journal of Petroleum Technology*. Society of Petroleum Engineers (SPE), 18(05), pp. 637–642. doi: 10.2118/1243-b-pa.

Al-Hussainy, R., Ramey, H. J. and Crawford, P. B. (1966) 'The Flow of Real Gases Through Porous Media', *Journal of Petroleum Technology*. Society of Petroleum Engineers, 18(05), pp. 624–636. doi: 10.2118/1243-A-PA.

Al-Khalifa, A. A., Horne, R. N. and Aziz, K. (1987) 'In-place determination of reservoir relative permeability using well test analysis', in *SPE Annual Technical Conference and Exhibition*. Dallas: Society of Petroleum Engineers, pp. 459-472 17973. doi: 10.2523/17973-ms.

Al-Marhoun, M. A. (1990) *New Correlations for FVFs of Oil and Gas Mixtures*. King Fahd University of Petroleum & Minerals.

Al-Meshari, A. *et al.* (2007) 'Measurement of Gas Condensate, Near-Critical and Volatile Oil Densities and Viscosities at Reservoir Conditions', in *Proceedings of SPE Annual Technical Conference and Exhibition*. California: Society of Petroleum Engineers. doi: 10.2523/108434-ms.

Al-Meshari, A. A. (2004) *New strategic method to tune equation-of-state to match experimental data for compositional simulation*. Texas. Available at: <http://repository.tamu.edu/handle/1969.1/1388>.

Al-Nasser, K. S. and Al-Marhoun, M. A. (2012) 'Development of New Gas Viscosity Correlations', in *SPE International Production and Operations Conference & Exhibition*. Doha: Society of Petroleum Engineers. doi: 10.2118/153239-ms.

Al-Shammasi, A. A. (2001) 'A review of bubblepoint pressure and oil formation volume factor correlations', *SPE Reservoir Evaluation and Engineering*. Society of Petroleum Engineers, 4(2), pp. 146–160. doi: 10.2118/71302-PA.

Al-Shawaf, A., Aramco, S. and Kelkar, M. (2014) 'A New Method To Predict the Performance of Gas-Condensate Reservoirs'. doi: 10.2118/161933-PA.

AlQuraishi, A. A. and Shokir, E. M. (2011) 'Artificial neural networks modeling for hydrocarbon gas viscosity and density estimation', *Journal of King Saud University - Engineering Sciences*. King Saud University, 23(2), pp. 123–129. doi: 10.1016/j.jksues.2011.03.004.

Altug, S., Mo-Yuen Chen and Trussell, H. J. (1999) 'Fuzzy inference systems implemented on neural architectures for motor fault detection and diagnosis', *IEEE Transactions on Industrial Electronics*, 46(6), pp. 1069–1079. doi: 10.1109/41.807988.

Arabloo, M., Heidari Sureshjani, M. and Gerami, S. (2014) 'A new approach for analysis of production data from constant production rate wells in gas condensate reservoirs', *Journal of Natural Gas Science and Engineering*. Elsevier, 21, pp. 725–731. doi: 10.1016/j.jngse.2014.09.028.

Arukhe, I. N. and Mason, W. E. (2012) 'The Use of Two Phase Compressibility Factors in Predicting Gas Condensate Performance', in *SPE Annual Technical Conference and Exhibition*. San Antonio: Society of Petroleum Engineers. doi: 10.2118/159080-ms.

Asklany, S. A. *et al.* (2011) 'Rainfall events prediction using rule-based fuzzy inference system', *Atmospheric Research*. Elsevier B.V., 101(1–2), pp. 228–236. doi: 10.1016/j.atmosres.2011.02.015.

Audonnet, F. and Pádua, A. A. . (2004) 'Viscosity and density of mixtures of methane and n-decane from 298 to 393 K and up to 75 MPa', *Fluid Phase Equilibria*. Elsevier, 216(2), pp. 235–244. doi: 10.1016/J.FLUID.2003.10.017.

Ayyalasomayajula, P., Silpngarmlers, N. and Kamath, J. (2005) 'Well Deliverability Predictions for a Low-Permeability Gas/Condensate Reservoir', in *SPE Annual Technical Conference and Exhibition*. Dallas, Texas: Society of Petroleum Engineers, pp. 9–12.

Azizi, N., Behbahani, R. and Isazadeh, M. A. (2010) 'An efficient correlation for calculating compressibility factor of natural gases', *Journal of Natural Gas Chemistry*, 19, pp. 642–645. doi: 10.1016/S1003-9953(09)60081-5.

Bagirov, A. M. (2008) 'Modified global k-means algorithm for minimum sum-of-squares clustering problems', *Pattern Recognition*. Pergamon, 41(10), pp. 3192–3199. doi:

10.1016/J.PATCOG.2008.04.004.

Bai, L. *et al.* (2017) 'Fast density clustering strategies based on the k-means algorithm', *Pattern Recognition*. Pergamon, 71, pp. 375–386. doi: 10.1016/J.PATCOG.2017.06.023.

Baled, H. O. *et al.* (2018) 'Viscosity models for pure hydrocarbons at extreme conditions: A review and comparative study', *Fuel*. Elsevier Ltd, 218, pp. 89–111. doi: 10.1016/j.fuel.2018.01.002.

Bandyopadhyay, S. and Maulik, U. (2002) 'An evolutionary technique based on K-Means algorithm for optimal clustering in RN', *Information Sciences*. Elsevier, 146(1–4), pp. 221–237. doi: 10.1016/S0020-0255(02)00208-6.

Beal, C. (1946) 'The Viscosity of Air, Water, Natural Gas, Crude Oil and Its Associated Gases at Oil Field Temperatures and Pressures', *Transactions of the AIME*, 165(01), pp. 94–115. doi: 10.2118/946094-g.

Beggs, H. D. and Brill, J. R. (1973) 'Study of two-phase flow in inclined pipes', *JPT, Journal of Petroleum Technology*. Society of Petroleum Engineers, 25(05), pp. 607–617. doi: 10.2118/4007-PA.

Beggs, H. D. and Robinson, J. R. (1975) 'Estimating the Viscosity of Crude Oil Systems', *Journal of Petroleum Technology*. Society of Petroleum Engineers, 27(09), pp. 1140–1141. doi: 10.2118/5434-PA.

Behera, S. S. and Chattopadhyay, S. (2012) 'A Comparative Study of Back Propagation and Simulated Annealing Algorithms for Neural Net Classifier Optimization', *Procedia Engineering*. Elsevier, 38, pp. 448–455. doi: 10.1016/J.PROENG.2012.06.055.

Behmanesh, H., Hamdi, H. and Clarkson, C. R. (2015) 'Production data analysis of tight gas condensate reservoirs', *Journal of Natural Gas Science and Engineering*. Elsevier, 22, pp. 22–34. doi: 10.1016/j.jngse.2014.11.005.

Behmanesh, H., Hamdi, H. and Clarkson, C. R. (2017) 'Production data analysis of gas condensate reservoirs using two-phase viscosity and two-phase compressibility', *Journal of Natural Gas Science and Engineering*. Elsevier B.V, 47, pp. 47–58. doi: 10.1016/j.jngse.2017.07.035.

Bell, J. (2014) *Machine Learning: Hands-On for Developers and Technical Professionals*. 1st edn. Canada: John Wiley & Sons, Incorporated.

Bergman, D. F. and Sutton, R. P. (2007a) 'A Consistent and Accurate Dead-Oil-Viscosity Method', in *SPE Annual Technical Conference and Exhibition*. Anaheim: Society of Petroleum Engineers, p. 30. doi: 10.2118/110194-MS.

Bergman, D. F. and Sutton, R. P. (2007b) 'An Update to Viscosity Correlations for Gas-Saturated Crude Oils', in *SPE Annual Technical Conference and Exhibition*. Anaheim: Society of Petroleum Engineers. doi: 10.2118/110195-MS.

Bezdek, J. and Pal, S. K. (1992) *Fuzzy models for pattern recognition, Fuzzy models for pattern recognition*. New York: IEEE Press.

Biezma, M. V., Agudo, D. and Barron, G. (2018) 'A Fuzzy Logic method: Predicting pipeline external corrosion rate', *International Journal of Pressure Vessels and Piping*, 163, pp. 55–62. doi: 10.1016/j.ijpvp.2018.05.001.

Black, M. (1937) 'Vagueness. An Exercise in Logical Analysis', *Philosophy of Science*, 4(4), pp. 427–455.

Bonyadi, M. *et al.* (2014) 'Theoretical and experimental determination of initial reservoir fluid in a lean gas condensate reservoir'. doi: 10.1016/j.petrol.2014.01.003.

Bonyadi, M., Rahimpour, M. R. and Esmaeilzadeh, F. (2012) 'A new fast technique for calculation of gas condensate well productivity by using pseudopressure method', *Journal of Natural Gas Science and Engineering*. Elsevier, 4, pp. 35–43. doi:

10.1016/J.JNGSE.2011.07.012.

Borges, P. R. (1991) 'Correction improves z-factor values for high gas density', *The Oil and Gas Journal*, 89(9), pp. 54–56.

Borthne, G. (1986) *Development of a materia balance and inflow performane model for oil and gas-condensate reservoirs*. The Norwegian Institute of Technolodgy.

Bourbiaux, B. J. (1994) 'Parametric Study of Gas-Condensate Reservoir Behavior During Depletion: A Guide for Development Planning', in *European Petroleum Conference*. London: Society of Petroleum Engineers. doi: 10.2118/28848-MS.

BP (2019) *BP invests in new artificial intelligence technology | News and insights | Home*. Available at: <https://www.bp.com/en/global/corporate/news-and-insights/press-releases/bp-invests-in-new-artificial-intelligence-technology.html> (Accessed: 8 April 2020).

Brooks, R. H. and Corey, A. T. (1964) *Hydraulic Properties of Porous Media*.

Calinski, T. and Harabasz, J. (1974) 'A dendrite method for cluster analysis', *Communications in Statistics - Theory and Methods*, 3(1), pp. 1–27. doi: 10.1080/03610927408827101.

Carnahan, N. F. and Starling, K. E. (1969) 'Equation of state for nonattracting rigid spheres', *The Journal of Chemical Physics*. American Institute of PhysicsAIP, 51(2), pp. 635–636. doi: 10.1063/1.1672048.

Carr, N. L., Kobayashi, R. and Burrows, D. B. (1954) 'Viscosity of Hydrocarbon Gases Under Pressure', *Journal of Petroleum Technology*. Society of Petroleum Engineers (SPE), 6(10), pp. 47–55. doi: 10.2118/297-g.

Chamkalani, A. *et al.* (2013) 'Utilization of support vector machine to calculate gas compressibility factor', *Fluid Phase Equilibria*, 358, pp. 189–202. doi: 10.1016/j.fluid.2013.08.018.

Chen, H. C. *et al.* (1993) 'Novel approaches to the determination of Archie parameters II: Fuzzy regression analysis', *Society of Petroleum Engineers of AIME, (Paper) SPE*. Society of Petroleum Engineers, 3(01), pp. 71–94. doi: 10.2118/26288-pa.

Chen, Z. *et al.* (2015) 'Self-Adaptive Prediction of Cloud Resource Demands Using Ensemble Model and Subtractive-Fuzzy Clustering Based Fuzzy Neural Network', *Computational and Mathematical Methods in Medicine*. Hindawi Limited, 2015(1), pp. 2–4. doi: 10.1155/2015.

Chew, J. . and Connally, C. (1959) 'A viscosity correlation for gas-saturated crude oils', *Pet. Trans. AIME*. Society of Petroleum Engineers, 216, pp. 23–25.

Chierici, G. L. (1984) 'Novel relation for drainage and imbibition relative permeabilities', *Society of Petroleum Engineers journal*. Society of Petroleum Engineers, 24(3), pp. 275–276. doi: 10.2118/10165-PA.

Chiu, S. L. (1994) 'Fuzzy model identification based on cluster estimation', *Journal of Intelligent and Fuzzy Systems*. IOS Press, 2(3), pp. 267–278. doi: 10.3233/IFS-1994-2306.

Chowdhury, N. *et al.* (2004) 'A Semi-Analytical Method to Predict Well Deliverability in Gas-Condensate Reservoirs', in *SPE Annual Technical Conference and Exhibition*. Houston: Society of Petroleum Engineers. doi: 10.2118/90320-MS.

Christensen, P. L. and Fredenslund, A. A. (1980) 'A corresponding states model for the thermal conductivity of gases and liquids', *Chemical Engineering Science*. Pergamon, 35(4), pp. 871–875. doi: 10.1016/0009-2509(80)85073-1.

Cios, K. J. and Shields, M. E. (1997) 'The handbook of brain theory and neural networks: By Micheal A. Arbib (Ed.)', MIT Press, Cambridge, MA, 1995, ISBN 0-262-01148-4, 1118 pp', *Neurocomputing*. Elsevier, 16(3), pp. 259–261. doi: 10.1016/S0925-2312(97)00036-2.

Coats, K. H. (1985) 'Simulation of gas-condensate reservoirs performance', *JPT, Journal of Petroleum Technology*, 37(11), pp. 1870–1886. doi: 10.2118/10512-pa.

Coats, K. H. and Smart, G. T. (1986) 'Application of a regression-based EOS PVT program to laboratory data', *SPE Reservoir Engineering (Society of Petroleum Engineers)*, 1(3), pp. 277–299. doi: 10.2118/11197-PA.

Coats, K. H., Thomas, L. K. and Pierson, R. G. (1995) 'Compositional and Black Oil Reservoir Simulation', in *SPE Reservoir Simulation Symposium*. San Antonio: Society of Petroleum Engineers. doi: 10.2118/50990-pa.

Corey, A. T. *et al.* (1956) 'Three-Phase Relative Permeability', *Journal of Petroleum Technology*. Society of Petroleum Engineers (SPE), 8(11), pp. 63–65. doi: 10.2118/737-g.

Cortes, C. and Vapnik, V. (1995) 'Support-vector networks', *Machine Learning*. Kluwer Academic Publishers, 20(3), pp. 273–297. doi: 10.1007/BF00994018.

Craft, B. and Hawkin, M. (2015) *Applied Petroleum Reservoir Engineering*. Third. Edited by T. Ronald and R. Brandon. New Jersey: Prentice Hall.

Cragoe, C. S. (1929) *Thermodynamic Properties of Petroleum Products*. Washington, DC.

Curilem, M. *et al.* (no date) 'Neural networks and support vector machine models applied to energy consumption optimization in semiautogeneous grinding', *folk.ntnu.no*. Available at: <http://folk.ntnu.no/skoge/prost/proceedings/pres2011-and-icheap10/PRES11/85Curilem.pdf> (Accessed: 12 March 2019).

Dake, L. (1983) *Fundamentals of reservoir engineering*. 19th edn. Oxford: Elsevier.

Dake, L. (2001) *The practice of reservoir engineering*. 3rd edn. Amsterdam: Elsevier.

Daltaban, T. (1985) *Numerical modelling of recovery processes from gas condensate reservoirs*. University of London.

Danesh, A. (1998) *PVT and phase behaviour of petroleum reservoir fluids*. 1st edn. Elsevier.

Davani, E. *et al.* (2013) 'HPHT viscosities measurements of mixtures of methane/nitrogen and methane/carbon dioxide', *Journal of Natural Gas Science and Engineering*, 12, pp. 43–55. doi: 10.1016/j.jngse.2013.01.005.

Dehane, A., Tiab, D. and Osisanya, S. O. (2000) 'Comparison of the Performance of Vertical and Horizontal Wells in Gas-Condensate Reservoirs', in *SPE Annual Technical Conference and Exhibition*. Society of Petroleum Engineers. doi: 10.2118/63164-MS.

Dempsey, J. R. (1965) 'Computer routine treats gas viscosity as a variable', *Oil and Gas Journal*, 63(8), pp. 141–143.

Dranchuk, P. M. and Abou-Kassem, J. H. (1974) 'Calculation of Z factors for natural gases using equations of state.', *Journal of Canadian Petroleum Technology*. Petroleum Society of Canada, 14(3), pp. 34–36. doi: 10.2118/75-03-03.

Dranchuk, P. M., Purvis, R. A. and Robinson, D. B. (1973) 'Computer Calculation Of Natural Gas Compressibility Factors Using The Standing And Katz Correlation', in. Edmonton: Society of Petroleum Engineers (SPE). doi: 10.2118/73-112.

Drohm, J. K., Goldthorpe, W. H. and Trengove, R. (1988) 'Enhancing the Evaluation of PVT Data', in *Offshore South East Asia Show*. Singapore: Society of Petroleum Engineers. doi: 10.2118/17685-MS.

Earlougher, R. C. (1977) *Advances in well test analysis*. SPE. Available at: <https://store.spe.org/Advances-in-Well-Test-Analysis-P8.aspx> (Accessed: 14 May 2019).

ECLIPSE (2014) *Eclipse Reservoir Simulation Reference Manual*.

Economides, M. J. *et al.* (1989) 'The Stimulation of a Tight, Very-High- Temperature Gas-Condensate Well', *SPE Formation Evaluation*. Society of Petroleum Engineers, 4(01), pp. 63–72. doi: 10.2118/15239-PA.

Economides, M. J. *et al.* (1989) 'The Stimulation of a Tight , Very-High- Temperature Gas-Condensate Well', *SPE Formation Evaluation*, Economides(March), pp. 63–72.

Egbogah, E. and Jack, N. (1990) 'An improved temperature-viscosity correlation for crude oil systems', *Journal of Petroleum Science and Engineering*, 5, pp. 197–200. Available at: <https://vdocuments.mx/an-improved-temperature-viscosity-correlation-for-crude-oil-systems.html>.

EIA (2020) *Open Data*, *eai.gov*. Available at: www.eia.gov (Accessed: 28 June 2020).

Eilerts, C. K. (1964) 'Integration of Partial Differential Equation for Transient Linear Flow of Gas-Condensate Fluids in Porous Structures', *Society of Petroleum Engineers Journal*. Society of Petroleum Engineers (SPE), 4(04), pp. 291–306. doi: 10.2118/111-pa.

Eilerts, C. K., Sumner, E. F. and Potts, N. L. (1965) 'Integration of Partial Differential Equation for Transient Radial Flow of Gas-Condensate Fluids in Porous Structures', *Society of Petroleum Engineers Journal*. Society of Petroleum Engineers (SPE), 5(02), pp. 141–152. doi: 10.2118/716-pa.

Eilerts, K. C. (1947) 'Gas-condensate reservoir engineering. 1. The reservoir fluid, its composition and phase behavior', *Oil Gas J.*, 45(39).

Elsharkawy, A. M. (2002) 'Predicting the Properties of Sour Gases and Condensates', in *2002 SPE International Petroleum Conference and Exhibition*. Society of Petroleum Engineers. doi: 10.2118/74369-MS.

Elsharkawy, A. M. (2006) 'Efficient methods for calculations of compressibility, density, and viscosity of natural gases', in *Journal of Canadian Petroleum Technology*. Petroleum Society of Canada, pp. 55–61. doi: 10.2118/06-06-04.

Elsharkawy, A. M. and Alikhan, A. A. (1999) 'Models for predicting the viscosity of Middle East crude oils', *Fuel*. Elsevier, 78(8), pp. 891–903. doi: 10.1016/S0016-2361(99)00019-8.

Elsharkawy, A. M. and Elkamel, A. (2001) 'The accuracy of predicting compressibility factor for sour natural gases', *Petroleum Science and Technology*. Taylor & Francis Group, 19(5–6), pp. 711–731. doi: 10.1081/LFT-100105285.

Elsharkawy, A. M. and Foda, S. G. (1998) 'EOS simulation and GRNN modeling of the constant volume depletion behavior of gas condensate reservoirs', in *SPE Asia Pacific Conference on Integrated Modelling for Asset Management*. Kuala Lumpur: Society of Petroleum Engineers. doi: 10.1021/ef970135z.

Elsharkawy, A. M., Hashem, Y. S. K. S. and Alikhan, A. A. (2000) 'Compressibility Factor for Gas Condensates', in *SPE Permian Basin Oil and Gas Recovery Conference*. Midland: Society of Petroleum Engineers. doi: 10.2118/59702-MS.

Eslamimanesh, A. *et al.* (2011) 'Phase Equilibrium Modeling of Structure H Clathrate Hydrates of Methane + Water "Insoluble" Hydrocarbon Promoter Using Group Contribution-Support Vector Machine Technique', *Ind. Eng. Chem. Res*, 50, pp. 12807–12814. doi: 10.1021/ie2011164.

Eslamimanesh, A. *et al.* (2012) 'Phase equilibrium modeling of clathrate hydrates of methane, carbon dioxide, nitrogen, and hydrogen+water soluble organic promoters using Support Vector Machine algorithm', *Fluid Phase Equilibria*. Elsevier, 316, pp. 34–45. doi: 10.1016/j.fluid.2011.11.029.

Evinger, H. H. and Muskat, M. (1942) 'Calculation of Theoretical Productivity Factor', *Transactions of the AIME*. Society of Petroleum Engineers, 146(01), pp. 126–139. doi:

10.2118/942126-g.

Fan, L. *et al.* (2005) 'Understanding Gas-Condensate Reservoirs', *Oilfield Review*, 17(4), pp. 14–27. Available at: <https://pdfs.semanticscholar.org/947f/0f6128844c3334638325ae38efe17bb802c7.pdf> (Accessed: 10 April 2020).

Fattah, K. A. *et al.* (2014) 'New Inflow Performance Relationship for solution-gas drive oil reservoirs', *Journal of Petroleum Science and Engineering*. Elsevier, 122, pp. 280–289. doi: 10.1016/j.petrol.2014.07.021.

Fayazi, A. *et al.* (2014) 'State-of-the-art least square support vector machine application for accurate determination of natural gas viscosity', *Industrial and Engineering Chemistry Research*, 53(2), pp. 945–958. doi: 10.1021/ie402829p.

Fazeli, H. *et al.* (2013) 'Experimental Study and Modeling of Ultrafiltration of Refinery Effluents Using a Hybrid Intelligent Approach', *Energy & Fuels*. American Chemical Society, 27(6), pp. 3523–3537. doi: 10.1021/ef400179b.

Fetkovich, M. D. *et al.* (1986) 'Oil and Gas Relative Permeabilities Determined From Rate-Time Performance Data', in *SPE Annual Technical Conference and Exhibition*. New Orleans: Society of Petroleum Engineers, pp. 1–44.

Fetkovich, M. J. (1973) 'The Isochronal Testing of Oil Wells', in *Fall Meeting of the Society of Petroleum Engineers of AIME*. Las Vegas, Nevada: Society of Petroleum Engineers, p. SPE 4529. doi: 10.2118/4529-MS.

Fevang, Ø. (1995) *Gas Condensate Flow Behavior and Sampling, October*. PhD Thesis. Petroleum Engineering and Applied Geophysics.

Fevang, Ø., Singh, K. and Whitson, C. H. (2000) 'Guidelines for choosing compositional and black-oil models for volatile oil and gas-condensate reservoirs', in *SPE Reservoir Engineering (Society of Petroleum Engineers)*. Dallas: Society of Petroleum Engineers. doi: 10.2118/63087-MS.

Fevang, Ø. and Whitson, C. H. (1996) 'Modeling Gas-Condensate Well Deliverability', *SPE Reservoir Engineering*. Society of Petroleum Engineers, 11(04), pp. 221–230. doi: 10.2118/30714-PA.

Flach, P. A. (2012) *Machine learning: the art and science of algorithms that make sense of data*. Cambridge: Cambridge University Press.

Fletcher, R. (1987) *Practical Methods of Optimization*. 2nd edn. Chichester: Wiley.

Forchheimer, P. (1901) 'Wasserbewegung durch Boden [Movement of Water through Soil]', *Zeitschrift des Vereins deutscher Ingenieur*, 45, pp. 1736–1749.

Forsyth, R. (1989) *Machine Learning*. 1st edn. London: Chapman and Hall.

Fuller, G. G. (1976) 'A Modified Redlich-Kwong-Soave Equation of State Capable of Representing the Liquid State', *Industrial & Engineering Chemistry Fundamentals*, 15(04), pp. 254–257.

Fussell, D. D. (1973) 'Single-well performance predictions for gas condensate reservoirs.', *JPT, Journal of Petroleum Technology*. Society of Petroleum Engineers, 25(07), pp. 860–870. doi: 10.2118/4072-PA.

Gazprom (2019) *Gas and oil reserves*. Available at: <https://www.gazprom.com/about/production/reserves/> (Accessed: 9 March 2020).

Ghaffari, A. *et al.* (2006a) 'Performance comparison of neural network training algorithms in modeling of bimodal drug delivery', *International Journal of Pharmaceutics*. Elsevier, 327(1–2), pp. 126–138. doi: 10.1016/J.IJPHARM.2006.07.056.

Ghaffari, A. *et al.* (2006b) 'Performance comparison of neural network training algorithms in modeling of bimodal drug delivery', *International Journal of*

Pharmaceutics. Elsevier, 327(1–2), pp. 126–138. doi: 10.1016/J.IJPHARM.2006.07.056.

Gharagheizi, F. *et al.* (2014) 'Development of a LSSVM-GC model for estimating the electrical conductivity of ionic liquids', *Chemical Engineering Research and Design*. Elsevier, 92(1), pp. 66–79. doi: 10.1016/J.CHERD.2013.06.015.

De Ghetto, G. *et al.* (1994) 'Reliability Analysis on PVT Correlations', in *European Petroleum Conference*. London: SPE.

Ghiasi, M. M. *et al.* (2014) 'Robust modeling approach for estimation of compressibility factor in retrograde gas condensate systems', *Industrial and Engineering Chemistry Research*. American Chemical Society, 53(32), pp. 12872–12887. doi: 10.1021/ie404269b.

Gilbert, W. E. (1954) 'Flowing and gas-lift well performance', in *API Drilling and Production Practice*. Los Angeles: American Petroleum Institute. doi: 10.2118.

Giri Nandagopal, M. S. and Selvaraju, N. (2016) 'Prediction of Liquid–Liquid Flow Patterns in a Y-Junction Circular Microchannel Using Advanced Neural Network Techniques', *Industrial & Engineering Chemistry Research*, 55(43), pp. 11346–11362. doi: 10.1021/acs.iecr.6b02438.

Glaso, O. (1980) 'Generalized Pressure-Volume-Temperature Correlations', *Journal of Petroleum Technology*, 32(05), p. 785.

Göktaş, B., Macmillan, N. A. and Thrasher, T. S. (2010) 'A systematic approach to modeling condensate liquid dropout in Britannia reservoir', in *SPE Latin American and Caribbean Petroleum Engineering Conference Proceedings*. Lima: Society of Petroleum Engineers, pp. 965–973. doi: 10.2118/139056-ms.

Gold, D. K., McCain, W. D. and Jennings, J. W. (1989) 'Improved method for the determination of the reservoir-gas specific gravity for retrograde gases', *Journal of*

Petroleum Technology. Society of Petroleum Engineers, 41(7), pp. 747–752. doi: 10.2118/17310-pa.

Gomes, H. P. and Corrêa, A. C. F. (1992) 'Fully implicit compositional modelling of gas condensate and volatile oil reservoirs', in *SPE Latin American and Caribbean Petroleum Engineering Conference Proceedings*. Caracas: Society of Petroleum Engineers, pp. 1–6. doi: 10.2523/23700-ms.

Gondouin, M., Iffly, R. and Husson, J. (1967) 'An Attempt to Predict the Time Dependence of Well Deliverability in Gas Condensate Fields', *Society of Petroleum Engineers Journal*. Society of Petroleum Engineers, 7(02), pp. 113–124. doi: 10.2118/1478-pa.

Gopal, V. (1977) 'Gas Z-Factor Equation Developed for computer.', *Oil and Gas Journal*, 75, pp. 58–60.

Gozalpour, F. *et al.* (2005) 'Viscosity, density, interfacial tension and compositional data for near critical mixtures of methane + butane and methane + decane systems at 310.95 K', *Fluid Phase Equilibria*. Elsevier, 233(2), pp. 144–150. doi: 10.1016/J.FLUID.2005.03.032.

Guehria, F. M. (2000) 'Inflow Performance Relationships for Gas Condensates', in *SPE Annual Technical Conference and Exhibition*. Society of Petroleum Engineers. doi: 10.2118/63158-MS.

Guo, B., Sun, K. and Ghalambor, A. (2008) *Well Productivity Handbook: Vertical, Fractured, Horizontal, Multilateral, and Intelligent Wells*. 1st edn, *Well Productivity Handbook: Vertical, Fractured, Horizontal, Multilateral, and Intelligent Wells*. 1st edn. Suite: Gulf Publishing Company. doi: 10.1016/C2013-0-15529-8.

Guo, T. M., Du, L. and School, B. G. (1989) *A New Three-Parameter Cubic Equation Of State For Fluids III. Application To Gas Condensates*.

Guo, X. *et al.* (1997) 'Viscosity model based on equations of state for hydrocarbon liquids and gases', *Fluid Phase Equilibria*. Elsevier, 139(1–2), pp. 405–421. doi: 10.1016/S0378-3812(97)00156-8.

Hagan, M. T. *et al.* (2014) *Neural network design*. 2nd edn. Frisco. Available at: <https://capitadiscovery.co.uk/teesside-ac/items/630382> (Accessed: 11 March 2019).

Hagan, M. T. and Menhaj, M. B. (1994) 'Training feedforward networks with the Marquardt algorithm', *IEEE Transactions on Neural Networks*, 5(6), pp. 989–993. doi: 10.1109/72.329697.

Hajirezaie, S. *et al.* (2015) 'A smooth model for the estimation of gas/vapor viscosity of hydrocarbon fluids', *Journal of Natural Gas Science and Engineering*. Elsevier, 26, pp. 1452–1459. doi: 10.1016/j.jngse.2015.07.045.

Hall, K. R. and Yarborough, L. (1973) 'A new equation of state for Z-factor calculations', *Oil and Gas Journal*, 71(25), pp. 82–92.

Hameed, I. A. (2011) 'Using Gaussian membership functions for improving the reliability and robustness of students' evaluation systems', *Expert Systems with Applications*, 38(6), pp. 7135–7142. doi: 10.1016/j.eswa.2010.12.048.

Hassan, A. *et al.* (2019) 'Gas condensate treatment: A critical review of materials, methods, field applications, and new solutions', *Journal of Petroleum Science and Engineering*. Elsevier, 177, pp. 602–613. doi: 10.1016/J.PETROL.2019.02.089.

Hatampour, A. and Ghiasi-Freez, J. (2013) 'A fuzzy logic model for predicting dipole shear sonic imager parameters from conventional well logs', *Petroleum Science and Technology*, 31(24), pp. 2557–2568. doi: 10.1080/10916466.2011.603005.

Hatzignatiou, D. G. and Reynolds, A. C. (1996) 'Determination of effective or relative permeability curves from well tests', *SPE Journal*. Publ by Soc of Petroleum Engineers of AIME, 1(01), pp. 89–100. doi: 10.2118/20537-pa.

Haykin, S. S. (1994) *Neural networks: a comprehensive foundation*. 1st edn. New York: Macmillan.

Heidaryan, E., Moghadasi, J. and Rahimi, M. (2010) 'New correlations to predict natural gas viscosity and compressibility factor', *Journal of Petroleum Science and Engineering*, 73(1–2), pp. 67–72. doi: 10.1016/j.petrol.2010.05.008.

Hekmatzadeh, M. and Gerami, S. (2018) 'A new fast approach for well production prediction in gas-condensate reservoirs', *Journal of Petroleum Science and Engineering*. Elsevier Ltd, 160(September 2017), pp. 47–59. doi: 10.1016/j.petrol.2017.10.032.

Hemmati-Sarapardeh, A. *et al.* (2014) 'Reservoir oil viscosity determination using a rigorous approach', *Fuel*. Elsevier, 116, pp. 39–48. doi: 10.1016/J.FUEL.2013.07.072.

Hemmati-Sarapardeh, A. *et al.* (2020) 'Modeling natural gas compressibility factor using a hybrid group method of data handling', *Engineering Applications of Computational Fluid Mechanics*, 14(1), pp. 27–37. doi: 10.1080/19942060.2019.1679668.

Hernandez, J. C. *et al.* (2002) 'Sensitivity of Reservoir Simulations to Uncertainties in Viscosity', in *SPE/DOE Improved Oil Recovery Symposium*. Oklahoma: Society of Petroleum Engineers, pp. 2–10. doi: 10.2118/75227-ms.

Hippert, H. S., Pedreira, C. E. and Souza, R. C. (2001) 'Neural networks for short-term load forecasting: a review and evaluation', *IEEE Transactions on Power Systems*, 16(1), p. 4333.

Horne, R. N. (1995) *Modern Well Test Analysis A Computer-Aided Approach*. Palo Alto: Petroway.

Horner, D. R. (1951) 'Pressure Build-up in Wells', in *3rd World Petroleum Congress*.

The Hague: World Petroleum Congress. Available at: <https://www.onepetro.org/conference-paper/WPC-4135> (Accessed: 14 May 2019).

Izgec, B. and Barrufet, M. A. (2005) 'Performance analysis of compositional and modified black-oil models for a rich gas/condensate reservoir', in *Offshore Europe Conference - Proceedings*. California: Society of Petroleum Engineers, pp. 1–14. doi: 10.2118/93374-ms.

Jain, A. K., Murty, M. N. and Flynn, P. J. (1999) 'Data Clustering: A Review', *ACM Computing Surveys*, 31(3), pp. 264–323.

Jalali, farhang, Abdy, Y. and Akbari, M. (2007) 'Dewpoint Pressure Estimation of Gas Condensate Reservoirs, Using Artificial Neural Network (ANN)', in *Proceedings of EUROPEC/EAGE Conference and Exhibition*. London: Society of Petroleum Engineers. doi: 10.2523/107032-MS.

Jang, J. S. R. (1993) 'ANFIS: Adaptive-Network-Based Fuzzy Inference System', *IEEE Transactions on Systems, Man and Cybernetics*, 23(3), pp. 665–685. doi: 10.1109/21.256541.

Jang, J. S. R., Sun, C. T. and Mizutani, E. (1997) 'Neuro-Fuzzy and Soft Computing- A Computational Approach to Learning and Machine Intelligence', *IEEE Transactions on Automatic Control*. Institute of Electrical and Electronics Engineers (IEEE), 42(10), pp. 1482–1484. doi: 10.1109/tac.1997.633847.

Jokhio, S. A. (2002) *Production Performance of Horizontal Wells In Gas-Condensate Reservoirs*. University of Oklahoma.

Jokhio, S. A. and Tiab, D. (2002) 'Establishing Inflow Performance Relationship (IPR) for Gas Condensate Wells', in *SPE Gas Technology Symposium*. Alberta: Society of Petroleum Engineers, pp. 1–20. doi: 10.2118/75503-MS.

Jokhio, S. A., Tiab, D. and Escobar, F. (2002) 'Forecasting Liquid Condensate and

Water Production In Two-Phase And Three-Phase Gas Condensate Systems', in. San Antonio: Society of Petroleum Engineers, pp. 1–13. doi: 10.2118/77549-ms.

Jones, J. R. and Raghavan, R. (1988) 'Interpretation of flowing well response in gas-condensate wells', *SPE Formation Evaluation*. Society of Petroleum Engineers, 3(3), pp. 578–594. doi: 10.2118/14204-PA.

Jones, J. R., Vo, D. T. and Raghavan, R. (1989) 'Interpretation of pressure-buildup responses in gas-condensate wells', *SPE Formation Evaluation*. Society of Petroleum Engineers, 4(1), pp. 93-104 15535. doi: 10.2118/15535-pa.

Jossi, J. A., Stiel, L. I. and Thodos, G. (1962) 'The viscosity of pure substances in the dense gaseous and liquid phases', *AIChE Journal*. John Wiley & Sons, Ltd, 8(1), pp. 59–63. doi: 10.1002/aic.690080116.

Kamari, A. *et al.* (2013) 'Prediction of sour gas compressibility factor using an intelligent approach', *Fuel Processing Technology*. Elsevier, 116, pp. 209–216. doi: 10.1016/J.FUPROC.2013.06.004.

Kamari, A., Mohammadi, A. H. and Ramjugernath, D. (2019) 'Petroleum Science and Technology Characterization of C7+ fraction properties of crude oils and gas-condensates using data driven models. doi: 10.1080/10916466.2019.1570254.

Kariznovi, M., Nourozieh, H. and Abedi, J. (2012) 'Experimental and thermodynamic modeling study on (vapor+liquid) equilibria and physical properties of ternary systems (methane+n-decane+n-tetradecane)', *Fluid Phase Equilibria*, 334, pp. 30–36. doi: 10.1016/j.fluid.2012.06.028.

Kartoatmodjo, T. R. S. and Schmidt, Z. (1991) 'New Correlations For Crude Oil Physical Properties'. USA: Society of Petroleum Engineers, p. 30.

Kartoatmodjo, T. and Schmidt, Z. (1994) 'Large data bank improves crude physical property correlations', *The Oil & gas journal*, 92(27), pp. 51–55.

Kashefi, K. *et al.* (2013) 'Viscosity of binary and multicomponent hydrocarbon fluids at high pressure and high temperature conditions: Measurements and predictions', *Journal of Petroleum Science and Engineering*. Elsevier, 112, pp. 153–160. doi: 10.1016/J.PETROL.2013.10.021.

Katz, D. L. (1942) 'Prediction Of The Shrinkage Of Crude Oils', *Drilling and Production Practic*. American Petroleum Institute, 137.

Katz, D. L. (1959) *Handbook of Natural Gas Engineering*. McGraw-Hill.

Kay, W. B. (1936) 'Density of Hydrocarbon', *Industrial and Engineering Chemistry*, 28(9), pp. 1014–1019. doi: 10.1021/ie50321a008.

Kenneth, L. (1944) 'A Method for the Solution of Certain Non-Linear Problem in Least Squares'. Chcago: American Mathematical Society, pp. 536–538. doi: 10.1090/qam/10666.

Kenyon, D. E. and Behie, G. A. (1987) 'Third SPE Comparative Solution Condensate Reservoirs Project: Gas Cycling of Retrograde', *Journal of Petroleum Technology*. Society of Petroleum Engineers, 39(8), pp. 981–997. doi: 10.2118/12278-PA.

Kesler, M. . and Lee, B. . (1976) 'Improved prediction of enthalpy fractions', *Hydrocarbon Processing*, 55, pp. 153–158.

Khamis, M. A. and Fattah, K. A. (2019) 'Estimating oil–gas ratio for volatile oil and gas condensate reservoirs: artificial neural network, support vector machines and functional network approach', *Journal of Petroleum Exploration and Production Technology*. Springer Verlag, 9(1), pp. 573–582. doi: 10.1007/s13202-018-0501-0.

Khanal, A., Khoshghadam, M. and Lee, W. J. (2016) 'Accurate forecasting of liquid rich gas condensate reservoirs with multiphase flow', in *SPE/AAPG/SEG Unconventional Resources Technology Conference 2016*. Unconventional Resources

Technology Conference (URTEC). doi: 10.15530/urtec-2016-2426222.

Khazali, N., Sharifi, M. and Ahmadi, M. A. (2019) 'Application of fuzzy decision tree in EOR screening assessment', *Journal of Petroleum Science and Engineering*, 177, pp. 167–180. doi: 10.1016/J.PETROL.2019.02.001.

Khorami, A. *et al.* (2017) 'Density, viscosity, surface tension, and excess properties of DSO and gas condensate mixtures', *Applied Petrochemical Research*. Springer Nature, 7(2–4), pp. 119–129. doi: 10.1007/s13203-017-0183-4.

Khosrojerdi, S. *et al.* (2016) 'Thermal conductivity modeling of graphene nanoplatelets/deionized water nanofluid by MLP neural network and theoretical modeling using experimental results', *International Communications in Heat and Mass Transfer*. Science Direct, 74, pp. 11–17. doi: 10.1016/J.ICHEATMASSTRANSFER.2016.03.010.

Klawonn, F., Kruse, R. and Winkler, R. (2015) 'Fuzzy clustering: More than just fuzzification', *Fuzzy Sets and Systems*. North-Holland, 281, pp. 272–279. doi: 10.1016/J.FSS.2015.06.024.

Kniazeff, V. J. and Naville, S. A. (1965) 'Two-Phase Flow of Volatile Hydrocarbons', *Society of Petroleum Engineers Journal*. Society of Petroleum Engineers, 5(01), pp. 37–44. doi: 10.2118/962-pa.

Kuenen, J. . (1892) *On Retrograde Condensation and the Critical Phenomena of Mixtures of Two Substances*, *Communications in Physics*. Netherlands.

Labedi, R. (1992) 'Improved correlations for predicting the viscosity of light crudes', *Journal of Petroleum Science and Engineering*. Elsevier, 8(3), pp. 221–234. doi: 10.1016/0920-4105(92)90035-Y.

Lawal, A. S. (1999) *Application of the Lawal-Lake-Silberberg equation-of-state to thermo- dynamic and transport properties of fluid and fluid mixtures*, *Technical Report*

TR-4-99. Lubbock.

Lee, A. L., Gonzalez, M. H. and Eakin, B. E. (1966) 'The Viscosity of Natural Gases', *Journal of Petroleum Technology*. Society of Petroleum Engineers, 18(08), pp. 997–1000. doi: 10.2118/1340-PA.

Lee, B. I. and Kesler, M. G. (1975) 'A Generalized Thermodynamic Correlation Based on Three-Parameter Corresponding States', *AIChE Journal*. John Wiley & Sons, Ltd, 21(3), pp. 981–983. doi: 10.1002/aic.690300615.

Lee, J. and Wattenbarger, R. (1995) *Gas Reservoir Engineering*. Richardson: Society of Petroleum Engineers (SPE).

Lee, K. H. (2005) *First Course on Fuzzy Theory and Applications*. Taejon: Springer Nature.

Leekwijck, W. Van and Kerre, E. E. (1999) 'Defuzzification: criteria and classification', *Fuzzy Sets and Systems*, 108(2), pp. 159–178. doi: 10.1016/s0165-0114(97)00337-0.

Liao, R. F. *et al.* (2008) 'Fuzzy logic control for a petroleum separation process', *Engineering Applications of Artificial Intelligence*, 21(6), pp. 835–845. doi: 10.1016/j.engappai.2007.09.006.

Liu, H. *et al.* (2013) 'Phase behavior and compressibility factor of two China gas condensate samples at pressures up to 95MPa', *Fluid Phase Equilibria*, 337, pp. 363–369. doi: 10.1016/j.fluid.2012.10.011.

Lohrenz, J., Bray, B. G. and Clark, C. R. (1964) 'Calculating Viscosities of Reservoir Fluids From Their Compositions', *Journal of Petroleum Technology*. Society of Petroleum Engineers, 16(10), pp. 1171–1176. doi: 10.2118/915-pa.

Londono, F. E., Archer, R. A. and Blasingame, T. A. (2002) 'Correlations for

Hydrocarbon Gas Viscosity and Gas Density - Validation and Correlation of Behavior Using a Large-Scale Database', *SPE Reservoir Evaluation & Engineering*. Society of Petroleum Engineers, 8(06), pp. 561–572. doi: 10.2118/75721-pa.

Londono, F. E., Archer, R. A. and Blasingame, T. A. (2005) 'Correlations for hydrocarbon-gas viscosity and gas density-validation and correlation of behavior using a large-scale database', *SPE Reservoir Evaluation and Engineering*. Society of Petroleum Engineers, 8(6), pp. 561–572. doi: 10.2118/75721-PA.

Louridas, P. and Ebert, C. (2016) 'Machine Learning', *IEEE Software*. IEEE Computer Society, 33(5), pp. 110–115. doi: 10.1109/MS.2016.114.

Lucas, K. (1981) 'Die Druckabhängigkeit der Viskosität von Flüssigkeiten – eine einfache Abschätzung', *Chemical Engineering Technology*, 53(12), pp. 959–960.

Mackay', D. J. C. (1992) 'Bayesian Interpolation', *Neural computation*, 4(3), pp. 415–447.

Majidi, S. M. J. *et al.* (2014) 'Evolving an accurate model based on machine learning approach for prediction of dew-point pressure in gas condensate reservoirs', *Chemical Engineering Research and Design*. Institution of Chemical Engineers, 92(5), pp. 891–902. doi: 10.1016/j.cherd.2013.08.014.

Mamdani, E. H. and Assilian, S. (1975) 'An experiment in linguistic synthesis with a fuzzy logic controller', *International Journal of Man-Machine Studies*. Academic Press, 7(1), pp. 1–13. doi: 10.1016/S0020-7373(75)80002-2.

Mansour, E. M. *et al.* (2013) 'Predicting PVT properties of Egyptian crude oils by a modified Soave–Redlich–Kowng equation of state', *Egyptian Journal of Petroleum*. Elsevier, 22(1), pp. 137–148. doi: 10.1016/J.EJPE.2012.09.005.

Maravi, Y. D. C. (2003) *New Inflow Performance Relationship for Gas-condensate reservoirs*. Texas A&M University.

MathWorks (2019) *Comparison of Sugeno and Mamdani Systems*. Available at: <https://uk.mathworks.com/help/fuzzy/comparison-of-sugeno-and-mamdani-systems.html> (Accessed: 31 July 2019).

Matthews, T. A. and Roland, C. H. (1942) 'High Pressure Gas Measurement', *Petroleum Refiner*, 20(6), p. 58.

McCain, W. D. and Cawley, G. (1991) 'Reservoir-Fluid Property Correlations-State of the Art', *SPE Reservoir Engineering*, 6(02), pp. 266–272. doi: 10.2118/18571-pa.

Mesbah, M., Soroush, E. and Rostampour Kakroudi, M. (2017) 'Predicting physical properties (viscosity, density, and refractive index) of ternary systems containing 1-octyl-3-methyl-imidazolium bis(trifluoromethylsulfonyl)imide, esters and alcohols at 298.15 K and atmospheric pressure, using rigorous classification', *Journal of Molecular Liquids*. Elsevier, 225, pp. 778–787. doi: 10.1016/J.MOLLIQ.2016.11.004.

Mmata, B. and Onyekonwu, M. (2014) 'Estimation of anhydrous oil density for accurate multiphase flow measurement: A comparative case study', in *SPE Nigeria Annual International Conference and Exhibition*. Lagos, Nigeria: Society of Petroleum Engineers, pp. 276–284. doi: 10.2118/172369-ms.

Mohaghegh, S. (2000) 'Virtual-Intelligence Applications in Petroleum Engineering', *Journal of Petroleum Technology*, 52(9)(November 2000), pp. 64–71. doi: 10.2118/62415-MS.

Mohamadi-Baghmolaei, M. *et al.* (2015) 'Prediction of gas compressibility factor using intelligent models', *Natural Gas Industry B*. Elsevier B.V., 2(4), pp. 283–294. doi: 10.1016/j.ngib.2015.09.001.

Moses, P. . (1986) 'Engineering Applications of Phase Behavior of Crude Oil and Condensate Systems', *Journal of Petroleum Technology*, pp. 715–723.

Moses, P. . and Donohoe, C. (1987) 'Gas-Condensate Reservoirs', in *In Petroleum Engineering Handbook*. Richardson: Society of Petroleum Engineers (SPE), p. 28. Available at: <https://www.onepetro.org/book/peh/spe-1987-39-peh> (Accessed: 6 July 2020).

Mott, R. (2002) 'Engineering Calculations of Gas-Condensate-Well Productivity', *SPE Reservoir Evaluation & Engineering*, 6(05), pp. 298–306. doi: 10.2118/86298-PA.

Muskat, M. (1949) *Physical principles of oil production*. 1st ed. New York, McGraw-Hill Book Co.

Naderi, M. and Khomehchi, E. (2019) 'Fuzzy logic coupled with exhaustive search algorithm for forecasting of petroleum economic parameters', *Journal of Petroleum Science and Engineering*. Elsevier, 176, pp. 291–298. doi: 10.1016/J.PETROL.2019.01.049.

Naseri, A., Nikazar, M. and Mousavi Dehghani, S. A. (2005) 'A correlation approach for prediction of crude oil viscosities', *Journal of Petroleum Science and Engineering*. Elsevier, 47(3–4), pp. 163–174. doi: 10.1016/J.PETROL.2005.03.008.

Nasrifar, K. and Moshfeghian, M. (2001) 'A new cubic equation of state for simple fluids: pure and mixture', *Fluid Phase Equilibria*, 190(1–2), pp. 73–88.

Nassar, I. S., El-Banbi, A. H. and Sayyoun, M. H. (2013) 'Modified black oil PVT properties correlations for volatile oil and gas condensate reservoirs', in *Society of Petroleum Engineers - North Africa Technical Conference and Exhibition 2013, NATC 2013*. Cairo: Society of Petroleum Engineers, pp. 998–1016. doi: 10.2118/164712-ms.

Nikravesh, M., Zadeh, A. and Aminzadeh, F. (2003) *Soft Computing and Intelligent Data Analysis in Oil Exploration*. 1st edn, *Developments in Petroleum Science*. 1st edn. Edited by M. Nikravesh L.A. Zadeh Fred Aminzadeh. Elsevier Science. doi: 10.1016/S0376-7361(03)80005-5.

Norton, S. (2018) *Shell Announces Plans to Deploy AI Applications at Scale - CIO*

Journal. - *WSJ, CIO Journal*. Available at: <https://blogs.wsj.com/cio/2018/09/20/shell-announces-plans-to-deploy-ai-applications-at-scale/> (Accessed: 8 April 2020).

Nowroozi, S. *et al.* (2009) 'Development of a neural fuzzy system for advanced prediction of dew point pressure in gas condensate reservoirs', *Fuel Processing Technology*, 90(3), pp. 452–457. doi: 10.1016/j.fuproc.2008.11.009.

O'Dell, H. and Miller, R. (1967) 'Successfully Cycling a Low-Permeability, High-Yield Gas Condensate Reservoir', *Journal of Petroleum Technology*, 19(01), pp. 41–47. doi: 10.2118/1495-PA.

Ogunrewo, O. (2014) *Imperial College London*. Imperial College London.

Ojha, S. P. *et al.* (2017) 'Relative permeability estimates for Wolfcamp and Eagle Ford shale samples from oil, gas and condensate windows using adsorption-desorption measurements', *Fuel*. Elsevier Ltd, 208, pp. 52–64. doi: 10.1016/j.fuel.2017.07.003.

Olds, R. H., Sage, B. H. and Lacey, W. N. (1945) 'Volumetric and Phase Behavior of Oil and Gas from Paloma Field', *Transactions of the AIME*. Society of Petroleum Engineers (SPE), 160(01), pp. 77–99. doi: 10.2118/945077-g.

Olds, R. H., Sage, B. H. and Lacey, W. N. (1949) 'Volumetric and Viscosity Studies of Oil and Gas from a San Joaquin Valley Field', *Transactions of the AIME*. Society of Petroleum Engineers (SPE), 179(01), pp. 287–302. doi: 10.2118/949287-g.

Ostermann, R. D. and Owolabi, O. O. (1983) 'Correlations for the Reservoir Fluid Properties of Alaskan Crudes', in *SPE California Regional Meeting*. Ventura: Society of Petroleum Engineers. doi: 10.2118/11703-MS.

Papay, P. (1968) 'A Termelotechnologiai Parameterek Valtozasa a Gazlepek Muvelese Soran', in *Ogil Musz*. Budapest, pp. 267–273.

Passino, K. and Yurkovich, S. (1998) *Fuzzy Control: The Basics, Fuzzy Control*. California: Addison Wesley Longman, Inc.

Pedersen, K. S. and Fredenslund, A. (1987) 'An improved corresponding states model

for the prediction of oil and gas viscosities and thermal conductivities', *Chemical Engineering Science*. Pergamon, 42(1), pp. 182–186. doi: 10.1016/0009-2509(87)80225-7.

Pedersen, K. S., Thomassen, P. and Fredenslund, A. (1984) 'Thermodynamics of Petroleum Mixtures Containing Heavy Hydrocarbons. 1. Phase Envelope Calculations by Use of the Soave-Redlich-Kwong Equation of State', *Industrial and Engineering Chemistry Process Design and Development*. American Chemical Society, 23(1), pp. 163–170. doi: 10.1021/i200024a027.

Pelckmans, K. *et al.* (2002) *LS-SVMlab: a MATLAB/C toolbox for Least Squares Support Vector Machines, Tutorial*. KULeuven- ESAT. Leuven-Heverlee. Available at: <ftp://ftp.esat.kuleuven.be/stadius/kpelckma/kp02-44.pdf>.

Peng, D. Y. and Robinson, D. B. (1976) 'A New Two-Constant Equation of State', *Industrial and Engineering Chemistry Fundamentals*. American Chemical Society, 15(1), pp. 59–64. doi: 10.1021/i160057a011.

Penula, G. (2003) 'Gas-Condensate Well-Test Analysis with and without the Relative Permeability Curves', in *Annual Technical Conference and Exhibition held in Dallas*. Dallas: SPE. doi: 10.1306/a9673950-1738-11d7-8645000102c1865d.

Petrosky, G. E. and Farshad, F. F. (1998) 'Viscosity correlations for gulf of Mexico crude oils', *SPE Reservoir Evaluation & Engineering*, 01(05), pp. 249–258. doi: 10.2523/29468-ms.

Piper, L. D., McCain, W. D. and Corredor, J. H. (1993) 'Compressibility Factors for Naturally Occurring Petroleum Gases', in *SPE Annual Technical Conference and Exhibition*. Houston: Society of Petroleum Engineers, pp. 661–671. doi: 10.2523/26668-ms.

Raghavan, R., Chu, W. C. and Jones, J. R. (1995) 'Practical Considerations in the Analysis of Gas-Condensate Well Tests', in *SPE Annual Technical Conference and*

Exhibition. Dallas, Texas: Society of Petroleum Engineers. doi: 10.2118/30576-MS.

Raghavan, R. and Jones, J. R. (1996) 'Depletion performance of gas-condensate reservoirs', *JPT, Journal of Petroleum Technology*. Society of Petroleum Engineers (SPE), 48(8), pp. 725–731. doi: 10.2118/36352-JPT.

Rahimzadeh, A. *et al.* (2016) 'Condensate blockage study in gas condensate reservoir', *Journal of Natural Gas Science and Engineering*. Elsevier, 33, pp. 634–643. doi: 10.1016/J.JNGSE.2016.05.048.

Rawlins, E. and Schellhardt, M. (1936) 'Back-Pressure Data on Natural Gas Wells and Their Application to Production Practices', in *Bureau of Mines Monograph*. Bureau of Mines Monograph.

Rayes, D. G. *et al.* (1992) 'Two-Phase Compressibility Factors for Retrograde Gases', *SPE Formation Evaluation*. Society of Petroleum Engineers, 7(01), pp. 87–92. doi: 10.2118/20055-PA.

Redlich, O. and Kwong, J. N. (1949) 'On the Thermodynamics of solutions. V An equation of state. Fugacities of gaseous solutions', *Chemical Reviews*, 44(1), pp. 233–244.

Riazi, M. R. and Daubert, T. E. (1987) 'Characterization Parameters for Petroleum Fractions', *Industrial and Engineering Chemistry Research*. American Chemical Society, 26(4), pp. 755–759. doi: 10.1021/ie00064a023.

Rollins, J. B., McCain, W. D. and Creeger, J. T. (1990) 'Estimation of solution GOR of black oils', *JPT, Journal of Petroleum Technology*. Society of Petroleum Engineers, 42(1), pp. 92–94. doi: 10.2118/18602-pa.

Ross, T. J. (2017) *Fuzzy Logic with Engineering Applications*. 4th edn. Chichester: Wiley.

Rostami, A., Hemmati-Sarapardeh, A. and Shamshirband, S. (2018) 'Rigorous

prognostication of natural gas viscosity: Smart modeling and comparative study', *Fuel*, 222, pp. 766–778. doi: 10.1016/j.fuel.2018.02.069.

Roussennac, B. (2001) *Gas condensate well test analysis*, Department of Petroleum Engineering. Stanford University. Available at: <https://pangea.stanford.edu/ERE/pdf/pereports/MS/Roussennac01.pdf> (Accessed: 30 April 2019).

Rowe, A. . (1978) *Internally Consistent Correlation for Predicting phase Composition of Heptane and Heavier Fractions*. Tulsa.

Rubin, B. and Buchanan, W. L. (1985) 'General purpose compositional model', *Society of Petroleum Engineers journal*. Society of Petroleum Engineers, 25(2), pp. 202–214. doi: 10.2118/11713-PA.

Safari, H. *et al.* (2014) 'Assessing the Dynamic Viscosity of Na–K–Ca–Cl–H₂O Aqueous Solutions at High-Pressure and High-Temperature Conditions', *Industrial & Engineering Chemistry Research*, 53, pp. 11488–11500. doi: 10.1021/ie501702z.

Saghafi, H. and Arabloo, M. (2018) 'Development of genetic programming (GP) models for gas condensate compressibility factor determination below dew point pressure', *Journal of Petroleum Science and Engineering*. Elsevier B.V., 171, pp. 890–904. doi: 10.1016/j.petrol.2018.08.020.

Samuel, A. L. (1959) 'Some Studies in Machine Learning Using the Game of Checkers', *IBM Journal of Research and Development*, 3(3), pp. 535–554.

Sanjari, E. and Lay, E. N. (2012) 'An accurate empirical correlation for predicting natural gas compressibility factors', *Journal of Natural Gas Chemistry*, 21, pp. 184–188. doi: 10.1016/S1003-9953(11)60352-6.

Sanni, M. (2018) *Petroleum engineering : principles, calculations, and workflows*. John Wiley & Sons, Incorporated. doi: 10.1002/9781119387985.

Sarkar, R., Danesh, A. S. and Todd, A. C. (1991) 'Phase Behavior Modeling of Gas-Condensate Fluids Using an Equation of State', in *SPE Annual Technical Conference and Exhibition*. Dallas: Society of Petroleum Engineers. doi: 10.2118/22714-MS.

Serra, K., Peres, A. M. and Reynolds, A. C. (1990) 'Well-Test Analysis for Solution-Gas-Drive Reservoirs: Part 1-Determination of Relative and Absolute Permeabilities', *SPE Formation Evaluation*, 05(02), pp. 124–132.

Serra, K. V., Peres, A. M. M. and Reynolds, A. C. (2007) 'Well-Test Analysis for Solution-Gas-Drive Reservoirs: Part 2-Buildup Analysis', *SPE Formation Evaluation*. Society of Petroleum Engineers, 5(02), pp. 133–140. doi: 10.2118/17048-pa.

Shi, C. (2009) *Flow Behavior of gas-condensate wells*. Stanford University.

Shokir, E. M. (2006) 'A Novel Model for Permeability Prediction in Uncored Wells', *SPE Reservoir Evaluation & Engineering*. Society of Petroleum Engineers, 9(03), pp. 266–273. doi: 10.2118/87038-pa.

Shokir, E. M. (2008) 'Novel Density and Viscosity Correlations for Gases and Gas Mixtures Containing Hydrocarbon and Non-Hydrocarbon Components', *Journal of Canadian Petroleum Technology*. Petroleum Society of Canada, 47(10). doi: 10.2118/08-10-45.

Smits, R. M. M., Van der Post, N. and Al Shaidi, S. M. (2001) 'Accurate Prediction of Well Requirements in Gas Condensate Fields', in *Proceedings of the Middle East Oil Show*. Manama: Society of Petroleum Engineers, pp. 611–621. doi: 10.2118/68173-ms.

Soave, G. (1972) *Equilibrium constants from a modified Redkh-Kwong equation of state*, *Chemical Engineering Science*. Pergamon Press.

Soroush, E. *et al.* (2015) 'Evolving a robust modeling tool for prediction of natural gas

hydrate formation conditions', *Journal of Unconventional Oil and Gas Resources*. Elsevier, 12, pp. 45–55. doi: 10.1016/J.JUOGR.2015.09.002.

Sousa, P. C. De, Garcia, A. P. and Waltrich, P. J. (2017) 'Analytical Development of a Dynamic IPR for Transient Two-Phase Flow in Reservoirs', in *SPE Annual Technical Conference and Exhibition*. San Antonio: Society of Petroleum Engineers. doi: 10.2118/187232-MS.

Spivak, A. and Dixon, T. N. (1973) 'Simulation Of Gas-Condensate Reservoirs', in *SPE Symposium on Numerical Simulation of Reservoir Performance*. Houston: Society of Petroleum Engineers. doi: 10.2118/4271-MS.

Standing, M. B. (1947) 'A Pressure-Volume-Temperature Correlation For Mixtures Of California Oils And Gases', *Drilling and Production Practice*. American Petroleum Institute, 275.

Standing, M. B. (1974) *Petroleum Engineering Data Book*. Trondheim: Norwegian Inst. of Technology.

Standing, M. B. (1979) *Calculating solutions gas drive reservoirs performance by Tarner's method*. doi: 10.1017/CBO9781107415324.004.

Standing, M. B. (1981) *Volumetric and Phase Behavior of Oil Field Hydrocarbon Systems*. 1st edn. Texas: SPE Richardson.

Standing, M. B. and Katz, D. L. (1942a) 'Density of Crude Oils Saturated with Natural Gas', *Transactions of the AIME*. Society of Petroleum Engineers (SPE), 146(01), pp. 159–165. doi: 10.2118/942159-g.

Standing, M. B. and Katz, D. L. (1942b) 'Density of Natural Gases', *Transactions of the AIME*. Society of Petroleum Engineers, 146(01), pp. 140–149. doi: 10.2118/942140-g.

Starling, K. E. and Ellington, R. T. (1964) 'Viscosity correlations for nonpolar dense

fluids', *AIChE Journal*. John Wiley & Sons, Ltd, 10(1), pp. 11–15. doi: 10.1002/aic.690100112.

Stewart, G. (2011) *Well Test Design and Analysis*. Tulsa: PennWell Corporation. Available at: <https://capitadiscovery.co.uk/teesside-ac/items/570433> (Accessed: 1 May 2019).

Stewart, W., Burkhardt, S. and Voo, D. (1959) 'Prediction of pseudocritical parameters for mixtures', in *AIChE Meeting*. Kansas City.

Stiel, L. I. and Thodos, G. (1962) 'The viscosity of polar gases at normal pressures', *AIChE Journal*, 8(2), pp. 229–232. doi: 10.1002/aic.690080220.

Stone, H. L. (1970) 'Probability model for estimating three-phase relative permeability', *Journal of Petroleum Technology*. Society of Petroleum Engineers, 22(2), pp. 214–218. doi: 10.2118/2116-pa.

Stone, H. L. (1973) 'Estimation of three -phase relative permeability and residual oil data', *Journal of Canadian Petroleum Technology*. Petroleum Society of Canada, 12(4), pp. 53–61. doi: 10.2118/73-04-06.

Strand, K. A. and Bjørkvik, B. J. A. (2019) 'Interface light-scattering on a methane–decane system in the near-critical region at 37.8 °C (100 °F)', *Fluid Phase Equilibria*. Elsevier B.V., 485, pp. 168–182. doi: 10.1016/j.fluid.2018.12.016.

Sumnu-Dindoruk, M. D. and Jones, J. R. (1998) 'Determination of Gas-Condensate Relative Permeabilities from Field Production Data', in *SPE Annual Technical Conference and Exhibition*. New Orleans: Society of Petroleum Engineers. doi: 10.2118/49267-MS.

Sun, C. Y. *et al.* (2012) 'Experiments and modeling of volumetric properties and phase behavior for condensate gas under ultra-high-pressure conditions', *Industrial and Engineering Chemistry Research*, 51(19), pp. 6916–6925. doi: 10.1021/ie2025757.

Sutton, R. P. (1985) 'Compressibility Factors for High-Molecular-Weight Reservoir Gases', in *SPE Annual Technical Conference and Exhibition*. Las Vegas: Society of Petroleum Engineers. doi: 10.2118/14265-ms.

Sutton, R. P. (2005a) 'Fundamental PVT Calculations for Associated and Gas-Condensate Natural Gas Systems', in *SPE Annual Technical Conference and Exhibition*. Dallas: Society of Petroleum Engineers. doi: 10.2118/97099-MS.

Sutton, R. P. (2005b) 'Fundamental PVT Calculations for Associated and Gas/Condensate Natural-Gas Systems', *SPE Reservoir Evaluation & Engineering*. Society of Petroleum Engineers, 10(03), pp. 270–284. doi: 10.2118/97099-pa.

Sutton, R. P. (2007) 'Fundamental PVT calculations for associated and gas/condensate natural-gas systems', *SPE Reservoir Evaluation and Engineering*. Society of Petroleum Engineers, 10(3), pp. 270–284. doi: 10.2118/97099-pa.

Sutton, R. P. and Farshad, F. (1990) 'Evaluation of Empirically Derived PVT Properties for Gulf of Mexico Crude Oils', *SPE Reservoir Engineering (Society of Petroleum Engineers)*, 5(01).

Suykens, J. A. K. *et al.* (2002) 'Weighted least squares support vector machines: robustness and sparse approximation', *Neurocomputing*. Elsevier, 48(1–4), pp. 85–105. doi: 10.1016/S0925-2312(01)00644-0.

Suykens, J. A. K. and Vandewalle, J. (1999) 'Least Squares Support Vector Machine Classifiers', *Neural Processing Letters*, 9(June), pp. 293–300. doi: 10.1023/A.

Takacs, G. (1976) 'Comparison Made for Computer Z-Factor Calculation', *Oil and Gas Journal*, pp. 64–66.

Takagi, T. and Sugeno, M. (1985) 'Fuzzy Identification of Systems and Its Applications to Modeling and Control', *IEEE Transactions on Systems, Man and Cybernetics*. IEEE,

SMC-15(1), pp. 116–132. doi: 10.1109/TSMC.1985.6313399.

Tanasa, D. E. *et al.* (2013) 'Photodegradation process of Eosin y using ZnO/SnO₂ nanocomposites as photocatalysts: Experimental study and neural network modeling', *Journal of Materials Science*. Springer, 48(22), pp. 8029–8040. doi: 10.1007/s10853-013-7617-x.

Tarner, J. (1944) 'How different size gas caps and pressure maintenance programs affect amount of recoverable oil', *Oil Weekly*, 144, pp. 32–34.

Thomas, F. B., Bennion, D. B. and Andersen, G. (2009) 'Gas Condensate Reservoir Performance', *Journal of Canadian Petroleum Technology*, 48(07), pp. 18–24. doi: 10.2118/09-07-18.

Thornton, F. (1946) 'Gas-Condensate Reservoirs-a Review', *Production Practice*, pp. 150–159.

Tillerson, R. (2015) *Natural Gas and the Policies of the Future*. Available at: https://corporate.exxonmobil.com/News/Newsroom/Speeches/2015/0602_Natural-Gas-and-the-Policies-of-the-Future (Accessed: 9 March 2020).

Ugwu, J. O. (2011) *A Semi-Emerical Approach To Modelling Well Deliverability In Gas Condensate Reservoirs*. Robert Gordon University Aberdeen. doi: 10.1177/0266242610391936.

Vazquez, M. and Beggs, H. D. (1980) 'Correlations for fluid physical property prediction', *Journal of Petroleum Technology*. Society of Petroleum Engineers (SPE), 32(06), pp. 968–970. doi: 10.2118/6719-pa.

Vo, D. T., Jones, J. R. and Raghavan, R. (1989) 'Performance predictions for gas-condensate reservoirs', *SPE Formation Evaluation*. Society of Petroleum Engineers, 4(4), pp. 576-584 16984. doi: 10.2118/16984-pa.

Vo, H. X. (2010) *Composition Variation During Flow of Gas-Condensate Wells*.

Stanford University.

Van der Waals, J. . (1873) *Over de Continuïteit van den Gas-en Vloeistofoestand (On the Continuity of the Gas and Liquid State)*. University of Leiden.

Walsh, M. and Lake, L. (2003) *A generalized approach to primary hydrocarbon recovery*. 1st edn. Amsterdam: Elsevier Ltd.

Warsito, B., Santoso, R. and Yasin, H. (2018) 'Cascade Forward Neural Network for Time Series Prediction', *Journal of Physics: Conference Series*, 1025, p. 12097. doi: 10.1088/1742-6596/1025/1/012097.

Wheaton, R. J. and Zhang, H. R. (2007) 'Condensate Banking Dynamics in Gas Condensate Fields: Compositional Changes and Condensate Accumulation Around Production Wells', in. doi: 10.2118/62930-ms.

Whitson, C. and Brulé, M. (2000) *Phase Behavior*. 1st edn, *Society of Petroleum Engineers*. 1st edn. Richardson: Society of Petroleum Engineers. doi: 10.1021/ma00080a014.

Whitson, C. H. (1983) 'Characterizing hydrocarbon plus fractions', *Society of Petroleum Engineers journal*. Society of Petroleum Engineers, 23(4), pp. 683–694. doi: 10.2118/12233-PA.

Whitson, C. H. (1989) 'Discussion of An Improved Method for the Determination of the Reservoir-Gas Specific-Gravity for Retrograde Gases', *Journal of Petroleum Technology*, 1216.

Whitson, C. H. (2006) 'Pressure/Volume/Temperature (PVT) treatment', in *Petroleum engineering handbook Volume V, Reservoir engineering and petrophysics*. Texas: Society of Petroleum Engineers, pp. 1458–1465.

Whitson, C. H., Fevang, Ø. and Yang, T. (1999) 'Gas Condensate PVT – What's Really

Important and Why?', in *Optimisation of Gas Condensate Fields*. London: Norwegian U. of Science and Technology. doi: 10.2118/117930-PA.

Whitson, C. H. and Kuntadi, A. (2005) 'Khuff gas condensate development', in *2005 International Petroleum Technology Conference Proceedings*. Doha, pp. 1191–1209. doi: 10.2523/iptc-10692-ms.

Whitson, C. H., Da Silva, F. and Soreide, I. (1988) 'Simplified compositional formulation for modified black-oil simulators', in *SPE Annual Technical Conference and Exhibition*. Houston: Society of Petroleum Engineers. doi: 10.2118/18315-MS.

Whitson, C. H. and Torp, S. B. (1983) 'Evaluating Constant Volume Depletion Data', *JPT, Journal of Petroleum Technology*, 35(3), pp. 610–620. doi: 10.2118/10067-PA.

Wichert, E. and Aziz, K. (1972) 'Calculation of Z's for Sour Gases', *Hydrocarbon Processing*, 51(5), pp. 119–122.

Wyllie, M. R. J. (1951) 'A Note on the Interrelationship Between Wetting and Nonwetting Phase Relative Permeability', *Journal of Petroleum Technology*. Society of Petroleum Engineers (SPE), 3(10), pp. 17–17. doi: 10.2118/951381-g.

Xiao, J. J. and Al-Muraikhi, A. J. (2004) 'A New Method for the Determination of Gas Condensate Well Production Performance', in *SPE Annual Technical Conference and Exhibition*. Texas: Society of Petroleum Engineers. doi: 10.2118/90290-MS.

Xu, S. and Lee, W. J. (1999) 'Two-phase well test analysis of gas condensate reservoirs', in *Proceedings - SPE Annual Technical Conference and Exhibition*. Houston, Texas: Soc Pet Eng (SPE). doi: 10.2118/56483-ms.

Yager, R. R. and Filev, D. P. (1994) 'Generation of Fuzzy Rules by Mountain Clustering', *Journal of Intelligent & Fuzzy Systems: Applications in Engineering and Technology*, 2(3), pp. 209–219.

Yan, K. Le *et al.* (2013) 'Measurement and calculation of gas compressibility factor for

condensate gas and natural gas under pressure up to 116 MPa', *Journal of Chemical Thermodynamics*. Academic Press, 63, pp. 38–43. doi: 10.1016/j.jct.2013.03.025.

Yang, T. *et al.* (2007) 'LBC Viscosity Modeling of Gas Condensate to Heavy Oil', in *SPE Annual Technical Conference and Exhibition*. Anaheim: Society of Petroleum Engineers. doi: 10.2523/109892-ms.

Yang, T., Chen, W. . and Guo, T. . (1997) 'Phase behavior of a near-critical reservoir fluid mixture', *Fluid Phase Equilibria*, 128, pp. 183–197.

Yarborough, L. and Hall, K. R. (1974) 'How to Solve EOS for Z-factors', *Oil and Gas Journal*, 86.

Zadeh, L. . (1965) 'Fuzzy Sets', *Information and control*, 8(3), pp. 338–353.

Zadeh, L. A. (1973) 'Outline of A New Approach to the Analysis of Complex Systems', *IEEE Trans. Syst. Man, Cybern.*, SMC-3(1), pp. 28–44.

Zendehboudi, S. *et al.* (2012) 'Prediction of Condensate-to-Gas Ratio for Retrograde Gas Condensate Reservoirs Using Artificial Neural Network with Particle Swarm Optimization', *Energy & Fuels*, 26(6), pp. 3432–3447. doi: 10.1021/ef300443j.

Zhang, W. *et al.* (2019) 'Production performance analysis for horizontal wells in gas condensate reservoir using three-region model', *Journal of Natural Gas Science and Engineering*. Elsevier B.V., 61, pp. 226–236. doi: 10.1016/j.jngse.2018.11.004.

Zhanggui, L. *et al.* (1998) 'Integration of Fuzzy Methods into Geostatistics for Petrophysical Property Distribution', in *SPE Asia Pacific Oil and Gas Conference and Exhibition*. Perth: Society of Petroleum Engineers (SPE). doi: 10.2118/49964-ms.

Zhao, X. *et al.* (2018) 'Reservoir geostatistical estimation of imprecise information using fuzzy kriging approach', in *SPE Western Regional Meeting Proceedings*. California: Society of Petroleum Engineers. doi: 10.2118/190051-pa.

Zhou, C. D., Wu, X. L. and Cheng, J. A. (1993) 'Determining reservoir properties in reservoir studies using a fuzzy neural network', in *Proceedings - SPE Annual Technical Conference and Exhibition*. Houston: Society of Petroleum Engineers, pp. 141–150. doi: 10.2523/26430-ms.

APPENDIX A: Sample of collected data for development of condensate viscosity models

Table A1: Sample data used for development of condensate viscosity of gas-condensate reservoirs.

Pressure (psia)	Temperature (F)	API Gravity	γ_{Gas}	Rs Standing	Condensate viscosity (cp)
2393	167	60	0.845	2661	0.04
2537	109	60	1.2514	4312	0.0404
2730	189	60	1.2514	4510	0.0433
2320	167	60	0.845	2574	0.045
2248	167	60	0.845	2488	0.0475
2175	167	60	0.845	2401	0.05
2103	167	60	0.845	2315	0.055
2030	167	60	0.845	2229	0.0575
1958	167	60	0.845	2143	0.06
2283	109	60	1.2514	3845	0.0649
1885	167	60	0.845	2057	0.065
1813	167	60	0.845	1972	0.0675
2184	189	65	1.2514	3573	0.0678
1740	167	60	0.845	1887	0.07
1667	167	60	0.845	1802	0.0725
1775	109	65	1.2514	2950	0.0739
1595	167	60	0.845	1717	0.075
1522	167	60	0.845	1633	0.0785
2457	189	60	1.2514	4026	0.0794
1450.4	167	60	0.845	1549	0.08
1522.2	109	65	1.2514	2493	0.0821
1377.88	167	60	0.845	1465	0.0825
2029.6	109	65	1.2514	3384	0.0849
1305.36	167	60	0.8451	1382	0.085
5801	248	62	0.5757	4577	0.086
1232.84	167	60	0.845	1299	0.0875
1268.5	109	65	0.7581	2043	0.0899

APPENDIX B: The developed Matlab codes for prediction of Two-phase Z factor

B1. Cascade Forward Neural Network (CFNN) code

```
% Calculating Two-phase compressibility factor of gas condensate reservoirs
% Input data:
% (Tem,Pres,H2S,CO2,N2,SGgas,C1,C2,C3,IC4,NC4,IC5,NC5,C6,C7+,MWC7+,SGc7+)
% Target data is 2-Phase compressibility factor
% One hidden layer /the x and t data should be defined for running the code
% Created by Foad Faraji on 30-Apr-2020 22:19:05
% This script assumes these variables are defined:
%
% x - input data.
% t - target data.

x = input';
t = target';

% Choose a Training Function
% For a list of all training functions type: help nntrain
% 'trainlm' is usually fastest.
% 'trainbr' takes longer but may be better for challenging problems.
% 'trainscg' uses less memory. Suitable in low memory situations.
trainFcn = 'trainlm'; % Levenberg-Marquardt backpropagation.

% Create a Fitting Network
hiddenLayerSize = 5;
net = cascadeforwardnet(hiddenLayerSize,trainFcn);

% Setup Division of Data for Training, Validation, Testing
net.divideParam.trainRatio = 70/100;
net.divideParam.valRatio = 15/100;
net.divideParam.testRatio = 15/100;

% Train the Network
[net,tr] = train(net,x,t);

% Test the Network
y = net(x);
e = gsubtract(t,y);
performance = perform(net,t,y)

% View the Network
view(net)
view(plotregression)

% Plots
% Uncomment these lines to enable various plots.
%figure, plotperform(tr)
%figure, plottrainstate(tr)
%figure, ploterrhist(e)
%figure, plotregression(t,y)
%figure, plotfit(net,x,t)
```

B2. Feed Forward Neural Network (FFNN) code

```
% Solve an Input-Output Fitting problem with a Neural Network
```

```

% Script generated by Neural Fitting app
% Created by Foad Faraji on 30-Apr-2020 22:01:22
%
% This script assumes these variables are defined:
%
% data - input data.
% data_1 - target data.

x = input';
t = target';

% Choose a Training Function
% For a list of all training functions type: help ntrain
% 'trainlm' is usually fastest.
% 'trainbr' takes longer but may be better for challenging problems.
% 'trainscg' uses less memory. Suitable in low memory situations.
trainFcn = 'trainlm'; % Levenberg-Marquardt backpropagation.

% Create a Fitting Network
hiddenLayerSize = 30;
net = fitnet(hiddenLayerSize,trainFcn);

% Setup Division of Data for Training, Validation, Testing
net.divideParam.trainRatio = 70/100;
net.divideParam.valRatio = 15/100;
net.divideParam.testRatio = 15/100;

% Train the Network
[net,tr] = train(net,x,t);

% Test the Network
y = net(x);
e = gsubtract(t,y);
performance = perform(net,t,y)

% View the Network
view(net)

% Plots
% Uncomment these lines to enable various plots.
%figure, plotperform(tr)
%figure, plottrainstate(tr)
%figure, ploterrhist(e)
%figure, plotregression(t,y)
%figure, plotfit(net,x,t)

```

B3. The Developed ANFIS code for prediction of two-phase Z factor

```

[Developed by Foad Faraji]
Name='Gas-condensate two-phase Zfactor'
Type='ANFIS'
Version=3.0

NumInputs=16
NumOutputs=1
NumRules=8

AndMethod='prod'
OrMethod='probor'

```

ImpMethod='prod'
AggMethod='sum'
DefuzzMethod='wtaver'

[Input1]

Name='in1'
Range=[86 325]
NumMFs=8
MF1='in1cluster1': 'gaussmf', [43.939616492805 212.000000668321]
MF2='in1cluster2': 'gaussmf', [43.9396154549174 104.000000079057]
MF3='in1cluster3': 'gaussmf', [43.9396152970173 235.000000099111]
MF4='in1cluster4': 'gaussmf', [43.9396155607974 139.999999943725]
MF5='in1cluster5': 'gaussmf', [43.9396153693023 279.999999687274]
MF6='in1cluster6': 'gaussmf', [43.9396154076292 175.99999970267]
MF7='in1cluster7': 'gaussmf', [43.9396157558023 255.000000125218]
MF8='in1cluster8': 'gaussmf', [43.9396152975791 251.000000132237]

[Input2]

Name='in2'
Range=[200 23244]
NumMFs=8
MF1='in2cluster1': 'gaussmf', [4236.58785306734 10581.9999999971]
MF2='in2cluster2': 'gaussmf', [4236.58785307214 11039]
MF3='in2cluster3': 'gaussmf', [4236.58785307423 2250.00000000649]
MF4='in2cluster4': 'gaussmf', [4236.58785307181 7263.00000000187]
MF5='in2cluster5': 'gaussmf', [4236.58785308286 14342.0000000042]
MF6='in2cluster6': 'gaussmf', [4236.58785307428 15368.9999999975]
MF7='in2cluster7': 'gaussmf', [4236.5878530787 5952.0000000046]
MF8='in2cluster8': 'gaussmf', [4236.58785307252 3014.9999999937]

[Input3]

Name='in3'
Range=[0 0.3182]
NumMFs=8
MF1='in3cluster1': 'gaussmf', [0.0585008072527943 2.93425098980129e-06]
MF2='in3cluster2': 'gaussmf', [0.0585003547682657 -4.35711822099071e-08]
MF3='in3cluster3': 'gaussmf', [0.0585125232360066 3.920654716736e-06]
MF4='in3cluster4': 'gaussmf', [0.0585003585012129 3.57358628042432e-09]
MF5='in3cluster5': 'gaussmf', [0.0585003749078678 2.37195865262904e-08]
MF6='in3cluster6': 'gaussmf', [0.0585003559359281 -3.53122863778846e-08]
MF7='in3cluster7': 'gaussmf', [0.0585003532042919 -4.60732216844032e-08]
MF8='in3cluster8': 'gaussmf', [0.0584877379626363 -6.75724218907177e-06]

[Input4]

Name='in4'
Range=[0.0001 0.2084]
NumMFs=8
MF1='in4cluster1': 'gaussmf', [0.0401613083121935 0.00458163909699585]
MF2='in4cluster2': 'gaussmf', [0.0382700153253149 0.00419517750559465]
MF3='in4cluster3': 'gaussmf', [0.0418651236512032 0.00983790276288075]
MF4='in4cluster4': 'gaussmf', [0.0382976043771252 0.00560357238162204]
MF5='in4cluster5': 'gaussmf', [0.0383076571498975 0.00419856705369914]
MF6='in4cluster6': 'gaussmf', [0.0382724375195043 0.00309742082476367]
MF7='in4cluster7': 'gaussmf', [0.0382677423396701 0.0055808663568813]
MF8='in4cluster8': 'gaussmf', [0.0330126699595674 0.00780999629460519]

```
[Input5]
Name='in5'
Range=[0 0.1284]
NumMFs=8
MF1='in5cluster1': 'gaussmf', [0.0238315335879429 0.00627438049210001]
MF2='in5cluster2': 'gaussmf', [0.0236044365109744 0.00621246344533544]
MF3='in5cluster3': 'gaussmf', [0.0234589814159074 0.000438829119254106]
MF4='in5cluster4': 'gaussmf', [0.023606925598594 0.00610490708916884]
MF5='in5cluster5': 'gaussmf', [0.023617800021654 0.00630146893508594]
MF6='in5cluster6': 'gaussmf', [0.0236032858024176 0.00618305313871095]
MF7='in5cluster7': 'gaussmf', [0.0236003856299571 0.00608143238616504]
MF8='in5cluster8': 'gaussmf', [0.0238839586551994 0.0116440844337897]
```

```
[Input6]
Name='in6'
Range=[0.0687 0.9668]
NumMFs=8
MF1='in6cluster1': 'gaussmf', [0.165150553187308 0.884578858736474]
MF2='in6cluster2': 'gaussmf', [0.165111896601757 0.88459081776779]
MF3='in6cluster3': 'gaussmf', [0.165210031746201 0.825402307244853]
MF4='in6cluster4': 'gaussmf', [0.165113507316405 0.964900845674523]
MF5='in6cluster5': 'gaussmf', [0.165107839743975 0.884578157602831]
MF6='in6cluster6': 'gaussmf', [0.165110322343173 0.966804385058771]
MF7='in6cluster7': 'gaussmf', [0.165121263844434 0.964881358891908]
MF8='in6cluster8': 'gaussmf', [0.165066896995706 0.755766146908575]
```

```
[Input7]
Name='in7'
Range=[0.0164 0.944]
NumMFs=8
MF1='in7cluster1': 'gaussmf', [0.170537156326957 0.0709951928989352]
MF2='in7cluster2': 'gaussmf', [0.170535976525295 0.0710045817804966]
MF3='in7cluster3': 'gaussmf', [0.170823693963334 0.0901375904915624]
MF4='in7cluster4': 'gaussmf', [0.170537007754508 0.0163991704194279]
MF5='in7cluster5': 'gaussmf', [0.170534925678062 0.0710112470165839]
MF6='in7cluster6': 'gaussmf', [0.170536114129939 0.0174970343925587]
MF7='in7cluster7': 'gaussmf', [0.170541037663105 0.0164129045437485]
MF8='in7cluster8': 'gaussmf', [0.170250455876678 0.0994769386419807]
```

```
[Input8]
Name='in8'
Range=[0.0022 0.1018]
NumMFs=8
MF1='in8cluster1': 'gaussmf', [0.0182785732196822 0.0131446902790636]
MF2='in8cluster2': 'gaussmf', [0.0183285883784814 0.0133242186889857]
MF3='in8cluster3': 'gaussmf', [0.0178949230235043 0.0454564001090557]
MF4='in8cluster4': 'gaussmf', [0.0183113629133724 0.00249286416737207]
MF5='in8cluster5': 'gaussmf', [0.0182357688175312 0.0134669529963677]
MF6='in8cluster6': 'gaussmf', [0.0182850669469996 0.0021667899903619]
MF7='in8cluster7': 'gaussmf', [0.0184157915219734 0.00270102537643144]
MF8='in8cluster8': 'gaussmf', [0.0180152760310817 0.0477535134282819]
```

```
[Input9]
Name='in9'
Range=[0.0005 0.0404]
NumMFs=8
MF1='in9cluster1': 'gaussmf', [0.00731487820979324 0.00248705844697268]
MF2='in9cluster2': 'gaussmf', [0.007333262442539 0.00273834693161455]
MF3='in9cluster3': 'gaussmf', [0.00604639249004752 0.00766948272983621]
MF4='in9cluster4': 'gaussmf', [0.00733666244176128 0.000595313425476853]
```

```
MF5='in9cluster5': 'gaussmf', [0.00729450032120393 0.00295481243543017]
MF6='in9cluster6': 'gaussmf', [0.00732367459622212 0.000474267243179914]
MF7='in9cluster7': 'gaussmf', [0.00738900334100898 0.00082534739516243]
MF8='in9cluster8': 'gaussmf', [0.0076818000584948 0.0125581351570796]
```

```
[Input10]
```

```
Name='in10'
```

```
Range=[0 0.0392]
```

```
NumMFs=8
```

```
MF1='in10cluster1': 'gaussmf', [0.00747277691174156 0.00274451654371034]
MF2='in10cluster2': 'gaussmf', [0.00738008536525681 0.0028322815061444]
MF3='in10cluster3': 'gaussmf', [0.00666993738573774 0.0125045152448831]
MF4='in10cluster4': 'gaussmf', [0.00721139358378071 0.000699342876967532]
MF5='in10cluster5': 'gaussmf', [0.00717791263011896 0.00300936669590871]
MF6='in10cluster6': 'gaussmf', [0.00721183693677959 0.000580641875893435]
MF7='in10cluster7': 'gaussmf', [0.00724359398144546 0.000906893188813673]
MF8='in10cluster8': 'gaussmf', [0.00510787308580824 0.020523686456587]
```

```
[Input11]
```

```
Name='in11'
```

```
Range=[0.0003 0.06]
```

```
NumMFs=8
```

```
MF1='in11cluster1': 'gaussmf', [0.010989628253451 0.00102876181349276]
MF2='in11cluster2': 'gaussmf', [0.0109804851472784 0.00103494165778055]
MF3='in11cluster3': 'gaussmf', [0.0110944296216656 0.00365004369558179]
MF4='in11cluster4': 'gaussmf', [0.0109758926313568 0.000299451581006178]
MF5='in11cluster5': 'gaussmf', [0.010975064190915 0.00106588632379741]
MF6='in11cluster6': 'gaussmf', [0.010975989920257 0.000298791894919426]
MF7='in11cluster7': 'gaussmf', [0.0109769927203072 0.000334011467299146]
MF8='in11cluster8': 'gaussmf', [0.0109001501554013 0.00885089077594512]
```

```
[Input12]
```

```
Name='in12'
```

```
Range=[0 0.0216]
```

```
NumMFs=8
```

```
MF1='in12cluster1': 'gaussmf', [0.00457778955022597 0.00111196522778592]
MF2='in12cluster2': 'gaussmf', [0.00423289799883626 0.00101248197634151]
MF3='in12cluster3': 'gaussmf', [0.00619416038926742 0.00558639453008147]
MF4='in12cluster4': 'gaussmf', [0.00397464927220307 0.000189386843120908]
MF5='in12cluster5': 'gaussmf', [0.00398812565111719 0.00110093043615154]
MF6='in12cluster6': 'gaussmf', [0.00398861318747511 0.000285119443082563]
MF7='in12cluster7': 'gaussmf', [0.00397097261582544 0.000396707083667242]
MF8='in12cluster8': 'gaussmf', [0.00398179998065765 0.00849152556357554]
```

```
[Input13]
```

```
Name='in13'
```

```
Range=[0.0002 0.0592]
```

```
NumMFs=8
```

```
MF1='in13cluster1': 'gaussmf', [0.0108684508337383 0.00126140042095949]
MF2='in13cluster2': 'gaussmf', [0.010870902974869 0.00126233616513022]
MF3='in13cluster3': 'gaussmf', [0.0116305743579675 0.00316351153430631]
MF4='in13cluster4': 'gaussmf', [0.0108468687521291 0.000191464708564138]
MF5='in13cluster5': 'gaussmf', [0.0108488403333567 0.0012516185013373]
MF6='in13cluster6': 'gaussmf', [0.0108492287135814 0.000596009458114832]
MF7='in13cluster7': 'gaussmf', [0.0108511139108379 0.000269921606950057]
MF8='in13cluster8': 'gaussmf', [0.0110647815223455 0.0082766796912394]
```

```
[Input14]
```

```
Name='in14'
```

```
Range=[0.0019 0.1719]
```

```
NumMFs=8
MF1='in14cluster1': 'gaussmf', [0.0313895504555309 0.0128126493856118]
MF2='in14cluster2': 'gaussmf', [0.0312690910203329 0.0127399065893526]
MF3='in14cluster3': 'gaussmf', [0.033945335994664 0.00369439822954486]
MF4='in14cluster4': 'gaussmf', [0.0312530103063453 0.00249646567033026]
MF5='in14cluster5': 'gaussmf', [0.0312385040941791 0.0127593524892205]
MF6='in14cluster6': 'gaussmf', [0.0312515251352922 0.00199422853454202]
MF7='in14cluster7': 'gaussmf', [0.0312739158522125 0.00256866844036951]
MF8='in14cluster8': 'gaussmf', [0.0307937319746233 0.0224414354898865]
```

```
[Input15]
Name='in15'
Range=[102 225]
NumMFs=8
```

```
MF1='in15cluster1': 'gaussmf', [22.6132755686906 224.999999792627]
MF2='in15cluster2': 'gaussmf', [22.6132753096855 224.999999820843]
MF3='in15cluster3': 'gaussmf', [22.6132738389611 137.000002857337]
MF4='in15cluster4': 'gaussmf', [22.6132747363538 225.000000097399]
MF5='in15cluster5': 'gaussmf', [22.6132743305156 225.000000254138]
MF6='in15cluster6': 'gaussmf', [22.6132753260657 195.999999803551]
MF7='in15cluster7': 'gaussmf', [22.6132753149952 224.999999724766]
MF8='in15cluster8': 'gaussmf', [22.613271651713 122.999996497212]
```

```
[Input16]
Name='in16'
Range=[0.046716897 1.410136517]
NumMFs=8
```

```
MF1='in16cluster1': 'gaussmf', [0.250719711771256 0.175492332239836]
MF2='in16cluster2': 'gaussmf', [0.250661991137857 0.175478576150735]
MF3='in16cluster3': 'gaussmf', [0.25091461673315 0.245266327423517]
MF4='in16cluster4': 'gaussmf', [0.250662064038314 0.0499995769632495]
MF5='in16cluster5': 'gaussmf', [0.250657890609538 0.17548566069849]
MF6='in16cluster6': 'gaussmf', [0.250705369797355 0.0467291163640506]
MF7='in16cluster7': 'gaussmf', [0.250671096084732 0.0500141702177388]
MF8='in16cluster8': 'gaussmf', [0.250615492824929 0.757005180901017]
```

```
[Output1]
Name='out1'
Range=[0.553 2.1627]
NumMFs=8
```

```
MF1='out1cluster1': 'linear', [-0.00755946821024183 8.86822083638194e-05 -
0.412276537299596 0.745026305035173 9.56344806960528 -2.89047524642926 -
7.5797641664173 2.94441542464119 0.679505589228421 1.86942166050559
0.560716546924377 0.855813168079827 0.429499405754188 -0.815630074279709 -
0.00965304624602736 1.60498727899211 6.88143509795696]
MF2='out1cluster2': 'linear', [-0.00460409002885835 0.000108459087557863 -
0.0062375138460695 3.74855041077772 2.54470760261085 2.15879531146028 -
16.3324009260478 0.376883823395303 0.015018869404537 1.41208249305524
0.462287501267406 0.906777719212053 0.882684655316704 2.83452350392611 -
0.00428859761793081 9.55855338304278 -0.708738887464017]
MF3='out1cluster3': 'linear', [0.000654969920065858 3.15514989381458e-06 -
1.38187325019845 -0.484591779456197 -4.59980740406345 -0.961475341734974
7.79296678187562 -11.8652879601992 -3.10545212298483 -24.2770009386534 -
35.412087739472 22.2766624459308 -34.3371337101806 7.24961947123729 -
0.00383584950248734 -0.388429258351758 2.48328480288172]
MF4='out1cluster4': 'linear', [-0.00184849889883234 9.49185556072603e-05 -
0.00014095174767368 2.25058904103199 -16.1831749939464 5.51839161925737
11.4546457747793 -4.77166490765641 -1.50880268005852 -2.32377763088734 -
0.909164647778335 -0.927806311399684 -0.225828088770019 4.84780947280657 -
0.00150769455910119 -1.389192049236 -4.30002498392912]
```

```

MF5='out1cluster5': 'linear', [-0.00489848807731454 1.67091758006954e-05 -
0.0887295942773967 1.68487226515761 -12.68583833339192 7.78537683563561
5.0887221862383 -3.95034999014721 -1.21509477194293 -1.75856087026495 -
0.682572244937583 -0.714591222236499 -0.152713713423265 3.62373006285843 -
0.00246435574546424 3.20612915974109 -4.22263078753113]
MF6='out1cluster6': 'linear', [-0.00180609861597681 9.52588235927679e-05 -
0.00204264406659315 2.84360244172998 -14.8735594657765 8.73949213298495
3.88166839803435 -4.46950500956205 -1.40535689468844 -1.95793684868143 -
0.813050133643518 -0.846995138006763 -0.361348044746124 3.05368444917823 -
0.00211678625950648 3.62802080920173 -7.50951241023598]
MF7='out1cluster7': 'linear', [-0.00219204652439519 5.10001229244977e-05 -
0.01773153949996 -1.28015744630374 7.72617783348421 -2.11658645471097 -
4.42934013531728 2.19127473716969 0.709237954037057 1.0509957945385
0.424597447499027 0.44089453206662 0.128646474136584 -2.14285603725373 -
3.37436828469696e-05 0.697452124271445 3.43216202064018]
MF8='out1cluster8': 'linear', [0.00022197675241711 5.66551503828279e-05 -
1.41094164824755 4.63301335859171 -0.102152414135072 -0.0208196609353636 -
0.244315490381672 -0.0203120179125655 0.740931989631539 -2.0461159783671 -
0.242012620863792 -15.5766598399363 4.08841008676089 0.885455014808267
0.00088095922505857 -0.330946185837141 0.872730470001803]

```

[Rules]

```

1 1 1 1 1 1 1 1 1 1 1 1 1 1 1, 1 (1) : 1
2 2 2 2 2 2 2 2 2 2 2 2 2 2 2, 2 (1) : 1
3 3 3 3 3 3 3 3 3 3 3 3 3 3 3, 3 (1) : 1
4 4 4 4 4 4 4 4 4 4 4 4 4 4 4, 4 (1) : 1
5 5 5 5 5 5 5 5 5 5 5 5 5 5 5, 5 (1) : 1
6 6 6 6 6 6 6 6 6 6 6 6 6 6 6, 6 (1) : 1
7 7 7 7 7 7 7 7 7 7 7 7 7 7 7, 7 (1) : 1
8 8 8 8 8 8 8 8 8 8 8 8 8 8 8, 8 (1) : 1

```

APPENDIX C: Sample calculation of inflow performance relationship (IPR) for HTHP gas condensate well

In this appendix the sample calculation of PVT properties for KAL – 05 is provided.

Please refer to the published paper for obtaining sample calculation of the IPR.
<https://www.sciencedirect.com/science/article/abs/pii/S0920410519305819>

APPENDIX D: The developed Eclipse – 300 code for prediction of well inflow performance of HPHT gas condensate well

The details of developed Eclipse 300 code is given in following.

```
=====
-- Study      : Gas-condensate HTHP/tight formation (KAL – 5)
-- Author     : F. Faraji
-- Simulator  : Eclipse-300
-- DATE      : 24 March 2020
=====
```

```
--RUNSPEC section-----
```

```
RUNSPEC
```

```
--Request the FIELD unit set
```

```
FIELD
```

```
--Water is present
```

```
WATER
```

```
--AIM solution method
```

```
AIM
```

```
--Nine components in study (plus water )
```

```
COMPS
```

```
9 /
```

```
--Peng-Robinson equation of state to be used
```

```
EOS
```

```
PR /
```

```
DIMENS
```

```
9 9 4 /
```

```
--ICP NTABSS=2
```

```
TABDIMS
```

```
2 1 40 40 /
```

```
--Is a gas condensate study
```

```
ISGAS
```

```
MULTSAVE
```

```
0 /
```

```
--ICP Debug
```

```
DEBUG3
```

```
81* 1 /
```

--ICP
SCFDIMS
4 /

FMTOUT

--Grid section-----

GRID

INIT

--Basic grid block sizes

DX
324*293.3 /

DY
324*293.3 /

DZ
162*30 162*50 /

--Cell top depths - only for first layer specified

TOPS
81*7400 /

PORO
324*0.13 /

PERMX
81*130 81*40 81*20 81*150 /

PERMY
81*130 81*40 81*20 81*150 /

PERMZ
81*13 81*4 81*2 81*15 /

CONDFRAC
'SCF3' 2 10.0 500.0 /
6 6 4 5 1 4 'X' /
6 7 5 5 1 4 'Y' /
7 7 5 6 1 4 'X' /
7 8 6 6 1 4 'Y' /
8 8 6 8 1 4 'X' /
8 9 8 8 1 4 'Y' /
9 9 8 9 1 4 'X' / <-- Intersects P1
/

--ICP
CONDFRAC
'SCF1' 2 10.0 500.0 /
4 7 2 2 1 4 'Y' /
/

CONDFRAC
'SCF2' 2 10.0 500.0 /
2 2 2 5 1 4 'X' /
/

--Properties section-----

PROPS

NCOMPS

9 /

EOS

PR /

--ICP

RPTPROPS

SWFN SGFN SOF3 /

-- Peng-Robinson correction

PRCORR

-- Standard temperature and pressure in Deg F and PSIA

STCOND

60.0 14.7 /

-- Component names

CNAMES

CO2 N2 C1 C2 C3 C4-6 C7+1 C7+2 C7+3 /

-- Critical temperatures Deg R

TCRIT

548.46000 227.16000 343.08000 549.77400 665.64000

806.54054 838.11282 1058.03863 1291.89071 /

-- Critical pressures PSIA

PCRIT

1071.33111 492.31265 667.78170 708.34238 618.69739

514.92549 410.74956 247.56341 160.41589 /

-- Critical Z-factors

ZCRIT

.27408 .29115 .28473 .28463 .27748

.27640 .26120 .22706 .20137 /

-- Acentric factors

ACF

.22500 .04000 .01300 .09860 .15240

.21575 .31230 .55670 .91692 /

-- Molecular Weights

MW

44.01000 28.01300 16.04300 30.07000 44.09700

66.86942 107.77943 198.56203 335.19790 /

-- Omega_A values

OMEGAA
.4572355 .4572355 .5340210 .4572355 .4572355
.4572355 .6373344 .6373344 .6373344 /

-- Omega_B values

OMEGAB
.0777961 .0777961 .0777961 .0777961 .0777961
.0777961 .0872878 .0872878 .0872878 /

-- Default fluid sample composition

ZMFVD
1.00000 .01210 .01940 .65990 .08690
.05910 .09670 .04745 .01515 .00330
10000.00000 .01210 .01940 .65990 .08690
.05910 .09670 .04745 .01515 .00330 /

-- Boiling point temperatures Deg R

TBOIL
350.46000 139.32000 201.06000 332.10000 415.98000
523.33222 689.67140 958.31604 1270.40061 /

-- Reference temperatures Deg R

TREF
527.40000 140.58000 201.06000 329.40000 415.80000
526.05233 519.67000 519.67000 519.67000 /

-- Reference densities LB/FT3

DREF
48.50653 50.19209 26.53189 34.21053 36.33308
37.87047 45.60035 50.88507 55.89861 /

-- Parachors (Dynes/cm)

PARACHOR
78.00000 41.00000 77.00000 108.00000 150.30000
213.52089 331.78241 516.45301 853.48860 /

-- Binary Interaction Coefficients

BIC
-.0200
.1000 .0360
.1300 .0500 .000000
.1350 .0800 .000000 .000
.1277 .1002 .092810 .000 .000
.1000 .1000 .130663 .006 .006 .0
.1000 .1000 .130663 .006 .006 .0 .0
.1000 .1000 .130663 .006 .006 .0 .0 .0 /

-- Reservoir temperature in Deg F

RTEMP
200.0 /

--Water saturation functions

SWFN

0.16	0	50
0.18	0	40
0.20	0.002	32
0.24	0.010	21
0.28	0.020	15.5
0.32	0.033	12.0
0.36	0.049	9.2
0.40	0.066	7.0
0.44	0.090	5.3
0.48	0.119	4.2
0.52	0.150	3.4
0.56	0.186	2.7
0.60	0.227	2.1
0.64	0.277	1.7
0.68	0.330	1.3
0.72	0.390	1.0
0.76	0.462	0.7
0.8	0.540	0.5
0.84	0.620	0.4
0.88	0.710	0.3
0.92	0.800	0.2
0.96	0.900	0.1
1.00	1.000	0.0

/

0.2	0	0
1.0	1	0

/

--Gas saturation functions

SGFN

0.00	0.000	0.0
0.04	0.005	0.0
0.08	0.013	0.0
0.12	0.026	0.0
0.16	0.040	0.0
0.20	0.058	0.0
0.24	0.078	0.0
0.28	0.100	0.0
0.32	0.126	0.0
0.36	0.156	0.0
0.40	0.187	0.0
0.44	0.222	0.0
0.48	0.260	0.0
0.52	0.300	0.0
0.56	0.349	0.0
0.60	0.400	0.0
0.64	0.450	0.0
0.68	0.505	0.0
0.72	0.562	0.0
0.76	0.620	0.0
0.80	0.680	0.0
0.84	0.740	0.0

/

/

--Oil saturation functions

SOF3

0.00	0.000	0.000
0.04	0.000	0.000
0.08	0.000	0.000
0.12	0.000	0.001
0.16	0.000	0.002
0.20	0.000	0.003
0.24	0.000	0.004
0.28	0.005	0.005
0.32	0.012	0.012
0.36	0.024	0.024
0.40	0.040	0.040
0.44	0.060	0.060
0.48	0.082	0.082
0.52	0.112	0.112
0.56	0.150	0.150
0.60	0.196	0.196
0.68	0.315	0.315
0.72	0.400	0.400
0.76	0.513	0.513
0.80	0.650	0.650
0.84	0.800	0.800

/
/

--Rock and water pressure data

ROCK

3550 0.000004 /

PVTW

3550 1.0 0.000003 0.31 0.0 /

--Surface density of water

DENSITY

1* 63.0 1* /

--Solution section-----

SOLUTION

--Equilibration data - initial pressure 3500 psi at 7500, which is
--the oil-water and the oil-gas contact depth

EQUIL

--Dep Pref Dow Pcow Dgo Pcog
7500 3550 7500 0 5000 0 / -- 1 1 0 /

RPTRST

BASIC=2 PRESSURE SOIL SWAT SGAS /

SUMMARY =====

ALL

RUNSUM

FOPR
FOPT
FGOR
FPR

--Schedule section-----

SCHEDULE

WELSPECS

I FIELD 1 1 7500 WATER /
P FIELD 9 9 7500 OIL /
/

COMPDAT

I 1 1 3 4 1* 1 /
P 9 9 1 2 1* 1 /
/

--ICP

-- Must come after COMPDAT

-- PI mult only used if NOCUT

-- <Well name> <CUT/NOCUT> <PI_Mult> <I> <J> <K> <C1> <C2>

WELLCF

P CUT 1.0 5* /
/

WCONPROD

P OPEN ORAT 2000 1* 1* 2* 500 /
/

WCONINJE

I WATER OPEN RATE 2000 /
/

TSTEP

36*10 /

END